

Site-selective C(sp³)-H Alkylation of Saccharide Derivatives by Photocatalysts

李, 艳茹

<https://hdl.handle.net/2324/7157370>

出版情報 : Kyushu University, 2023, 博士 (理学), 課程博士
バージョン :
権利関係 :

Site-selective C(sp³)-H Alkylation of Saccharide Derivatives by Photocatalysts

LI Yanru

September 2023

Department of Interdisciplinary Engineering

Kyushu University

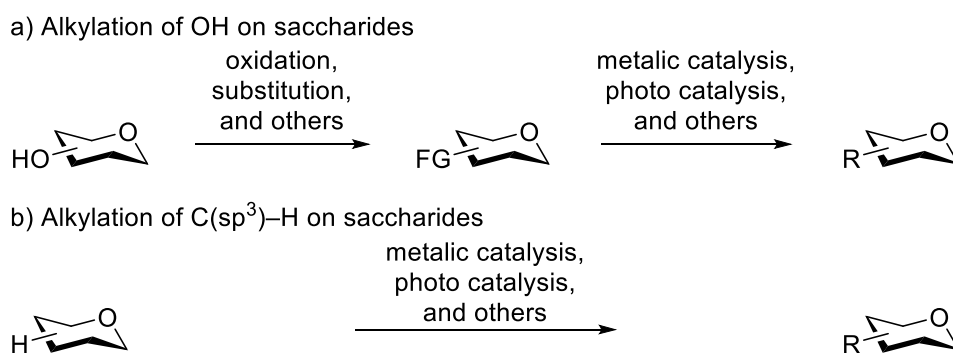
Contents

Abstract	1
Chapter 1. Introduction: Site-selective Alkylation of Saccharide Derivatives and Its Expected Applications	4
1.1 Introduction	4
1.2 Hydroxy Group Modification of Saccharides at Anomeric Position	10
1.3 Site-selective Hydroxy Groups Modification of Saccharides at Non-Anomeric Positions	18
1.4 Site-selective C(sp ³)-H Alkylation of Saccharides.....	24
1.5 Importance, Purpose, and Design of This Research.....	31
Chapter 2. Site-selective C(sp³)-H Alkylation of a Fructopyranose Derivative by 1,6-HAT	43
2.1 Introduction	43
2.2 Results and Discussion.....	46
2.3 Conclusion.....	64
2.4 Experimental Section	65
2.5 References	75
Chapter 3. Site-selective Direct Intermolecular C(sp³)-H Alkylation of Saccharides and Switching of Reaction Sites by Changing Photocatalysts	77
3.1 Introduction	77
3.2 Results and Discussion.....	83
3.3 Conclusion.....	127
3.4 Experimental Section	129
3.5 References	152
3.6 Supporting Information	155
Chapter 4. Conclusion	181
Publication List	185
Acknowledgements	186

Abstract

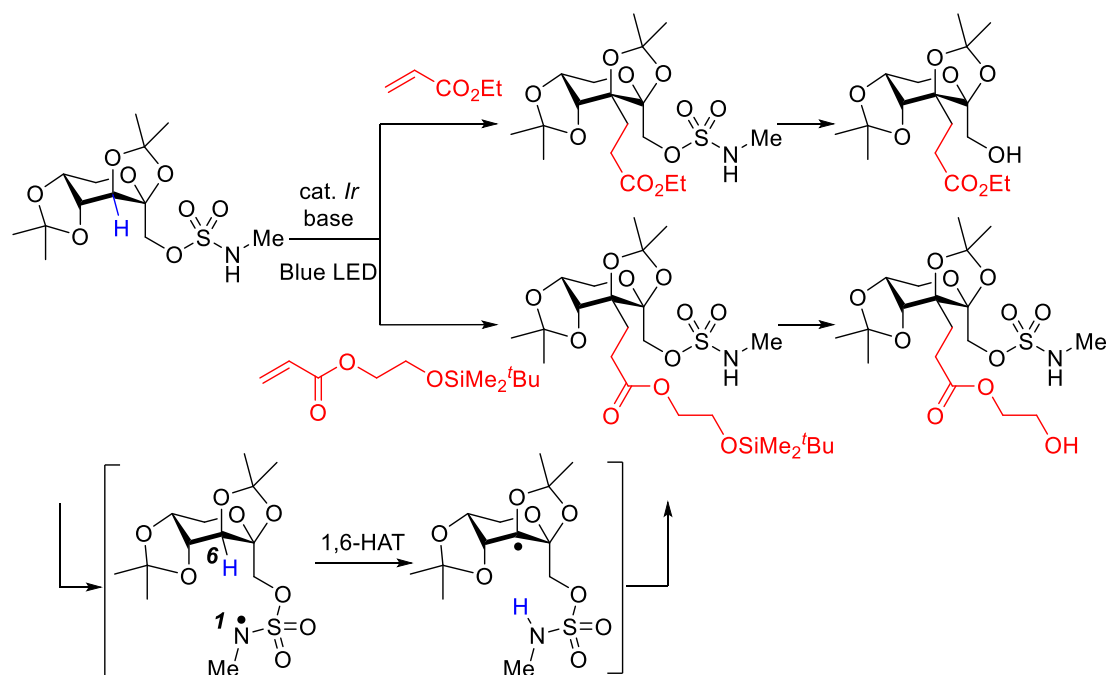
Site-selective functionalization of complex molecules is a major challenge in organic synthesis. Saccharides are key building blocks in bioactive and natural compounds. In this thesis, three novel methods for the site-selective C(sp³)-H alkylation of saccharide derivatives using photocatalysts were developed. The methods offer unique and efficient approaches to functionalize saccharides.

In Chapter 1, I introduced the site-selective alkylation of saccharide derivatives and its potential applications in various fields. Saccharides are important natural products, and their modification provides versatile derivatives for studies in glycobiology and glycochemistry. The modification of hydroxy groups and C(sp³)-H bonds of saccharides are important methods in synthetic glycochemistry. The site-selective C(sp³)-H alkylation of saccharides, which preserves the biological activity and functions of saccharides, is a significant research area. This chapter briefly discussed the different approaches for modifying saccharides, emphasizing the importance and application of the site-selective C(sp³)-H alkylation of saccharides.

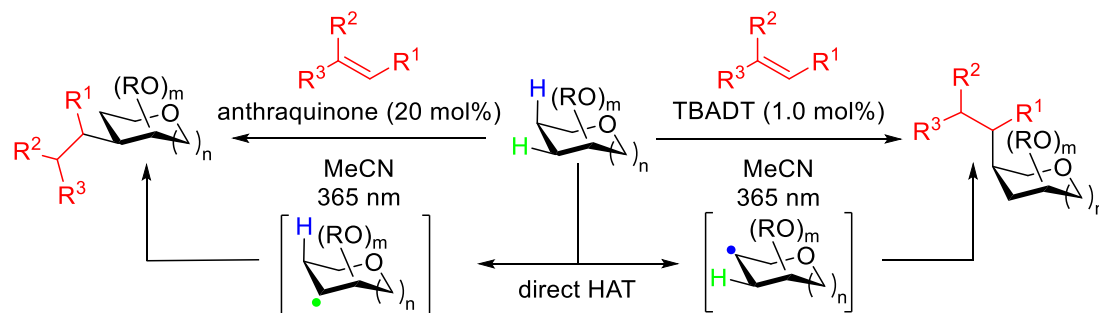


In Chapter 2, we investigated of C(sp³)-H alkylation of 2,3:4,5-bis-*O*-(1-ethylethylidene)- β -D-fructopyranose methyl sulfamate using an iridium photocatalyst under blue LED. This reaction enabled the introduction of various functional groups (such as ester, carbonyl, cyano, and sulfonyl groups) to the fructopyranose derivative by 1,6-HAT strategy. Furthermore, the *N*-methyl sulfamate group, acting as a hydrogen abstractor from the fructopyranose derivative, was converted to a hydroxy group.

Additionally, the siloxy group located at the introduced alkyl chain could be easily removed, providing a free hydroxy group.



In Chapter 3, we developed site-selective C(sp³)-H alkylation of saccharides with electron-deficient alkenes using anthraquinone and tetrabutylammonium decatungstate (TBADT). Interestingly, the reaction sites were switched by changing the photocatalysts. Anthraquinone-catalyzed C(sp³)-H alkylation occurred at the weak bond dissociation energy (BDE) of C(sp³)-H bond of saccharides. On the other hand, the site-selectivity of TBADT-catalyzed C(sp³)-H alkylation was dominated by steric effects. In the TBADT-catalyzed C(sp³)-H alkylation, the mono-alkylated product was obtained in excellent yield, even on a gram scale. The reactions were compatible with several electron-deficient alkenes and some saccharides, and provided a variety of C-saccharides.



Overall, the results presented in this thesis offer promising methods for the site-selective C(sp³)-H alkylation of saccharides and provide new platforms for the construction of complex saccharide derivatives. These methods can potentially be used in the synthesis of new bioactive molecules, which have important applications in the field of drug discovery.

Chapter 1. Introduction: Site-selective Alkylation of Saccharide Derivatives and Its Expected Applications

1.1 Introduction

Saccharides are aldehydes or ketones with multiple hydroxy groups and are composed of carbon, hydrogen, and oxygen atoms. In addition, saccharides are widely distributed in nature, including monosaccharides, disaccharides, and polysaccharides.

In the initial studies of saccharides, they are traditionally classified into 'energy substances,' such as glycogen and starch, which serve as stored sources of energy, and 'structural substances,' such as cellulose and proteoglycans, which play vital roles in cell walls, cartilage, and connective tissues, providing support and organization.¹ Until 1970s, their structures and many biological functions are gradually revealed.² At present, saccharide derivatives play important roles in the investigations and developments of new drugs, biological materials, and other life sciences.³ For example, Topiramate **1-1** is a medication used to treat epilepsy,⁴ and sialic acids **1-2** are widely distributed in animal tissues and are closely associated with the development of many diseases, such as, myopathy, cardiovascular diseases, and tumors (Scheme 1-1).⁵

Scheme 1-1. Structures of Topiramate and sialic acids.



The history of glycochemistry was traced back to the discovery and cultivation of sugarcane as sweeteners. Over time, people learned to extract sugars from sugarcane and beets, making sugars an important component of the human diet. The early research activities on saccharides were developed slowly, limited by the scientific research level at that time. Until 1806, Georg Ernst Stahl established that a functional group of saccharides was an aldehyde or a ketone.⁶ In the early 20th century, scientists, such as Emil Fischer and Henri Braconnot, investigated saccharide synthesis, structures, and

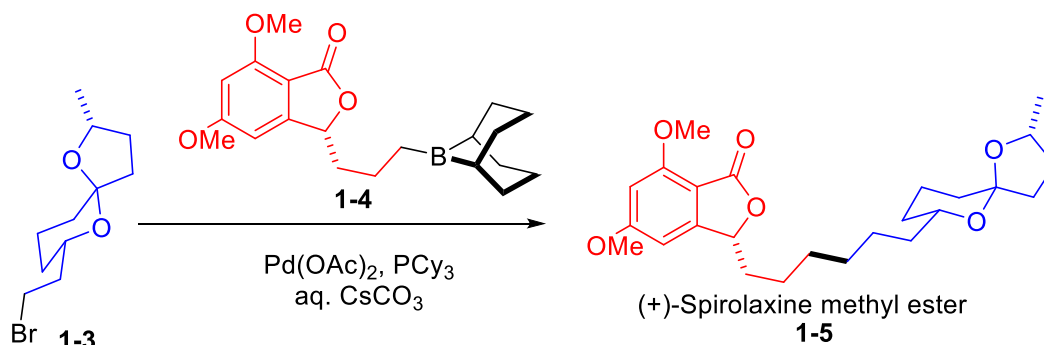
properties, which provided the basis for modern studies of saccharide chemistry.⁷ In recent years, significant progress has been made in saccharide chemistry, largely due to the continuous development of advanced imaging and molecular biology technologies.

However, the study of saccharides lags behind that of proteins and nucleic acids. Due to their complex and diverse structures, it is challenging to extract saccharides from natural sources that meet research needs. As a result, chemical synthesis remains an important method for obtaining pure saccharides.⁸ Therefore, the studies on the chemical synthesis and modification methods of saccharides are very vital to the development of glycochemistry and glycobiology. In this chapter, I will briefly summarize the research activities and development prospects of site-selective modification of saccharide derivatives.

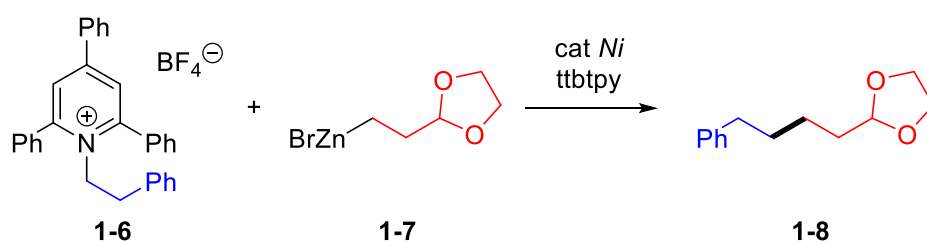
C–C bonds are found extensively in organic compounds, and their construction plays a crucial role in enhancing substance diversity and synthesizing compounds with novel chemical properties. This is particularly important in the development of new drugs, agrochemicals, and functional materials. Aryl-aryl cross-coupling reactions, such as Negishi, and Suzuki-Miyaura reactions, have been developed relatively maturely, with a wide substrate scope and good functional group compatibility. However, alkyl-alkyl coupling is still challenging to improve the compatibility and suppress the byproducts from homocoupling and β -hydride elimination.⁹ In 1855, Wurtz reported the $C(sp^3)–C(sp^3)$ homocoupling of two alkyl halides in the presence of sodium. Although the yields of the products were low, it encouraged the development of $C(sp^3)–C(sp^3)$ coupling reactions.¹⁰ The traditional methods of constructing alkyl-alkyl structures are based on Suzuki-Miyaura and Negishi reactions and nucleophilic reaction using Grignard reagent. Most nucleophiles used in the traditional methods are primary nucleophiles, and there are few studies except for nickel and palladium catalysts. For example, the Phillips group published palladium-catalyzed Suzuki-Miyaura $C(sp^3)–C(sp^3)$ cross-coupling in the total synthesis of the polyketide (+)-spiroloxine methyl ether **1-5** (Scheme 1-2a).¹¹ The Watson group reported a nickel-catalyzed Negishi $C(sp^3)–C(sp^3)$ cross-coupling between the alkylpyridinium salt **1-6** and organozinc **1-7** (Scheme 1-2b).¹² In addition, Kambe et.al succeeded in the development of copper-catalyzed $C(sp^3)–C(sp^3)$ cross-coupling with the Grignard reagent **1-10** in the presence of 1,3-butadiene or phenylpropyne (Scheme 1-2c).¹³

Scheme 1-2. C(sp³)-C(sp³) cross-coupling reactions.

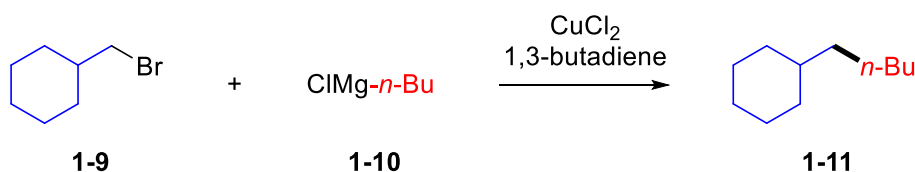
a) Suzuki-Miyaura C(sp³)-C(sp³) cross-coupling



b) Negishi C(sp³)-C(sp³) cross-coupling



c) C(sp³)-C(sp³) cross-coupling with Grignard reagent

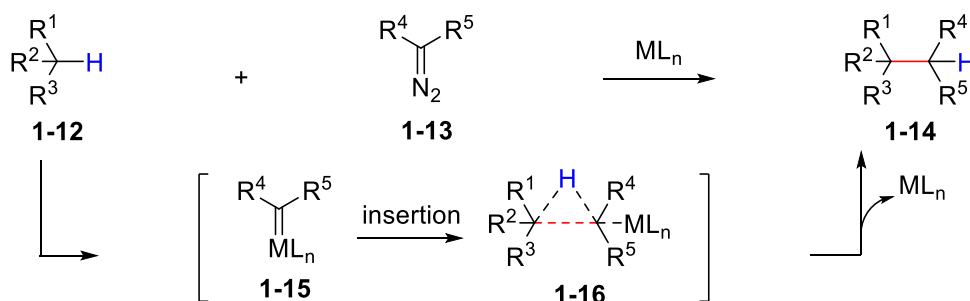


The direct transformations of C(sp³)-H bonds to construct C(sp³)-C(sp³) bonds are atom economy because they do not require the prefunctionalization of substrates.¹⁴ These strategies can be summarized into three categories: a) insertion of highly reactive metalcarbenes into C(sp³)-H bond.¹⁵ The rate-determining step in this reaction is to form the metalcarbene intermediate **1-15** from the metal complex and diazo compound **1-13**. Subsequently, the reactive intermediate **1-15** undergoes an attack on the C(sp³)-H bond, resulting in the formation of the alkylated product **1-14** through the three-membered ring transition state **1-16** (Scheme 1-3a); b) directing group-assisted C(sp³)-H transformations.¹⁶ The reaction energy barriers are reduced by the chelation of the directing group with the metal complex, allowing C(sp³)-H bond cleavage by metalation and deprotonation pathways. Then, the electrophilic substrate **1-20** is transformed into the metallacycle **1-21** through oxidative addition. The reactive intermediate **1-21** allows reductive elimination to generate the desired alkylation

product **1-19** and release the catalyst (Scheme 1-3b); and c) photocatalyzed C(sp³)-H transformation.¹⁷ Excited photocatalyst induces C(sp³)-H cleavage to form the carbon radical **1-25**, which reacts with the electron-deficient alkene **1-23** to generate C(sp³)-C(sp³) bond. Then, the alkyl radical intermediate **1-26** is hydrogenated to produce the alkylated product **1-24** (Scheme 1-3c). Hence, site-selective C(sp³)-H transformation of saccharides is a prominent subject and challenging work due to the inert C(sp³)-H bonds with similar reactivities.

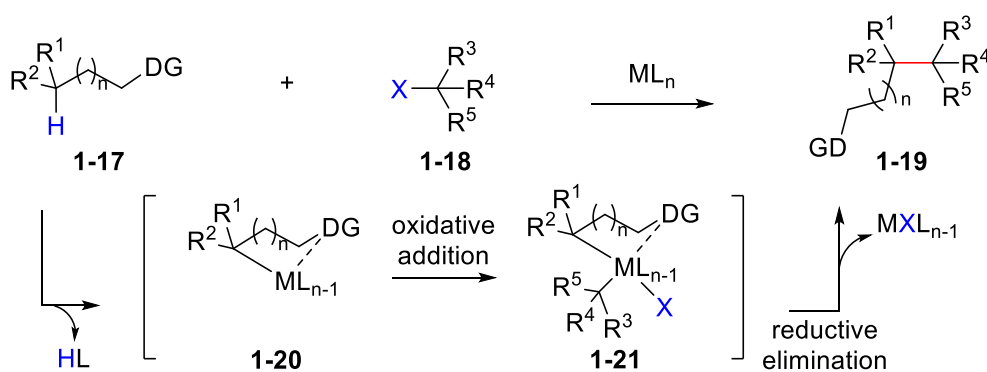
Scheme 1-3. Transformations of C(sp³)-H bond to form C(sp³)-C(sp³) bond.

a) Insertion of metallocarbene into C(sp³)-H bond

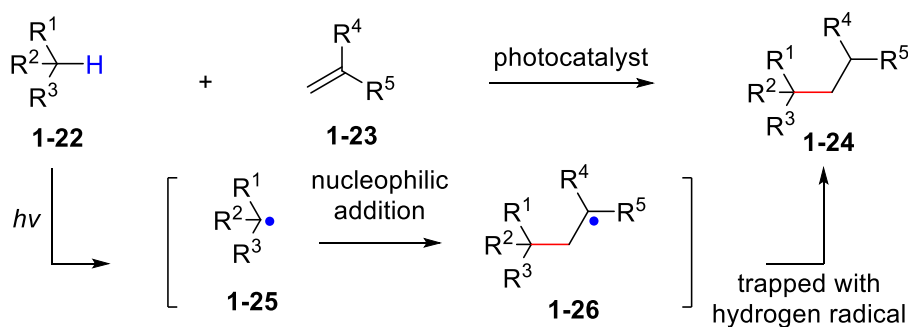


M: Fe, Cu, Ru, Rh, Ag, Au, etc.

b) Directing group-assisted C(sp³)-H transformations



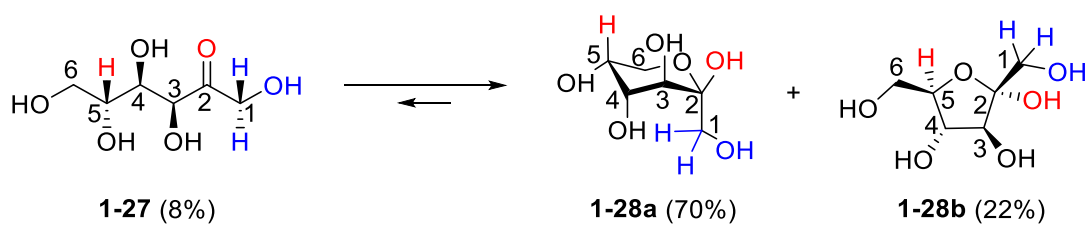
c) Photocatalyzed C(sp³)-H transformations



The site-selective modification of saccharides plays a crucial role in glycochemistry, as it allows for the precise manipulation of saccharide structures and properties. In particular, the selective C–H bonds activation of saccharides to construct C–C bonds has become an intriguing and challenging research area. This is attributed to the inertness and chemically similar properties of C(sp³)–H bonds of saccharides. In my research, I aim to address this challenge by developing methods for the selective C–H alkylation of saccharides, enabling the construction of desired C–C bond.

Fructose, as a crucial carbohydrate molecule with significant importance in metabolism, nutrition, and as a sweetening agent in the food industry, serves as a fundamental substrate in my research. By utilizing a fructose derivative as model substrate, I aim to investigate the site-selective C(sp³)–H alkylation. Here, I briefly analyze the structure of fructose to facilitate the understanding of fundamental characteristics of saccharides (Scheme 1-4). Fructose has chain and ring forms. In aqueous solution, approximately 70% of fructose exists as pyranose (a six-membered ring), 22% of it as furanose (five-membered ring), and the remaining portion adopts other forms, including open-chain structures. The ring configuration **1-28a** is formed by the nucleophilic attack of the OH group at C6 onto the carbonyl group at C2 of the chain configuration **1-27**. In its natural state, the ring configuration **1-28a** is more stable than chain configuration **1-27**. In the modification of ring configuration **1-28a**, only O–H and C–H bonds can be modified without altering the carbon skeleton. There are three types of hydroxy groups in fructose: 1) a primary hydroxy group at C1; 2) secondary hydroxy groups at C3, C4, and C5; 3) a tertiary hydroxy group at C2. The OH at C2 is known as anomeric OH, and it more easily subject to functionalization. The modification of saccharides can be simply classified into three types: 1) the modification of OH group at the anomeric position, 2) the site-selective protection and oxidation of OH group(s) at other positions, and 3) the site-selective C–H bond(s) modification of saccharides.

Scheme 1-4. Chain and ring configurations of fructose.

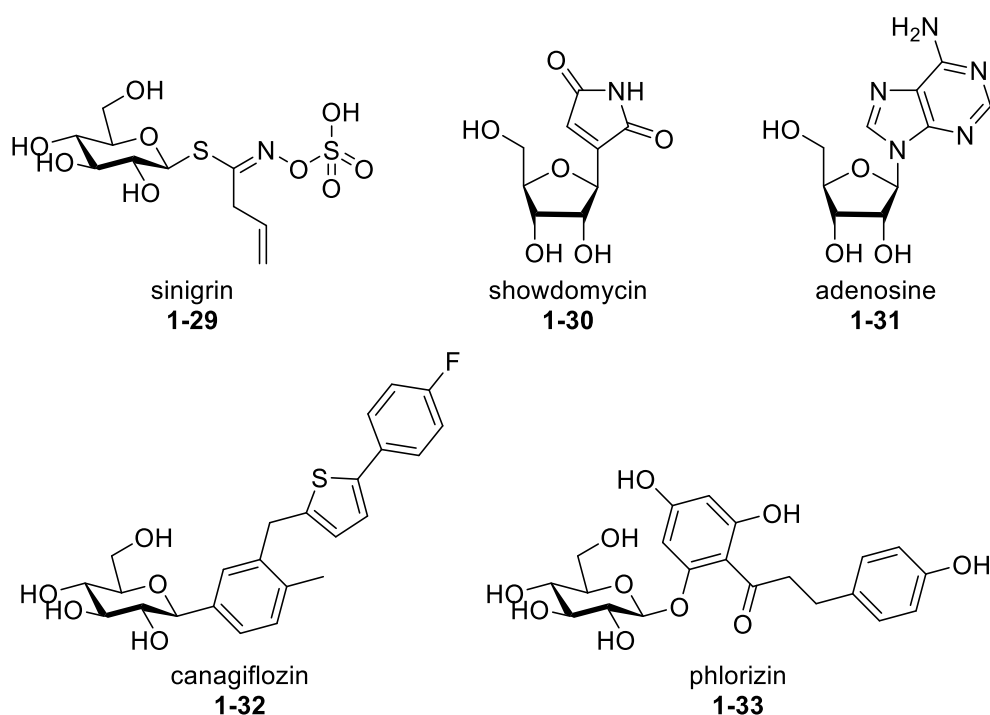


1.2 Hydroxy Group Modification of Saccharides at Anomeric Position

1.2.1 Traditional Methods

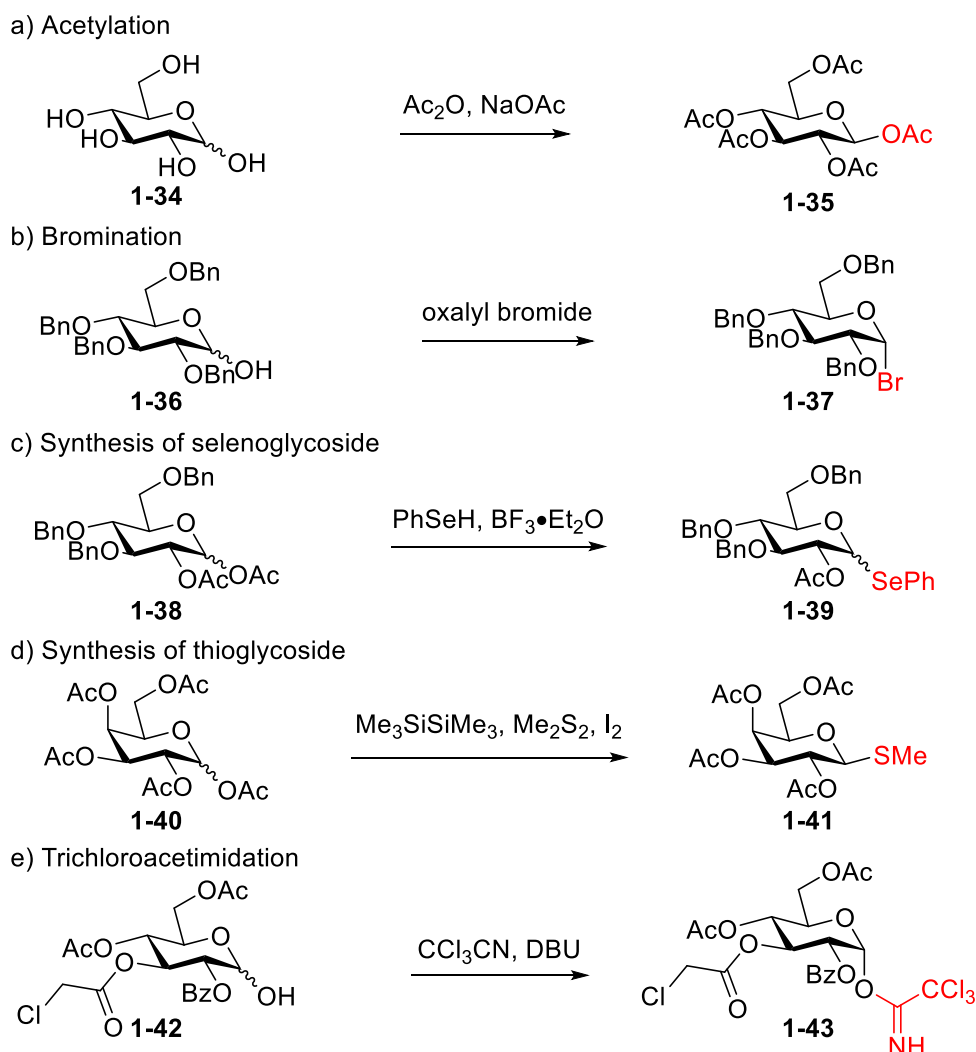
Glycoconjugates are important biomolecules that consist of saccharides linked to proteins, lipids, peptides, and other compounds. They play essential roles in various biological processes. Research in glycobiology is relevant to fields such as molecular and cellular biology, proteomics, and medicine, as it helps us understand how disruptions in these processes can lead to severe diseases. Glycoconjugates are typically large molecules, and researchers have synthesized simplified versions, known as artificial glycosides, to explore their potential in drug development.¹⁸ For instance, Canagliflozin **1-32** (*C*-glycoside) and Phlorizin **1-33** (*O*-glycoside) are recognized as inhibitors of sodium-glucose co-transporter 2 (SGLT2) and have demonstrated their effectiveness in lowering plasma glucose levels.¹⁹ The proximity of the anomeric hydroxy group to the oxygen atom facilitates its conversion into a suitable leaving group, such as acetoxy, alkylthio groups, or halogen atoms. Subsequently, a substitution reaction occurs at this position, resulting in the formation of *C*-glycosides,²⁰ *N*-glycosides,²¹ *O*-glycosides,²² and *S*-glycosides.²³ Various natural and artificial glycosides exist, and specific examples can be found in Scheme 1-5.

Scheme 1-5. Several natural and artificial glycosides.



In Scheme 1-6, acetoxy group, bromine atom and other suitable leaving groups were introduced at the anomeric position by reactions, such as acetylation and bromination. For example, selenoglycoside **1-39** was synthesized by the reaction of acetyl group-substituted saccharide **1-38** with benzeneselenol (Scheme 1-6c). Thioglycoside **1-41** was synthesized by the reaction between acetyl group-substituted saccharide **1-40** and dimethyl disulfide in the presence of hexamethyldisilane and iodine (Scheme 1-6d). Saccharide **1-42** reacted with trichloroacetonitrile to introduce trichloroacetimidate moiety, resulted in the formation of **1-43** (Scheme 1-6e). Subsequently, α -bromoglycosides (Scheme 1-6b) are utilized as initial substrates to outline the synthetic routes for *C*-glycosides, *N*-glycosides, *O*-glycosides, and *S*-glycosides.²⁴

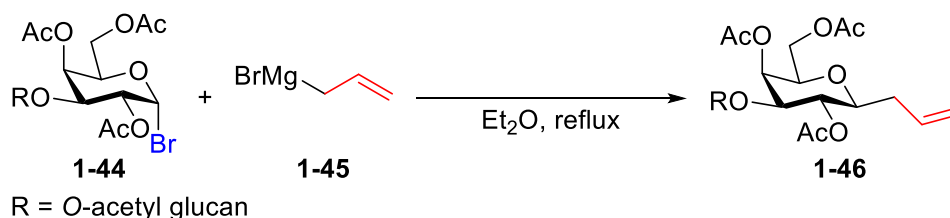
Scheme 1-6. Introduction of several leaving groups at the anomeric position.



1) Synthesis of C-glycosides

Merino *et al.* reported that the S_N2 nucleophilic addition of allyl Grignard reagent **1-45** to α -bromoglycoside **1-44** gave C-glycoside **1-46** (Scheme 1-7).²⁵

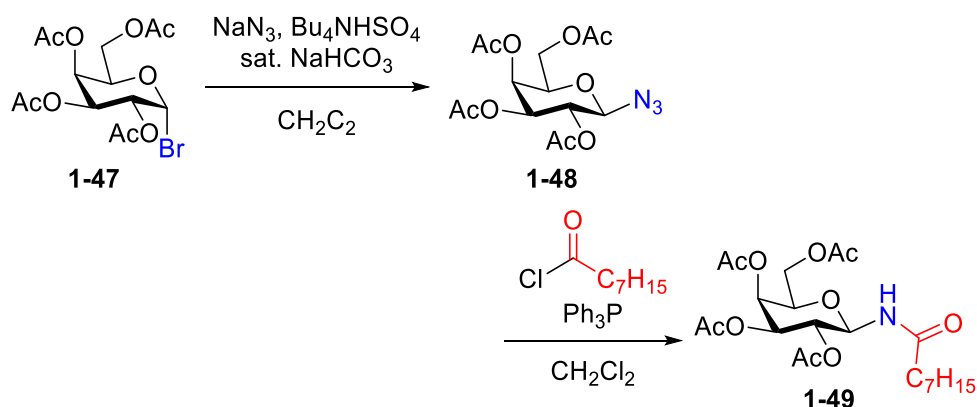
Scheme 1-7. Synthesis of C-glycoside from α -bromoglycoside.



2) Synthesis of N-glycosides

To realize the synthesis of N-glycoside **1-49**, one way is the reaction of the α -bromo saccharide **1-47** with NaN₃ to give glycosyl azide **1-48** under mild conditions,²⁶ and the successive treatment of glycosyl azide **1-48** with acyl chloride to produce glycosyl amide **1-49**. In this method, the stereoselectivity was well controlled (Scheme 1-8).²⁷

Scheme 1-8. Synthesis N-glycoside from α -bromoglycoside.

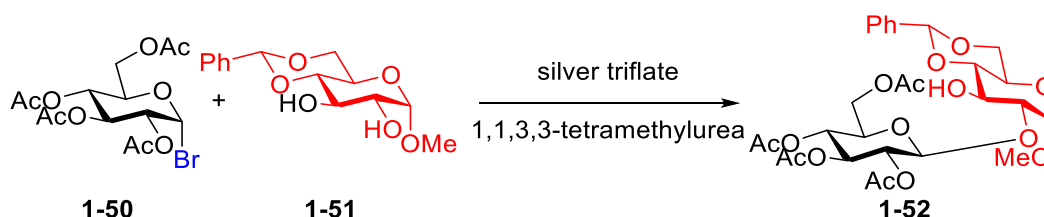


3) Synthesis of O-glycosides

Compared with the synthetic methods of other glycosides, there have been many research efforts on O-glycosides which contains some mature synthesis methods, such as Koenigs–Knorr glycosylation,²⁸ Schmidt glycosylation,²⁹ and Yu glycosylation.³⁰ In 1901, Koenigs and Knorr reported the substitution reaction of α -bromosaccharides with

an alcohol under silver carbonate as the promoter.²⁸ Based on the report, the synthesis of diverse oligosaccharides was developed. The example is that Hanessian and Banoub reported the synthesis of disaccharide **1-52** by the silver salt-promoted etherification of acetobromoglucose **1-50** with methyl 4,6-*O*-benzylidene- α -D-glucopyranoside **1-51** (Scheme 1-9).³¹

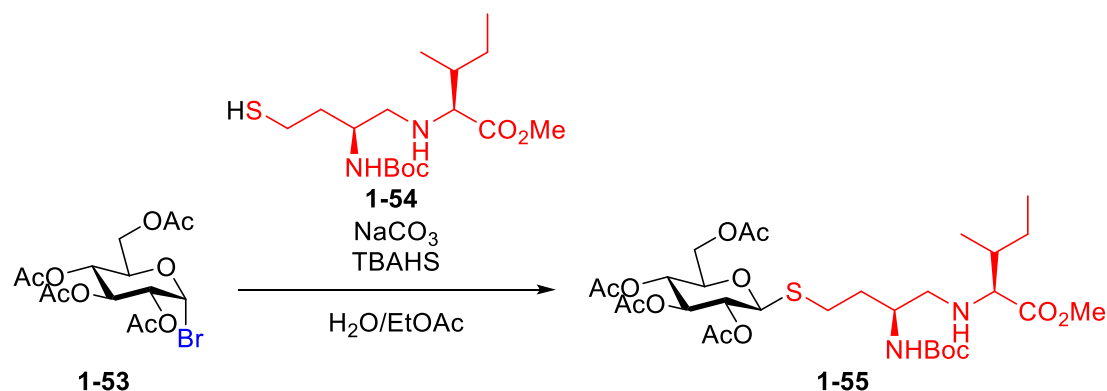
Scheme 1-9. Synthesis of *O*-glycoside from α -bromoglycoside.



4). Synthesis of *S*-glycosides

The anomeric oxygen of *O*-glycosides was replaced with sulfur, nitrogen, and carbon nucleophiles, providing *S*-, *N*-, and *C*-glycosides, respectively. They are tolerated under acidic and basic conditions and enzymatic hydrolysis in organisms.³² And some *S*-glycoproteins were reported.³³ The synthetic method of thioglycosides involves treating α -bromosaccharides with compounds containing a thiol group, taking advantage of the higher nucleophilicity of the thiol group compared to the hydroxy group. For example, Schmidt's group reported the synthesis of *S*-glycopeptide **1-55** by the reaction of α -bromosaccharide **1-53** with SH-containing amino acid derivative **1-54** in aqueous solution (Scheme 1-10).³⁴

Scheme 1-10. Synthesis of *S*-glycoside from α -bromoglycoside.



TBAHS = tetra-*n*-butylammonium hydrogen sulfate

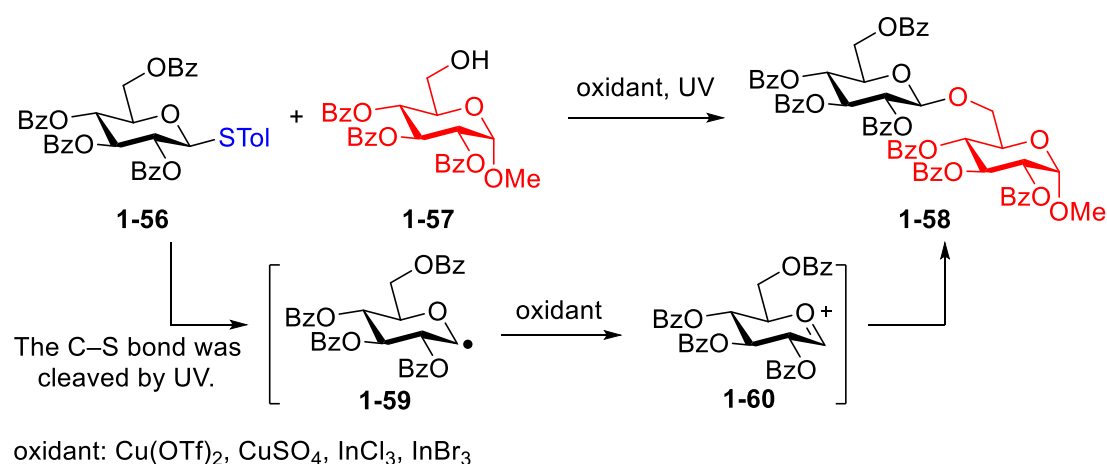
1.1.2 Light-mediated Glycosylation Reactions: Direct Photolysis and Photocatalysis

In recent years, researchers such as MacMillan, Stephenson, Rovis, and others have made significant advancements in photocatalytic C–C cross-coupling reactions. This emerging field of photocatalysis offers a promising approach to construct C(sp³)–C(sp³) structures in saccharides.³⁵ The light-mediated glycosylation has facilitated the synthesis of *O*-glycosides and *C*-glycosides in recent years, owing to its environmentally low toxicity and mild reaction conditions.³⁶

1) Light-mediated *O*-glycosylation

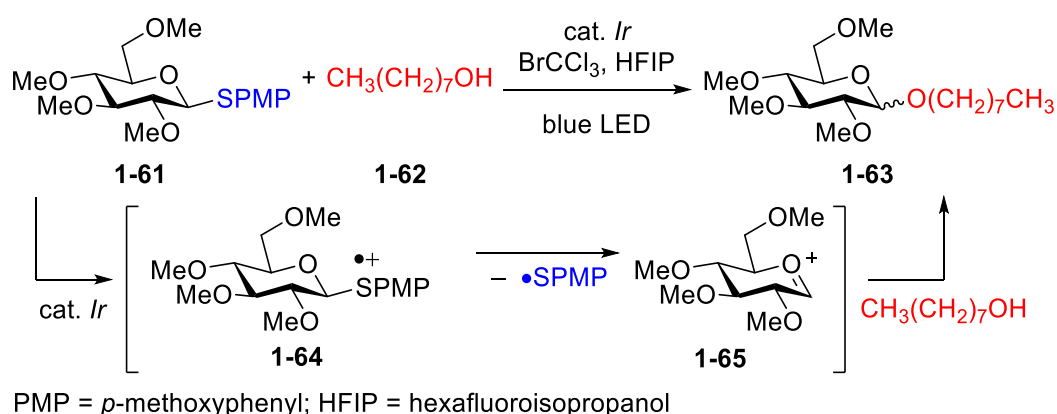
Ultraviolet (UV) and visible light are used as the light sources to mediate glycosylation. UV light has high energy, which can directly cleave the C–X (C–S, C–Se) bonds and generate a glycosyl radical. The disadvantage of the ultraviolet light-excited reactions is that free radical by-products is easily generated because the excitation energy is high. Ye's group reported the transformation of thiosaccharides to *O*-glycosides under UV light irradiation in the absence of photocatalysts.³⁷ Thioglycoside **1-56** was homolytically cleaved under UV irradiation to produce C radical **1-59**, which was oxidized to oxocarbenium ion **1-60** by an oxidant, and then reacted with hydroxy-containing compound **1-57** to form *O*-glycoside **1-58** (Scheme 1-11).

Scheme 1-11. UV-mediated *O*-glycosylation.



Visible light-mediated reactions usually necessitate the use of photocatalysts, in contrast to UV-mediated reactions. This is due to the lower energy of visible light compared to UV. Notably, photocatalysts have been utilized in the synthesis of thiosaccharides. Bowers's group reported that the single electron transfer (SET) from the *p*-methoxyphenyl-tetra-*O*-benzyl-thioglycoside **1-61** to the excited iridium catalyst resulting in the formation of the radical cation of thioglycoside **1-64**. Subsequently, it dissociated to oxocarbenium intermediate **1-65** and *p*-methoxyphenylthio radical. The intermediate **1-65** reacted with the alcohol **1-62** to give *O*-glycosylated product **1-63** (Scheme 1-12).³⁸

Scheme 1-12. Photoredox-catalyzed *O*-glycosylation.

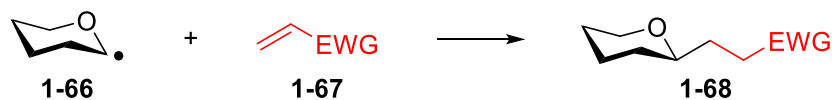


2) Light-mediated C-glycosylation

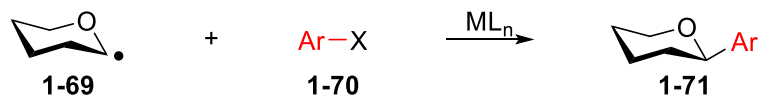
For light-mediated *C*-glycosylation, there are two reported methods. First method is that the generated nucleophilic C radical **1-66** reacted with electron-deficient alkene **1-67** to form a new C–C bond (Scheme 1-13a). Second method is the addition between the generated C radical **1-69** and aryl halide **1-70** in the presence of a transition metal catalyst to form a high-valence metal complex, and subsequently, the reductive elimination occurred to form a new C–C bond (Scheme 1-13b).

Scheme 1-13. Two methods of light-mediated C-glycosylation.

a) Addition process without metal catalysts



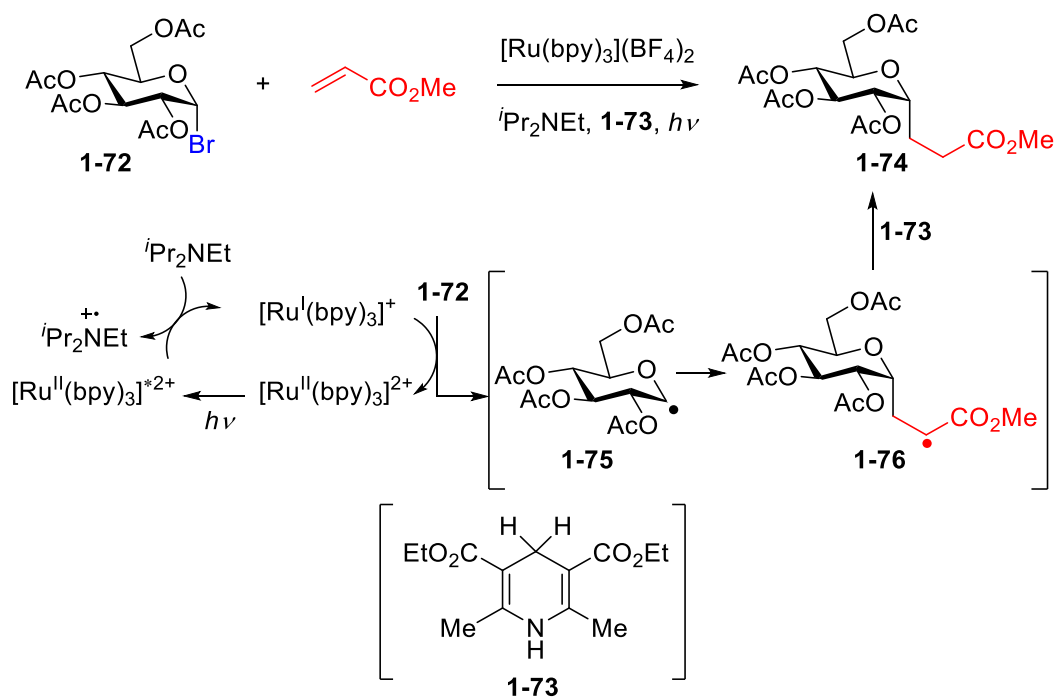
b) Addition process with metal catalysts



EWG: electron-withdrawing group; X: halogen; M: metal; L: ligand

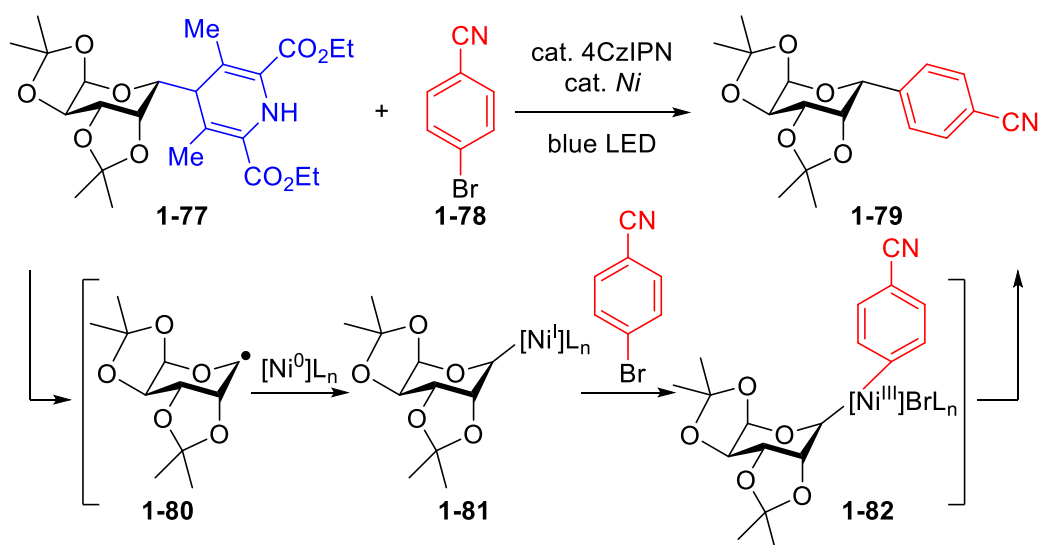
Gagné's group investigated the reaction of brominated saccharides with electron-deficient alkenes in the presence of photocatalyst, $\text{Ru}(\text{bpy})_3(\text{BF}_4)_2$.³⁹ One electron was transferred from $[\text{Ru}(\text{bpy})_3]^+$ to brominated saccharide **1-72**, generating glycosyl radical **1-75**. The radical species **1-75** had nucleophilicity and reacted with methyl acrylate (an electron-deficient alkene) to obtain alkyl radical **1-76**. Then, the radical species **1-76** trapped a hydrogen atom from Hantzsch ester **1-73**, resulting in the formation of C-glycosylated product **1-74** (Scheme 1-14).

Scheme 1-14. Alkylation of brominated saccharides.



Molander's group reported a method for synthesizing non-classical C-glycosides by reacting saccharides, which have 1,4-dihydropyridine derivatives (DHPs) as leaving groups, with aryl bromides. In this method, an electron transfer occurred from saccharide derivative **1-77** to an excited 4CzIPN photocatalyst, resulting in the formation of an unstable radical cation of **1-77**. Swiftly, the radical cation underwent cleavage, yielding the glycosyl radical **1-80** and a DHP derivative. Subsequently, the radical **1-80** reacted with the nickel(0) catalyst to form the alkyl nickel(I) species **1-81**. Following that, the oxidative addition of aryl bromide **1-78** took place with the species **1-81**, giving rise to the aryl nickel(III) complex **1-82**. Ultimately, complex **1-82** underwent reductive elimination, resulting in the formation of the novel C-glycoside **1-79** (Scheme 1-15).⁴⁰

Scheme 1-15. Arylation of a saccharide derivative with 1,4-dihydropyridine moiety.



After briefly reviewing the modification methods of saccharides at the anomeric position, it becomes evident that main approaches involve pre-functionalization of saccharides. This is achieved by introducing effective leaving groups (such as $-\text{SPh}$, $-\text{OTf}$, $-\text{DHPs}$, etc.) or forming relatively weak bonds (such as $\text{C}-\text{Br}$, $\text{C}-\text{S}$, $\text{C}-\text{Se}$, etc.) at the anomeric position. However, when it comes to directly and selectively modifying other positions, particularly converting $\text{C}-\text{OH}$ to active $\text{C}-\text{X}$ bonds like $\text{C}-\text{Br}$ and $\text{C}-\text{SPh}$, significant challenges arise. Therefore, achieving selective modifications at positions other than the anomeric position typically involves more complex strategies.⁴¹

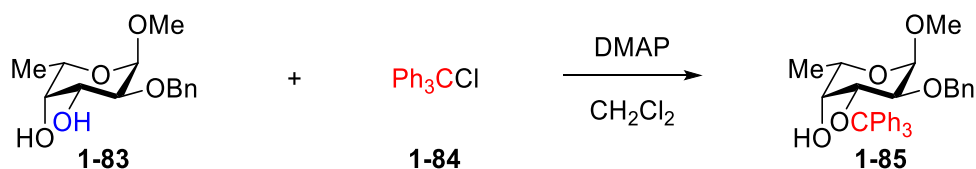
1.3 Site-selective Hydroxy Group Modification of Saccharides at Non-Anomeric Positions

1.3.1 Site-selective Protection of Hydroxy Groups of Saccharides

1) Equatorial-selective Protection of Hydroxy Group of Saccharide

Hernandez found that the reactivity of the equatorial hydroxy group with trityl chloride was higher than that of the axial one due to kinetic factor.⁴² In 1980, Matta reported that trityl chloride selectively reacted with the equatorial hydroxy group at C3-position of methyl 2-*O*-benzyl- α -L-fucopyranoside **1-83** under DMAP catalysis (Scheme 1-16).⁴³

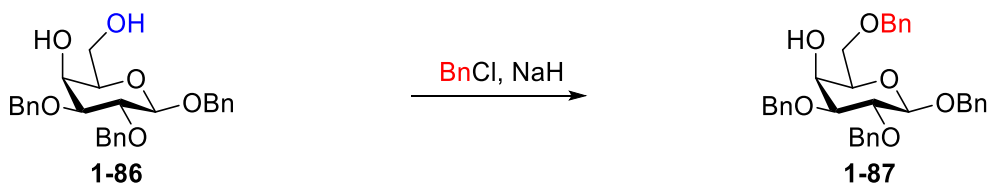
Scheme 1-16. Tritylation of equatorial hydroxy group.



2) Site-selective Protection of the Hydroxy Group of Saccharide Controlled by Steric Effect

Bulky protecting groups, such as benzyl, trityl, and trimethylsilane groups, are more likely to react with the primary hydroxy group due to less steric hindrance than that of secondary or tertiary hydroxy groups. Flowers reported the benzylation of methyl 2,3-di-*O*-benzyl- α -D-galactopyranoside **1-86** with benzyl chloride in the presence of sodium hydride as a base in DMF to give methyl 2,3,6-tri-*O*-benzyl- α -D-galactopyranoside **1-87** as a major product (Scheme 1-17).⁴⁴

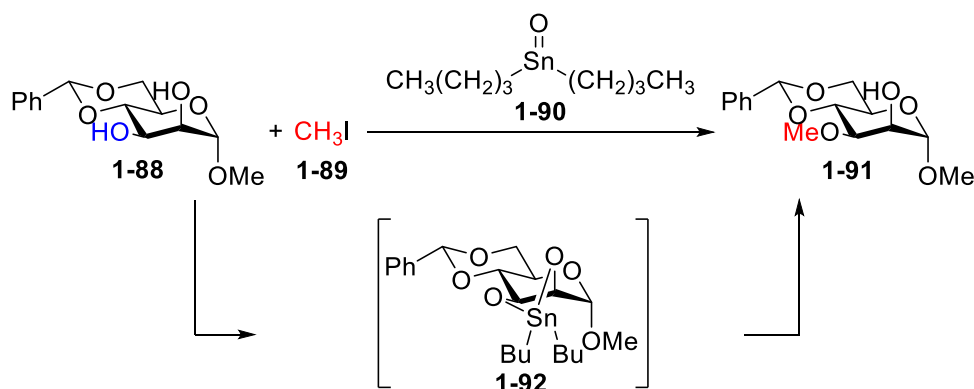
Scheme 1-17. Benzylation of primary hydroxy group.



3) Site-selective Protection of the Hydroxy Group of Saccharide Controlled by Chelation

The site-selective modification of hydroxy group(s) of saccharides was achieved using the chelation of two hydroxy groups with metal compounds, such as organotin,⁴⁵ silver,⁴⁶ copper,⁴⁷ and other transition complexes,⁴⁸ and organic compounds, such as organoboron and organosilicon compounds. Among them, organotin reagent is simple to operate and has high selectivity and compatibility in sulfonation, glycosylation, and oxidation. Nashed reported that the reaction of methyl 4,6-*O*-benzylidene- α -D-mannopyranoside **1-88** with methyl iodide **1-89** in the presence of dibutyltin oxide **1-90** gave methyl 4,6-*O*-benzylidene-3-*O*-methyl- α -D-mannopyranoside **1-91** (Scheme 1-18).⁴⁹

Scheme 1-18. Methylation of the equatorial hydroxy group by chelation.

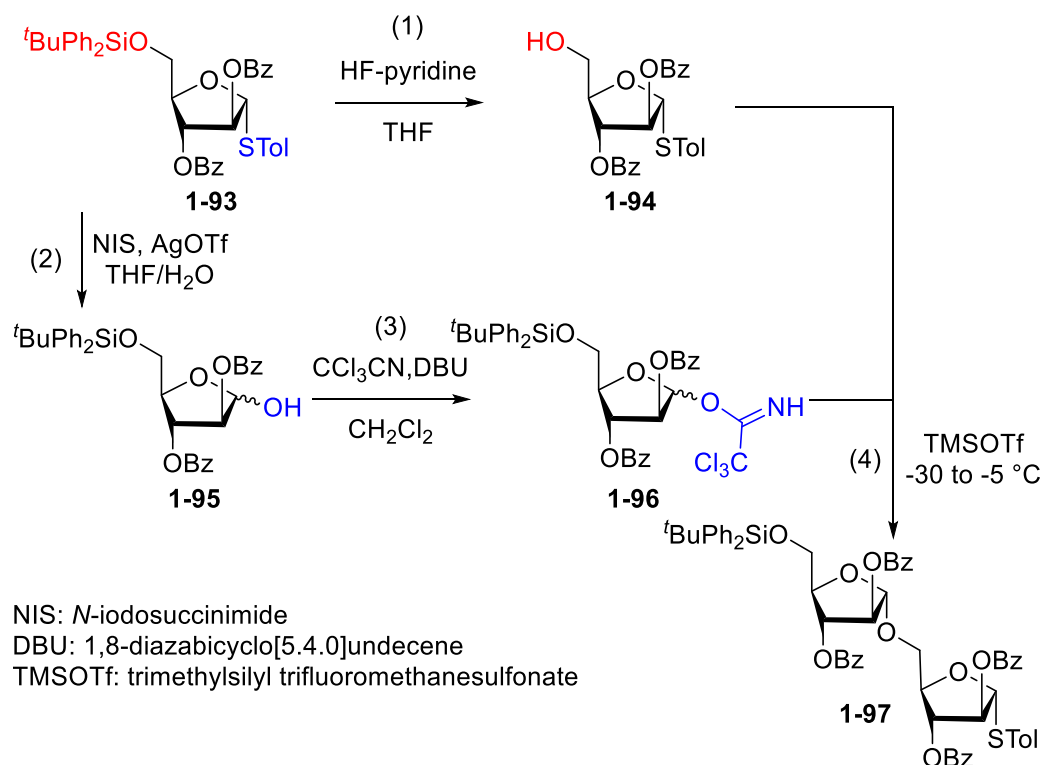


4) Site-selective Protection of Hydroxy Groups of Saccharide Supported by Different Protecting Groups

In the synthesis of oligosaccharides and glycoconjugates, a common strategy for achieving site-selectivity is the selective protection and deprotection of hydroxy groups, utilizing protecting groups with varying reactivities and steric hindrance. In this method, undesired reaction sites (hydroxy groups) are converted to inert groups, and only the exposed hydroxy group reacts with various compounds with functional groups. After the sequential reaction is completed, the protection groups can be removed.⁵⁰ Lowary reported the synthetic process of a disaccharide (Scheme 1-19). The starting monosaccharide, (*p*-tolyl 5-*O*-*t*-butyldiphenylsilyl-2,3-di-*O*-benzoyl-1-thio- α -D-

arabinofuranoside), possessed three types of protecting groups: thio-*p*-tolyl, tert-butyldiphenylsilyl, and benzyl groups. In the presence of HF–pyridine, only the *tert*-butyldiphenylsilyl group of saccharide **1-93** was deprotected to give compound **1-94**. In contrast, in presence of *N*-iodosuccinimide (NIS) and silver triflate, the thio-*p*-tolyl group of **1-93** was deprotected to give compound **1-95**. Then, the hydroxy group of **1-95** reacted with trichloroacetonitrile in the presence of 1,8-diazabicyclo[5.4.0]undecane (DBU) to afford compound **1-96**. Finally, the hydroxy group of **1-94** reacted with compound **1-96** in the presence of trimethylsilyl trifluoromethanesulfonate (TMSOTf) to obtain di-D-arabinofuranoside derivative **1-97**.⁵¹

Scheme 1-19. Stepwise synthesis of disaccharide.

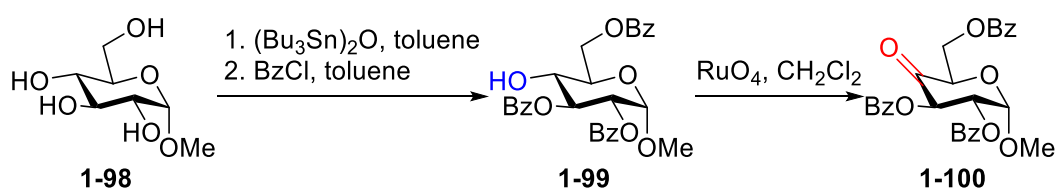


1.3.2 Site-selective Hydroxy Groups Oxidations of Saccharides

1) Site-selective Oxidation Followed by Site-selective Protection of Hydroxy Groups

Selective protection of hydroxy groups is widely employed in the synthesis of polysaccharides and glycoconjugates, serving as a crucial step in achieving site-selective modifications. In order to achieve selective oxidation of hydroxy groups of the saccharide, a common approach involves the prior selective protection of hydroxy groups. Then the unprotected hydroxy group is oxidized to a carbonyl group by an oxidant, such as RuO_4 and DMSO. Renaudet and Dumy reported the selective protection of methyl-D-glucopyranoside **1-98** and subsequent oxidation of the unprotected hydroxy group of **1-98** to a carbonyl group using RuO_4 to give 4-ketose **1-100** (Scheme 1-20).⁵²

Scheme 1-20. Site-selective oxidation of hydroxy group via selective protection of hydroxy groups on the saccharide.

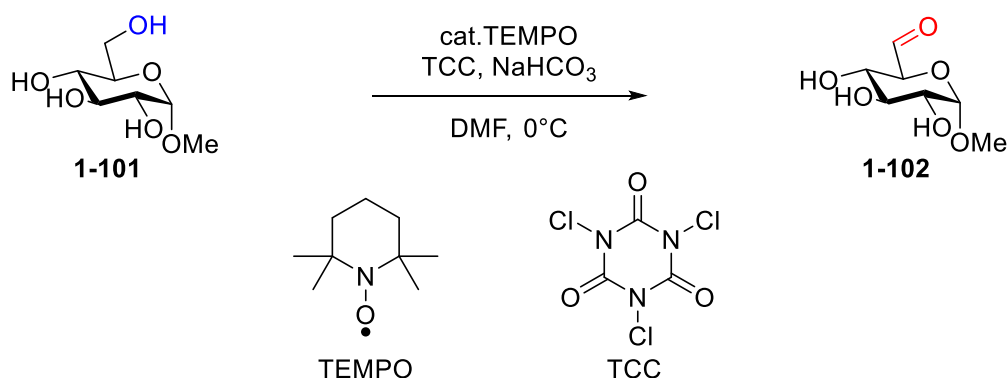


2) Directly Site-selective Oxidation

Site-selective oxidation of unprotected or less protected saccharides is a promising method to reduce reaction steps in the synthesis of glycoconjugates.⁵³ Because both primary and secondary hydroxy groups exist on most unprotected saccharides, selective oxidation of them is challenging in the modification of saccharides.

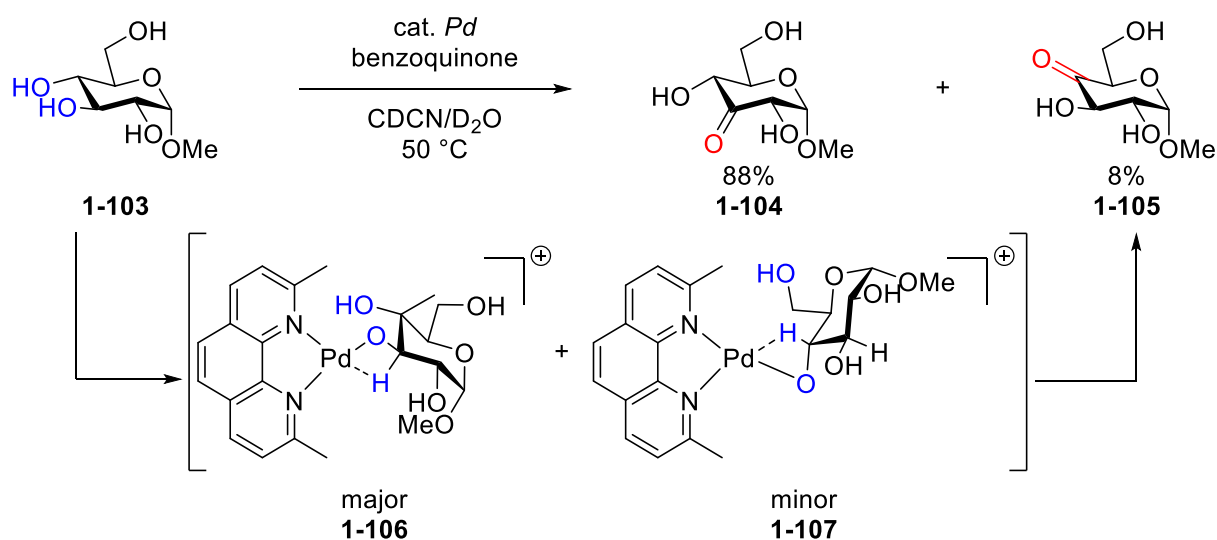
There are several reports on the selective oxidation of the primary hydroxy group, such as oxidation using organic catalysts,⁵⁴ enzymatic catalysts,⁵⁵ and solid catalysts.⁵⁶ Ramström's group reported that (2,2,6,6-tetramethylpiperidin-1-yl)oxyl (TEMPO) efficiently and selectively oxidized the primary hydroxy group of unprotected dialdo-glycoside **1-101** to the corresponding aldehyde **1-102** (Scheme 1-21).^{54b}

Scheme 1-21. Selective oxidation of primary hydroxy group using TEMPO.



To achieve the selective oxidation of the secondary hydroxy group, organotin reagents,⁵⁷ palladium compounds,⁵⁸ and glycoxidases⁵⁹ are mainly used as oxidants. Minnaard's group reported Pd-catalyzed site-selective oxidation at the C3-position of methyl α -D-glucopyranoside **1-103**.^{58a} Later, Chung and Waymouth pointed out that the palladium catalyst simultaneously locked the two hydroxy groups at the C3- and C4-positions of **1-103**, and the hydroxy group at C3-position was preferentially oxidized. Because the β -hydride elimination at C3-position of intermediate **1-106** is more favorable (Scheme 1-22).^{58b}

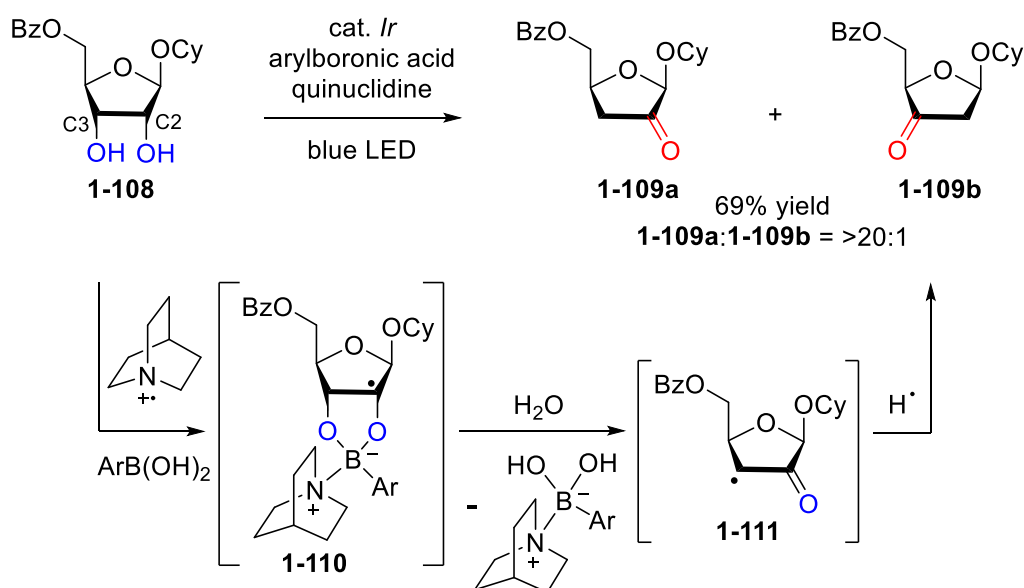
Scheme 1-22. Selective oxidation of secondary hydroxy group using Pd catalyst.



3) Selective Oxidation by Photocatalyst

Recently, photoreaction has become an important research direction in the modification of natural products due to the mild reaction conditions and environmentally friendliness. Taylor's group has made outstanding contributions to the selective modification of saccharides under photoredox catalysis. They realized the site-selective oxidation of saccharides using iridium photocatalyst, arylboronic acid, and quinuclidine as a cooperative catalyst (Scheme 1-23). Cyclohexyl 5-*O*-benzoyl β -D-ribofuranoside **1-108** was protected with arylboronic acid to lower the bond dissociation energy of the C2–H bond. The hydrogen atom of C2–H bond was then abstracted by the quinuclidine radical cation, leading to the formation of intermediate **1-110**. Subsequently, **1-110** underwent the cleavage of the C3–O bond, resulting in the formation of C3 radical **1-111**. Finally, **1-111** was trapped with a hydrogen atom, yielding product **1-109a**, which was 2-ketone 3-deoxyfuranoside.⁶⁰

Scheme 1-23. Site-selective photocatalytic oxidation of D-ribofuranoside derivatives.



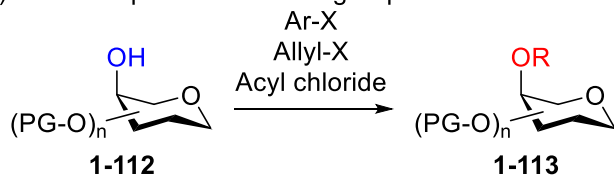
1.4 Site-selective C(sp³)-H Alkylation of Saccharides

The selective introduction of alkyl or aryl groups into saccharides using previous methods is summarized in Scheme 1-24: 1) by the selective protection of hydroxy group: Achieving the selective protection of a hydroxy group is accomplished by using protecting groups, such as aryl, alkyl, and acyl groups (Scheme 1-24a). 2) oxidation of unprotected alcohol: the unprotected hydroxy group is oxidized to a carbonyl group, and then nucleophiles, such as the Grignard reagent, react with the carbonyl group to form a new C-C bond (Scheme 1-24b). 3) by introducing a leaving group at the anomeric position: by using promoters (silver carbonate, etc.), the saccharide with a leaving group is converted to an oxocarbenium intermediate, which subsequently reacts with an alcohol (Scheme 1-24c). 4) by introducing a functional group at the anomeric carbon position: saccharides with a functional group to form oxocarbenium intermediates in presence of oxidizing agents or photocatalysts under light irradiation, which reacts with hydroxy-containing nucleophiles to give *O*-glycosides. If a glycosyl C radical is generated by photocatalyst, the C radical reacts with electron-deficient alkenes to produce *C*-glycosides (Scheme 1-24d).

Generally, in these methods, the hydroxy group of the saccharide serves as the initial reactive moiety. However, direct transformation of the hydroxy group into an alkyl group is challenging and necessitates a multistep process. If the C(sp³)-H bond of saccharides could be directly arylated or alkylated, the reaction process would be more concise and would not require the pre-functionalization of the starting saccharides.

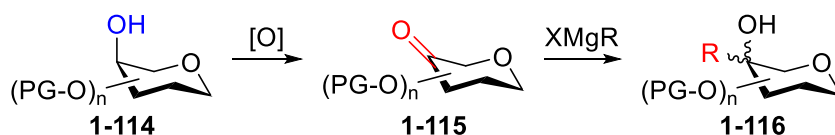
Scheme 1-24. Several methods of selective introduction of alkyl or aryl groups of saccharides.

a) Selective protection of OH group on saccharide



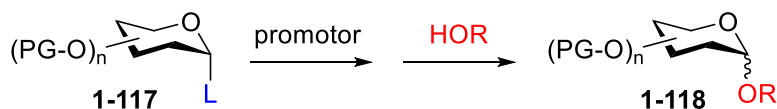
PG = protecting group; R = Ar, Allyl, Acyl

b) Selective oxidation of OH group on saccharide



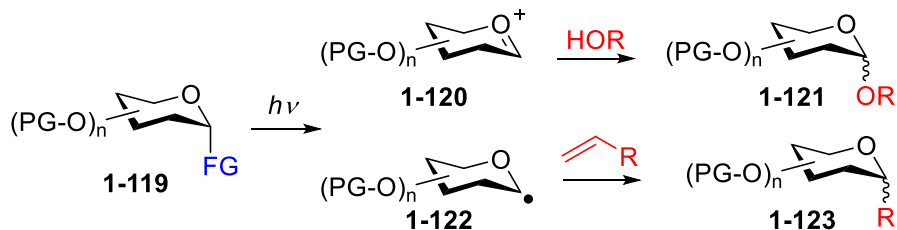
PG = protecting group; X = halogen; R = Ar, Alkyl

c) Modification of OH group at anomeric position by introduction of leaving group



PG = protecting group; LG = leaving group (-SPh, -OTf, -DHPs etc.); R = Ar, Alkyl

d) Modification of OH group at anomeric position by photocatalyst

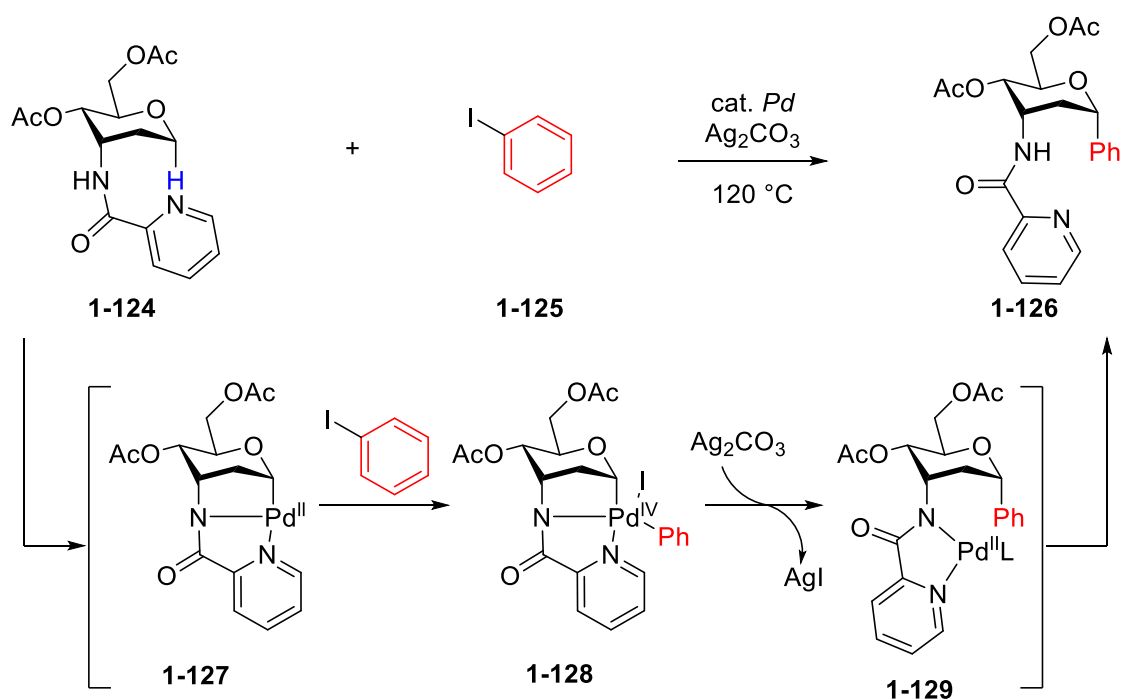


PG = protecting group; FG = functional group (-SAr, -OAr, -halogen, etc.); R = Ar, Alkyl

1.4.1 Pd-catalyzed Site-selective Arylation of C(sp³)-H of Saccharide Using Directing Group

Messaoudi's group reported Pd-catalyzed C(sp³)-H arylation of saccharide. Saccharide **1-124**, which possessed picolinic amide as a directing group, reacted with Pd(OAc)₂ to generate Pd(II) intermediate **1-127** through the metalation-deprotonation process. Then the oxidative addition of phenyl iodide **1-125** to **1-127** to produce Pd(IV) intermediate **1-128**. The arylated saccharide **1-126** was obtained via reductive elimination (Scheme 1-25).⁶¹

Scheme 1-25. Pd-catalyzed C(sp³)-H arylation of saccharide.

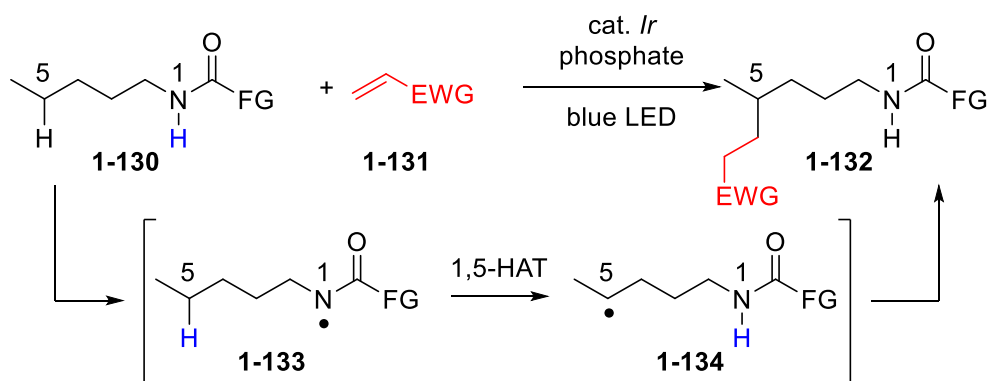


1.4.2 Site-selective Alkylation of C(sp³)-H of Saccharide Through Remote Hydrogen Atom Transfer under Photocatalysis

Transition metal-catalyzed activation of C(sp³)-H bond of saccharides typically requires high reaction temperatures. However, the use of photocatalysts allows for a decrease in reaction temperatures. In 2016, Knowles and Rovis independently reported the N-H bond of amide substrates **1-130** can be oxidized by iridium photocatalyst to generate amidyl radical intermediate **1-133**, which abstracted the hydrogen atom of unactivated C(sp³)-H to generate C radical **1-134** via 1,5-hydrogen atom transfer (1,5-HAT) process. Finally, the nucleophilic C radical reacted with electron-deficient alkene **1-131** to form **1-132** (Scheme 1-26a).⁶² The direct C(sp³)-H alkylation via a remote HAT process provides a new way to achieve regioselective transformation of unactivated C(sp³)-H.⁶³ Later, Rovis's group reported a reaction in which the saccharide derivative **1-135** reacted with electron deficient alkene **1-136** in the presence of an iridium photocatalyst and K₃PO₄ under blue LED irradiation, resulting in the formation of the alkylated product **1-137**.⁶⁴

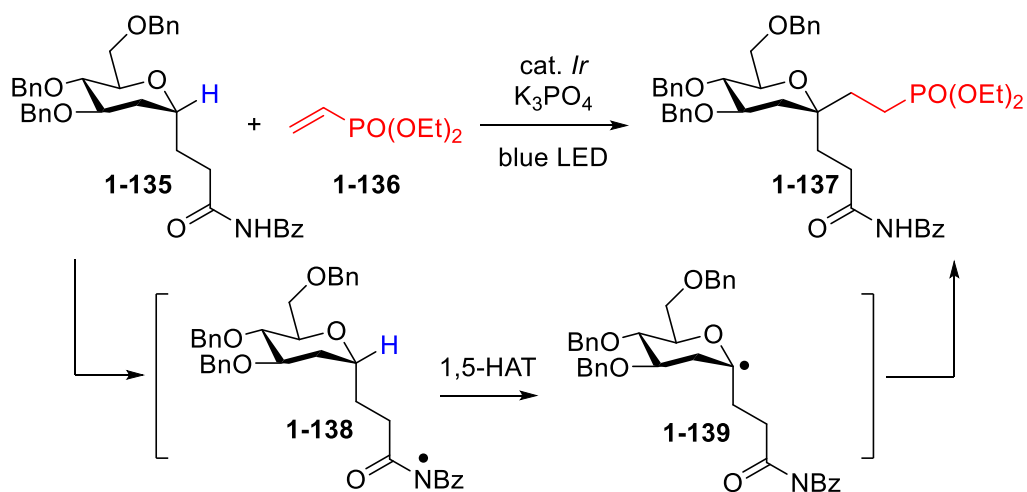
Scheme 1-26. Direct C(sp³)-H alkylation via 1,5-HAT.

a) Knowles/Rovis's work



FG = functional group; EWG = electron-withdrawing group

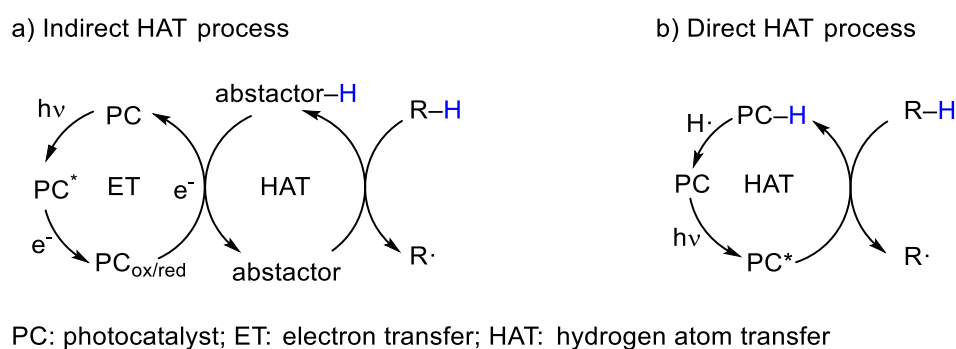
b) Rovis's work



1.4.3 Site-selective Photocatalytic C(sp³)-H Alkylation of Saccharides Controlled by Bond Dissociation Energy

In the indirect HAT process, the photocatalyst is only responsible for electron transfer with the abstractor. Then, the active abstractor abstracts the hydrogen atom from the substrate (R-H). This process requires a photoredox catalyst and HAT catalyst. For example, iridium complex and quinuclidine are photoredox and HAT catalysts, respectively, (Scheme 1-28a). In the case of the direct HAT process, the excited photocatalyst is the abstractor. For example, in Chapter 3, I investigated the C-H alkylation of saccharides using anthraquinone and TBADT photocatalysts via the direct HAT processes (Scheme 1-27).⁶⁵

Scheme 1-27. Indirect and direct HAT processes.

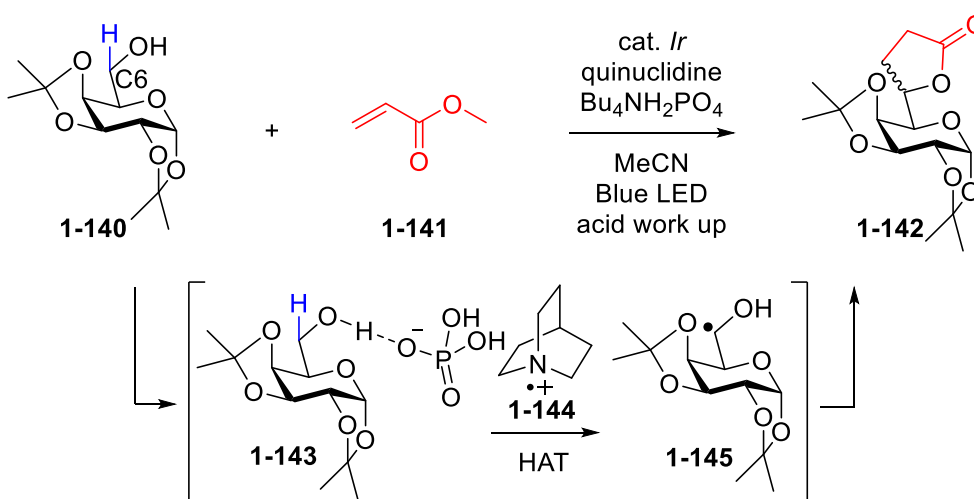


In 2015, MacMillan *et al.* introduced an indirect HAT process for achieving C(sp³)-H alkylation. They utilized an iridium photocatalyst to facilitate electron transfer, which led to the formation of N radical cation **1-144** through interaction with quinuclidine. This radical cation was able to abstract a hydrogen atom from the C6-H bond of saccharide **1-140**. To enhance the activation of the C6-H bond, the presence of a hydrogen bond between tetrabutylammonium dihydrogen phosphate (TBAP) and hydroxy group at C6-position was crucial, and TBAP lowered the C6-H bond dissociation energy (Scheme 1-28a).⁶⁶ Several research groups, including Minnaard, Wang, and Taylor, independently explored diverse applications of the indirect HAT process and successfully realized the alkylation of saccharide derivatives using a similar photocatalyst system coupled with quinuclidine and various cocatalysts, such as TBAP, diarylborinic acid, and diorganotin dihalide.⁶⁷ In Minnaard's work, the C(sp³)-H

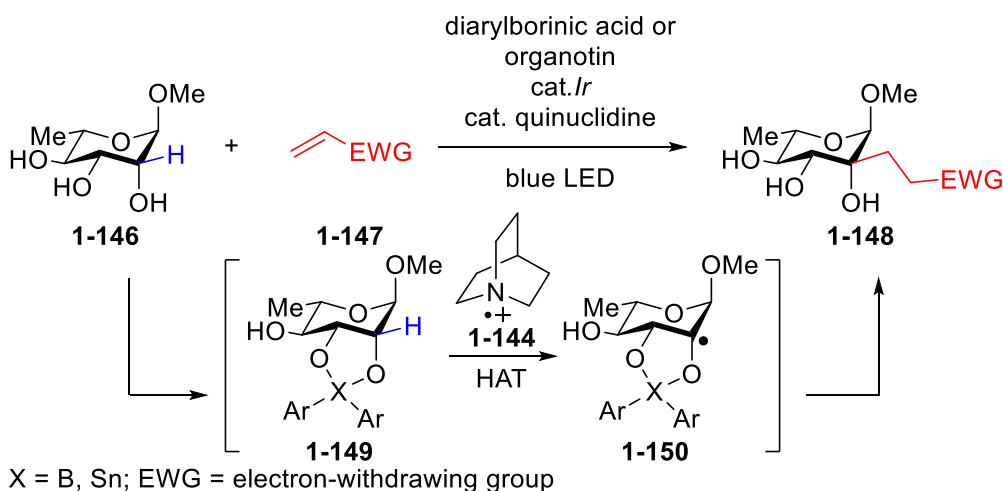
alkylation of less protected saccharides was achieved in the presence of iridium photocatalyst, quinuclidine and TBAP. ^{67a} Taylor's group found that diarylborinic acid (or organotin reagents) and the *cis*-diol of saccharide **1-146** formed intermediate **1-149** with 5-membered ring which affected the bond dissociation energies of C(sp³)–H bonds linked to the *cis*-diol. The quinuclidine generated N radical cation **1-144** to abstract the H atom of the C(sp³)–H bond with smaller bond dissociation energy to generate glycosyl radical **1-150**. And then, this radical reacted with electron-deficient alkene **1-147** to obtain alkylated saccharide product **1-148** (Scheme 1-28).^{67b,c}

Scheme 1-28. C(sp³)–H alkylation of saccharide derivatives via indirect HAT process.

a) C–H alkylation at C6-position by hydrogen bond



b) C–H alkylation by the protection of *cis*-1,2-diol with diarylborinic acid

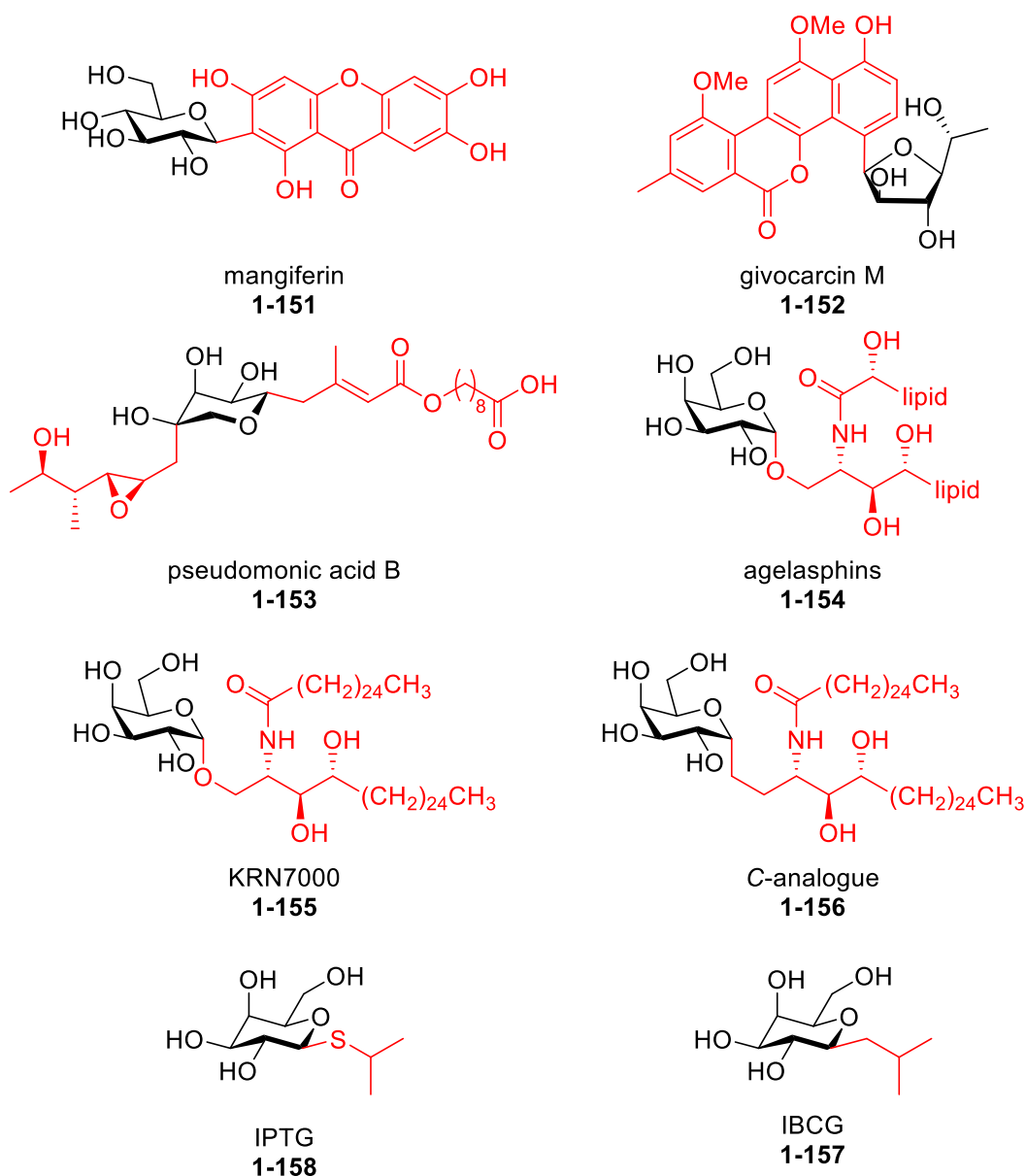


1.5 Importance, Purpose, and Design of This Research

1.5.1 Importance of This Research

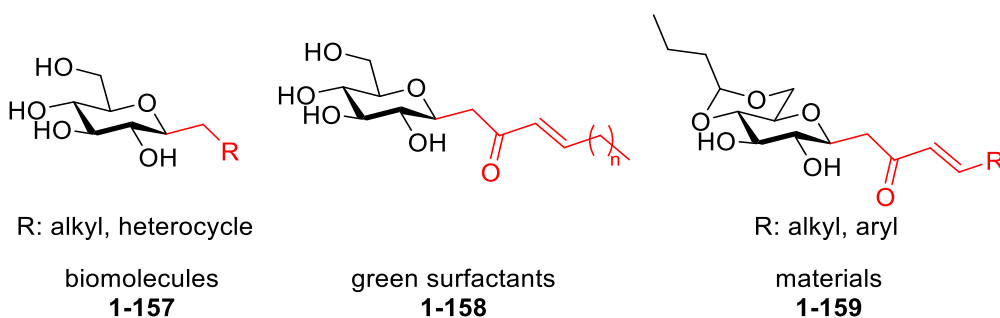
Many modification methods of O–H and C–H bonds of saccharides were introduced in sections 1.2, 1.3, and 1.4. *C*-glycosides and *O*-glycoside were synthesized through these methods. *C*-glycosides are stable for acid, base, and enzymatic hydrolysis than *O*-glycoside. At present, many natural *C*-saccharides have been discovered and investigated, and artificial *C*-saccharides have been invented and applied for drug molecules and biological materials (Scheme 1-29).⁶⁸ Kirin's group demonstrated that agelasphins **1-154** have a potent antitumor activity, and they proved that KRN7000 **1-155** is a slightly simpler analogue of the natural agelasphins and displayed key biological effects.⁶⁹ Franck and Tsuji used KRN7000 **1-155** and its *C*-analogue **1-156** as immunostimulant drugs to perform an experimental model of malaria in mice and *C*-analogue showed excellent activity.⁷⁰ In addition, Pohl's group also reported isobutyl- β -D-galactoside (IBCG) **1-158** can replace isopropyl- β -D-thiogalactopyranoside (IPTG) **1-157** to control gene expression (Scheme 1-29). Moreover, IBCG has long half-life and stable in gene induction system of animals.⁷¹

Scheme 1-29. Several C-saccharides.



Molecules composed of saccharides bearing alkyl and aryl groups can be used in the treatment of neurological diseases (biomolecules **1-157**) and engineering biomaterials (materials **1-159**).⁷² In the case of C-glycosides linking to linear and cyclic alkyl groups, they are used as surfactants **1-158**.⁷³ Carbohydrates are involved in almost all life activities. Hence, glycochemistry is one of the important research areas in biological, material, and organic chemistry (Scheme 1-30).⁷⁴

Scheme 1-30. Saccharides bearing alkyl and aryl groups.

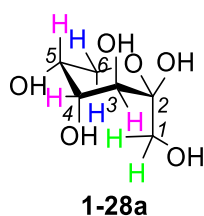


However, saccharides are complex and challenging to purify from natural sources (such as plants, algae, bacteria), which hinders their synthesis, characterization, and the exploration of their biological properties. Therefore, there is a significant need to develop simple and practical synthetic approaches for site-selective modification of saccharides. These methods would not only enable the synthesis of saccharides with novel structures but also facilitate the study of their biological, material, and pharmaceutical properties.

1.5.2 Purpose of This Research

The direct transformation of C(sp³)-H bonds in a substrate using a photocatalyst not only simplifies the experimental steps but also allows the reaction to proceed under mild conditions. Therefore, we investigated selective C(sp³)-H alkylation of saccharides using photocatalysts. Saccharides contain multiple C(sp³)-H bonds with similar reactivities. Taking fructose as an example, C(sp³)-H bonds are present at the C3-, C4-, and C5-positions (Scheme 1-31). The objective of this study is to switch the reaction sites of C(sp³)-H alkylation at these positions by employing different photocatalysts.

Scheme 1-31. The ring configuration of fructose.



1.5.3 Design of This Research

I considered alkylation at C3–H bond using a remote HAT approach. Firstly, HAT moiety was introduced at C1, and the N–H bond of the sulfamate ester was homogeneously cleaved by the iridium photocatalyst and K_3PO_4 to obtain N radical, and then the N radical abstracted the hydrogen atom of $C3(sp^3)$ –H via 1,6-HAT process, to give C3 radical. Subsequently, the C3 radical reacted with an electron-deficient alkene to give an alkyl radical, which was then trapped by a hydrogen atom to give an alkylated product (the detail is described in Chapter 2).

In the section 3.2.1, we calculated the BDEs of C–H bonds of all possible reaction sites of 2,3:4,5-di-*O*-isopropylidene- β -D-fructopyranose to predict the reaction site for the C–H alkylation of saccharides. I screened aromatic ketones with different size as photocatalysts for this reaction. When using anthraquinone as a photocatalyst, the main product was alkylated at the $C4(sp^3)$ –H bond of 2,3:4,5-di-*O*-isopropylidene- β -D-fructopyranose. For the higher BDE of $C5(sp^3)$ –H, its steric hindrance is the lowest compared to the C3- and C4- positions. When using bulky TBADT as a photocatalyst, the alkylation proceeded at $C5(sp^3)$ –H bond of 2,3:4,5-di-*O*-isopropylidene- β -D-fructopyranose (the detail is described in Chapter 3).

Based on these three catalytic methods, the site-selective alkylation of other saccharide derivatives was explored.

1.6 References

1. (a) Varki, A. *Glycobiology* **1993**, *3*, 97–130. (b) Regassa, T. H.; Wortmann, C. S. *Biomass Bioenergy* **2014**, *64*, 348–355.
2. (a) Fischer, E. *Berichte der Deutschen Chemischen Gesellschaft* **1901**, *34*, 2249–2262. (b) Pauling, L. *J. Chem. Phys.* **1945**, *13*, 766–771. (c) Presper, J. H.; Axel, R. *Chem. Rev.* **1984**, *84*, 323–362.
3. (a) Rudd, P. M.; Elliott, T.; Cresswell, P.; Wilson, I. A.; Dwek, R. A. *Science* **2001**, *291*, 2370–2376. (b) Atsumi, S.; Hanai, T.; Liao, J. C. *Nature* **2008**, *451*, 86–89. (c) Guo, Z.; Boons, G. J. Carbohydrate-based vaccines and immunotherapies; John Wiley & Sons: Hoboken, NJ, **2009**. (d) Miura, Y.; Hoshino, Y.; Seto, H. *Chem. Rev.* **2016**, *116*, 1673–1692. (e) Tiwari, V. K.; Mishra, B. B.; Mishra, K. B.; Mishra, N.; Singh, A. S.; Chen, X. *Chem. Rev.* **2016**, *116*, 3086–3240.
4. Maryanoff, B. E.; Nortey, S. O.; Gardocki, J. F.; Shank, R. P.; Dodgson, S. P. *J. Med. Chem.* **1987**, *30*, 880–887.
5. Ghosh, S. Sialic acids and sialoglycoconjugates in the biology of life, health and disease; Academic Press: Cambridge, MA, USA, **2020**.
6. Lehninger, A. L.; Nelson, D. L.; Cox, M. M. Principles of Biochemistry; W. H. Freeman and Company: New York, **2017**.
7. (a) Fischer, E. *Ber. Dtsch. Chem. Ges.* **1901**, *34*, 2249–2262. (b) Dam, T. K.; Brewer, C. F. Carbohydrates (Saccharides). In *Comprehensive Glycoscience*; Elsevier: Oxford, UK, **2007**, pp 1–38.
8. Bertozzi, C. R.; Kiessling, L. L. *Science* **2001**, *291*, 2357–2364.
9. (a) Cárdenas, D. J. *Angew. Chem., Int. Ed.* **2003**, *42*, 384–387. (b) Choi, J. Fu, G. C. *Science* **2017**, *356*, eaaf7230. (c) Kranthikumar, R. *Organometallics* **2022**, *41*, 667–679.
10. Wurtz, Ann. *Chem. Pharm.* **1855**, *96*, 364–375.
11. K. A. Keaton and A. J. Phillips, *Org. Lett.* **2007**, *9*, 2717–2719.
12. Plunkett, S.; Basch, C. H.; Santana, S. O.; Watson, M. P. *J. Am. Chem. Soc.* **2019**, *141*, 2257–2262.
13. Iwasaki, T.; Imanishi, R.; Shimizu, R.; Kuniyasu, H.; Terao, J.; Kambe, N. *J. Org. Chem.* **2014**, *79*, 8522–8532.
14. (a) Girard, S. A.; Knauber, T.; Li, C. J. *Angew. Chem. Int. Ed.* **2014**, *53*, 74–100. (b) Chu, J. C.; Rovis, T. *Angew. Chem. Int. Ed.* **2018**, *57*, 62–101

15. (a) Díaz-Requejo, M. M.; Belderraín, T. R.; Nicasio, M. C.; Trofimenko, S.; Pérez, P. J. *J. Am. Chem. Soc.* **2002**, *124*, 896–897. (b) Davies, H. M.; Manning, J. R. *Nature* **2008**, *451*, 417–424. (c) McLarney, B. D. Hanna, S.; Musaev D. G.; France, S. *ACS Catal.* **2019**, *9*, 4526–4538.
16. (a) He, J.; Wasa, M.; Chan, K. S. L.; Shao, Q.; Yu, J.-Q. *Chem. Rev.* **2017**, *117*, 8754–8786.
17. (a) McNally, A.; Prier, C. K.; MacMillan, D. W. *Science* **2011**, *334*, 1114–1117. (b) Holmberg-Douglas, N.; Nicewicz, D. A. *Chem. Rev.* **2021**, *122*, 1925–2016.
18. (a) Zhu, Y.; van der Donk, W. A. *Org. Lett.* **2001**, *3*, 1189–1192. (b) Macmillan, D.; Daines, A. M.; Bayrhuber, M.; Flitsch, S. L. *Org. Lett.* **2002**, *4*, 1467–1470.
19. Chao, E. C.; Henry, R. R. *Nat. Rev. Drug Discovery* **2010**, *9*, 551–559.
20. (a) Andrews, R. S.; Becker, J. J.; Gagné, M. R. *Angew. Chem. Int. Ed.* **2010**, *49*, 7474–7276. (b) Chen, D.; Chen, R.; Wang, R.; Li, J.; Xie, K.; Bian, C.; Dai, J. *Angew. Chem. Int. Ed.* **2015**, *54*, 12678–12682. (c) Yang, Y.; Yu, B. *Chem. Rev.* **2017**, *117*, 12281–12356. (d) Zhu, F.; Rodriguez, J.; Yang, T.; Kevlishvili, I.; Miller, E.; Yi, D.; Walczak, M. A. *J. Am. Chem. Soc.* **2017**, *139*, 17908–17922.
21. (a) Fosso, M. Y.; Nziko, V. P.; Chang, C. W. T. *J. Carbohydr. Chem.* **2012**, *31*, 603–619. (b) Sangwan, R.; Khanam, A.; Mandal, P. K. *Eur. J. Org. Chem.* **2020**, *37*, 5949–5977.
22. (a) Wulff, G.; Röhle, G. *Angew. Chem. Int. Ed.* **1974**, *13*, 157–216. (b) Nicolaou, K. C.; Seitz, S. P.; Papahatjis, D. P. *J. Am. Chem. Soc.* **1983**, *105*, 2430–2434. (c) Hanessian, S.; Lou, B. *Chem. Rev.* **2000**, *100*, 4443–4464. (d) Sherry, B. D.; Loy, R. N.; Toste, F. D. *J. Am. Chem. Soc.* **2004**, *126*, 4510–4511. (e) Hu, Y.; Yu, K.; Shi, L. L.; Liu, L.; Sui, J. J.; Liu, D. Y.; Sun, J. S. *J. Am. Chem. Soc.* **2017**, *139*, 12736–12744.
23. Pachamuthu, K.; Schmidt, R. R. *Chem. Rev.* **2006**, *106*, 160–187.
24. Osborn, H. M.; I.; Harwood, L. M. *In Best Synthetic Methods: Carbohydrates*; Academic Press: San Diego, CA, 2003.
25. (a) Ko, K.-S.; Kruse, J.; Pohl, N. L. *Org. Lett.* **2003**, *5*, 1781–1783. (b) Marca, E.; Valero-Gonzalez, J.; Delso, I.; Tejero, T.; Hurtado-Guerrero, R.; Merino, P. *Carbohydr. Res.* **2013**, *382*, 9–18.
26. Tropper, F. D.; Andersson, F. O.; Braun, S.; Roy, S. *Synthesis* **1992**, 618–620
27. Maunier, V.; Boullanger, P.; Lafont, D.; *J. Carbohydr. Chem.* **1997**, *16*, 231–235.

28. Koenigs, W.; Knorr, E. *Ber. Dtsch. Chem. Ges.* **1901**, *34*, 957–981.
29. Schmidt, R. R.; Michel, J. *Angew. Chem. Int. Ed.* **1980**, *19*, 731–732.
30. Li, Y.; Yang, Y.; Yu, B. *Tetrahedron Lett.* **2008**, *49*, 3604–3608.
31. Hanessian S.; Banoub, J. *Carbohydr. Res.* **1977**, *53*, C13–C16.
32. (a) Horton, D.; Wander, J. D. *Carbohydrates: Chemistry and Biochemistry*; Academic Press: New York, **1990**. (b) Witczak, Z. J.; Chhabra, R.; Chen, H.; Xie, X.-Q. *Carbohydr. Res.* **1997**, *301*, 167–175.
33. (a) Lote, C. J.; Weiss, J. B. *FEBS Lett.* **1971**, *16*, 81–85. (b) Lote, C. J.; Weiss, J. B. *Biochem. J.* **1971**, *123*, 25P. (c) Weiss, J. B.; Lote, C. J.; Bobinski, H. *Nature New Biol.* **1971**, *234*, 25–26.
34. Zhu, X.; Pachamuthu, K.; Schmidt, R. R. *J. Org. Chem.* **2003**, *68*, 5641–5651.
35. (a) Nicewicz, D. A.; MacMillan, D. W. C. *Science* **2008**, *322*, 77–80. (b) Nguyen, J. D.; D'Amato, E. M.; Narayanam, J. M. R.; Stephenson, C. R. J. *Nat. Chem.* **2012**, *4*, 854–859. (c) Chu, J. C. K.; Rovis, T. *Nature* **2016**, *539*, 272–275.
36. Sangwan, R.; Mandal, P. K. *RSC Adv.* **2017**, *7*, 26256–26321.
37. (a) Mao, R.-Z.; Guo, F.; Xiong, D.-C.; Li, Q.; Duan, J.; Ye, X.-S. *Org. Lett.* **2015**, *17*, 5606–5609. (b) Mao, R.-Z.; Xiong, D.-C.; Guo, F.; Li, Q.; Duan, J.; Ye, X.-S. *Org. Chem. Front.* **2016**, *3*, 737–743.
38. (a) Wever, W. J.; Cinelli, M. A.; Bowers, A. A. *Org. Lett.* **2013**, *15*, 30–33. (b) Yu, Y.; Xiong, D.-C.; Mao, R.-Z.; Ye, X.-S. *J. Org. Chem.* **2016**, *81*, 7134–7138.
39. (a) Andrews, R. S.; Becker, J. J.; Gagné, M. R. *Angew. Chem. Int. Ed.* **2010**, *122*, 7432–7434. (b) Andrews, R. S.; Becker, J. J.; Gagné, M. R. *Angew. Chem. Int. Ed.* **2012**, *124*, 4216–4219.
40. Dumoulin, A.; Matsui, J. K.; Gutiérrez-Bonet, Á.; Molander, G. A. *Angew. Chem. Int. Ed.* **2018**, *130*, 6724–6728.
41. Dimakos, V.; Taylor, M. S. *Chem. Rev.* **2018**, *118*, 11457–11517.
42. Chaudhary, S. K.; Hernandez, O. *Tetrahedron Lett.* **1979**, *20*, 95–98.
43. Rana, S. S.; Piskorz, C. F.; Barlow, J. J.; Matta, K. L. *Carbohydr. Res.* **1980**, *83*, 170–174.
44. Flowers, H. M. *Carbohydr. Res.* **1975**, *39*, 245–251.
45. (a) Tsuda, Y.; Haque, M. E.; Yoshimoto, K. *Chem. Pharm. Bull.* **1983**, *31*, 1612–1624. (b) Haque, M. E.; Kiuchi, T.; Yoshimoto, K.; Tsuda, Y. *Chem. Pharm. Bull.* **1985**,

33, 2243–2255. (c) Helm, R. F.; Ralph, J.; Anderson, L. *J. Org. Chem.* **1991**, *56*, 7015–7021. (d) Muramatsu, W.; Tanigawa, S.; Takemoto, Y.; Yoshimatsu, H.; Onomura, O. *Chem. Eur. J.* **2012**, *18*, 4850–4853. (e) Muramatsu, W. *J. Org. Chem.* **2012**, *77*, 8083–8091. (f) Zhou, Y.; Li, J.; Zhan, Y.; Pei, Z.; Dong, H. *Tetrahedron* **2013**, *69*, 2693–2700. (g) Giordano, M.; Iadonisi, A. *J. Org. Chem.* **2014**, *79*, 213–222. (h) Xu, H.; Lu, Y.; Zhou, Y.; Ren, B.; Pei, Y.; Dong, H.; Pei, Z. *Adv. Synth. Catal.* **2014**, *356*, 1735–1740.

46. (a) Wang, H.; She, J.; Zhang, L. H.; Ye, X. S. *J. Org. Chem.* **2004**, *69*, 5774–5777. (b) Yang, Q.; Lei, M.; Yin, Q. J.; Yang, J. S. *Carbohydr. Res.* **2007**, *342*, 1175–1181.

47. (a) Matsumura, Y.; Maki, T.; Murakami, S.; Onomura, O. *J. Am. Chem. Soc.* **2003**, *125*, 2052–2053. (b) Evtushenko, E. V. *Carbohydr. Res.* **2012**, *359*, 111–119. (c) Allen, C. L.; Miller, S. J. *Org. Lett.* **2013**, *15*, 6178–6181.

48. (a) Gangadharmath, U. B.; Demchenko, A. V. *Synlett.* **2004**, 2191–2193. (b) Evtushenko, E. V. *Synth. Commun.* **2006**, *36*, 1593–1599. (c) Evtushenko, E. V. *J. Carbohydr. Chem.* **2010**, *29*, 369–378. (d) Bourdreux, Y.; Lemetais, A.; Urban, D.; Beau, J. M. *Chem. Commun.* **2011**, *47*, 2146–2148. (e) Kuriyama, M.; Takeichi, T.; Ito, M.; Yamasaki, N.; Yamamura, R.; Demizu, Y.; Onomura, O. *Chem. Eur. J.* **2012**, *18*, 2477–2480.

49. Nashed, M. A. *Carbohydr. Res.* **1978**, *60*, 200–205

50. Cheon, H. S.; Lian, Y.; Kishi, Y. *Org. Lett.* **2007**, *9*, 3323–3326.

51. Joe, M.; Bai, Y.; Nacario, R. C.; Lowary, T. L. *J. Am. Chem. Soc.* **2007**, *129*, 9885–9901.

52. Renaudet, O.; Dumy, P. *Tetrahedron* **2002**, *58*, 2127–2135.

53. (a) Liu, X.-C.; Dordick, J. S. *J. Am. Chem. Soc.* **1999**, *121*, 466–467. (b) Peri, F.; Jimenez-Barbero, J.; Garcia-Aparicio, V.; Tvaroska, I.; Nicotra, F. *Chem. Eur. J.* **2004**, *10*, 1433–1444. (c) Blasdel, L. K.; Myers, A. G. *Org. Lett.* **2005**, *7*, 4281–4283.

54. (a) Davis, N. J.; Flitsch, S. L.; *Tetrahedron Lett.* **1993**, *34*, 1181–1184. (b) Angelin, M.; Hermansson, M.; Dong, H.; Ramström, O. *Eur. J. Org. Chem.* **2006**, *19*, 4323–4326.

55. (a) Avigad, G.; Amaral, D.; Asensio, C.; Horecker, B. L. *J. Biol. Chem.* **1962**, *237*, 2736–2743. (b) Toone, E. J.; Simon, E. S.; Whitesides, G. M. *J. Org. Chem.* **1991**, *56*, 5603–5606.

56. Waki, M.; Muratsugu, S.; Tada, M. *Chem. Commun.* **2013**, *49*, 7283–7285.

57. (a) Tsuda, Y.; Hanajima, M.; Matsuhira, N.; Okuno, Y.; Kanemitsu, K. *Chem. Pharm. Bull.* **1989**, *37*, 2344–2350. (b) Liu, H.-M.; Sato, Y.; Tsuda, Y. *Chem. Pharm. Bull.* **1993**, *41*, 491–501. (c) Muramatsu, W. *Org. Lett.* **2014**, *16*, 4846–4849.
58. (a) Jäger, M.; Hartmann, M.; de Vries, J. G.; Minnaard, A. J. *Angew. Chem. Int. Ed.* **2013**, *52*, 7809–7812. (b) Chung, K.; Waymouth, R. M. *ACS Catal.* **2016**, *6*, 4653–4659.
59. Freimund, S.; Huwig, A.; Giffhorn, F.; Kçpper, F. *Chem. Eur. J.* **1998**, *4*, 2442–2455.
60. (a) Dimakos, V.; Gorelik, D.; Su, H. Y.; Garrett, G. E.; Hughes, G.; Shibayama, H.; Taylor, M. S. *Chem. Sci.* **2020**, *11*, 1531–1537; (b) Gorelik, D. J.; Dimakos, V.; Adrianov, T.; Taylor, M. S. *Chem. Commun.* **2021**, *57*, 12135–12138.
61. (a) Probst, N.; Grelier, G.; Ghermani, N.; Gandon, V.; Alami, M.; Messaoudi, S. *Org. Lett.* **2017**, *19*, 5038–5041. (b) Probst, N.; Grelier, G.; Dahaoui, S.; Alami, M.; Gandon, V.; Messaoudi, S. *ACS Catal.* **2018**, *8*, 7781–7786. (c) Ghouilem, J.; Tran, C.; Grimblat, N.; Retailleau, P.; Alami, M.; Gandon, V.; Messaoudi, S. *ACS Catal.* **2021**, *11*, 1818–1826.
62. (a) Choi, G. J.; Zhu, Q.; Miller, D. C.; Gu, C. J.; Knowles, R. R. *Nature* **2016**, *539*, 268–271. (b) Chu, J. C. K.; Rovis, T. *Nature* **2016**, *539*, 272–275.
63. Several reports of regioselective transformation of unactivated C(sp³)-H via remote HAT: (a) Liang, W.; Jiang, K.; Du, F.; Yang, J.; Shuai, L.; Ouyang, Q.; Wei, Y. *Angew. Chem. Int. Ed.* **2020**, *59*, 19222–19228. (b) Nobile, E.; Castanheiro, T.; Besset, T. *Angew. Chem. Int. Ed.* **2021**, *133*, 12278–12299. (c) Yue, W. J.; Day, C. S.; Martin, R. *J. Am. Chem. Soc.* **2021**, *143*, 6395–6400. (d) Li, N.; Li, J.; Qin, M.; Li, J.; Han, J.; Zhu, C.; Xie, J. *Nat. Commun.* **2022**, *13*, 4224. (e) Sarkar, S.; Wagulde, S.; Jia, X.; Gevorgyan, V. *Chem.* **2022**, *8*, 3096–3108. (f) Simons, R. T.; Nandakumar, M.; Kwon, K.; Ayer, S. K.; Venneti, N. M.; Roizen, J. L. *J. Am. Chem. Soc.* **2023**, *145*, 3882–3890. (g) a review: Guo, W.; Wang, Q.; Zhu, J. *Chem. Soc. Rev.* **2021**, *50*, 7359–7377.
64. Chen, D.; Chu, J. C. K.; Rovis, T. *J. Am. Chem. Soc.* **2017**, *139*, 14897–14900.
65. Capaldo, L.; Ravelli, D.; Fagnoni, M. *Chem. Rev.* **2021**, *122*, 1875–1924.
66. Jeffrey, J. L.; Terrett, J. A.; MacMillan, D. W. *Science* **2015**, *349*, 1532–1536.
67. (a) Wan, I. C. S.; Witte, M. D.; Minnaard, A. J. *Chem. Commun.* **2017**, *53*, 4926–4929 (b) Dimakos, V.; Su, H. Y.; Garrett, G. E.; Taylor, M. S. *J. Am. Chem. Soc.* **2019**, *141*, 5149–5153. (c) Gorelik, D. J.; Turner, J. A.; Virk, T. S.; Foucher, D. A.; Taylor, M. S. *Org. Lett.* **2021**, *23*, 5180–5185. (d) Mouthaan, M. L.; Pouwer, K.; Borst, M. L.;

Witte, M. D.; Minnaard, A. J. *Synthesis* **2022**, *54*, 4683–4689 (e) Cao, H.; Guo, T.; Deng, X.; Huo, X.; Tang, S.; Liu, J.; Wang, X. *Chem. Commun.* **2022**, *58*, 9934–9937 (f) Guo, T.; Yan, X.; Cao, H.; Lu, L.; Gao, L.; Tang, S.; Liu, J.; Wang, X. *ChemRxiv* **2022**, DOI: 10.26434/chemrxiv-2022-s2p4k.

68. (a) Yang, Y.; Yu, B. *Chem. Rev.* **2017**, *117*, 12281–12356. (b) Kitamura, K.; Ando, Y.; Matsumoto, T.; Suzuki, K. *Chem. Rev.* **2018**, *118*, 1495–1598. Shatskiy, A.; Stepanova, E. V.; Kärkäs, M. D. *Nat. Rev. Chem.* **2022**, *6*, 782–805.

69. (a) Natori, T.; Morita, M.; Akimoto, K.; Koezuka, Y. *Tetrahedron* **1994**, *50*, 2771–2784. (b) Nakagawa, R.; Motoki, K.; Ueno, H.; Iijima, H.; Nakamura, H.; Kobayashi, E.; Shimosaka, A.; Koezuka, Y. *Cancer Res.* **1998**, *58*, 1202–1207. (c) Kakimi, K.; Guidotti, L. G.; Koezuka, Y.; Chisari, F. V. *J. Exp. Med.* **2000**, *192*, 921–930. (d) Hong, S.; Wilson, M. T.; Serizawa, I.; Wu, L.; Singh, N.; Naidenko, O. V.; Miura, T.; Haba, T.; Scherer, D. C.; Wei, J.; Kronenberg, M.; Koezuka, Y.; Van Kaer, L. *Nat. Med.* **2001**, *7*, 1052–1056. (e) Miyamoto, K.; Miyake, S.; Yamamura, T. *Nature* **2001**, *413*, 531–534. (f) Kikuchi, A.; Nieda, M.; Schmidt, C.; Koezuka, Y.; Ishihara, S.; Ishikawa, Y.; Tadokoro, K.; Durrant, S.; Boyd, A.; Juji, T.; Nicol, A. *Br. J. Cancer* **2001**, *85*, 741–746. (g) Matsumoto, G.; Nagai, S.; Toi, M.; Ishiyama, S.; Kuroi, K.; Turuta, K.; Okamoto, A.; Takahashi, T. *Nippon Geka Gakkai Zasshi* **2001**, *102*, 421–421. (h) Hayakawa, Y.; Rovero, S.; Forni, G.; Smyth, M. J. *Proc. Natl. Acad. Sci. USA* **2003**, *100*, 9464–469. (i) Costantino, V.; Fattorusso, E.; Imperatore, C.; Mangoni, A. *J. Org. Chem.* **2004**, *69*, 1174–1179.

70. (a) Yang, G.; Schmieg, J.; Tsuji, M.; Franck, R. W. *Angew. Chem. Int. Ed.* **2004**, *43*, 3818–3822. (b) Franck, R. W.; Tsuji, M. *Acc. Chem. Res.* **2006**, *39*, 692–701.

71. (a) Riggs, A. D.; Suzuki, H.; Bourgeois, S. *J. Mol. Biol.* **1970**, *48*, 67–83. (b) Bell, C. E.; Lewis, M. *Curr. Opin. Struct. Biol.* **2001**, *11*, 19–25. (c) Liu, L.; Abdel Motaal, B.; Schmidt-Supprian, M.; Pohl, N. L. *J. Org. Chem.* **2012**, *77*, 1539–1546.

72. (a) Russell, T. P. *Science* **2002**, *297*, 964–967. (b) Zhang, S. *Nat. Biotechnol.* **2003**, *21*, 1171–1178. (c) Percec, V.; Dulcey, A. E.; Balagurusamy, V. S. K.; Miura, Y.; Smidrkal, J.; Peterca, M.; Nummelin, S.; Edlund, U.; Hudson, S. D.; Heiney, P. A.; Duan, H.; Maganov, S. N.; Vinogradov, S. A. *Nature* **2004**, *430*, 764–768. (d) Gao, X. Y.; Matsui, H. *Adv. Mater.* **2005**, *17*, 2037–2050. (e) Nagarajan, S.; Shanmugam, M. J.;

Das, T. M. *Carbohydr. Res.* **2011**, *346*, 722–727. (f) Balachandran, V. S.; Jadhav, S. R.; Vemula, P. K.; John, G. *Chem. Soc. Rev.* **2013**, *42*, 427–438.

73. (a) Griffin, W. C. *J. Soc. Cosmet. Chem.* **1949**, *1*, 311–326. (b) Ranoux, A.; Lemiegre, L.; Benoit, M.; Gueganand, J. P.; Benvegna, T. *Eur. J. Org. Chem.* **2010**, *7*, 1314–1323. (c) Foley, P. M.; Phimpachanh, A.; Beach, E. S.; Zimmerman, J. B.; Anastas, P. T. *Green Chem.* **2011**, *13*, 321–325.

74. Lalitha, K.; Muthusamy, K.; Prasad, Y. S.; Vemula, P. K.; Nagarajan, S. *Carbohydr. Res.* **2015**, *402*, 158–171.

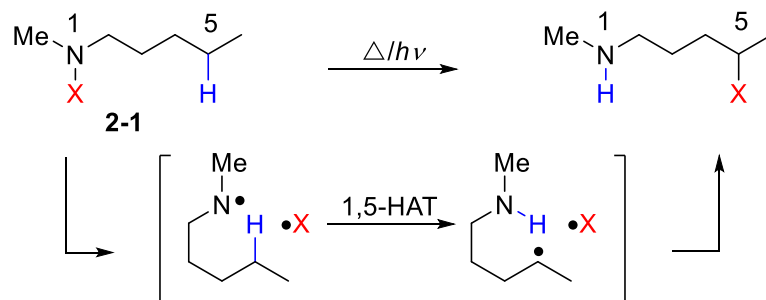
Chapter 2. Site-selective C(sp³)-H Alkylation of a Fructopyranose Derivative by 1,6-HAT

2.1 Introduction

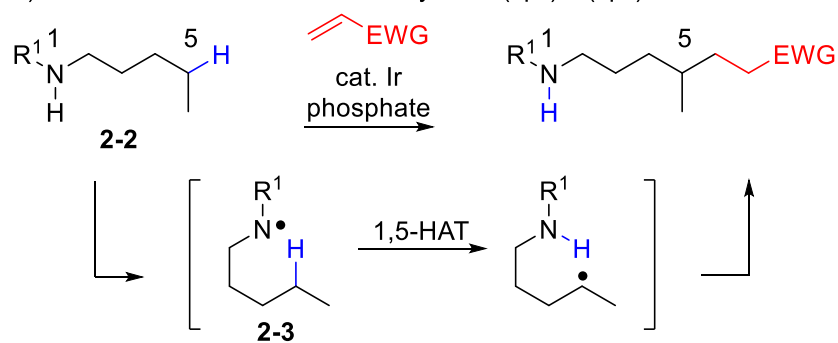
The Hofmann-Löffler-Freytag reaction was discovered in 1882, which involves the light- or heat-induced homolysis of nitrogen-halogen (N-X) bond of the amine **2-1** to form a N radical. The N radical then undergoes 1,5-hydrogen atom transfer (HAT) through a six-membered transition state to generate a carbon-centered radical, which combines with the halogen (X) radical to form a carbon-halogen (C-X) bond (Scheme 2-1a).¹ Because the bond dissociation energy (BDE) of the nitrogen-hydrogen (N-H) bond in amide groups (BDE = 107–110 kcal/mol)² is higher than that of the carbon-hydrogen (C-H) bond in alkanes (BDE = 88–100 kcal/mol),³ the generation of the C radical proceeds easily. In Hofmann-Löffler-Freytag reaction, a C-X bond is ultimately formed. To generate a new carbon-carbon (C-C) bond, it is necessary to replace the N-X bond with N-H bond, allowing for the avoidance of introducing a halogen radical. Recently, Knowles and Rovis *et al.* discovered that iridium catalysts could cleave the N-H bond of amide **2-2** in the presence of a phosphate. Then, the generated N radical reacted with electron-deficient alkenes as alkylation reagents to construct a C(sp³)-C(sp³) bond (Scheme 2-1b).⁴ Roizen *et al.* followed the reaction and performed regioselective C(sp³)-H alkylation of **2-4** to abstract the H atom via 1,6-HAT (Scheme 2-1c). They considered that the 1,6-HAT process formed a 7-membered ring, due to the smaller O-S-N bond angle in the transition state **2-5** (Scheme 2-1c) compared to the C-C-N bond angle in the 6-membered ring transition state **2-3** (Schemes 2-1a and b). The N radical and the C-H bond were linearly aligned, bringing the N radical in close proximity to the H atom. This linear arrangement facilitated geometrically favorable interaction, allowing the N radical to abstract the H atom from the C-H bond.⁵

Scheme 2-1. Site-selective C(sp³)-H transformations via 1,5- or 1,6-HAT.

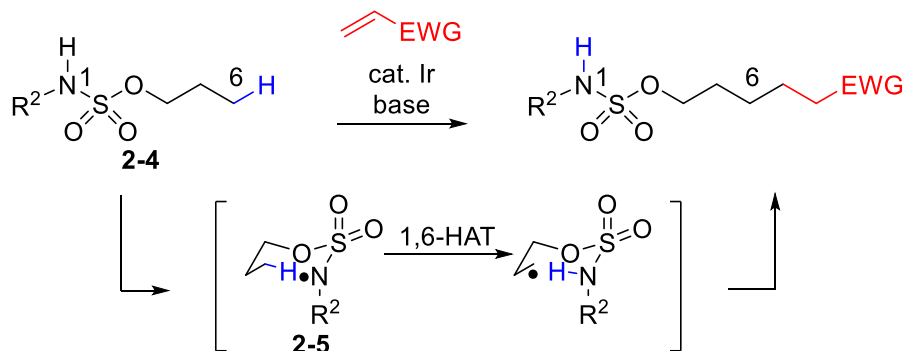
a) Hofmann-Löfer-Freytag reaction



b) Knowles and Rovis : Photocatalyzed C(sp³)-C(sp³) bond formation via 1,5-HAT

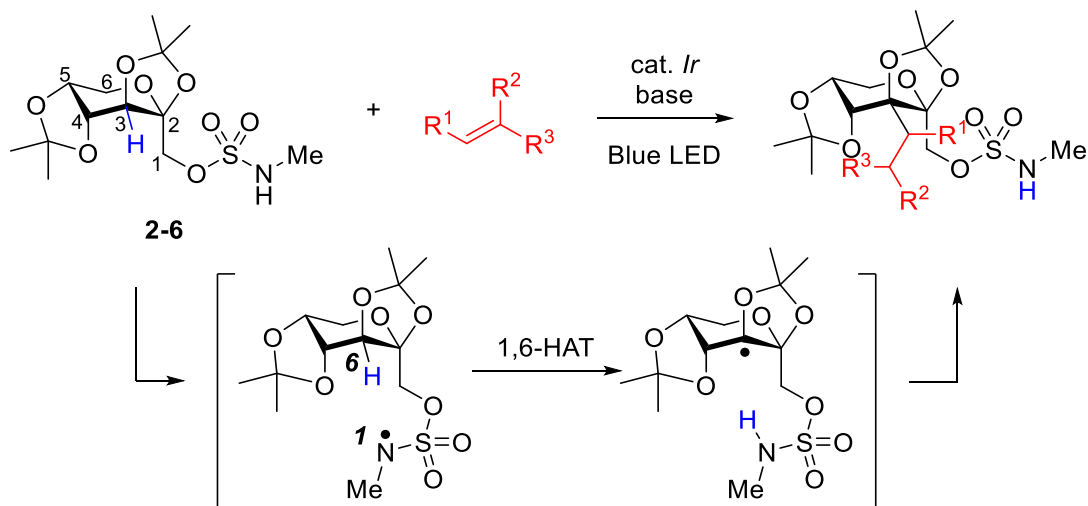


c) Roizen : Photocatalyzed C(sp³)-C(sp³) bond formation via 1,6-HAT



In this chapter, 2,3:4,5-bis-*O*-(1-ethylethylidene)- β -D-fructopyranose methyl sulfamate **2-6a** was used as a model substrate to investigate C3(sp³)-H alkylation via 1,6-HAT using iridium photocatalyst under blue LED irradiation (Scheme 2-2).⁶

Scheme 2-2. This work: site-selective C(sp³)-H alkylation of **2-6a** by 1,6-HAT.



2.2 Results and Discussion

2.2.1 Optimization of Reaction Conditions

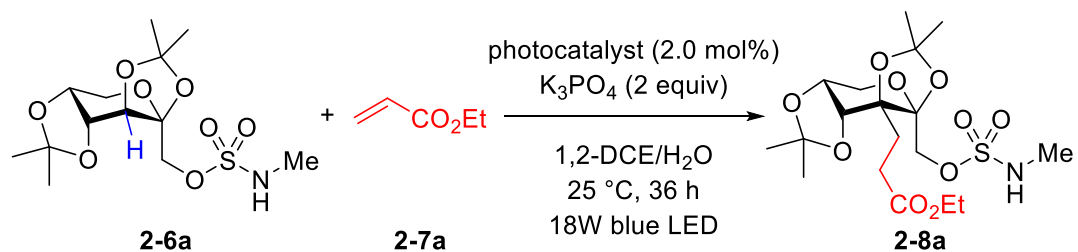
1) Screening of Photocatalysts

Photocatalysts **2-P1–P8** were screened in the reaction, and the results are summarized in Table 2-1. When **2-P1** ($[\text{Ir}\{\text{dF}(\text{CF}_3)\text{ppy}\}_2(\text{bpy})]\text{PF}_6$) was used as the photocatalyst (entry 1), the yield of C–H alkylated product **2-8a** was 32%. The yield was slightly improved to 34% when using **2-P2** ($[\text{Ir}\{\text{dF}(\text{CF}_3)\text{ppy}\}_2(\text{dtbpy})]\text{PF}_6$) as the photocatalyst (entry 2). However, **2-P3** ($[\text{Ir}\{\text{dF}(\text{CF}_3)\text{ppy}\}_2(\text{phen})]\text{PF}_6$), **2-P4** ($[\text{Ir}\{\text{dF}(\text{CH}_3)\text{ppy}\}_2(\text{dtbpy})]\text{PF}_6$), and **2-P5** ($[\text{Ir}\{\text{dF}(\text{CH}_3)\text{ppy}\}_2(\text{dtbpy})]\text{PF}_6$) did not significantly change the yield of **2-8a** (entries 3–5). Overall, the use of **2-P1** to **2-P5** as photocatalysts resulted in the formation of desired product **2-8a**. On the other hand, **2-P6** ($[\text{Ir}\{\text{dF}(\text{CH}_3)\text{ppy}\}_2(5,5'\text{-dCF}_3\text{bpy})]\text{PF}_6$) and **2-P7** ($[\text{Ir}\{\text{dF}(\text{CF}_3)\text{ppy}\}_2(5,5'\text{-dCF}_3\text{bpy})]\text{PF}_6$) dramatically decreased the yields of **2-8a** to 11% and 3% respectively (entries 6, 7). The formation of **2-8a** was not observed using **2-P8** ($\text{Ru}(\text{phen})_3\text{Cl}_2$) as the photocatalyst (entry 8).

Subsequently, the requirement of photocatalysts was considered. The following two conditions are required to promote the reaction between the excited photocatalyst and **2-6a**: (1) the generation of a sufficient amount of excited photocatalyst, and (2) the electron transfer between the excited photocatalyst and the aminosulfonyl group of **2-6a**. Regarding condition (1), the wavelength of the light source used in the experiments should be important for the efficient photocatalyst cycle. In this study, the light source wavelength ranged from 450 to 455 nm, which is close to the maximum absorption wavelengths of the used photocatalysts **2-P1–P8**. Regarding condition (2), the redox potential of the excited photocatalyst need to be higher than the redox potential of the sulfamate ester **2-6a**. According to the report by the Duan group, the oxidation peak potential of the sulfamate ester is over +2 V (vs. saturated calomel electrode, 0.05 M in DMF). When KO^tBu was added to the solution, the peak potential shifted to +1.16 V.⁷ The redox potentials of the reported photocatalysts are as follows: 1) **2-P2**: $E_{1/2}^{\text{red}}[*\text{Ir}(\text{III})/\text{Ir}(\text{II})] = +1.21 \text{ V}$, $\lambda_{\text{max}} = 470 \text{ nm}$ (entry 2),⁸ 2) **2-P8**²⁺: $E_{1/2}^{\text{red}}[*\text{Ru}(\text{II})/\text{Ru}(\text{I})] = +0.82 \text{ V}$, $\lambda_{\text{max}} = 442 \text{ nm}$ (entry 8).⁹ Therefore, iridium catalyst can oxidize the anion of substrate. Since the redox potential of the excited state of **2-P8** is lower than the redox potential of sulfamate ester (+1.16 V), the reaction did not occur using **2-P8** as

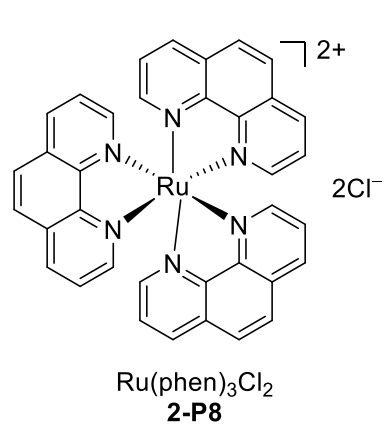
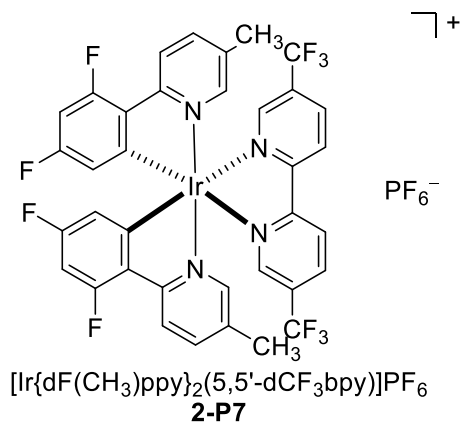
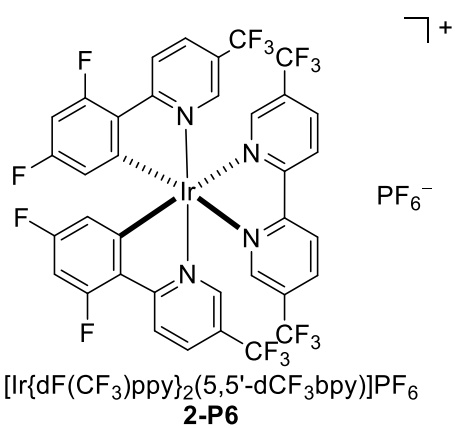
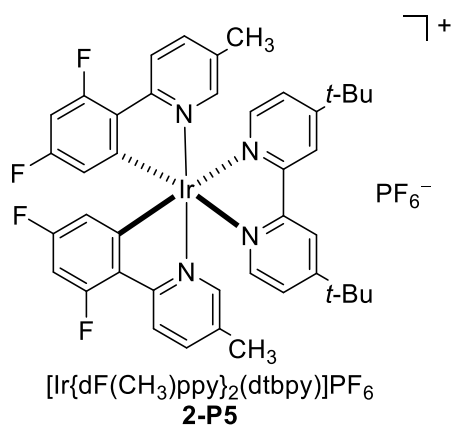
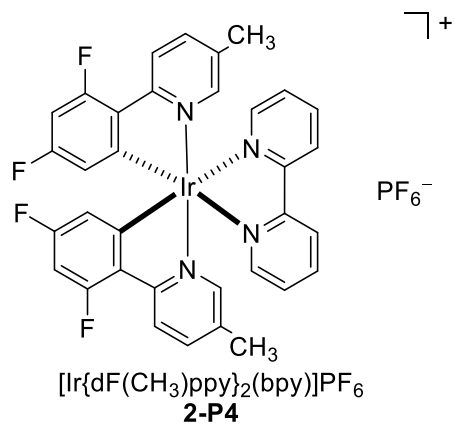
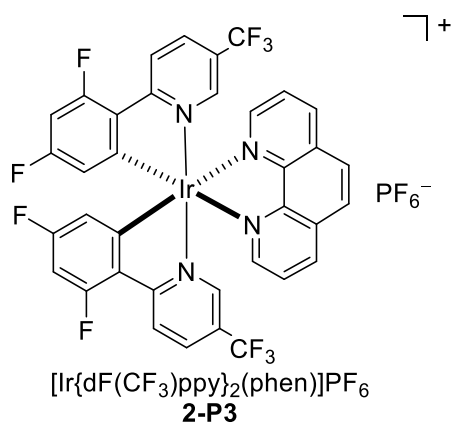
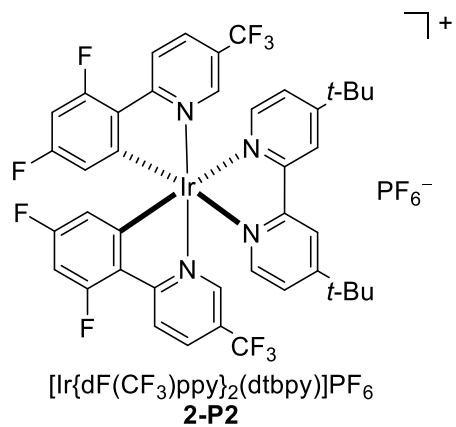
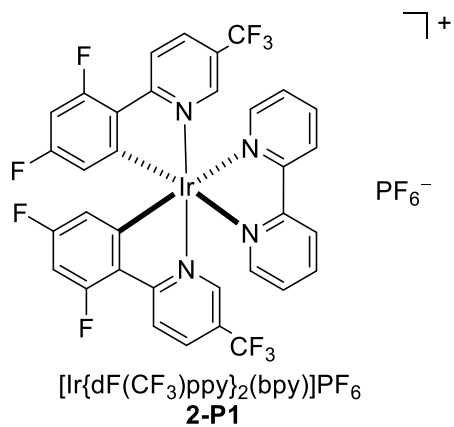
the photocatalyst (entry 8). In conclusion, the reaction requires the sufficient oxidizing ability of the excited state of photocatalysts.

Table 2-1. Screening of photocatalysts.^a



entry	photocatalyst	GC conv. (%)	GC yield (%)
1	2-P1	85	32
2	2-P2	96	34
3	2-P3	84	31
4	2-P5	99	31
5	2-P6	85	29
6	2-P4	16	3
7	2-P7	36	11
8	2-P8	29	<1

^a**2-7a** (3 equiv); 1,2-DCE/ H_2O (2:1, 0.05 M).



2) Screening of Bases

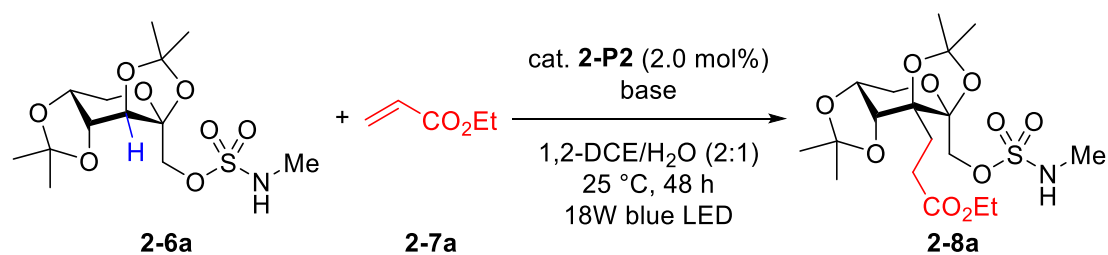
Several bases were screened to improve the yield of **2-8a** (Table 2-2-1). The reaction proceeded smoothly using K_3PO_4 , K_2CO_3 , Na_2CO_3 , and Cs_2CO_3 (entries 1–4). Among them, the best yield (35%) was obtained using K_3PO_4 (entry 1). In contrast, the reaction did not proceed using NaH_2PO_4 , Na_2HPO_4 , $\text{Na}_2\text{HPO}_4 \cdot 2\text{H}_2\text{O}$, KH_2PO_4 , K_2HPO_4 , AcONa , AcOK , and NEt_3 (entries 5–12), demonstrating that the base was important in the conversion of **2-6a**. Knowles *et al.* reported that iridium-catalyzed C–H alkylation of aliphatic amides **2-9** with electron-deficient alkenes in the presence of tetrabutylammonium dibutyl phosphate as a base via 1,5-HAT. And they proposed that the electron transfer process between the excited iridium photocatalyst and the N–H bond was accompanied with the proton transfer between the base and the N–H bond. This process was called proton-coupled electron transfer (PCET) (Scheme 2-3).¹⁰ Therefore, I considered that the PCET process occurred among the excited iridium catalyst **2-P2**, the N–H bond of **2-6a**, and the inorganic base (K_3PO_4 , K_2CO_3 , Na_2CO_3 , and Cs_2CO_3) to generate N radical in this reaction.

To further explain the different results by different bases, I analyzed them based on the pK_b values of the bases.¹¹ The pK_b value of the N–H bond of aminosulfonyl group is approximately 2.2 in water.¹² From the pK_b values of the bases used, it can be observed that the pK_b value of PO_4^{3-} ($\text{pK}_b \approx 1.7$) and the pK_b value of CO_3^{2-} ($\text{pK}_b \approx 3.7$) are close to the pK_b value of the N–H bond of aminosulfonyl group (entries 1-4). Therefore, phosphates and carbonates can act as weak bases in this reaction. Considering the pK_b values of H_2PO_4^- and HPO_4^{2-} ($\text{pK}_b \approx 6.8, 11.9$), it is evident that their basicity is weaker than that of **2-6a**. As a result, NaH_2PO_4 , Na_2HPO_4 , $\text{Na}_2\text{HPO}_4 \cdot 2\text{H}_2\text{O}$, KH_2PO_4 , and K_2HPO_4 did not promote the reaction (entries 5-7 and 10-11). Furthermore, the pK_b value of AcO^- is 9.2, which is larger than that of **2-6a**, indicating that its basicity is weaker than that of **2-6a**. Hence, acetates (AcONa and AcOK) were also unsuitable bases (entries 8-9). However, despite having a pK_b value close to that of **2-6a**, triethylamine did not lead to the conversion of **2-6a** (entry 12). I considered that the triethylamine reacted with the catalyst **2-P2**. Because the redox potential of triethylamine is +0.83 V that is smaller than that of **2-6a** (+1.16 V).¹³

In summary, the selection of bases and their pK_b values played crucial roles in the reaction outcome. Bases, such as phosphates and carbonates, with pK_b values close to

or slightly lower than that of the N–H bond of aminosulfonyl group were effective in promoting the reaction, while bases, such as acetates, bicarbonates, monohydrogen phosphates and dihydrogen phosphates, with weaker basicity did not facilitate the desired conversion of **2-6a**.

Table 2-2-1. Screening of bases.^a

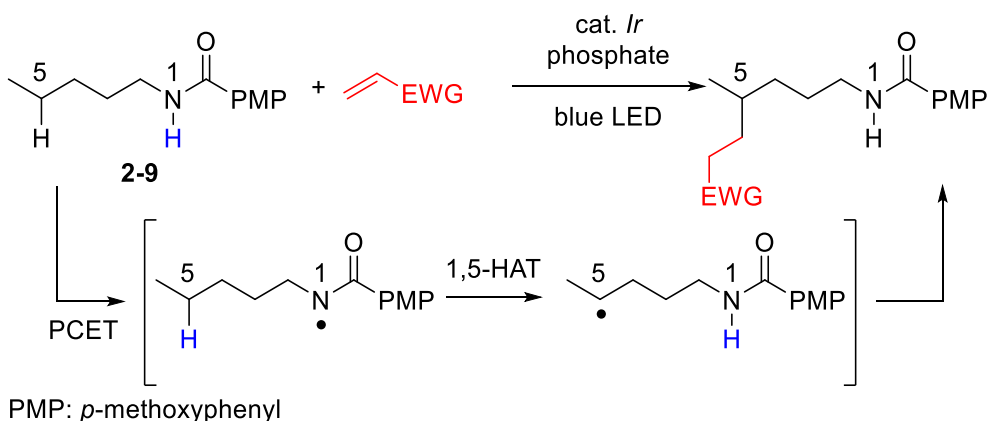


entry	base (2 equiv)	pK _b (in H ₂ O)	GC conv. (%)	GC yield (%)
1	K ₃ PO ₄	1.7	95	35
2	K ₂ CO ₃	3.7	85	27
3	Na ₂ CO ₃	3.7	94	31
4	Cs ₂ CO ₃	3.7	96	28
5	NaH ₂ PO ₄	6.8	<1	<1
6	KH ₂ PO ₄	6.8	<1	<1
7	K ₂ HPO ₄	6.8	<1	<1
8	AcONa	9.2	<1	<1
9	AcOK	9.2	<1	<1
10	Na ₂ HPO ₄	11.9	<1	<1
11	Na ₂ HPO ₄ •2H ₂ O	11.9	<1	<1
12	NEt ₃	3.4	<1	<1

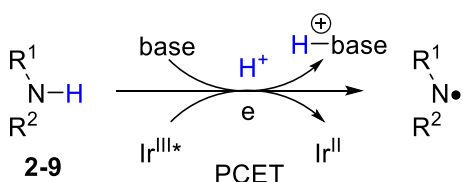
^a**2-7a** (3 equiv); 1,2-DCE/H₂O (2:1, 0.05 M).

Scheme 2-3. The PCET process.

a) Knowles's work



b) The PCET process



To optimize the yield of **2-8a**, the amount of K_3PO_4 was further investigated, and the results are summarized in Table 2-2-2. Adding 1.0 equivalent of K_3PO_4 resulted in the formation of **2-8a** in 29% yield (entry 1). Increasing the amount of K_3PO_4 to 2 equivalents led to the improvement of the yield to 35% (entry 2). However, further increasing the amount of K_3PO_4 to 3.0 equivalents did not enhance the yield of **2-8a** (entry 3).

Table 2-2-2. Screening of the amount of K_3PO_4 .^a

entry	K_3PO_4 (equiv)	GC conv. (%)	GC yield (%)
1	1.0	99	29
2	2.0	95	35
3	3.0	97	33

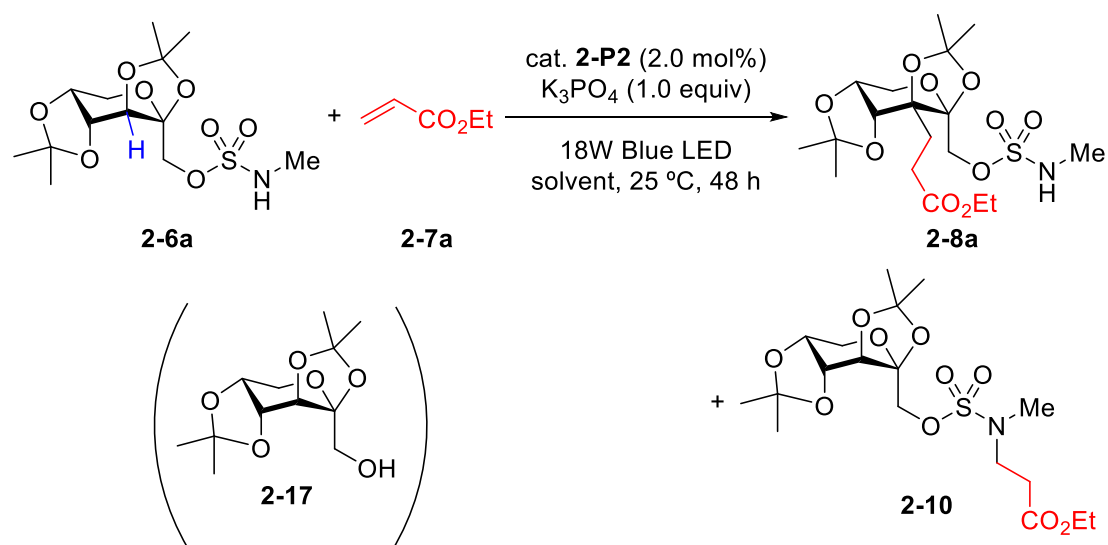
^a**2-7a** (3 equiv); 1,2-DCE/ H_2O (2:1, 0.05 M).

3) Screening of Solvents

Several solvents were also investigated to improve the yield of **2-8a** (Table 2-3-1). By using 1,2-DCE as the solvent, and the yields of **2-8a** and *N*-alkylated product **2-10** were 20% and 1%, respectively, and the ratio between **2-8a** and **2-10** was 96:4 (entry

1). When the solvent was changed to DCM, the yield of **2-8a** did not increase, but the ratio between **2-8a** and **2-10** was 83:17, indicating the yield of **2-10** increased (entry 2). When using PhCl, the yield of **2-8a** decreased to 15%, and the ratio between **2-8a** and **2-10** was 59:41 (entry 3). When PhCF₃ was used as the solvent, the yield of **2-8a** dropped to 8%, and the ratio between **2-8a** and **2-10** became 27:73 (entry 4). At this point, the main product became to be the N–H alkylated product **2-10**. When using strong polar solvents DMF or MeCN, **2-6a** was converted almost completely, and only N–H alkylated product **2-10** was obtained in 42% and 63% yields, respectively (entries 5 and 6). We found that C–H alkylated product **2-8a** was obtained using solvents with smaller dielectric constants, such as 1,2-DCE, DCM, PhCl, and PhCF₃. When using solvents with larger dielectric constant, such as DMF and MeCN, only N–H alkylated product **2-10** was obtained. As shown in Scheme 2-4, the formation of C–H alkylated product **2-8a** and N–H alkylated product **2-10** were competitive reactions in this system. Only *N*-alkylated product **2-10** was obtained using polar solvent MeCN under dark conditions (Table 3-3-2). This result indicates that K₃PO₄ abstracts proton from N–H bond of **2-6a** to form N anionic intermediate, which easily attacks electron deficient alkene in MeCN. In contrast, the formation of **2-10** was difficult in less polar solvents. When the mixed solvent (1,2-DCE/H₂O (2:1, 0.05 M)) was used, the yield of **2-8a** increased to 29% and the formation of by-product **2-10** was also suppressed, and the ratio between **2-8a** and **2-10** was improved to 98:2 (entry 7). In organic solvents without adding water, small amount of decomposition product **2-17** was formed (entries 1-6). I considered that K₃PO₄ served as a base to promote the decomposition of **2-6a**. When the mixed solvent (1,2-DCE/H₂O (2:1, 0.05 M)) was used, the formation of **2-17** was inhibited (entry 7). I considered that K₃PO₄ was dissolved in the aqueous phase, which made the less content of K₃PO₄ in the organic phase (1,2-DCE). Thus, the decomposition of **2-6a** was suppressed.

Table 2-3-1. Screening of solvents.^a

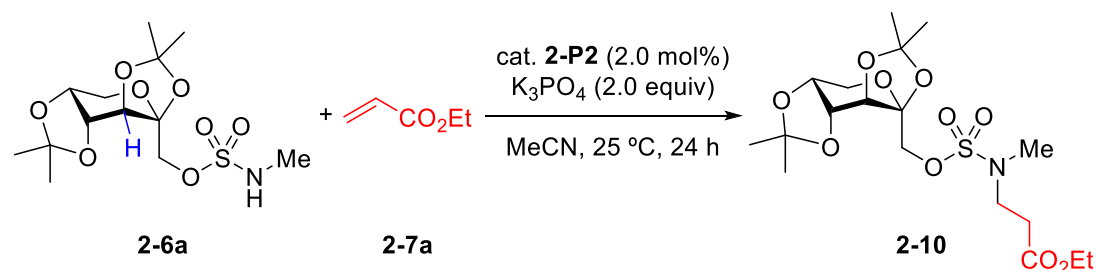


entry	solvent	dielectric constant ¹⁴	conv. (%)	2-17 GC yield (%)	2-8a GC yield (%)	2-10 GC yield (%)	isomer 2-8a : 2-10
1	1,2-DCE	10	97	11	20	1.0	96:4
2	DCM	8.9	83	15	20	4.1	83:17
3	PhCl	5.6	89	10	15	10	59:41
4	PhCF ₃	9.4	86	11	8.2	22	27:73
5	DMF	37	98	21	<1.0	42	<1:99>
6	MeCN	38	99	19	<1.0	63	<1:99>
7	1,2-DCE/H ₂ O ^b	-	94	2	29	<1.0	98:2

^a**2-7a** (2 equiv); K_3PO_4 (2 equiv); solvent (0.05 M);

^b1,2-DCE/H₂O (2:1).

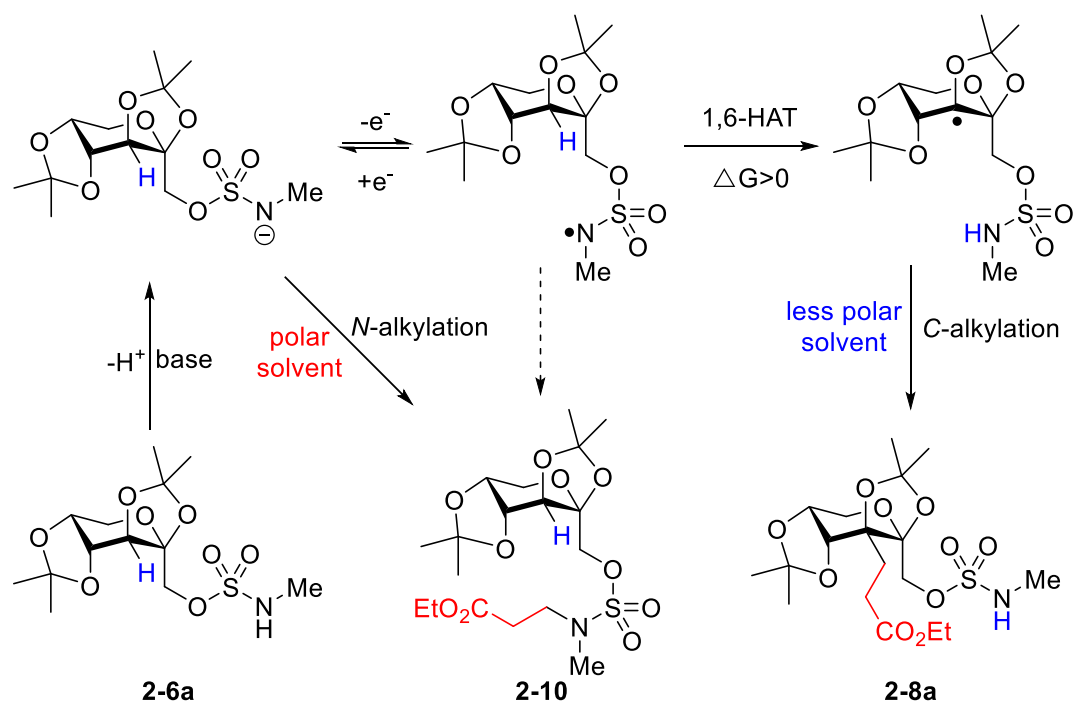
Table 2-3-2. Experiments under dark condition.^a



entry	photocatalyst	conv. (%)	2-8a GC yield (%)	2-10 GC yield (%)
1	2-P2	67	-	65
2	-	69	-	68

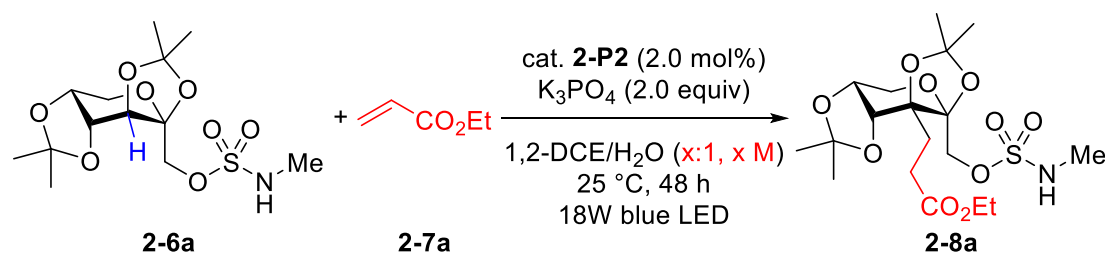
^a**2-7a** (2 equiv); MeCN (0.05 M).

Scheme 2-4. Explanation of the formation of **2-8a** and **2-10**.



A series of experiments were investigated for determining the optimal ratio of 1,2-DCE/H₂O and the concentration (Table 2-3-2). By using 1,2-DCE/H₂O, the yield of **2-8a** was increased, and the formation of N–H alkylated product **2-10** was suppressed (Table 2-3-1, entry 7). Therefore, experiments were conducted using different ratios of 1,2-DCE to H₂O (0.05 M) (Table 2-3-2 entries 1-3). The results indicated that the highest yield of **2-8a** was obtained when the ratio of 1,2-DCE/H₂O was 2:1 (35% yield, entry 2), while the yields were lower when the ratio was either increased (31% yield, entry 1) or decreased (30% yield, entry 3) from this ratio.

After fixing the ratio of 1,2-DCE/H₂O at 2:1, the effect of the concentration on the yield of **2-8a** was investigated. The results showed that when the concentration was higher than 0.05 M, the yield of **2-8a** decreased (entries 4 and 5). Similarly, when the concentration was lower than 0.05 M, the yield of **2-8a** also decreased (entry 6). It is speculated that the use of the mixed solvent, 1,2-DCE/H₂O, improved the yield of **2-8a** because the inorganic base used in the reaction was easily soluble in water. A small amount of water was unfavorable to the dissolution of the base, while excess water was unfavorable to the stability of the transition state of **2-8a**.

Table 2-3-2 Screening of ratio of 1,2-DCE/H₂O and concentration.^a

entry	1,2-DCE/H ₂ O	conc. (mol/L)	GC yield (%)
1	3/1	0.05	31
2	2/1	0.05	35
3	1/1	0.05	30
4	2/1	0.20	23
5	2/1	0.10	21
6	2/1	0.04	30

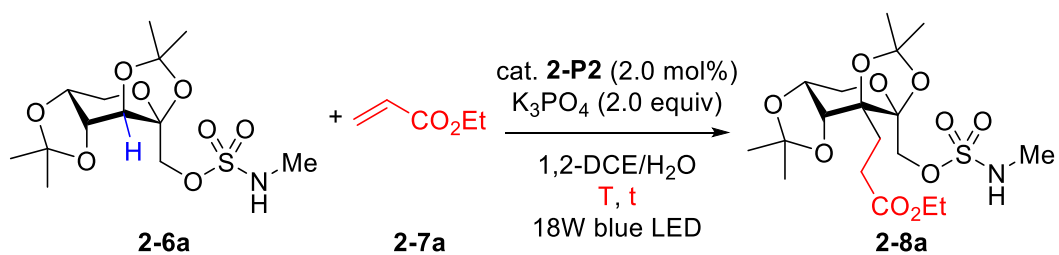
^a**2-7a** (3 equiv).

4) Screening of Reaction Time and Temperature

The reaction time and temperature were investigated to improve the yield of **2-8a** (Table 4). At 24 h, there was almost complete conversion of **2-6a**, but the yield of **2-8a** was slightly lower than that at 36 h (29%, entry 1). This could be attributed to the incomplete conversion of some reaction intermediates into products. Prolonging the reaction time to 48 h resulted in the slightly lower yield of **2-8a** (35%, entry 3). These results showed that the optimal yield was 41% at 36 h (entry 2).

After determining the optimal reaction time, the temperature was investigated (entries 4-7). The yield of **2-8a** increased from 30% to 46% with increasing temperature from 15 °C to 60 °C. This may be because some elementary reactions were endothermic, and much lower temperature was not conducive to their progress. For instance, Dorigo and Houk reported that the ΔG value of 1,6-HAT process from the 7-membered ring transition state was greater than 0, indicating that the 1,6-HAT process was thermodynamically unfavorable. However, the ΔH value was greater than 0 indicating that the 1,6-HAT process was an endothermic reaction. Therefore, increasing the temperature would facilitate the occurrence of this process.¹⁵ However, temperature above 60 °C was unfavorable for the reaction (entry 7). From the above results, the optimal reaction temperature was 60 °C at 36 h (entry 6), and temperatures lower or higher than 60 °C were not favorable for the reaction.

Table 4. Screening of reaction time and temperature.^a



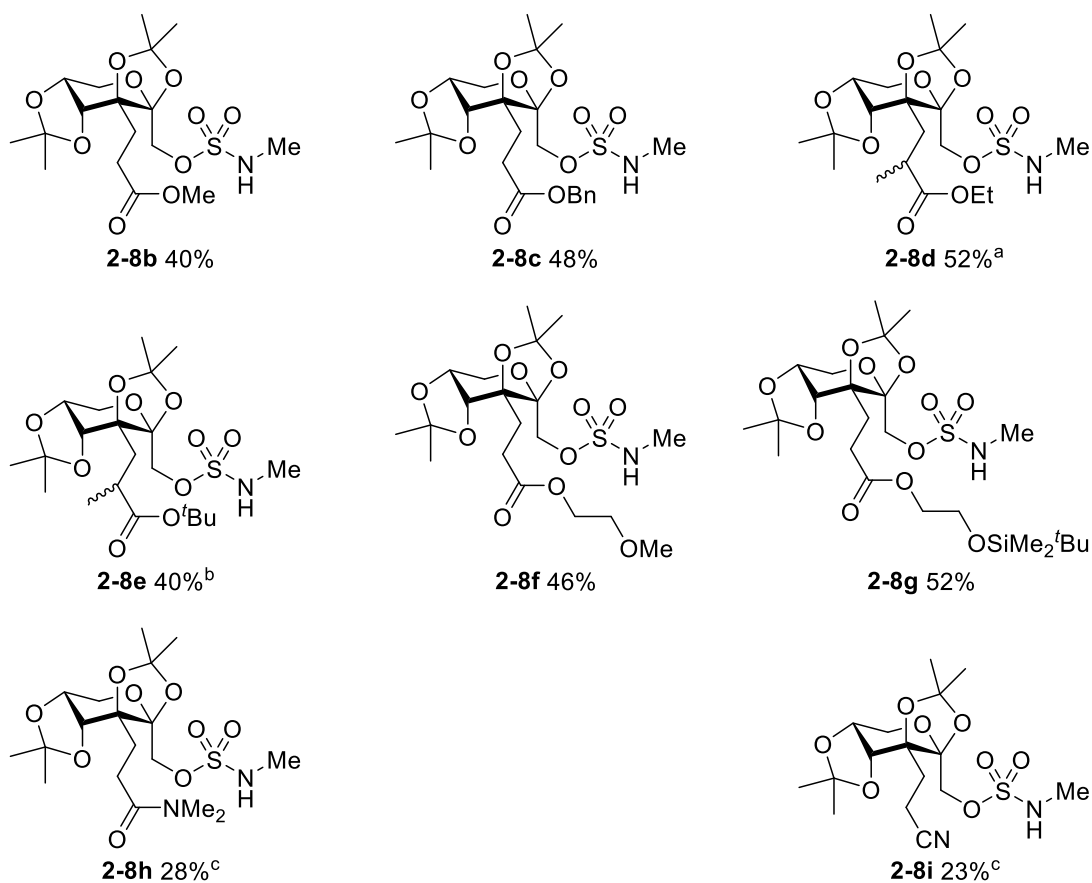
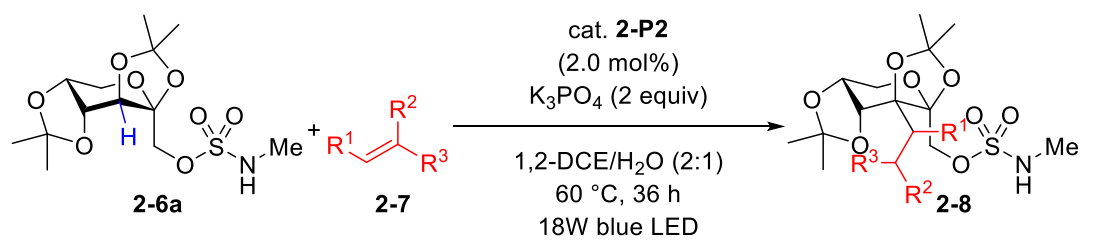
entry	time (h)	T (°C)	GC conv. (%)	GC yield (%)
1	24	25	99	29
2	36	25	99	41
3	48	25	95	35
4	36	15	97	30
5	36	40	92	45
6	36	60	86	46
7	36	75	95	38

^a**2-7a** (3 equiv); 1,2-DCE/ H_2O (2:1, 0.05 M).

2.2.2 Scope of Alkenes

Under the optimized reaction conditions shown in Table 4, entry 6, the substrate scope of alkylation reagents was investigated (Scheme 2-5). Treatment of 2,3:4,5-bis-*O*-(1-ethylethylidene)- β -D-fructopyranose methyl sulfamate **2-6a** with methyl acrylate (**2-7b**) or benzyl acrylate (**2-7c**) provided alkylated products **2-8b** and **2-8c** in 40% and 48% yields, respectively. The alkylation also proceeded using methacrylates **2-7d** and **2-7e**, and the corresponding alkylated products **2-8d** and **2-8e** were obtained in 52% and 40% yields, respectively, as a mixture of diastereomers. The reactions were not inhibited by the steric hindrance from a methyl group at the β -carbon of the acrylate. Acrylates **2-7f** and **2-7g** bearing a methoxy or siloxy group were also suitable for this reaction and produced **2-8f** and **2-8g** in 46% and 52% yields, respectively. The alkylation also proceeded using acrylamide **2-7h** and acrylonitrile **2-7i**, and the corresponding alkylated products **2-8h** and **2-8i** were obtained in 28% and 23% yields, respectively. The alkyl, aryl, methoxy, siloxy, amide, and cyano groups were versatile functional groups that can be easily transformed to other functional groups and find broad applications in organic synthesis, materials science, and pharmaceuticals.

Scheme 2-5. Scope of alkenes.



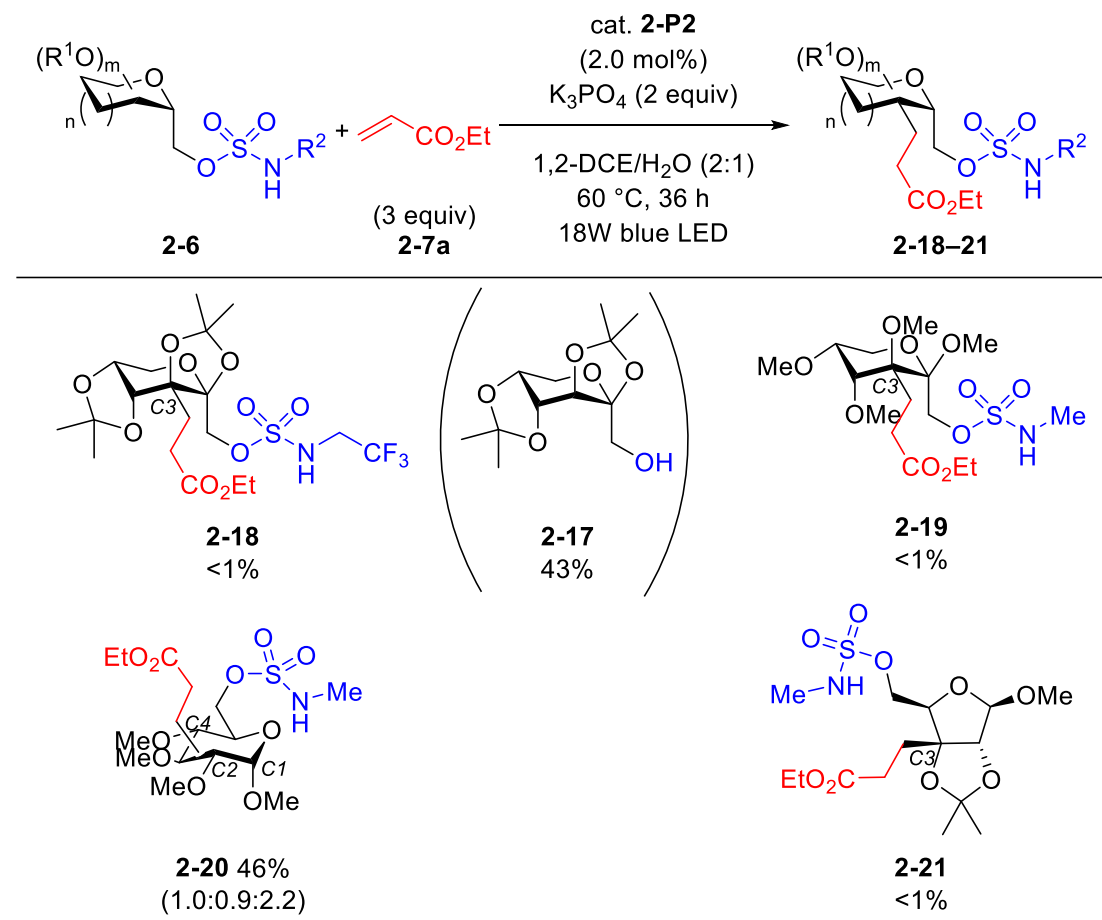
^aMixture of diastereomers (52:48). ^b25 °C, 48 h, mixture of diastereomers (76:24).

^c25 °C, 48 h.

2.2.3 Scope of Saccharides

Under the optimized reaction conditions shown in Table 4, entry 6, the substrate scope of saccharides was investigated (Scheme 2-6). When **2-6b** was used as a substrate, in which an electron-withdrawing trifluoroethyl group was attached to the sulfamate group, the alkylated product **2-18** was not obtained. Instead, decomposition product **2-17** was obtained in 43% yield. I considered that it becomes difficult to transfer one electron from the sulfamate group to the excited iridium catalyst due to the electron-withdrawing trifluoroethyl group. In addition, **2-6b** underwent a decomposition reaction to produce **2-17** in the presence of a base. When using **2-6c** as a substrate, in which protecting groups was replaced to methyl groups, alkylated product **2-19** was not obtained. This result probably due to the steric hindrance of the methoxy group on C4, which affected the 1,6-HAT reaction at C3-H. The yields of alkylated product was 46% using **2-6d**, but the site-selectivity was low (C1:C3:C4 = 1.0:0.9:2.2). This result probably due to that these three places (C1, C3 and C4) are all suitable in space to form 7-membered ring transition state of 1,6-HAT. When using ribofuranose derivative **2-6e**, alkylated product **2-21** was not formed. It may be due to the close distance between C3-H and aminosulfonyl group, and thus the 7-membered ring transition state cannot be formed. To achieve C(sp³)-H alkylation, the following points should be fulfilled: 1) one electron of nitrogen atom of aminosulfonyl group can transfer to the excited iridium catalyst; 2) there is less steric hindrance around the C-H bond; and 3) the distance between C-H bond and aminosulfonyl group should be appropriate.

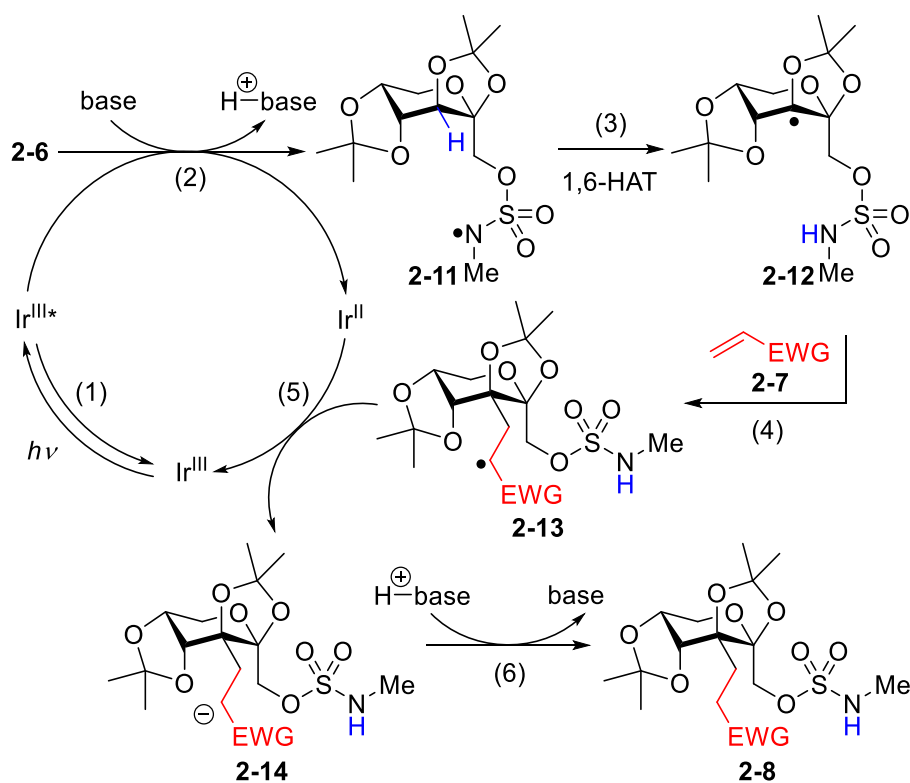
Scheme 2-6. Scope of saccharides.



2.2.4 Proposed Reaction Mechanism

The proposed reaction mechanism of the site-selective C(sp³)-H alkylation of fructopyranose derivative **2-6a** is shown in Scheme 2-6: (1) upon blue LED irradiation, the iridium photocatalyst (Ir^{III}) is excited to Ir^{III}* species; (2) sulfamyl radical **2-11** is formed through a proton-coupled electron transfer (PCET) by the excited Ir^{III}* and a base. At the same time, Ir^{III}* species is deactivated and reduced to Ir^{II}; (3) carbon radical **2-12** is formed by 1,6-HAT; (4) the nucleophilic carbon radical reacts with an electron-deficient alkene **2-7** to generate an alkyl radical intermediate **2-13**; (5) Ir^{II} reduces the radical intermediate **2-13** to give anionic intermediate **2-14** and Ir^{III} is regenerated; and (6) intermediate **2-14** is subsequently protonated to produce the alkylated product **2-8**.

Scheme 2-7. Proposed reaction mechanism.

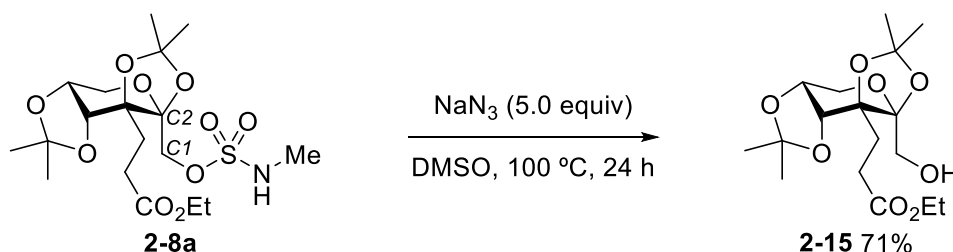


2.2.5 Exploring the Application Potential of This Reaction

The *N*-methyl sulfamate group of alkylated fructopyranose derivative **2-8a** can be converted to a hydroxy group (Scheme 2-8). This can be used in organic synthesis because hydroxy groups can participate in a wide range of chemical reactions, including oxidation, esterification, and glycosylation, allowing for the synthesis of various compounds. The hydroxy group can also act as a hydrogen bond donor, influencing the physical and chemical properties, such as solubility and boiling point.

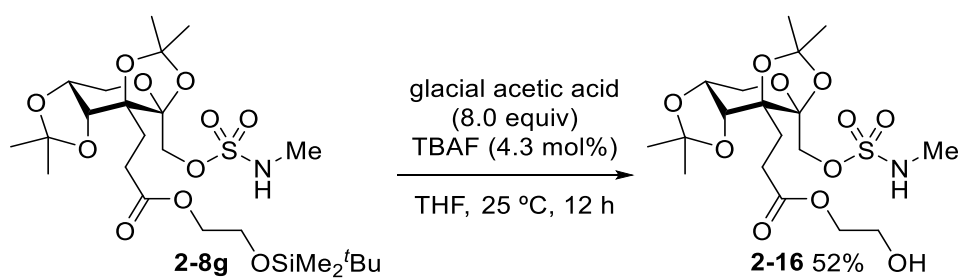
In this work, the treatment of fructopyranose derivative **2-8a** with NaN₃ in DMSO at 100 °C for 24 h gave the deprotected product **2-15** in 71% yield. Interestingly, the hydroxylation proceeded whereas an azide group is generally introduced by the elimination of the *N*-methyl sulfamate group under the reaction conditions.¹⁶ This is possibly due to the steric hindrance of C1 atom or the potential inhibitory effect by the C2–O bond in the S_N2 reaction.

Scheme 2-8. Conversion of *N*-methyl sulfamate group of alkylated fructopyranose derivative **2-8a** to a hydroxy group.



The silyl group of the alkylated fructopyranose derivative **2-8g** can be easily removed by the treatment of **2-8g** with TBAF and glacial acetic acid, giving **2-16** bearing a free hydroxy group (Scheme 2-9). The hydroxy group of **2-16** offers various possibilities for further functionalization.

Scheme 2-9. Deprotection of silyl group of **2-16**.



2.3 Conclusion

This work achieved site-selective C(sp³)-H alkylation of a fructopyranose derivative using 1,6-HAT, which is a departure from the conventional functionalization approach of saccharides that involves converting the highly reactive primary and secondary hydroxy groups and anomer positions. Notably, the hydroxy groups of the fructopyranose derivative were preserved after the C(sp³)-H alkylation process.

During the investigation of optimal reaction conditions, it was found that the choice of a catalyst and base had a substantial impact on the conversion of **2-6a**. Since fructopyranose derivative **2-6a** undergoes a proton-coupled electron transfer (PCET) process by the photocatalyst and base, resulting in the formation of sulfamyl radical. The E_{1/2}^{red} value of the catalyst and the pK_b value of the base play a crucial role in determining the feasibility of this process. Among the catalysts tested, [Ir{dF(CF₃)ppy}₂(dtbpy)]PF₆ was found to be the most effective photocatalyst, while K₃PO₄ was identified as the optimal base. During the investigation of the solvent effect on the reaction, it was observed that while the solvent had a negligible impact on the conversion of **2-6a**, it had a significant effect on the proportion and yield of the product **2-8a** and the by-product **2-10**. The mixed solvent of 1,2-dichloroethane (1,2-DCE) and water (2:1, 0.05 M) was the most optimal solvent for this reaction.

This reaction allows for the introduction of various functional groups by employing electron-deficient alkenes with different functional groups. Moreover, the *N*-methyl sulfamate group, which acts as a hydrogen abstractor from the fructopyranose derivative, can be transformed into a hydroxy group. Additionally, the silyl group located at the terminal position of the introduced alkyl chain can be easily removed by the treatment with TBAF, thus providing a free hydroxy group.

The findings of this study offer valuable insights into sugar chemistry and C-H transformations. Moreover, these results have a potential to drive further advancements in saccharide chemistry as C(sp³)-H transformations can produce saccharide derivatives that are not accessible through transformations at the hydroxy groups or anomer position.

2.4 Experimental Section

2.4.1 General

All reactions were carried out under nitrogen atmosphere unless otherwise noted. Fructopyranose derivative **2-6** was prepared according to the literature procedure.¹⁷ 1,2-Dichloroethane (1,2-DCE, Wako) was distilled over CaH₂ prior to use. H₂O (deionized, Takasugi Seiyaku), tetrahydrofuran (THF, anhydrous, Wako), *N,N*-dimethylformamide (DMF, anhydrous, Wako), and dichloromethane (DCM, anhydrous, Wako) were used as received from commercial sources. Other reagents were purchased from commercial sources and used without further purification.

¹H (400 MHz) and ¹³C (100 MHz) NMR spectra were recorded using a JEOL ECZ400 spectrometer. Proton chemical shifts are reported relative to residual solvent peak (CDCl₃ at δ 7.26 ppm). Carbon chemical shifts are reported relative to CDCl₃ at 77.0 ppm. IR spectra were recorded on a JASCO FT/IR-4200. High resolution mass spectra were recorded on JEOL JMS-700 (EI, FAB) spectrometer. Gel Permeation Chromatography (GPC) was performed by Japan Analytical Industry LC-5060 with series-connected JAIGEL-1H (φ 20 mm x 600 mm) and JAIGEL-2H (φ 20 mm x 600 mm). Photo reactions were carried out using PhotoRedOx TC (HepatoChem) with 18W Blue LED (450 nm).

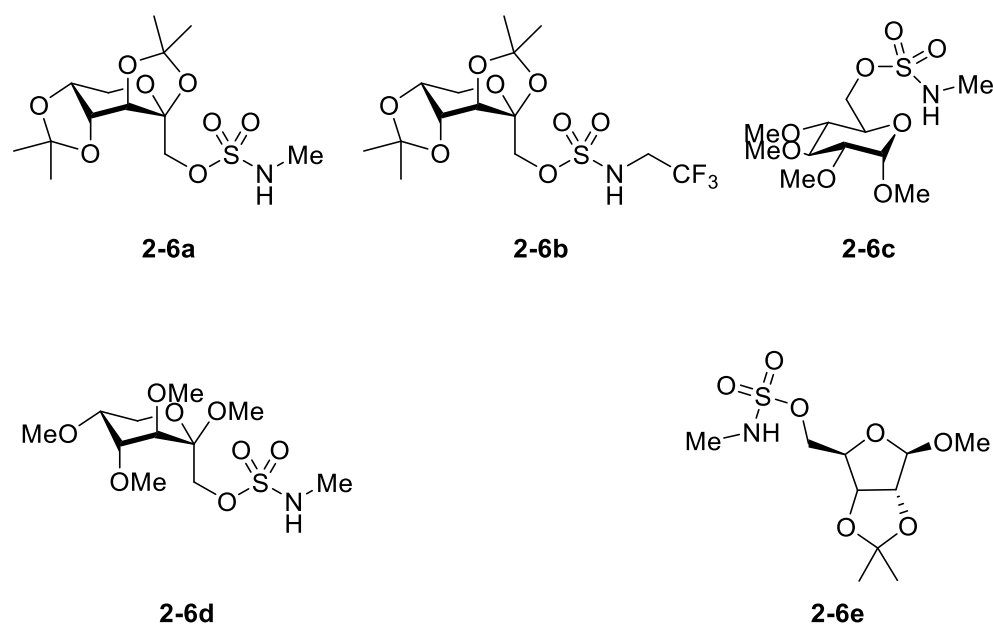


Figure 2-1. Scope of saccharides.

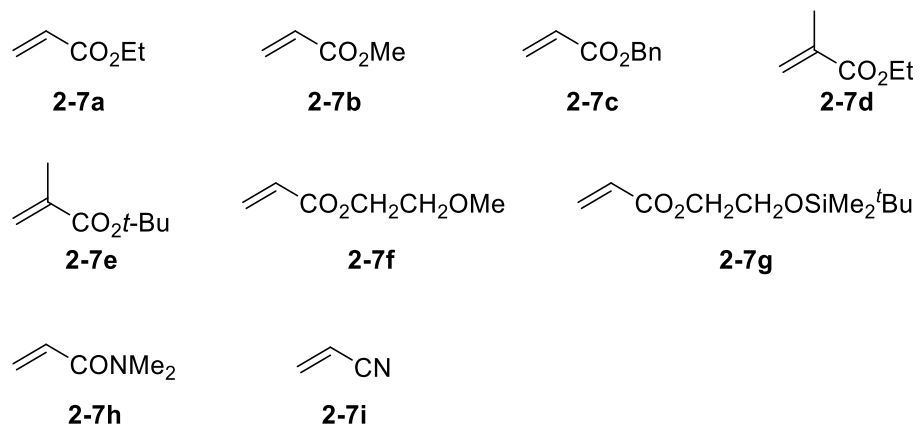


Figure 2-2. Scope of alkenes.

2.4.2 Synthesis and Characterization of Substrates

1) Confirm the Reaction Site

In the DEPT-135 spectrum of **2-8a**, eight signals were observed for CH₃ and CH signals, and five signals were observed for CH₂ signals (Figure 2-3), indicating that the results were consistent with the expected structure of **2-8a**. DEPT-135 spectra of **2-8b**–**2-8i** were also measured and showed consistent results with the C–H alkylated products.

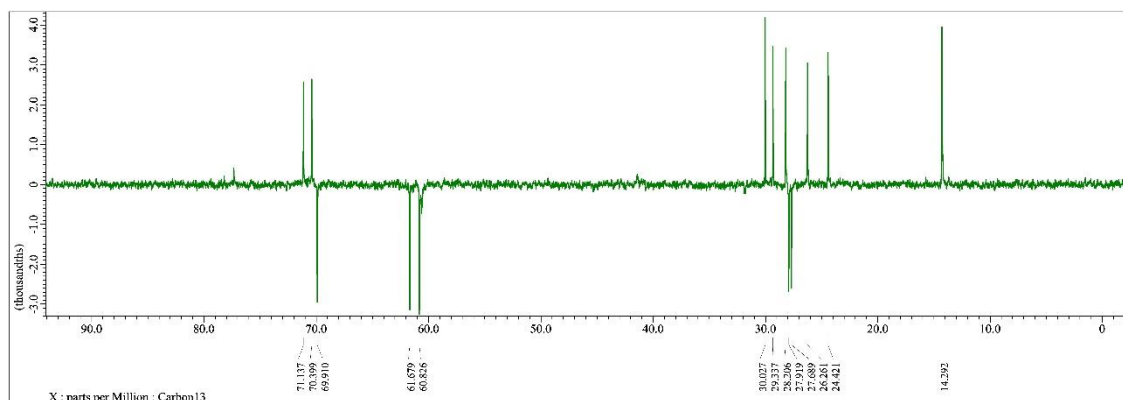


Figure 2-3. DEPT-135 spectrum of **2-8a**.

The NOESY spectrum of **2-8a** showed a correlation between the hydrogen atoms on carbons 1 and 2, indicating their proximity in space (Figure 2-4). This supports the proposed structure of **2-8a**. NOESY spectra were also obtained for **2-8b**–**2-8i**, and the results were consistent with the C(sp³)–H alkylation products.

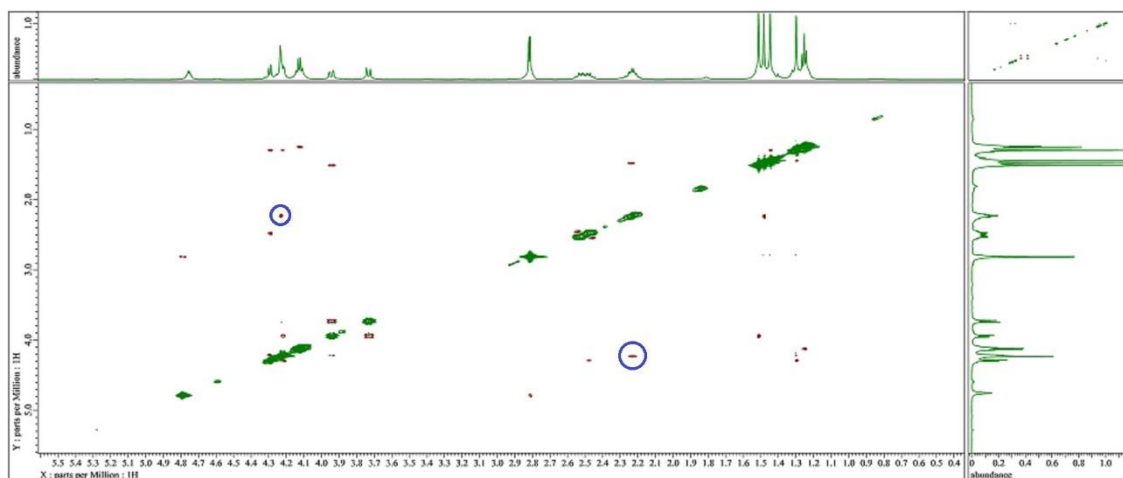
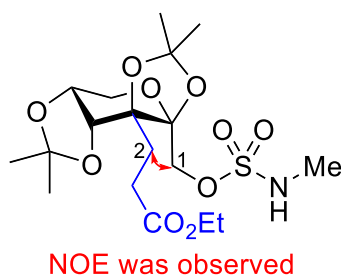
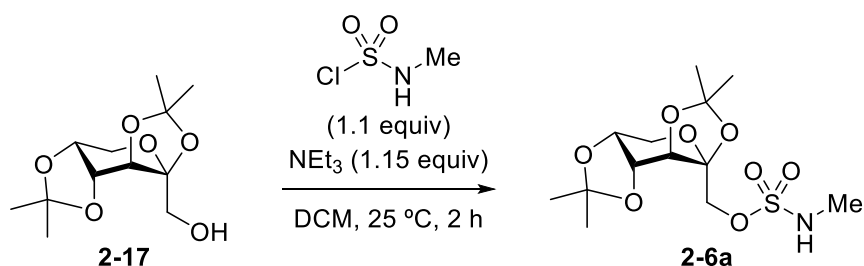


Figure 2-4. NOESY spectrum of **2-8a** (600 MHz, CDCl₃).



2) Synthesis of Compounds

Synthesis of compound 2-6a



To a dichloromethane (18 mL) solution of methylsulfamoyl chloride, which was prepared by the reaction of methylsulfamic acid (0.940 g, 8.50 mmol) with PCl_5 (1.94 g, 9.30 mmol) in toluene (16 mL) at 80 °C for 5 h, was added **2-17** (2.00 g, 7.70 mmol). Et_3N (0.896 g, 8.85 mmol) was added dropwise to the mixture, and stirred at 25 °C. After 2 h, the reaction was quenched by slow addition of 1.0 M aq. HCl (9.2 mL). The organic layer was collected, and the aqueous layer was extracted with dichloromethane (1 x 18 mL) and ethyl acetate (1 x 18 mL). The combined organic fractions were dried over Na_2SO_4 , filtered, and concentrated under reduced pressure. The crude product was purified by column chromatography on silica gel to give compound **2-6a** (2.72 g, 98%). ^1H NMR (400 MHz, CDCl_3) δ 1.33 (s, 3H), 1.41 (s, 3H), 1.47 (s, 3H), 1.54 (s, 3H), 2.83 (d, $J = 5.2$ Hz, 3H), 3.74 (d, $J = 12.8$ Hz, 1H), 3.89 (d, $J = 12.8$ Hz, 1H), 4.07-4.12 (m, 2H), 4.18 (d, $J = 10.4$ Hz, 1H), 4.23 (d, $J = 8.0$ Hz, 1H), 4.32 (d, $J = 2.0$ Hz, 1H), 4.57-4.61 (m, 1H); ^{13}C NMR (100 MHz, CDCl_3) δ 24.0, 25.1, 25.8, 26.5, 29.8, 61.3, 69.9, 70.1, 70.2, 70.6, 100.8, 109.18, 109.24.

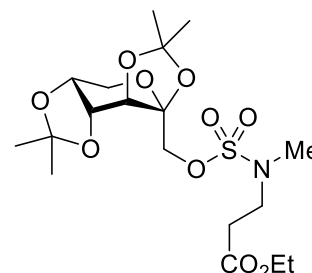
General procedure: To a test tube, **2-P2** (2.20 mg, 2.0 μmol , 2.0 mol%), K_3PO_4 (42.4 mg, 0.200 mmol, 2.0 equiv), **2-6a** (35.3 mg, 0.100 mmol), 1,2-DCE (1.33 mL) and H_2O (0.67 mL) were added, and the mixture was frozen-thaw two times to remove air of the

system. To the mixture, ethyl acrylate (**2-7a**, 30.0 mg, 0.300 mmol, 3.0 equiv) was added via syringe, and the tube was sealed with a Teflon lined screw cap. The mixture was stirred under the irradiation of 18W Blue LED at 60°C for 36 h. After cooling to room temperature, the mixture was diluted with dichloromethane, washed with water, brine, dried over Na₂SO₄ and concentrated in vacuo. The crude product was purified by GPC.

Synthesis of compound 2-10

Following Procedure in Table 2-3-1 entry 6 (ethyl acrylate (**2-7a**, 0.200 mmol), 25 °C, 48 h). Compound **2-10** was obtained as a colorless oil (19.8 mg, 44%) by GPC.

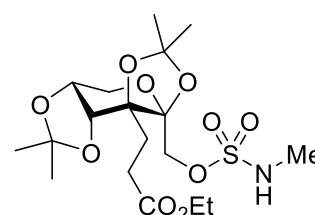
¹H NMR (400 MHz, CDCl₃) δ 1.28 (t, *J* = 7.6 Hz, 3H), 1.35 (s, 3H), 1.43 (s, 3H), 1.49 (s, 3H), 1.56 (s, 3H), 2.67 (t, *J* = 6.9 Hz, 2H), 2.96 (s, 3H), 3.56 (t, *J* = 6.9 Hz, 2H), 3.77 (d, *J* = 12.8, 1H), 3.92 (d, *J* = 12.8, 1H), 4.10-4.19 (m, 4H), 4.25 (d, *J* = 7.8 Hz, 1H), 4.36 (d, *J* = 2.4 Hz, 1H) 4.62 (dd, *J* = 7.8, 2.4 Hz, 1H); ¹³C NMR (100 MHz, CDCl₃) δ 14.1, 23.9, 25.2, 25.8, 26.5, 33.2, 36.4, 47.0, 60.9, 61.3, 69.3, 69.8, 70.0, 70.6, 100.7, 109.13, 109.18, 171.1; HRMS (EI) exact mass calculated for C₁₇H₂₈NO₁₀S [M-CH₃]⁺ 438.1434, found 438.1434; IR (v/cm⁻¹) 2986, 2936, 1734.



Synthesis of compound 2-8a

Following General Procedure (ethyl acrylate (**2-2a**, 0.300 mmol), 60 °C, 36 h). Compound **3a** was obtained as a colorless oil (18.1 mg, 40%) by GPC.

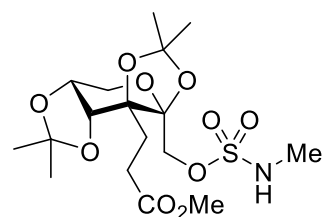
¹H NMR (400 MHz, CDCl₃) δ 1.26 (t, *J* = 7.0 Hz, 3H), 1.30 (s, 3H), 1.45 (s, 3H), 1.49 (s, 3H), 1.52 (s, 3H), 2.20-2.26 (m, 2H), 2.43-2.58 (m, 2H), 2.82 (d, *J* = 6.8 Hz, 3H), 3.73 (d, *J* = 14.4 Hz, 1H), 3.95 (dd, *J* = 12.8, 2.8 Hz, 1H), 4.13 (dd, *J* = 14.4, 7.6 Hz, 2H), 4.21-4.24 (m, 3H), 4.30 (d, *J* = 7.6 Hz, 1H), 4.65 (d, *J* = 15.2 Hz, 1H); ¹³C NMR (100 MHz, CDCl₃) δ 14.2, 24.4, 26.2, 27.4, 27.9, 29.2, 29.7, 30.1, 60.6, 61.5, 69.8, 70.4, 71.1, 80.5, 104.0, 108.6, 110.0, 173.4; HRMS (EI) exact mass calculated for C₁₈H₃₁NO₁₀S [M+H]⁺ 453.1669, found 453.1670; IR (v/cm⁻¹) 2981, 1734.



Synthesis of compound 2-8b

Following General Procedure (methyl acrylate (**2-7a**, 0.300 mmol), 60 °C, 36 h). Compound **2-8b** was obtained as a colorless oil (17.6 mg, 40%) by GPC.

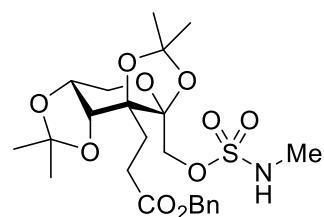
¹H NMR (400 MHz, CDCl₃) δ 1.30 (s, 3H), 1.45 (s, 3H), 1.48 (s, 3H), 1.52 (s, 3H), 2.20-2.28 (m, 2H), 2.45-2.59 (m, 2H), 2.83 (d, *J* = 5.2 Hz, 3H), 3.68 (s, 3H), 3.73 (d, *J* = 13.6 Hz, 1H), 3.95 (d, *J* = 13.6 Hz, 1H), 4.21-4.24 (m, 3H), 4.30 (d, *J* = 8.0 Hz, 1H), 4.48 (s, 1H); ¹³C NMR (100 MHz, CDCl₃) δ 24.4, 26.2, 27.74, 27.76, 28.1, 29.3, 30.0, 51.9, 61.6, 69.8, 70.3, 71.2, 80.6, 103.7, 108.7, 109.9, 173.7; HRMS (EI) exact mass calculated for C₁₇H₂₉NO₁₀S [M+H]⁺ 439.1512, found 439.1512; IR (ν/cm⁻¹) 2981, 1739.



Synthesis of compound 2-8c

Following General Procedure (benzyl acrylate (**2-7c**, 0.300 mmol), 60 °C, 36 h). Compound **2-8c** was obtained as a colorless oil (24.7 mg, 48%) by GPC.

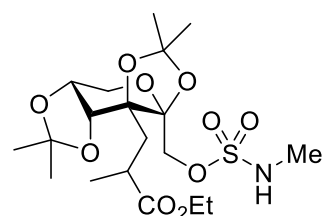
¹H NMR (400 MHz, CDCl₃) δ 1.29 (s, 3H), 1.45 (s, 3H), 1.48 (s, 3H), 1.51 (s, 3H), 2.24-2.30 (m, 2H), 2.54-2.61 (m, 2H), 2.80 (d, *J* = 5.2 Hz, 3H), 3.73 (d, *J* = 12.8 Hz, 1H), 3.96 (d, *J* = 12.8 Hz, 1H), 4.20-4.30 (m, 6H), 4.50 (d, *J* = 5.6 Hz, 1H), 7.32-7.39 (m, 5H); ¹³C NMR (100 MHz, CDCl₃) δ 24.4, 26.2, 27.7, 27.9, 28.1, 29.3, 30.0, 61.6, 66.6, 69.8, 70.4, 71.1, 80.4, 103.5, 108.9, 109.7, 128.3 (2C), 128.4, 128.7 (2C), 135.8, 173.0; HRMS (EI) exact mass calculated for C₂₃H₃₃NO₁₀S [M+H]⁺ 515.1825, found 515.1824; IR (ν/cm⁻¹) 2956, 1734.



Synthesis of compound 2-8d

Following General Procedure (ethyl methacrylate (**2-7d**, 0.300 mmol), 60 °C, 36 h). Compound **2-8d** was obtained as a colorless oil (24.3 mg, 52%) by GPC.

¹H NMR (400 MHz, CDCl₃) δ 1.20-1.26 (m, 6H), 1.33 (s, 3H), 1.42-1.49 (m, 6H), 1.61 (s, 3H), 1.87-1.98 (m, 1H), 2.28-2.47 (m, 1H), 2.76-2.86 (m, 4H), 3.70 (d, *J* = 14.4 Hz, 1H), 3.93 (dd, *J* = 13.4, 13.4 Hz, 1H), 4.01-4.16 (m, 1H), 3.96-4.38 (m, 5H), 4.61 (d, *J* = 8.4 Hz, 1H); ¹³C NMR (100 MHz, CDCl₃) δ 14.2, 19.3,

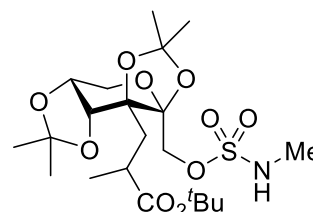


24.6, 26.3, 28.1, 29.1, 29.9, 34.9, 37.4, 60.4, 61.8, 69.8, 70.4, 71.6, 81.0, 103.7, 108.6, 110.0, 176.6; HRMS (EI) exact mass calculated for C₁₉H₃₃NO₁₀S [M+H]⁺ 467.1825, found 467.1826; IR (ν/cm⁻¹) 2961, 1724.

Synthesis of compound 2-8e

Following General Procedure (*tert*-butyl methacrylate (2-7e, 0.300 mmol), 25 °C, 48 h). Compound 2-8e was obtained as a colorless oil (19.8 mg, 40%) by GPC.

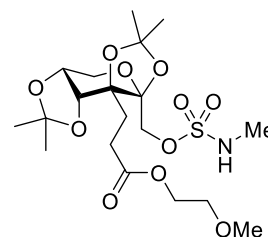
¹H NMR (400 MHz, CDCl₃) δ 1.34 (s, 3H), 1.44-1.48 (m, 21H), 1.89 (dd, *J* = 14.0, 4.0 Hz, 1H), 2.30 (*J* = 14.0, 9.6 Hz, 1H), 2.65-2.75 (m, 1H), 2.83 (d, *J* = 5.2 Hz, 3H), 3.72 (dd, *J* = 14.4, 5.2 Hz, 1H), 3.94 (dd, *J* = 12.8, 2.8 Hz, 1H), 4.23-4.25 (m, 3H), 4.55-4.65 (m, 2H); ¹³C NMR (100 MHz, CDCl₃) δ 19.5, 24.5, 26.3, 28.0, 28.2, 29.3, 30.0, 35.6, 36.9, 61.8, 70.0, 70.7, 71.6, 80.1, 81.1, 103.8, 108.7, 110.1, 175.9; HRMS (EI) exact mass calculated for C₂₁H₃₇NO₁₀S [M+H]⁺ 496.2216, found 496.2216; IR (ν/cm⁻¹) 2981, 1729.



Synthesis of compound 2-8f

Following General Procedure (2-methoxyethyl acrylate (2-7f, 0.300 mmol), 60 °C, 36 h). Compound 2-8f was obtained as a colorless oil (22.2 mg, 46%) by GPC.

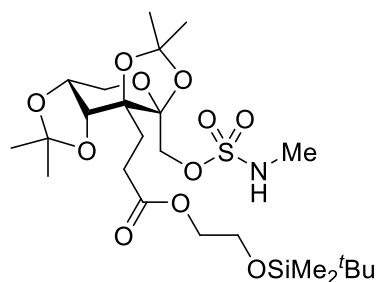
¹H NMR (400 MHz, CDCl₃) δ 1.29 (s, 3H), 1.45 (s, 3H), 1.48 (s, 3H), 1.51 (s, 3H), 2.21-2.28 (m, 2H), 2.54-2.60 (m, 2H), 2.82 (d, *J* = 5.2 Hz, 3H), 3.35-3.38 (m, 3H), 3.59-3.61 (m, 2H), 3.73 (d, *J* = 13.2 Hz, 1H), 3.95 (d, *J* = 12.8 Hz, 1H), 4.24-4.29 (m, 6H), 4.70 (d, *J* = 4.8 Hz, 1H); ¹³C NMR (100 MHz, CDCl₃) δ 24.4, 26.2, 27.6, 27.8, 28.2, 29.3, 30.0, 59.0, 61.6, 63.8, 69.6, 70.3, 70.4, 71.1, 81.3, 103.5, 108.8, 109.7, 173.2; HRMS (EI) exact mass calculated for C₁₉H₃₃NO₁₁S [M+H]⁺ 483.1774, found 483.1773; IR (ν/cm⁻¹) 2956, 1729.



Synthesis of compound 2-8g

Following General Procedure (2-((*tert*-butyldimethylsilyl)oxy)ethyl acrylate (**2-7g**, 0.300 mmol), 60 °C, 36 h). Compound **2-8g** was obtained as a colorless oil (30.4 mg, 52%) by GPC.

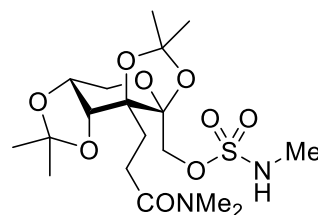
¹H NMR (400 MHz, CDCl₃) δ 0.06 (s, 6H), 0.89 (s, 9H), 1.31 (s, 3H), 1.46 (s, 3H), 1.49 (s, 3H), 1.53 (s, 3H), 2.20-2.28 (m, 2H), 2.48-2.62 (m, 2H), 2.84 (d, *J* = 5.2 Hz, 3H), 3.74 (dd, *J* = 12.8, 1.6 Hz 1H), 3.80-3.82 (m, 2H), 3.96 (dd, *J* = 13.2, 2.8 Hz, 1H), 4.14-4.17 (m, 2H), 4.22-4.17 (m, 3H), 4.31 (d, *J* = 7.2 Hz, 1H) 4.56-4.60 (m, 1H); ¹³C NMR (100 MHz, CDCl₃) δ -5.2, 18.4, 24.4, 25.9, 26.3, 27.7, 27.8, 28.2, 29.4, 30.0, 61.3, 61.7, 66.0, 69.9, 70.4, 71.2, 80.5, 103.6, 108.9, 109.8, 173.2; HRMS (EI) exact mass calculated for C₂₄H₄₅NO₁₁SSi [M+H]⁺ 583.2483, found 583.2482; IR (ν/cm⁻¹) 2941, 1734.



Synthesis of compound 2-8h

Following General Procedure (*N,N*-dimethylacrylamide (**2-7h**, 0.300 mmol), 25 °C, 48 h). Compound **2-8h** was obtained as a colorless oil (12.8 mg, 28%) by GPC.

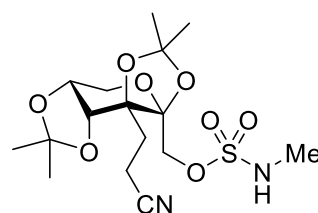
¹H NMR (400 MHz, CDCl₃) δ 1.31 (s, 3H), 1.45 (s, 3H), 1.49 (s, 3H), 1.65 (s, 3H), 2.14-2.22 (m, 1H), 2.27-2.35 (m, 1H), 2.43-2.56 (m, 2H), 2.83 (d, *J* = 5.2 Hz, 3H), 2.94 (s, 3H), 3.03 (s, 3H), 3.75 (d, *J* = 13.2 Hz, 1H), 3.97 (d, *J* = 13.2 Hz, 1H), 4.22-4.36 (m, 4H), 5.12 (d, *J* = 5.2 Hz, 1H); ¹³C NMR (100 MHz, CDCl₃) δ 24.6, 26.2, 26.7, 28.0, 28.2, 29.4, 30.0, 35.6, 37.2, 61.6, 69.7, 70.5, 71.5, 80.7, 103.7, 108.9, 109.6, 172.4; HRMS (EI) exact mass calculated for C₁₈H₃₂N₂O₉S [M+H]⁺ 452.1829, found 452.1831; IR (ν/cm⁻¹) 2940, 1624.



Synthesis of compound 2-8i

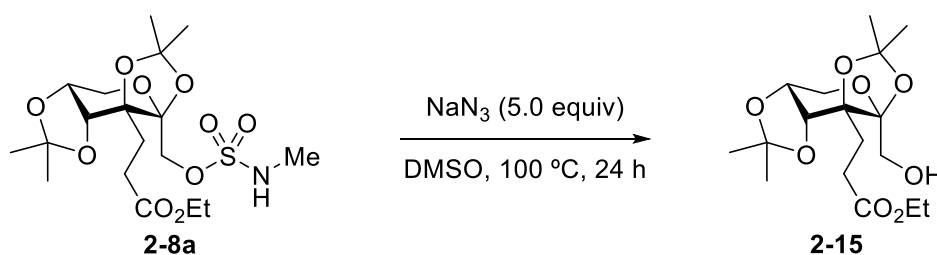
Following General Procedure (acrylonitrile (**2-7i**, 0.300 mmol), 25 °C, 48 h). Compound **2-8i** was obtained as a colorless oil (9.2 mg, 23%) by GPC.

¹H NMR (400 MHz, CDCl₃) δ 1.32 (s, 3H), 1.46 (s, 3H), 1.51 (s, 3H), 1.54 (s, 3H), 2.22-2.29 (m, 1H), 2.38-2.45 (m,



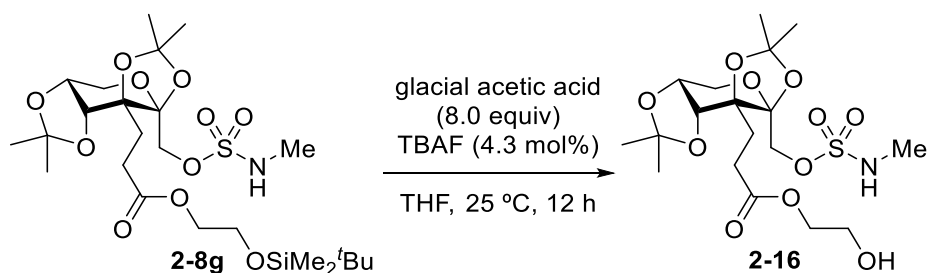
1H), 2.54-2.58 (m, 2H), 2.82 (d, $J = 5.6$ Hz, 3H), 3.76 (d, $J = 12.8$ Hz, 1H), 3.94 (d, $J = 15.6$ Hz, 1H), 4.14-4.19 (m, 2H), 4.22-4.26 (m, 1H), 4.32 (d, $J = 7.6$ Hz, 1H), 4.49 (d, $J = 4.8$ Hz, 1H); ^{13}C NMR (100 MHz, CDCl_3) δ 11.3, 24.3, 26.1, 28.0, 28.5, 29.5, 29.9, 61.4, 69.4, 70.2, 70.6, 80.0, 103.4, 109.1, 110.0, 119.3; HRMS (EI) exact mass calculated for $\text{C}_{16}\text{H}_{26}\text{N}_2\text{O}_8\text{S}$ $[\text{M}+\text{H}]^+$ 406.1410, found 406.1411; IR (v/cm^{-1}) 2930, 2323.

Synthesis of compound 2-15



To a test tube charged with a stir bar was added **2-8a** (31.7 mg, 0.0700 mmol), NaN_3 (22.7 mg, 0.350 mmol) and DMSO (0.10 M, 0.70 mL). The mixture was then heated to 100 °C and stirred for 24 h. The mixture was diluted with water (7.0 mL) and extracted with dichloromethane (2 x 7.0 mL). The combined organic phase was washed with water and brine. The solvent was removed under vacuum. The residue was further purified by column chromatography on silica gel (eluted by hexane:ethyl acetate= 3:1) to give compound **2-15** as colorless oil (17.9 mg, 71% yield). ^1H NMR (400 MHz, CDCl_3) δ 1.26 (t, $J = 7.2$ Hz, 3H), 1.32 (s, 3H), 1.45 (s, 3H), 1.48 (s, 3H), 1.52 (s, 3H), 2.14 (t, $J = 6.0$ Hz, 1H), 2.28-2.38 (m, 2H), 2.43-2.58 (m, 2H), 3.74 (d, $J = 6.4$ Hz, 2H), 3.77 (dd, $J = 12.8, 0.8$ Hz, 1H), 4.01 (dd, $J = 12.8, 2.0$ Hz, 1H), 4.13 (q, $J = 14.4, 6.8$ Hz, 2H), 4.21-4.24 (m, 1H), 4.31 (d, $J = 8.0$ Hz, 1H); ^{13}C NMR (100 MHz, CDCl_3) δ 14.3, 24.4, 26.2, 27.6, 28.0, 28.2, 29.5, 60.7, 61.7, 64.5, 70.9, 71.0, 80.4, 105.5, 108.6, 109.1, 173.4. HRMS (EI) exact mass calculated for $\text{C}_{17}\text{H}_{28}\text{O}_8$ $[\text{M}+\text{H}]^+$ 360.1784, found 360.1784; IR (v/cm^{-1}) 2986, 1729.

Synthesis of compound 2-16



Alkylated fructopyranose derivative **2-8g** (68.2 mg, 0.117 mmol, 1.0 equiv) was dissolved in anhydrous THF (0.50 mL, 0.23 M) at 0 °C under nitrogen. To the solution, glacial acetic acid (53.0 μ L, 0.936 mmol, 8.0 equiv) and tetrabutylammonium fluoride (0.10 M TBAF in THF, 50.9 μ L, 4.3 mol%) were added dropwise. The mixture was warmed to room temperature and stirred for 18 h. The reaction mixture was diluted with EtOAc (2 x 2.0 mL) and was washed with sat. NaHCO₃ (2.0 mL) and brine (2.0 mL). The organic layer was dried over Na₂SO₄, filtered and concentrated under reduced pressure. The residue was further purified by column chromatography on silica gel (eluted by hexane:ethyl acetate = 1:5) to give compound **2-16** as colorless oil (28.3 mg, 52% yield). ¹H NMR (400 MHz, CDCl₃) δ 1.31 (s, 3H), 1.45 (s, 3H), 1.49 (s, 3H), 1.52 (s, 3H), 1.87 (br, 1H), 2.23-2.37 (m, 2H), 2.50-2.64 (m, 2H), 3.81 (d, J = 5.2 Hz, 3H), 3.74 (dd, J = 13.2, 1.6 Hz, 1H), 3.82 (q, 2H), 3.95 (dd, J = 13.6, 2.8 Hz, 1H), 4.15-4.27 (m, 5H), 4.31 (d, J = 7.2 Hz, 1H), 4.93-4.97 (m, 1H); ¹³C NMR (100 MHz, CDCl₃) δ 24.4, 26.2, 27.8, 28.0, 28.1, 29.3, 29.9, 61.0, 61.6, 66.3, 69.5, 70.4, 80.5, 103.6, 108.9, 109.7, 173.5; HRMS (EI) exact mass calculated for C₁₈H₃₁NO₁₁S [M+H]⁺ 469.1618, found 469.1617; IR (v/cm⁻¹) 2925, 1729.

2.5 References

1. (a) Hofmann, A. W. *Ber. Dtsch. Chem. Ges.* **1882**, *15*, 762–775. (b) Löffler, K.; Freytag, C. *Ber. Dtsch. Chem. Ges.* **1909**, *42*, 3427–3431. (c) Corey, E. J.; Hertler, W. R. *J. Am. Chem. Soc.* **1960**, *82*, 1657–1668.
2. (a) Bordwell, F. G.; Ji, G.-Z. *J. Am. Chem. Soc.* **1991**, *113*, 8398–8401. (b) Bordwell, F. G.; Zhang, S.; Zhang, X.-M.; Liu, W.-Z. *J. Am. Chem. Soc.* **1995**, *117*, 7092–7096.
3. (a) Blanksby, S. J.; Ellison, G. B. *Acc. Chem. Res.* **2003**, *36*, 255–263. (b) Li, N.; Li, J.; Qin, M.; Li, J.; Han, J.; Zhu, C.; Li, W.; Xie, J. *Nat. Commun.* **2022**, *13*, 4224.
4. (a) Choi, G. J.; Zhu, Q.; Miller, D. C.; Gu, C. J.; Knowles, R. R. *Nature* **2016**, *539*, 268–271. (b) Chu, J. C. K.; Rovis, T. *Nature* **2016**, *539*, 272–275. (c) Chen, D. F.; Chu, J. C.; Rovis, T. *J. Am. Chem. Soc.* **2017**, *139*, 14897–14900.
5. For examples of C(sp³)–H transformations by 1,6-HAT (a) Short, M. A.; Blackburn J. M.; Roizen, J. L. *Angew. Chem. Int. Ed.* **2018**, *57*, 296–299. (b) Ma, Z.-Y.; Guo, L.-N.; You, Y.; Yang, F.; Hu, M.; Duan, X.-H. *Org. Lett.* **2019**, *21*, 5500–5504. (c) Shu, W.; Zhang, H.; Huang, Y. *Org. Lett.* **2019**, *21*, 6107–6111.
6. Li, Y.; Miyamoto, S.; Torigoe, T.; Kuninobu, Y. *Org. Biomol. Chem.* **2021**, *19*, 3124–3127.
7. Ma, Z. Y.; Guo, L. N.; You, Y.; Yang, F.; Hu, M.; Duan, X. H. *Org. Lett.* **2019**, *21*, 5500–5504.
8. Lowry, M. S.; Goldsmith, J. I.; Slinker, J. D.; Rohl, R.; Pascal, R. A.; Malliaras, G. G.; Bernhard, S. *Chem. Mater.* **2005**, *17*, 5712–5719.
9. Prier, C. K.; Rankic, D. A.; MacMillan, D. W. *Chem. Rev.* **2013**, *113*, 5322–5363.
10. Choi, G. J.; Zhu, Q.; Miller, D. C.; Gu, C. J.; Knowles, R. R. *Nature* **2016**, *539*, 268–271.
11. Ripin, D. H.; Evans, D. A. PKa's of Inorganic and Oxo-Acids Chem 206, <https://pdfslide.net/documents/dh-ripin-da-evans-pkas-of-inorganic-and-oxo-acids-chem-206.html> (accessed on December 28, 2020).
12. Seebach, D.; Beck, A. K.; Bichsel, H. U.; Pichota, A.; Sparr, C.; Wünsch, R.; Schweizer, W. B. *Helv. Chim. Acta.* **2012**, *95*, 1303–1324.
13. Roth, H. G.; Romero, N. A.; Nicewicz, D. A. *Synlett* **2016**, *27*, 714–723.

14. (a) https://depts.washington.edu/eoopic/linkfiles/dielectric_chart%5b1%5d.pdf (b) Haynes, W. M. *CRC Handbook of Chemistry and Physics*; CRC Press: Boca Raton, FL, **2016**.
15. Dorigo, A. E.; Houk, K. N. *J. Am. Chem. Soc.* **1987**, *109*, 2195–2197.
16. Shu, W.; Zhang, H.; Huang, Y. *Org. Lett.* **2019**, *21*, 6107–6111.
17. (a) Laughrey, Z. R.; Kiehna, S. E.; Riemen, A. J.; Waters, M. L. *J. Am. Chem. Soc.* **2008**, *130*, 14625–14633. (b) Pichavant, L.; Celine G.; Xavier C. *Biomacromolecules* **2010**, *11*, 2415–2421. (c) Matwiejuk, M.; Thiem, J. *Eur. J. Org. Chem.* **2011**, 5860–5878. (d) Callari, M.; De Souza, P. L.; Rawal, A.; Stenzel, M. H. *Angew. Chem. Int. Ed.* **2017**, *56*, 8441–8445.

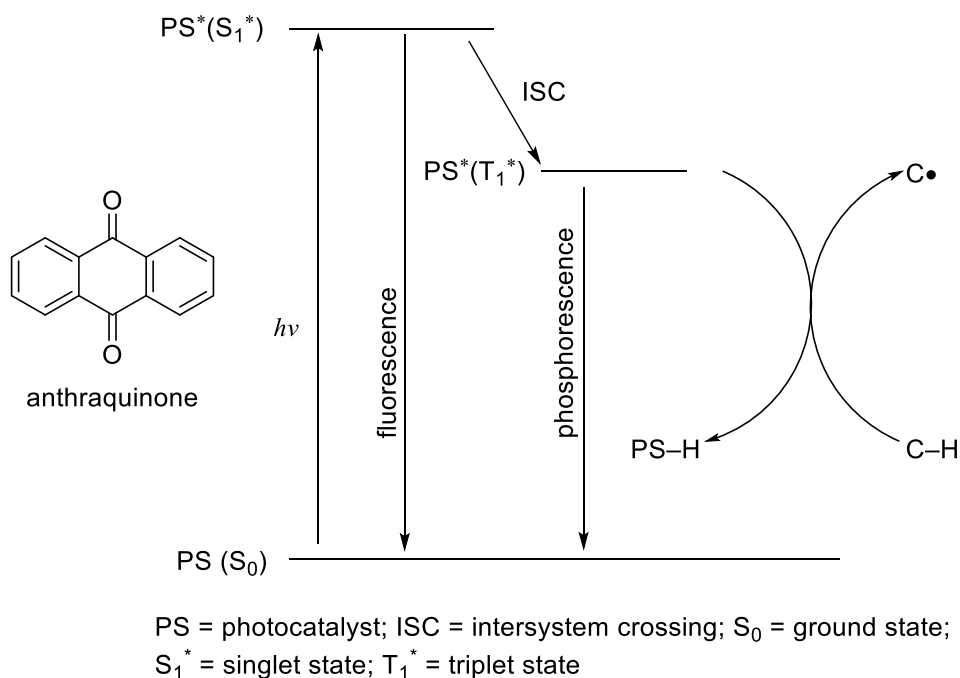
Chapter 3. Site-selective Direct Intermolecular C(sp³)-H Alkylation of Saccharides and Switching of Reaction Sites by Changing Photocatalysts

3.1 Introduction

3.1.1 Introduction of Anthraquinone Photocatalyst

Anthraquinones are a class of natural products widely distributed in nature. Anthraquinones not only exhibit potential drug value due to their antibacterial, anticancer, and other biological properties,¹ but they also find applications as organic dyes in the textile industry.² Moreover, anthraquinones have garnered significant attention as photoredox catalysts due to their affordability, commercial availability, and relatively low toxicity.³ Here, the activation process of C-H bonds using anthraquinones was introduced, taking anthraquinone as an example, as illustrated in Scheme 3-1. Initially, anthraquinone absorbs visible light and transitions to an excited state. Subsequently, the excited anthraquinone abstracts a hydrogen atom from the substrate, leading to the formation of a C radical, which is then further functionalized.

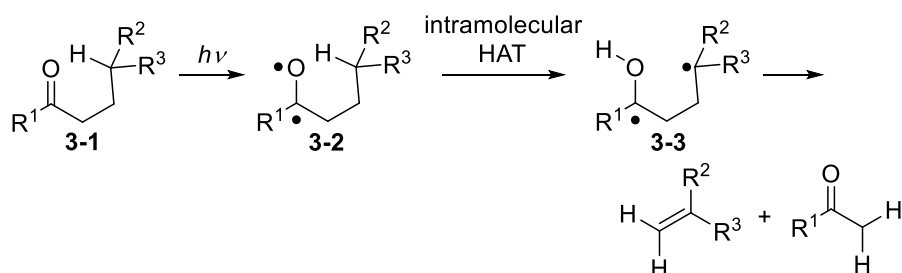
Scheme 3-1. Activation of C-H bond through HAT via anthraquinone.



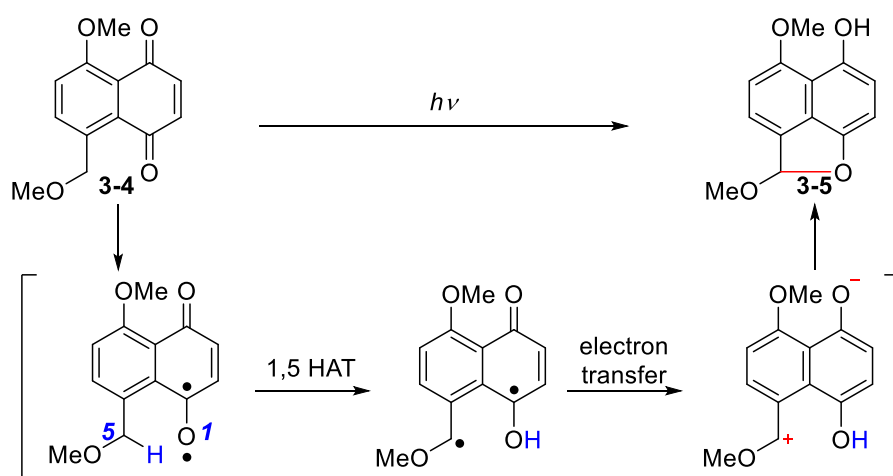
The mechanism of the anthraquinone-photocatalyzed reaction is similar to the Norrish type II reaction reported by Norrish in 1937. In this reaction, the photoexcited carbonyl compound **3-2** produced 1,4-diradical **3-3** via the intramolecular γ -hydrogen atom transfer (Scheme 3-2a).⁴ Since then, there has been a growing body of research on this intramolecular photochemical process of quinones, with numerous studies reporting its mechanisms and applications.⁵ For example, Suzuki *et al.* reported the intramolecular redox process of naphthoquinone derivative **3-5** including 1,5-hydrogen atom transfer (HAT), in which the C(sp³)–H bond was oxidized and quinone was reduced, and the ring-forming product **3-5** was obtained (Scheme 3-2b).⁶ Recently, Murafuji *et al.* reported on the C(sp³)–H alkylation of mono-alkylated tetrahydrofuran **3-6** using 2-chloroanthraquinone as photocatalyst. This reaction involved the intermolecular HAT process between the excited 2-chloroanthraquinone and the C(sp³)–H bond of **3-6**. By employing 1,1-bis(phenylsulfonyl)ethylene **3-7** as the alkylating agent, dialkylated product **3-8** was obtained. (Scheme 3-2c).⁷ However, the site-selective C(sp³)–H alkylation of saccharides is challenging since they have multiple C(sp³)–H bonds adjacent to oxygen atoms. In this work, site-selective C(sp³)–H alkylation of fructopyranose derivatives with electron-deficient alkenes was achieved (Scheme 3-2d).

Scheme 3-2. Several photocatalytic reactions using anthraquinones and the related compounds.

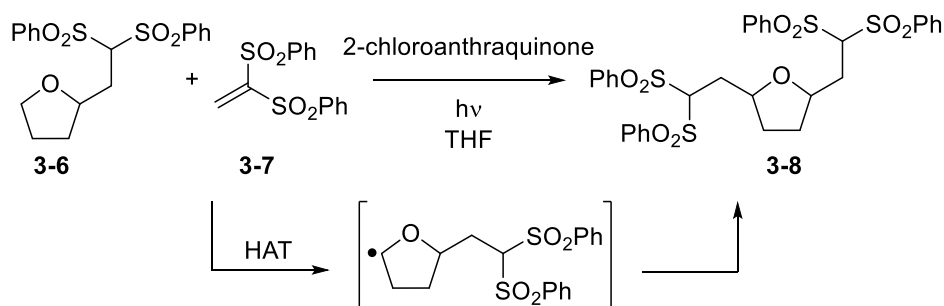
a) Norrish type II reaction via intramolecular HAT



b) Photoinduced quinone derivatives redox reaction including 1,5-HAT

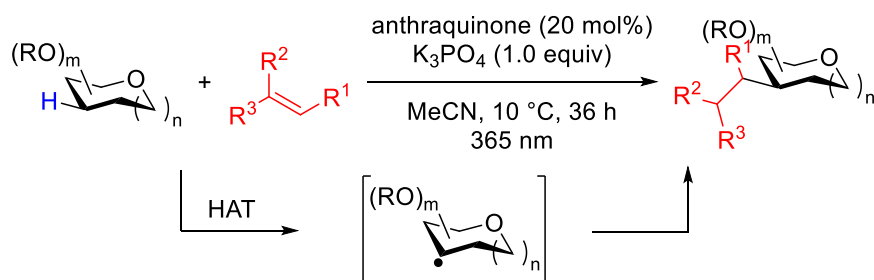


c) Quinone derivatives-catalyzed C-H akylation via intermolecular HAT



d) This work:

anthraquinone-catalyzed C-H alkylation of saccharides via intermolecular HAT



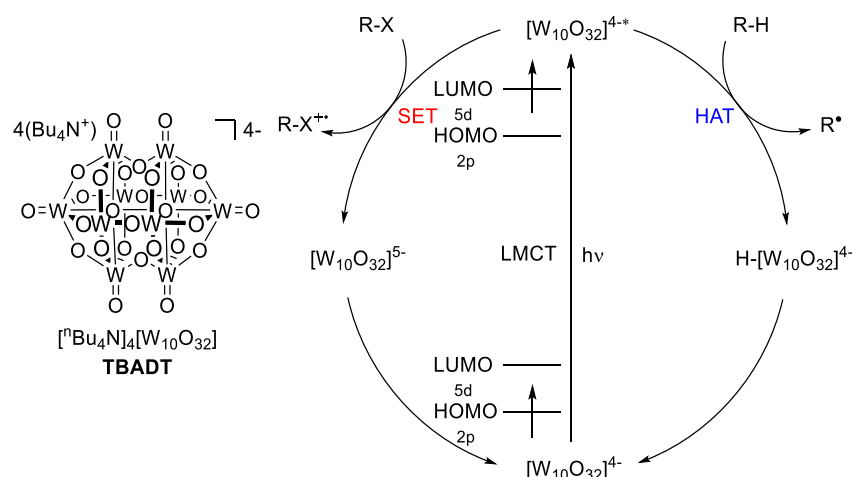
OR = protecting group

3.1.2 Introduction of TBADT Photocatalyst

Tetrabutylammonium decatungstate (TBADT) is a polyoxometalate and its anion composed by tungsten and oxygen atoms. Polyoxometalates, as versatile compounds, possess multiple functionalities, including catalysis, ion exchange and supramolecular chemistry. This multifunctionality allows for their wide application in fields such as chemistry, energy, materials science, and the environment.⁸ TBADT has emerged as a promising photocatalyst for C(sp³)-H transformations, offering several advantages.⁹ Specifically, it can be excited by sunlight under mild reaction conditions. Furthermore, after the reaction, it can be easily separated from the reaction system as a metal oxide salt.

Notably, the highest occupied molecular orbital (HOMO) of TBADT is primarily located on the oxygen atom, while the lowest unoccupied molecular orbital (LUMO) is predominantly found on the tungsten atom. Under light irradiation, the ligand-to-metal charge transfer (LMCT) effect occurs, enabling the transfer of one electron from the 2p orbital of the oxygen atom to the 5d orbital of the tungsten atom, resulting in the formation of an excited state.¹⁰ This excited state possesses +2.44 V oxidation potential (vs. saturated calomel electrode, SCE). The reaction outcome is determined by the oxidation potential of the reactant R-X. If the oxidation potential of R-X is lower than +2.44 V (vs. SCE), single electron transfer (SET) occurs from R-X to the excited state, generating the corresponding radical cation R-X^{•+}. On the other hand, if the oxidation potential of the reactant R-H is higher than +2.44 V (vs. SCE), hydrogen atom transfer (HAT) takes place, producing radical species R[•] (Scheme 3-3).¹¹

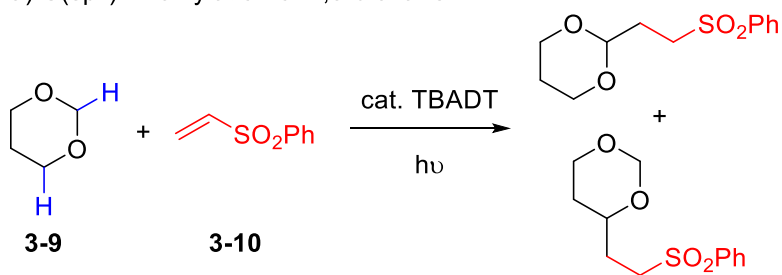
Scheme 3-3. Mechanism of decatungstate-catalyzed reaction via SET and HAT.



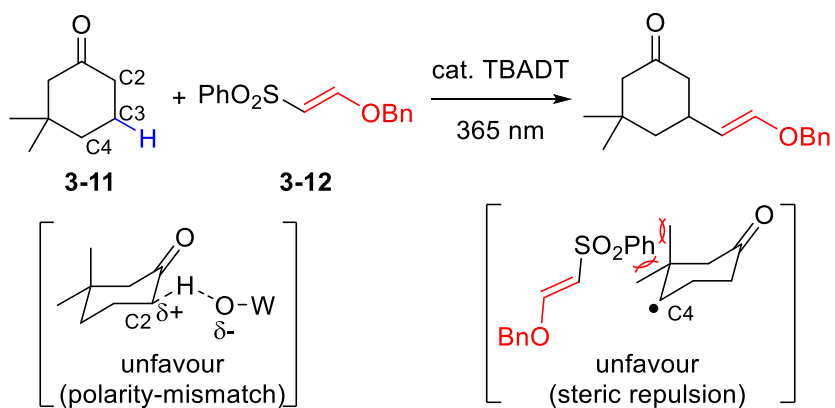
Ravelli *et al.* previously reported TBADT-catalyzed α -position-selective C(sp³)-H alkylation of 1,3-dioxane **3-9** using phenyl vinyl sulfone **3-10** as an alkylation reagent. However, determining the specific reaction site in oxygen heterocycles with multiple oxygen atoms is challenging (Scheme 3-4a).¹² Recently, Ryu's group reported site-selective TBADT-catalyzed alkenylation of 3,3-dimethylcyclohexanone **3-11**. In this reaction, the C2- and C4-positions did not react with the alkenylation reagent **3-12**, due to the polarity mismatch of the transition state and the steric hindrance between the bulky PhSO₂ and methyl groups, respectively (Scheme 3-4b).¹³ Herein we present a novel approach utilizing TBADT for the mild and site-selective C(sp³)-H alkylation of saccharides (Scheme 3-4c). By leveraging the unique electronic properties and steric hindrance of TBADT, we aim to address the challenge of selective alkylation of saccharides, which possess multiple C(sp³)-H bonds adjacent to oxygen atoms.

Scheme 3-4. Several examples of TBADT-catalyzed C(sp³)-H transformations.

a) C(sp³)-H alkylation of 1,3-dioxane

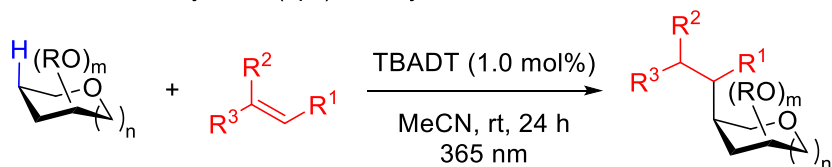


b) C(sp³)-H alkenylation of 3,3-dimethylcyclohexanone



c) **This work:**

TBADT-catalyzed C(sp³)-H alkylation of saccharides



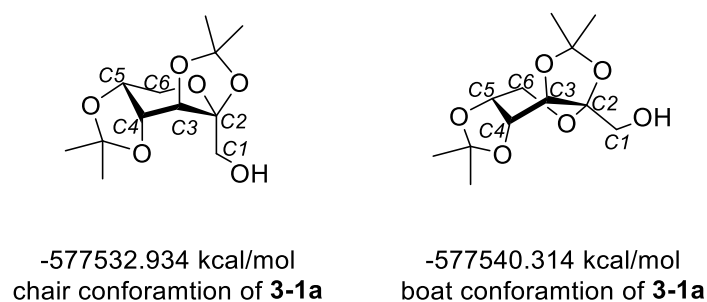
3.2 Results and Discussion

3.2.1 Analysis of Reaction Sites of Boat Conformation of **3-1a**

1) Chair and boat conformations of **3-1a**

The free energy of boat conformation of **1a** was 7.4 kcal/mol lower than that of chair conformation of **1a** using the B3LTP/6-31G(d) method¹⁵ in Gaussian 16¹⁶ (for data and 3D images, see the Supporting Information). Because of the diaxial interaction between C2 and C4 of chair conformation, which increases the energy of the system.

Scheme 3-5. Chair and boat conformations of **3-1a**.

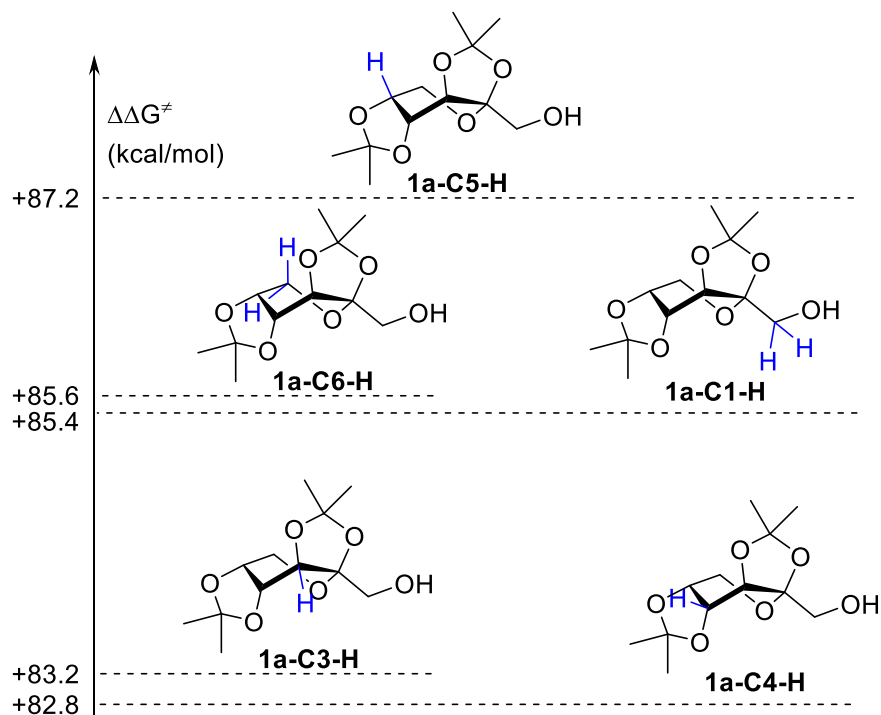


2) DFT Calculations of Bond Dissociation Energies of boat conformation of **3-1a**

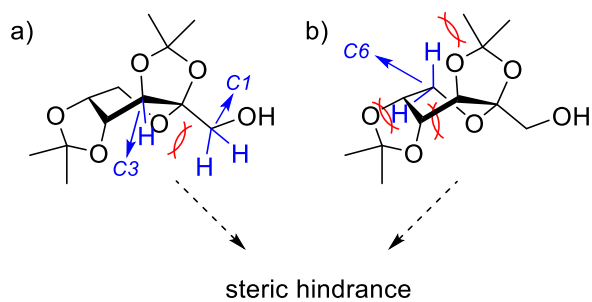
In 2005, Matsuo and Mayer observed that the log of the rate constants is proportional to the bond dissociation energies (BDEs) of C–H bonds in HAT reactions.¹⁴ Their findings indicated that HAT reactions tend to occur at the weakest C(sp³)–H bond of organic molecules. We performed BDE calculations for all C–H bonds at potential reaction sites of fructopyranose derivative boat conformation of **3-1a** using the UB3LTP/6-31G(d) method¹⁵ in Gaussian 16¹⁶. The obtained results are illustrated in Scheme 3-6. The results showed that the C–H bond at the C4-position has the weakest BDE (**3-1a-C4-1**, $\Delta\Delta G^\ddagger = + 82.8$ kcal/mol), and the BDE of the C–H bond at the C3-position was + 83.2 kcal/mol, which was close to the BDEs of C–H bonds at the C4-position. There was steric hindrance between two C1–H bonds and C3–H (Scheme 3-7a). Similarly, axial C6–H is affected by steric hindrance from the methyl group of isopropylidene moiety on C2 and C3, whereas equatorial C6–H faced steric hindrance from the adjacent oxygen atoms on C5 and C6 (Scheme 3-7b). These steric interactions limited the accessibility of excited photocatalyst to the C–H bonds. The

steric hindrance is observed from the 3D images of boat conformation of **3-1a** (Figure 3-1). Therefore, alkylation proceeded at C4-H and C5-H due to less steric hindrance.

Scheme 3-6. C(sp³)-H bond dissociation energies of boat conformation of **3-1a**.



Scheme 3-7. Minor reaction sites



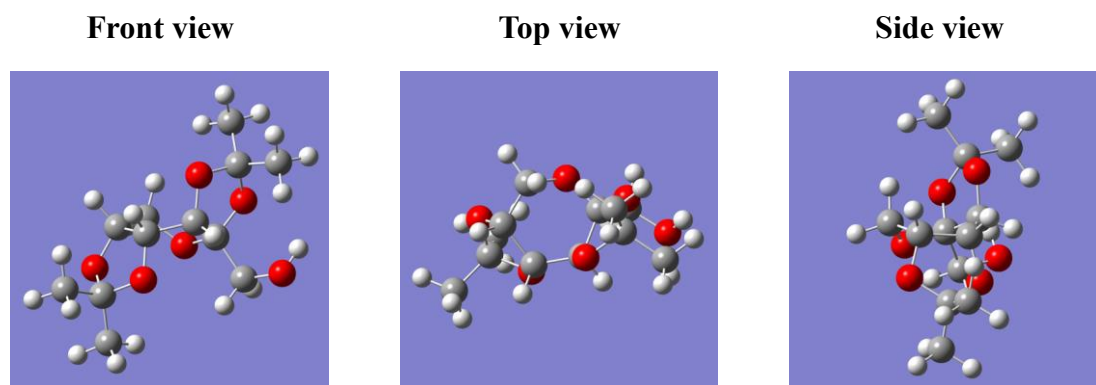


Figure 3-1. Boat conformation of **3-1a**.

According to the Nernst equation ($\Delta G = -RT \ln K_{eq}$), the ratio of the equilibrium constant (K_{eq}) of the C–H bond cleavage at C4- and C5-positions was estimated by calculating the value of K_{C4}/K_{C5} at 298K, without being affected by steric hindrance. The calculation result was that the ratio of the equilibrium constants for the C4–H to C5–H bond cleavage was 1691. Therefore, without considering being affected by steric hindrance, the yield of C–H alkylation at C4-position was much higher than that at C5-position.

The calculation process is as follows:

$$\Delta G_{C5} = -RT \ln K_{C5} \quad (1)$$

$$\Delta G_{C4} = -RT \ln K_{C4} \quad (2)$$

(1)-(2):

$$\Delta G_{C5} - \Delta G_{C4} = -RT \ln K_{C5} + RT \ln K_{C4}$$

$$\Delta G_{C5} - \Delta G_{C4} = RT(\ln K_{C4} - \ln K_{C5})$$

$$(\Delta G_{C5} - \Delta G_{C4})/RT = \ln(K_{C4} / K_{C5})$$

$$\frac{K_{C4}}{K_{C5}} = e^{(\Delta G_{C5} - \Delta G_{C4})/RT}$$

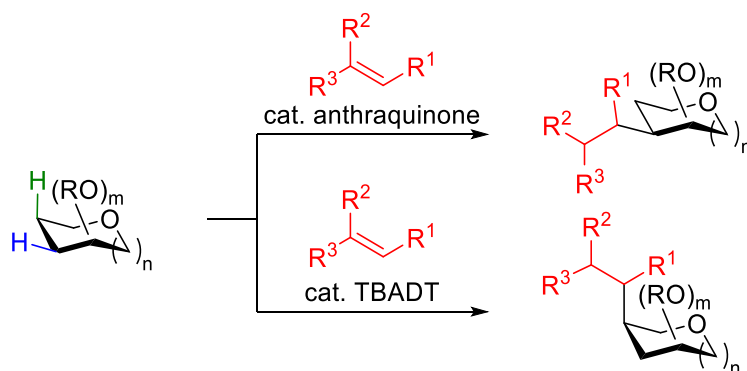
Putting the values:

$$\frac{K_{C4}}{K_{C5}} = 2.718^{(87.2-82.8)*4.184*1000/(8.31*298)}$$

$$\frac{K_{C4}}{K_{C5}} \approx 1691$$

We observed that the C(sp³)–H bond at the C4- and C5-positions exhibited lower hindrance compared to the C3- and C6- positions. Moreover, the C(sp³)–H bond at the C5 position possessed a higher BDE ($\Delta\Delta G^\ddagger = +87.2$ kcal/mol (**3-1a-C5-1**)) than that at the C4 position. With these factors in mind, we conducted screening of several aromatic ketones as potential photocatalysts for alkylation reaction. Interestingly, when anthraquinone was employed as photocatalyst, the major product obtained was the C4-alkylated derivative (**3-3a**). To facilitate the selective alkylation at the C5 position, we utilized the bulky TBADT as the photocatalyst. Encouraged by these results, we expanded our investigation to explore the site-selective alkylation of other saccharide derivatives. Additionally, we proposed reaction mechanisms to elucidate the processes involved (Scheme 3-8).

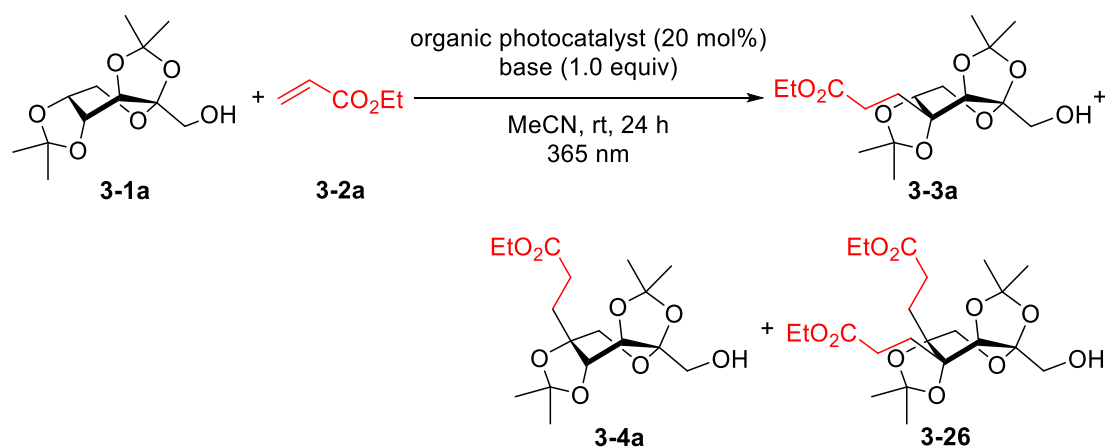
Scheme 3-8. Switching the reaction sites by catalyst control (**This work**).



3.2.2 Screening of HAT Photocatalysts

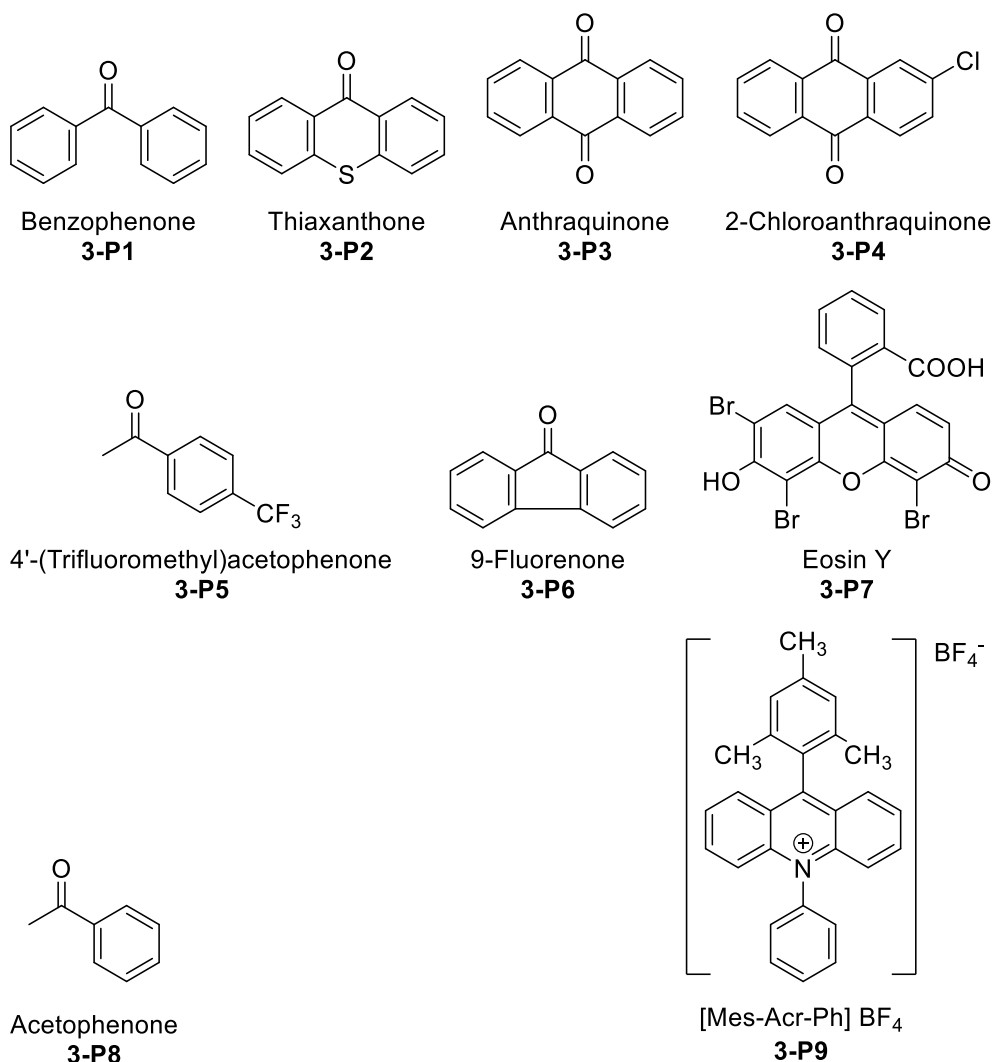
Fructopyranose derivative **3-1a** and ethyl acrylate (**3-2a**) were selected as a model substrate and alkylation reagent, respectively, to investigate C(sp³)-H alkylation by screening several organic photocatalysts (Table 3-1-1). When using benzophenone as the photocatalyst, the total yields of alkylated products **3-3a**, **3-4a**, and **3-26** was 5% (entry 1). The total yields increased to 58% when thioxanthenone was used as the photocatalyst (entry 2). It is worth noting that when anthraquinone was employed, the total yields of alkylated products **3-3a**, **3-4a**, and **3-26** was increased to 80% (entry 3). However, the main product was dialkylated product where both the C-H bonds at C4- and C5-positions were alkylated, and the ratio of **3-3a** to **3-4a** was 5.2 (entry 3). The good performance of anthraquinone, due to big π -conjugation structure making the excited state more active. When the base was changed to K₃PO₄, the total yields of alkylated products **3-3a**, **3-4a**, and **3-26** was increased to 95% (entry 4). At the same time, the formation of dialkylated products was suppressed, and the alkylated product **3-3a** became the main product, and the ratio of **3-3a**, **3-4a**, and **3-26** was 2.8:1.0:1.2 (entry 4). Using 2-chloroanthraquinone resulted in total yields of 87% for alkylated products, with a ratio of 2.7:1.0:0.8 for **3-3a**, **3-4a**, and **3-26** (entry 5). When 4'-(trifluoromethyl)acetophenone was employed, the total yields of alkylated products was 34% (entry 6). When using 4'-(trifluoromethyl)acetophenone, a decrease in the ratio of **3-3a** to **3-4a** was observed compared to anthraquinone. Although the size of 4'-(trifluoromethyl)acetophenone is smaller than anthraquinone. The steric hindrance still affected the reaction with the C-H bond of **3-1a**. The alkylated products were not formed using 9-fluorenone, eosin Y, [Mes-Acr-Ph]BF₄, and acetophenone as photocatalysts, with NaHCO₃ as the base (entries 7-10). Finally, in the absence of photocatalyst, the formation of alkylated products was not observed (entry 11). It indicated that anthraquinone play as the catalyst in this reaction system.

Table 3-1-1. Screening of organic photocatalysts for C(sp³)-H alkylation of **3-1a**.^a



entry	organic photocatalysts	base (1 equiv)	GC conv. (%)	GC yield ^b (%)	ratio (3-3a : 3-4a : 3-26)
1	Benzophenone	NaHCO ₃	33	5	1.8:1.0:0.46
2	Thioxanthenone	NaHCO ₃	60	58	2.7:1.0:1.5
3	Antraquinone	NaHCO ₃	>99	80	5.2:1.0:6.6
4	Antraquinone	K ₃ PO ₄	97	95	2.8:1.0:1.2
5	2-Chloroantraquinone	K ₃ PO ₄	92	87	2.7:1.0:0.8
6	4'-(Trifluoromethyl)acetophenone	K ₃ PO ₄	38	34	2.1:1.0:0.3
7	9-Fluorenone	NaHCO ₃	<1	-	-
8	Eosin Y	NaHCO ₃	2	-	-
9	[Mes-Acr-Ph]BF ₄	NaHCO ₃	<1	-	-
10	Acetophenone	NaHCO ₃	<1	-	-
11	-	NaHCO ₃	-	-	-

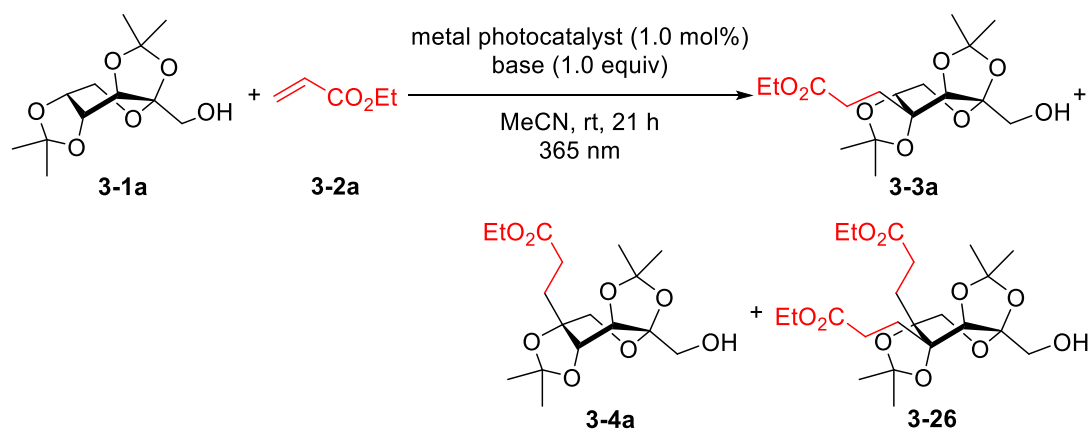
^a**3-2a** (2 equiv), MeCN (0.1 M); ^bTotal yields of **3-3a**, **3-4a**, and **3-26**.



To further explore the possibilities, we extended the investigation by screening several metal photocatalysts (Table 3-1-2). When using TBADT as a catalyst, the total yields of **3-3a**, **3-4a**, and **3-26** was 80%, and the ratio of them was <1:98:2 (entry 1). Similarly, when NaDT was employed, the total yields of **3-3a**, **3-4a**, and **3-26** was 86%, and the ratio of them was <1:91:9 (entry 2). The higher selectivity observed with TBADT compared to NaDT can be attributed to the larger size of tetrabutylammonium as the cation, which influences reaction outcomes (entries 1 and 2). When using iridium photocatalysts **3-P12** ([Ir{dF(CF₃)ppy}₂(dtbpy)]PF₆) and **3-P13** (Ir(ppy)₃), and ruthenium photocatalysts **3-P14** (RuCl₂(phen)₃), **3-P15** (Ru(bpy)₃Cl₂•6H₂O) and **3-P16** (Ru(bpy)₃(PF₆)₂), the desired reaction did not proceed (entries 3 and 5-8). However, in the presence of **3-P12**, quinuclidine, and Na₂CO₃, alkylated products were formed with 40% yield and a ratio of <1:6:94 for **3-3a**, **3-4a**, and **3-26** (entry 4). This highlights the

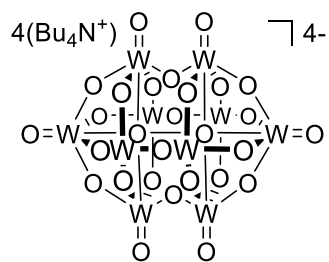
crucial roles of quinuclidine and Na₂CO₃ in the reaction. Only iridium photocatalyst **3-P12** is unable to directly activate the C–H bond of fructose derivative **3-1a**. The involvement of quinuclidine is necessary, as it undergoes electron transfer with **3-P12**, generating N–radical that act as abstractors for the C–H bond of **3-1a**. The mechanism is shown in Scheme 3-9. Therefore, when using iridium photocatalyst **3-P12** as the catalyst, the addition of quinuclidine and Na₂CO₃ is required for successful alkylation. The experiments showed that both TBADT and NaDT produced alkylated product **3-4a** with high yield and site-selectivity (entries 1 and 2), indicating that the reaction predominantly occurred at the C5–H bond, which has a larger bond dissociation energy. However, based on the calculation results using the Nernst equation (section 3.2.1), the reaction was expected to occur more favorably at the C4-position. I consider TBADT and NaDT are larger size compared to anthraquinone, exhibited steric hindrance that inhibited hydrogen abstraction from the C4-position.

Table 3-1-2. Screening of metal photocatalysts for C(sp³)–H Alkylation of **3-1a**.^a

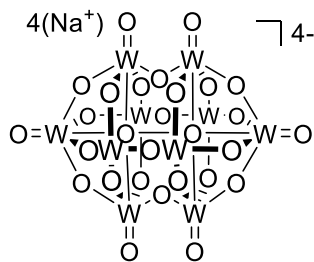


entry	metal photocatalysts	base (1 equiv)	GC conv. (%)	GC yield ^b (%)	ratio (3-3a : 3-4a : 3-26)
1	TBADT	NaHCO ₃	87	80	<1:98:2
2	NaDT	NaHCO ₃	92	86	<1:91:9
3	[Ir{dF(CF ₃)ppy} ₂ (dtbpy)]PF ₆	NaHCO ₃	<1	-	-
4 ^c	[Ir{dF(CF ₃)ppy} ₂ (dtbpy)]PF ₆	Na ₂ CO ₃	45	40	<1:6:94
5	Ir(ppy) ₃	NaHCO ₃	<1	-	-
6	RuCl ₂ (phen) ₃	NaHCO ₃	<1	-	-
7	Ru(bpy) ₃ Cl ₂ •6H ₂ O	NaHCO ₃	<1	-	-
8	Ru(bpy) ₃ (PF ₆) ₂	NaHCO ₃	<1	-	-

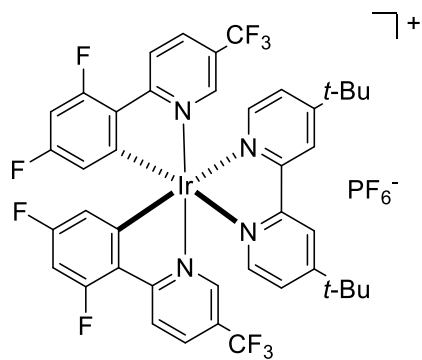
^a**3-2a** (3 equiv), MeCN (0.1 M); ^byield of **3-3a**; ^cQuinuclidine (30 mol%), Na₂CO₃ (1.5 equiv).



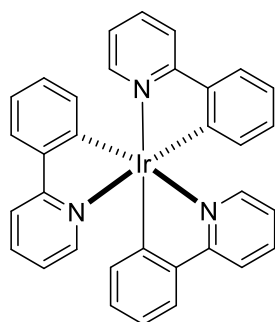
TBADT
3-P10



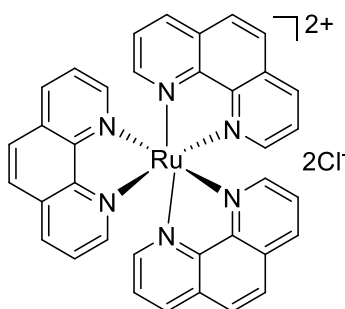
NaDT
3-P11



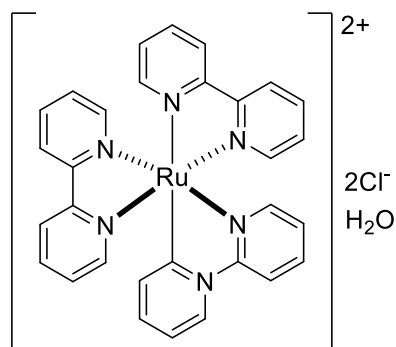
[Ir{dF(CF₃)ppy}₂(dtbbpy)]PF₆
3-P12



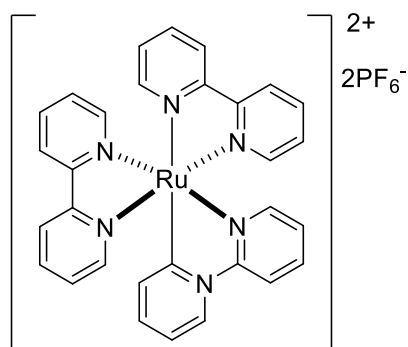
Ir(ppy)₃
3-P13



Ru(phen)₃Cl₂
3-P14

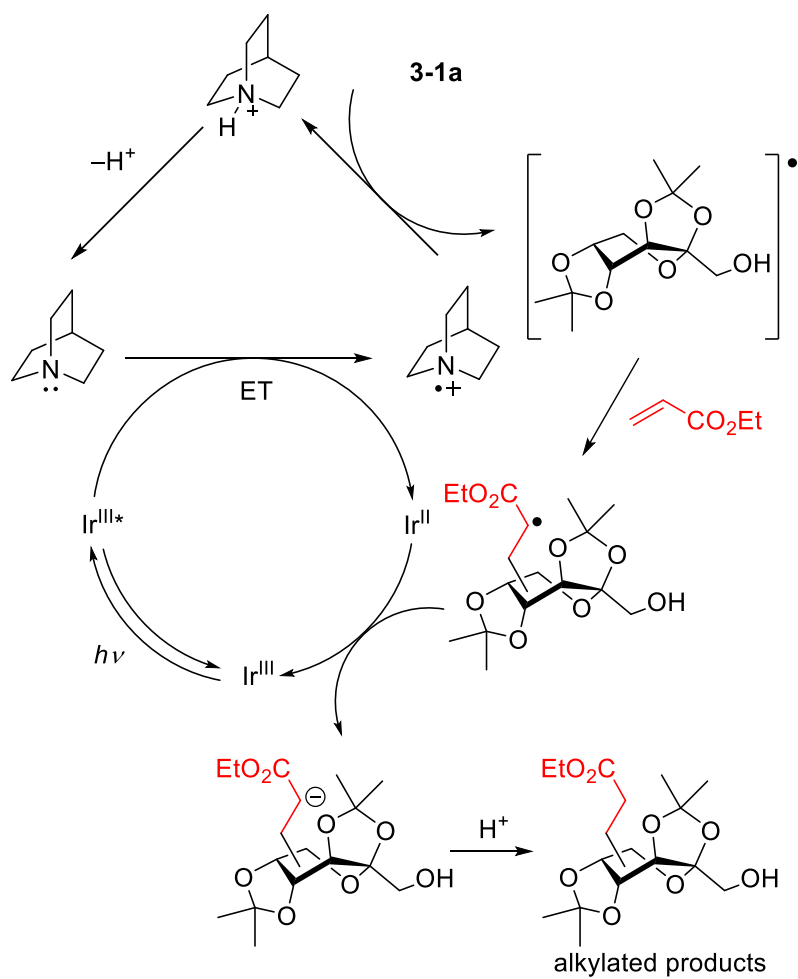


Ru(bpy)₃Cl₂·H₂O
3-P15



Ru(bpy)₃(PF₆)₂
3-P16

Scheme 3-9. The possible mechanism of Table 3-1-2, entry 4.



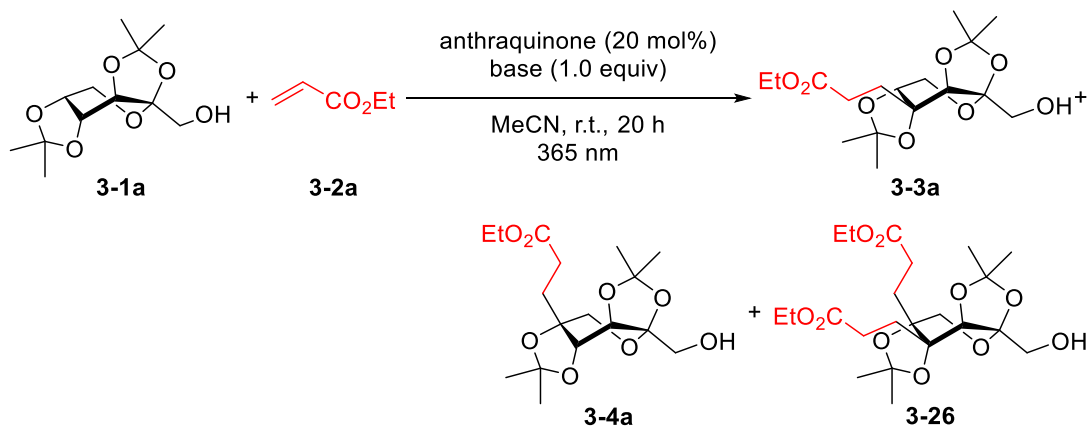
3.2.3 Optimization of Reaction Conditions for Anthraquinone-catalyzed C(sp³)-H Alkylation of **3-1a**

1) Screening of Bases

In the experiments using anthraquinone as the photocatalyst, good conversion of **3-1a** and yield of alkylated products were achieved (Table 3-1-1). Additionally, base was found to impact the product ratio. Therefore, the influence of bases in anthraquinone-catalyzed system was investigated to improve the yield of **3-3a** (Table 3-2). when no base was added to the reaction system, the total yields of **3-3a** and **3-4a** was 49% with a ratio of **3-3a:3-4a:3-26** of 2.5:1.0:0.75 (entry 1). This indicates that the reaction process is different from proton-coupled electron transfer (PCET) process observed in Chapter 2, where the involvement of a base is necessary for the PCET process. When NaHCO₃ was used as the base (entry 2), the total yields of **3-3a** and **3-4a** was 54% with a ratio of **3-3a:3-4a:3-26** of 3.0:1.0:2.1. Similarly, when Na₂CO₃, KHCO₃, K₂HPO₄ KH₂PO₄, and Cs₂CO₃ were employed as the base (entries 3–7), the total yields of **3-3a** and **3-4a** were 56%, 49%, 57%, 46% and 65% respectively. Finally, when K₃PO₄ was used as the base (entry 8), the total yields of **3-3a** and **3-4a** increased to 71% with a ratio of **3-3a:3-4a:3-26** of 2.7:1.0:0.85. Comparing the result in entry 1, the yield of **3-3a** and **3-4a** were improved by adding the base (NaHCO₃, Na₂CO₃, KHCO₃, K₂HPO₄ and Cs₂CO₃), indicating that the addition of a base can inhibit the formation of by-products. Specially, compare the results of adding KHCO₃ and K₃PO₄, when adding K₃PO₄, the C5-H alkylated product **3-4a** was inhibited. Hence, I considered that the addition of base may inhibit the formation of by-products by altering the activity of the C-H bond. This effect can be attributed to the influence of inorganic salts on the reactivity of C-H bond activation. Photoexcited anthraquinone has strong electrophilic oxygen and tends to abstract the hydrogen atom of the nucleophilic C-H bond (Scheme 3-10a). And this normal HAT process is through three-center electron¹⁷ In MacMillan's work they reported the hydrogen bonding was formed between oxygen anion of phosphate and hydrogen atom of hydroxy group in HAT process, changing the activity of C-H linking to the hydroxy group (Scheme 1-28b).¹⁸ I considered the hydrogen bonding effected the three-center electron HAT process showed in Scheme 3-8b. The addition of a base may make low reaction activity of several C-H bonds of **3-1a** and the excited anthraquinone, and thus be inhibited. From the above experimental

results and discussion, it was observed that the alkylation reaction could promote by adding K_3PO_4 (entry 8).

Table 3-2. Screening of bases for anthraquinone-catalyzed $C(sp^3)$ -H alkylation of **3-1a**.^a

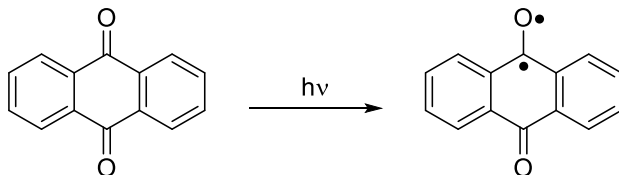


entry	base	GC conv. (%)	GC yield ^b (%)	ratio (3-3a : 3-4a : 3-26)
1	-	92	49	2.5:1.0:0.75
2	$NaHCO_3$	97	54	3.0:1.0:2.1
3	Na_2CO_3	>99	56	3.4:1.0:2.9
4	$KHCO_3$	>99	49	5.4:1.0:6.4
5	K_2HPO_4	>99	57	3.2:1.0:2.3
6	KH_2PO_4	90	46	2.5:1.0:0.76
7	CS_2CO_3	80	65	2.3:1.0:0.49
8	K_3PO_4	93	71	2.7:1.0:0.85

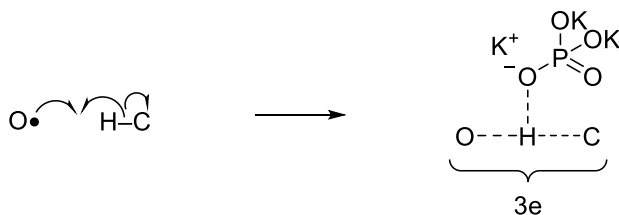
^a**3-2a** (2 equiv); MeCN (0.1 M); ^bTotal yields of **3-3a**, **3-4a**.

Scheme 3-10. The effect of bases.

a) Anthraquinone excited by light to generate abstractor O radical



b) The three center transition state of HAT between O radical and C-H effected by K_3PO_4

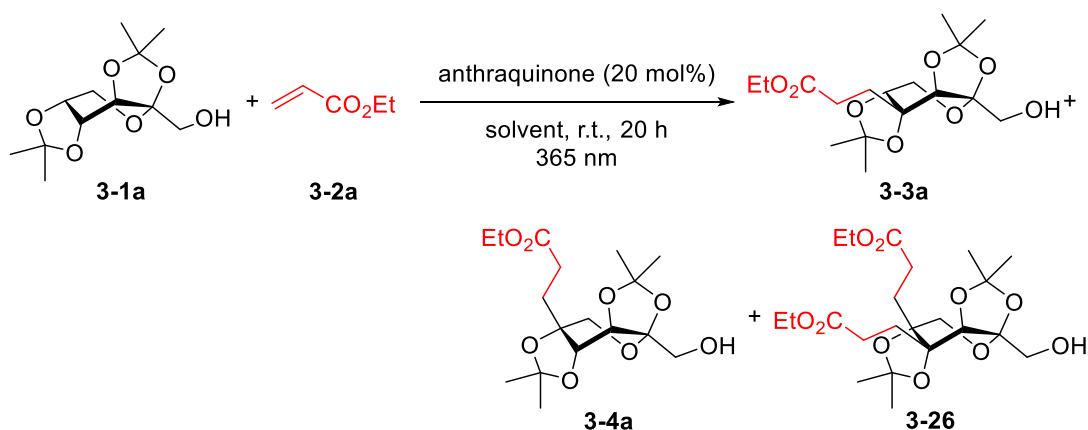


2) Screening of Solvents and the Amount of Alkenes

Since the reaction was also occurred smoothly without adding base. Therefore, when discussing the influence of the solvent effect, there was no base added (Table 3-2-1). When using CHCl_3 , the conversion of **3-1a** was 29% and the total yields of mono-alkylated products (**3-3a** and **3-4a**) was only 7% (entry 1). In contrast, when ethyl acetate was used, the conversion of **3-1a** increased to 55% and the total yields of mono-alkylated products increased to 18% (entry 2). Using DCM, the conversion of **3-1a** was 48% and the total yields of mono-alkylated products was only 12% (entry 4). When acetone was used, the conversion of **3-1a** was 87% and but the total yields of mono-alkylated products was only 29% (entry 6). In case of using MeCN as a solvent, the conversion of **3-1a** was 92% and the total yields of mono-alkylated products was only 49% (entry 8). When THF, pyridine, DMF and DMSO were used, no alkylated product was formed (entry 3, 5, 7, 9)

From the experimental results, alkylated products were obtained in CHCl_3 , ethyl acetate, DCM, acetone, and MeCN. These solvents have dielectric constants of 4.2, 6.0, 8.9, 21, and 38, respectively. On the other hand, the reaction did not occur in THF, pyridine, DMF, and DMSO, with dielectric constants of 7.6, 12, 37, and 47, respectively. In conclusion, the dielectric constant was not the primary factor influencing the occurrence of this reaction.

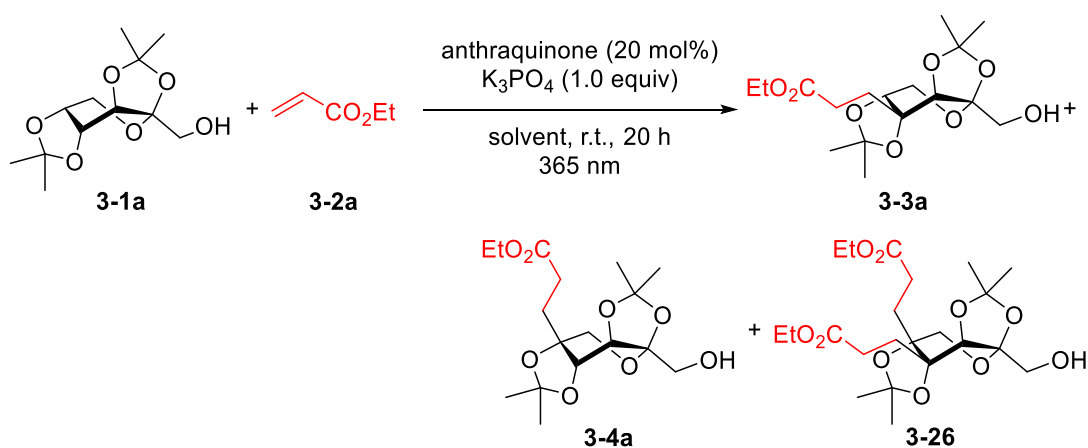
The HAT processes were similar in anthraquinone-catalyzed and TBADT-catalyzed systems. In section 3.2.4.2, the excited decatungstate anion was converted to reactive transient **wO**, which possessed the oxyradical-like character. According to the investigation by Seghrouchni *et al.*, the transient **wO** species of the decatungstate anion exhibited high reactivity towards various organic solvents. However, $\text{W}_{10}\text{O}_{32}^{4-}$ formed strong precomplexes with MeCN and acetone, enabling effective reactivity of the **wO** species in these solvents.¹⁹ In section 3.1.1, the excited anthraquinone also possessed the reactive oxygen radical. I hypothesized that the excited anthraquinone also formed strong precomplexes with MeCN and acetone, ensuring the effectiveness of the **reactive species**. Therefore, we observed smooth formation of alkylated products **3-3a** and **3-4a** in both acetone and MeCN (entries 1, 2, 4, 6, and 8).

Table 3-2.1. Screening of solvents.^a

entry	solvent	dielectric constant	GC conv. (%)	GC yield ^b (%)	ratio (3-3a : 3-4a : 3-26)
1	CHCl ₃	4.2	29	7	1.9:1.0:<0.1
2	ethyl acetate	6.0	55	18	1.5:1.0:<0.1
3	THF	7.6	1	-	-
4	DCM	8.9	48	12	2.1:1.0:<0.1
5	pyridine	12	<1	-	-
6	acetone	21	87	29	2.3:1.0:<0.1
7	DMF	37	40	-	-
8	MeCN	38	92	49	2.5:1.0:0.75
9	DMSO	47	33	-	-

^a**3-2a** (2 equiv); solvent (0.1 M); ^bTotal yields of **3-3a**, **3-4a**.

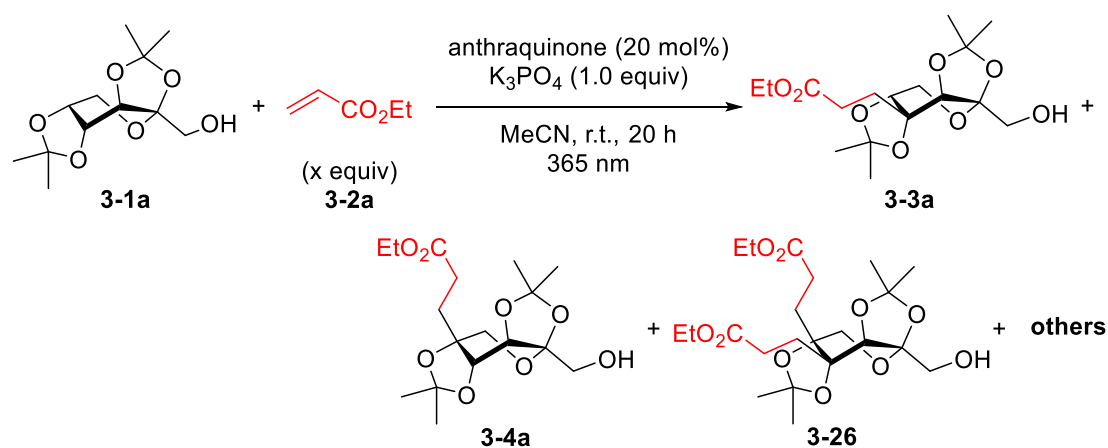
To investigate the influence of mixed solvents, a combination of MeCN and water, the addition of K₃PO₄ as an inorganic base was considered (Table 3-2-2). When a mixed solvent of MeCN/H₂O (2:1) was used, the conversion of **3-1a** was 74%, and the total yields of **3-3a** and **3-4a** was 51% (entry 1). Increasing the MeCN/H₂O ratio to 5:1 resulted in a higher conversion of **3-1a** at 82%, and the total yields of **3-3a** and **3-4a** increased to 63% (entry 2). Further increasing the MeCN/H₂O ratio to 10:1 led to a conversion of **3-1a** at 88%, with 65% yield of **3-3a** and **3-4a** (entry 3). Based on the experimental results, the addition of water to the reaction system had a negative impact on the alkylation process. As the amount of water increased from 1/10 to 1/2, the yield of mono-alkylated products decreased from 65% to 51%. Moreover, the proportion of **3-3a** in the alkylation products did not increase. When anhydrous MeCN was used as the solvent, the conversion of the reaction reached 93%, and the total yields of **3-3a** and **3-4a** was 71% (entry 4). Therefore, adding water in this reaction system was not conducive to alkylation.

Table 3-2.2. Screening of mixed solvents.^a

entry	MeCN/H ₂ O	conc. (mol/L)	GC conv. (%)	GC yield ^b (%)	ratio (3-3a:3-4a:3-26)
1	2:1	0.1	74	51	1.7:1.0:0.37
2	5:1	0.1	82	63	2.1:1.0:0.68
3	10:1	0.1	88	65	2.7:1.0:1.0
4	anhydrous MeCN	0.1	93	71	2.7:1.0:0.85

^a3-2a (2 equiv); MeCN (0.1 M); ^bTotal yields of 3-3a, 3-4a.

To improve the yield of 3-3a, the amount of ethyl acrylate (3-2a) was investigated (Table 3-2-3). When adding 1 equivalent of 3-2a, the total yields of 3-3a and 3-4a was 46% and the ratio of 3-3a:3-4a:3-26:others (alkylated products) was 1.6:1.0:0.20:<0.1 (entry 1). It was observed that the reaction was incomplete, resulting in lower yields of multi-alkylated products. Increasing the amount to 2 equivalents of 3-2a resulted in 71% total yields of 3-3a and 3-4a, with a ratio of 3-3a:3-4a:3-26:others of 2.7:1.0:0.85:<0.1 (entry 2). When 3 or 4 equivalents of 3-2a were added, the total yields of 3-3a and 3-4a decreased to 35% and 21% respectively, and the ratio of 3-3a:3-4a:3-26:others changed significantly (entries 3-4). Even with 6 equivalents of 2a, the total yields of 3-3a and 3-4a was only 22%, with a ratio of 3-3a:3-4a:3-26:others of 3.5:1.0:5.7:3.0 (entry 5). The addition of more than 2 equivalents of 3-2a resulted in increased yields of multi-alkylated products and a decrease in the proportion of mono-alkylated products (entries 2-5). Therefore, the amount of ethyl acrylate (3-2a) was 2 equivalents, leading to best results.

Table 3-2.3. Screening of the amount of alkenes.^a

entry	2a (equiv)	GC yield (%) ^b	ratio (3-3a:3-4a: 3-26:others)
1	1	46	1.6:1.0:0.20: <0.1
2	2	71	2.7:1.0:0.85:<0.1
3	3	35	14:1.0:28:5.2
4	4	21	3.5:1.0:2.7:0.2
5	6	22	3.5:1.0:5.7:3.0

^aMeCN (0.1 M); ^bTotal yields of 3-3a, 3-4a.

3) Screening of Reaction Time and Temperature

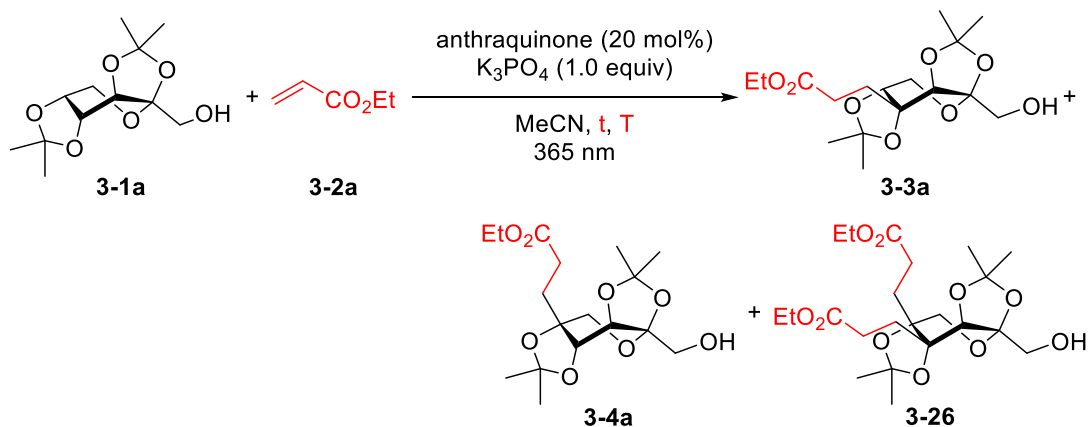
In Table 3-3, the effects of reaction time and temperature were investigated to improve the yield of 3-3a. When the reaction time was 12 h (entry 1), total yields of mono-alkylated products 3-3a and 3-4a was 65% with a ratio of 2.3:1.0:0.5 (3-3a:3-4a:3-26). It indicated that the conversion of 3-1a was incomplete. Increasing the reaction time to 24 h (entry 2) resulted in total yields of 72% for mono-alkylated products, with a ratio of 2.8:1.0:1.2. However, extending the reaction time to 36 h (entry 3) led to a decrease in the total yields to 53%, with a ratio of 2.9:1.0:1.8, while the yields of multi-substituted products increased.

Regarding the reaction temperature, at 15 °C (entry 4), total yields of mono-alkylated products 3-3a and 3-4a were 69% with a ratio of 2.9:1.0:1.0. Lowering the temperature to 10 °C (entry 5) resulted in a slightly higher total yields of 72% for mono-alkylated products with a ratio of 3.4:1.0:0.6. Further decreasing the temperature to 5 °C (entry 6) led to a decrease in the total yields to 61% with a ratio of 2.3:1.0:0.2.

The experimental results reveal that both reaction time and temperature play significant roles in the yield and selectivity of the mono-alkylated products. In summary,

the results suggested that optimal reaction time of 24 h and temperature of 10 °C provide the highest yield and selectivity for the desired mono-alkylated products.

Table 3-3. Screening of reaction time and temperature.^a



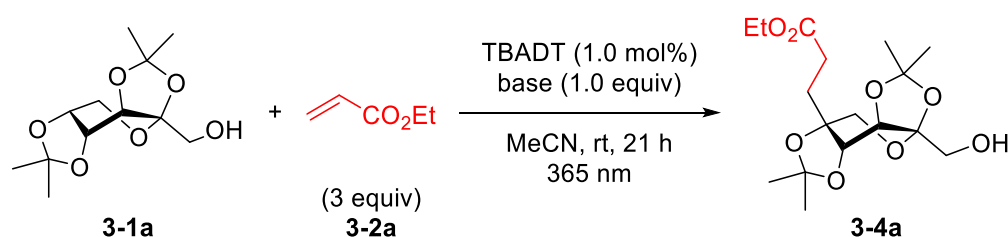
entry	time (h)	T (°C)	GC yield (%) ^b	ratio (3-3a:3-4a:3-26)
1	12	rt	65	2.3:1.0:0.5
2	24	rt	72	2.8:1.0:1.2
3	36	rt	53	2.9:1.0:1.8
4	24	15	69	2.9:1.0:1.0
5	24	10	72	3.4:1.0:0.6
6	24	5	61	2.3:1.0:0.2

^a3-2a (2 equiv); MeCN (0.1 M); ^bTotal yields of 3-3a, 3-4a.

3.2.4 Optimization of Reaction Conditions for TBADT-catalyzed C(sp³)-H Alkylation of **3-1a**

1) Screening of Bases

Several bases were screened to improve the yield of **3-4a** (Table 3-4). When Na₂CO₃ was used as the base (entry 1), the conversion of **3-1a** was 96% and the yield of **3-4a** was 86%. Similarly, using KHCO₃, Na₂HPO₄, NaH₂PO₄ and K₃PO₄ as bases resulted in conversions of **3-1a** were 97%, 95%, 89%, and 77%, respectively, and yields of **3-4a** were 83%, 89%, 88%, and 63%, respectively (entries 2–5). Interestingly, the addition of K₃PO₄ to the TBADT-catalyzed system led to a decrease in both the conversion of **3-1a** and the yield of **3-4a**, indicating its inhibitory effect on the alkylation of C5–H. This observation was consistent with the findings in the anthraquinone catalytic system, where the addition of K₃PO₄ inhibited the alkylation of C5–H, leading to an increase in the proportion of **3-3a** (at C4–H alkylation) and a decrease in the yield of multi-alkylated products. When Cs₂CO₃ was added as the base (entry 6), a significant decrease in both the conversion of **3-1a** and the yield of **3-4a** was observed, reaching 30% and 9% respectively. The results observed that the yield of **3-4a** was inhibited in the presence of any base. According to the report by Hill *et al.*, the HAT process of the excited dectungstate anion with C–H bonds of substrates did not require a base, as discussed in section 3.1.2.²⁰ The reason of decreasing the yield of **3-4a** by adding a base likely inhibits the formation of the transition state of hydrogen atom abstraction of C5–H bond by oxygen radical (similar to Scheme 3-7b).²¹ Therefore, the best result was obtained without adding a base, where the conversion of **3-1a** was 93% and the yield of **3-4a** was 92% (entry 7).

Table 3-4. Screening of bases.^a

entry	base	GC conv. (%)	GC yield (%)
1	Na ₂ CO ₃	96	86
2	KHCO ₃	97	83
3	Na ₂ HPO ₄	95	89
4	NaH ₂ PO ₄	89	88
5	K ₃ PO ₄	77	63
6	Cs ₂ CO ₃	30	9
7	-	93	92

^aMeCN (0.1 M).

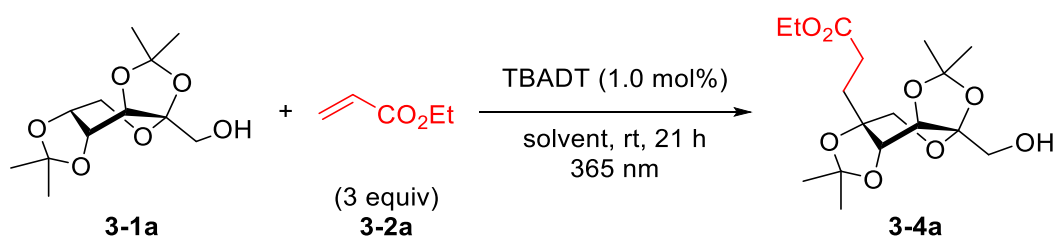
2) Screening of Solvents and the Amounts of Alkenes

Several solvents were investigated to improve the yield of mono-alkylated product **3-4a** (Table 3-5-1). When solvents, such as CHCl₃, ethyl acetate, THF, DMF and DMSO were used, **3-4a** was not obtained (entries 1-3, 6, and 8). However, when pyridine was used as the solvent, the yield of mono-alkylated product **3-4a** was only 4% (entry 4). On the other hand, when acetone was used as the solvent, the yield of **3-4a** was 64% (entry 5). The highest yield of **3-4a**, reaching 92%, using MeCN as the solvent (entry 7).

From the above results, alkylated product **3-4a** was observed using pyridine, acetone, and MeCN as solvents, despite their different dielectric constants. The dielectric constants of these solvents are 12, 21, and 38, respectively. In contrast, CHCl₃, ethyl acetate, THF, DMF, and DMSO have dielectric constants of 4.2, 6.0, 7.6, 37, and 47, respectively, but no significant formation of alkylation products was observed. These results suggested that the yield of **3-4a** did not show a clear correlation with the dielectric constants of the solvents used in this study. In section 3.2.3, the solvent effect was discussed in anthraquinone catalytic system, which shared similarities with HAT reaction processes in TBADT catalytic system. Notably, similar results were obtained in both systems, where acetone and MeCN were found to be favorable solvents.

Seghrouchni, *et al.* investigated solvent effect of HAT reaction process. They found that transient **wO** species of the decatungstate anion exhibited high reactivity with various organic solvents. However, $W_{10}O_{32}^{4-}$ formed strong precomplexes with MeCN and acetone, allowing the **wO** to react effectively in these solvents. Our experimental results were consistent with these findings, as we observed good yields of alkylated product **3-4a** in both acetone and MeCN (entries 5 and 7).

Table 3-5-1. Screening of solvents.^a



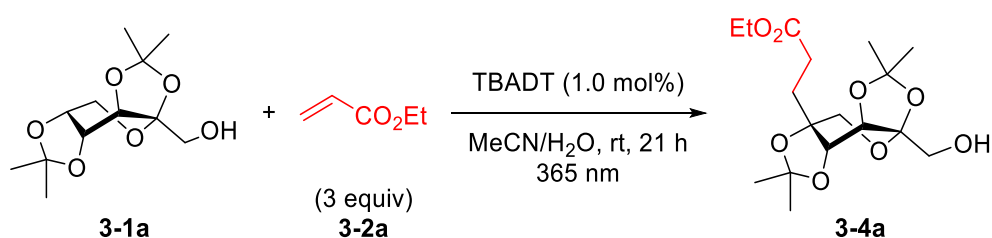
entry	solvent (1.0 mL)	dielectric constant	GC conv. (%)	GC yield (%)
1	CHCl ₃	4.2	<1	-
2	ethyl acetate	6.0	1	-
3	THF	7.6	<1	-
4	pyridine	12	7	4
5	acetone	21	67	64
6	DMF	37	43	-
7	MeCN	38	94	92
8	DMSO	47	8	-

^asolvent (0.1 M).

The ratio between MeCN and H₂O in the mixed solvent was investigated to improve the yield of **3-4a** (Table 3-5-2). When H₂O was used as the sole solvent, the yield of **3-4a** was only 2% (entry 1). This result indicates that the reaction was significantly inhibited by H₂O. When the mixed solvent MeCN/H₂O (1:1) was added, the yield of **3-4a** was increased to 31% (entry 2). Increasing the MeCN/H₂O ratio to 5:1 resulted in a higher yield of **3-4a** at 55% (entry 3). Further increasing the MeCN/H₂O ratio to 20:1 led to the yield of **3-4a** at 84% (entry 4). These results demonstrated that as the amount of water decreased in the solvent mixture, the yield of **3-4a** increased. When anhydrous MeCN was used, the yield of **3-4a** reached 92% (entry 5). Hence, the addition of water in this reaction system was found to be unfavorable for the alkylation process.

The effect of solvent concentration on the reaction was also investigated. When the concentration was increased to 0.2 M, the yield of **3-4a** decreased to 89% (entry 6). Similarly, when the concentration was reduced to 0.05 M and 0.025 M, the yields of **3-4a** decreased further to 63% and 46%, respectively (entries 7 and 8). These results indicate that as the reaction concentration decreased, the yield of **3-4a** gradually decreased as well. The lower concentration may have hindered the reaction between the excited TBADT and **3-1a**, resulting in lower yields (entries 5, 7, and 8). Based on these observations, it can be concluded that the optimized conditions for the reaction involve using anhydrous MeCN with a concentration of 0.1 M.

Table 3-5-2. Screening of ratio of MeCN/H₂O and concentration.



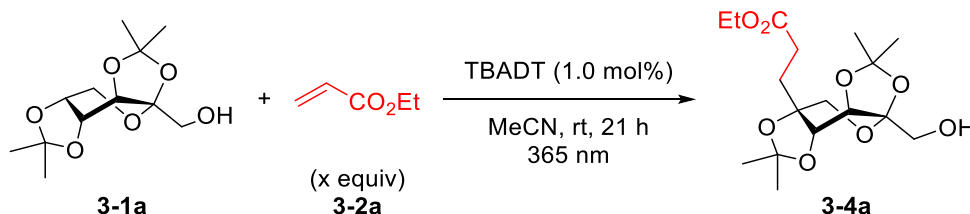
entry	MeCN/H ₂ O	conc. (mol/L)	GC conv. (%)	GC yield (%)
1	H ₂ O	0.1	20	2
2	1:1	0.1	33	31
3	5:1	0.1	69	55
4	20:1	0.1	90	84
5	anhydrous MeCN	0.1	94	92
6	anhydrous MeCN	0.2	91	89
7	anhydrous MeCN	0.05	68	63
8	anhydrous MeCN	0.025	51	46

^aMeCN (0.1 M).

The amount of ethyl acrylate (**3-2a**) was investigated (in Table 3-5-2). When 1 equivalent of **3-2a** was added, the yield of **3-4a** was 42% (entry 1). Increasing the amount to 2 equivalents led to an improved yield of 77% (entry 2). However, in both cases (entries 1 and 2), **3-1a** did not completely react, likely due to an insufficient amount of **3-2a**. To address this, 3 equivalents of **3-2a** were added, resulting in the highest yield of 92% (entry 3). However, when the amount of **3-2a** was further increased to 4 equivalents, the yield of **3-4a** decreased to 86% due to the formation of some by-

products (entry 4). In summary, the optimal amount of **3-2a** to achieve the highest yield of **3-4a** was found to be 3 equivalents.

Table 3-5-3. Screening of the amount of alkenes.^a



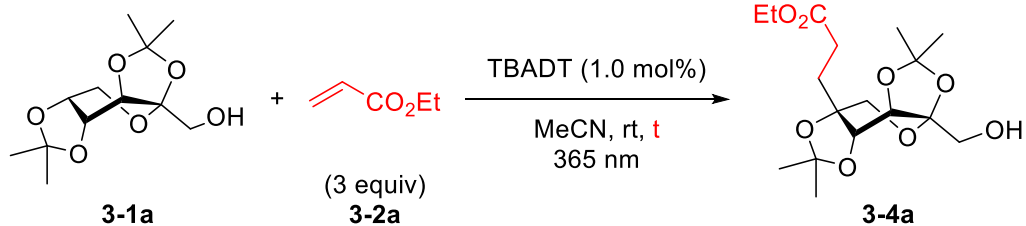
entry	3-2a (equiv)	GC conv. (%)	GC yield (%)
1	1	46	42
2	2	85	77
3	3	94	92
4	4	97	86

^aAnhydrous MeCN (0.1 M).

3) Screening of Reaction Time

From the above experimental results, when the reaction time was 12 h, the yield of **3-4a** was 72% and **3-1a** was not fully converted (entry 1). Therefore, the reaction time was extended to 24 h (entry 2). As a result, the yield of **3-4a** was 96%. Although by the reaction time was prolonged to 36 h, the yield of **3-4a** was slightly decreased and by-products were formed (entry 3). Judging from the above experiments, the optimal reaction time was 24 h.

Table 3-6. Screening of reaction time.^a



entry	time (h)	GC conv. (%)	GC yield (%)
1	12	77	72
2	24	97	96
3	36	99	95

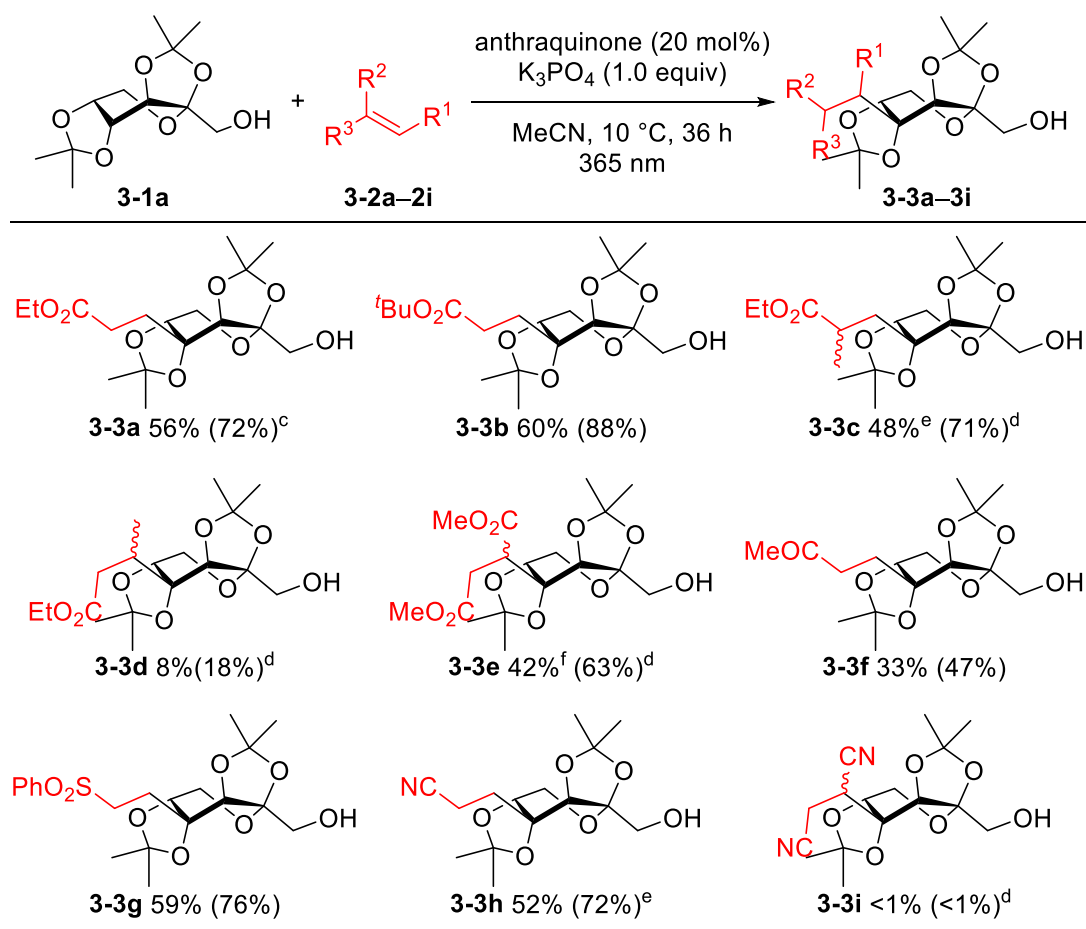
^aAnhydrous MeCN (0.1 M).

3.2.5 Scope of Alkenes

1) Scope of Alkenes for Anthraquinone-catalyzed C(sp³)-H Alkylation of 3-1a

Under the optimized reaction conditions shown in Table 3-3, entry 6, the alkylation reagents were investigated (Scheme 3-11). By using ethyl acrylate (**3-2a**), mono-alkylated fructopyranose derivative **3-3a** was obtained in 56% yield (total yields of **3-3a** and **3-4a** were 72%). When *tert*-butyl acrylate (**3-2b**) was used, the corresponding alkylated product **3-3b** was produced in 60% yield, and total yields of **3-3a** and **3-4a** were increased to 88%. This might be attributed to the larger size of the *tert*-butyl group, which inhibited the formation of multi-alkylated products. When using ethyl methacrylate (**3-2c**) or ethyl crotonate (**3-2d**), the corresponding alkylated products **3-3c** and **3-3d** were obtained in 48% and 8% yields, respectively. The yield of **3-3d** was lower than that of **3-3c**, probably due to the steric repulsion between the methyl group of **3-2d** and the substituents of **3-1a**. Dimethyl fumarate (**3-2e**) gave mono-alkylated product **3-3e** in 42% yield. By using vinyl ketone **3-2f**, vinyl sulfone **3-2g** or acrylonitrile **3-2h** as the alkylation reagents, the corresponding alkylated products **3-3f**, **3-3g**, and **3-3h** were obtained in 33%, 59%, and 52% yields, respectively. The C(sp³)-H alkylation did not proceed in the case of fumaronitrile (**3-2i**).

Scheme 3-11. Scope of alkenes for anthraquinone-catalyzed C(sp³)-H alkylation of **3-1a**.



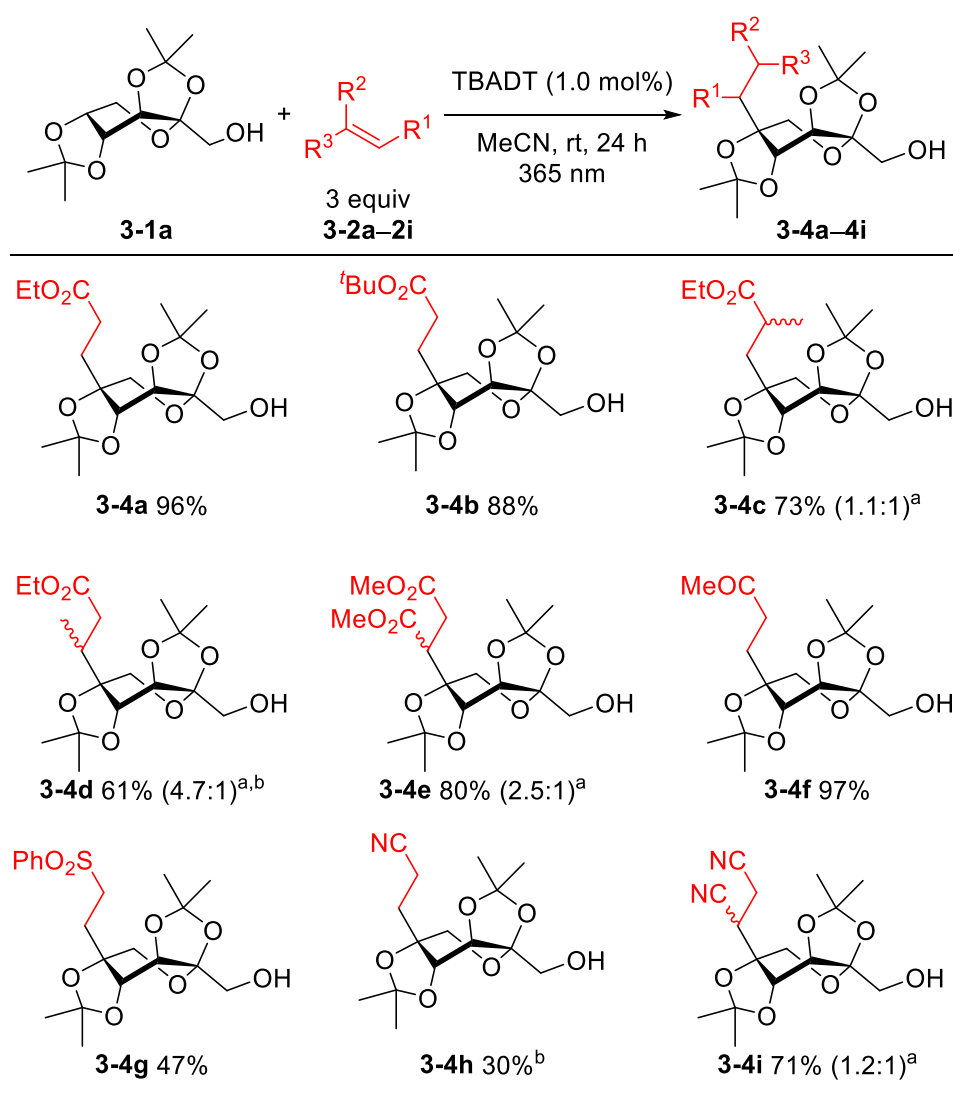
^a**3-2a** (2.0 equiv). ^bThe total yields of mono-alkylated products **3-3a-3i** and **3-4a-4i** (see **Scheme 3-6**) is reported in parentheses. ^c24 h. ^dr.t. ^eDiastereomers (1.4:1.0). ^fDiastereomers (1.6:1.0).

2) Scope of Alkenes for TBADT-catalyzed C(sp³)-H Alkylation of **3-1a**

Under the optimized reaction conditions shown in Table 3-6, entry 2, the alkylation reagents were investigated (**Scheme 3-12**). Treatment of fructopyranose derivative **3-1a** with ethyl acrylate (**3-2a**) or tert-butyl acrylate (**3-2b**) provided alkylated products **3-4a** and **3-4b** in 96% and 88% yields, respectively. The use of ethyl methacrylate (**3-2c**) or ethyl crotonate (**3-2d**) as substrates produced the corresponding alkylated products **3-4c** and **3-4d** in 73% and 61% yields, respectively, as a mixture of diastereomers. In the case of **3-2d**, the alkylation reaction proceeded by avoiding steric hindrance from the methyl group. Dimethyl fumarate (**3-2e**) provided **3-4e** in 80% yield,

with a diastereomeric ratio of 2.5:1. Methyl vinyl ketone (**3-2f**) gave the desired alkylated product **3-4f** in 97% yield. Phenyl vinyl sulfone (**3-2g**) and acrylonitrile (**3-2h**) also yielded the corresponding alkylated products **3-4g** and **3-4h** in 47% and 30%, respectively. Finally, fumaronitrile (**3-2i**) was used as an alkylation reagent, and alkylated product **3-4i** was obtained in 71% yield. Overall, these results demonstrate the broad alkenes scope and site-selectivity of the TBADT photocatalyzed C(sp³)-H alkylation reaction, and its potential utility in the synthesis of complex molecules.

Scheme 3-12. Scope of alkenes for TBADT-catalyzed C(sp³)-H alkylation of **3-1a**.



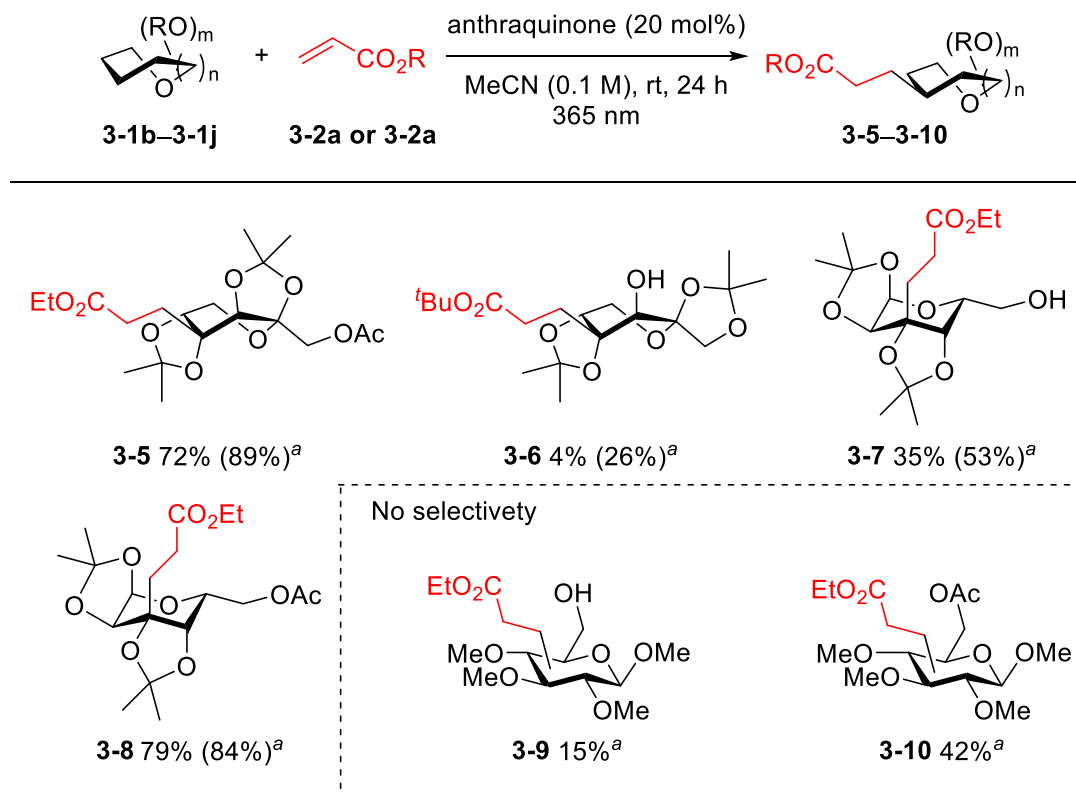
^aRatio of diastereomers. ^bTBADT (5.0 mol%), 36 h.

3.2.6 Scope of Saccharides

1) Scope of Saccharides for Anthraquinone-catalyzed C(sp³)-H Alkylation

Under the optimized reaction conditions shown in Table 3-3, entry 6, the scope of saccharides was investigated (Scheme 3-13). The structures of saccharides **3-1b-1j** are shown in the Experimental Section. C(sp³)-H alkylation of **3-1b** with **3-2a** gave the corresponding mono-alkylated product **3-5** in 72% yield (the total yields of mono-alkylated products was 89%). C(sp³)-H alkylated product **3-6** was formed from **3-1c** and **3-2b**, and the yield of **3-6** was low. The corresponding mono-alkylated products **3-7** and **3-8** were obtained in 35% and 79% yields, respectively. Using **3-1e** and its acetylated saccharide **3-1f** as the substrates, C(sp³)-H alkylation proceeded and the corresponding alkylated products **3-9** and **3-10** formed whereas the yields of the products were not satisfactory and there was no selectivity observed in the formation of alkylated products **3-9** and **3-10**. Five mono-alkylated products were detected by GC-MS in the reaction mixtures of **3-9** and **3-10**.

Scheme 3-13. Scope of saccharides for anthraquinone-catalyzed C(sp³)-H alkylation.

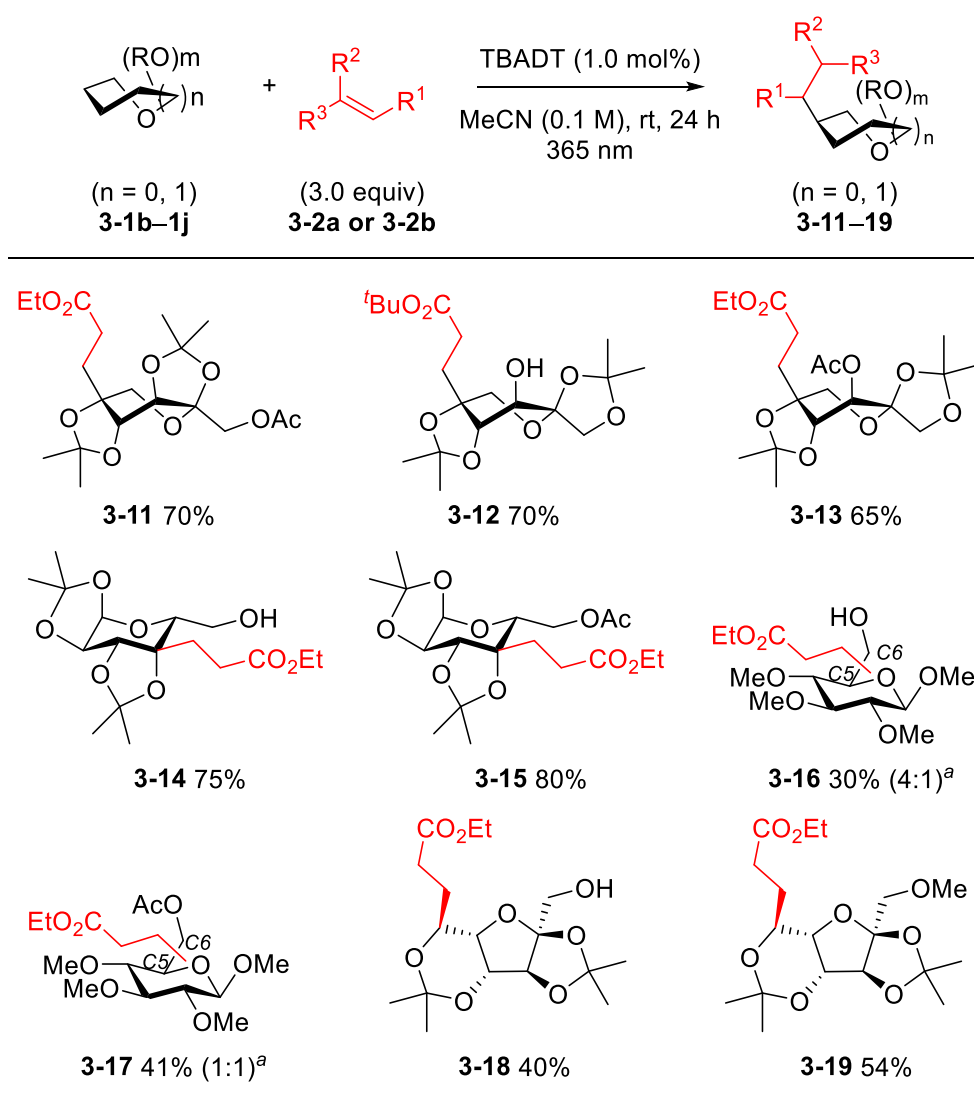


^aThe total yields of mono-alkylated products is reported in parentheses.

2) Scope of Protected Saccharides for TBADT-catalyzed C(sp³)-H Alkylation

Under the optimized reaction conditions shown in Table 3-6, entry 2, the scope of saccharides was investigated (Scheme 3-14). The alkylation of **3-1b**, in which the primary hydroxy group of **3-1a** was protected by acetyl group, with ethyl acrylate (**3-2a**) gave mono-alkylated fructopyranose derivative **11** in 70% yield. Saccharide **3-1c** bearing a different protecting pattern compared with **3-1a** reacted with *tert*-butyl acrylate (**2b**) to give mono-alkylated product **12** in 70% yield. The alkylation of saccharide **3-1d**, which is the acetylated compound of **3-1c**, with ethyl acrylate (**3-2a**) gave **13** in 65% yield. The desired mono-alkylated product **14** was obtained in 75% yield by the reactions of D-galactopyranose derivatives **3-1e** with **3-2a**. The alkylation also proceeded site-selectively using furanose as a substrate. Using **3-1i** and its acetylated saccharide **3-1j** as the substrates, C(sp³)-H alkylation proceeded and the corresponding alkylated products **16** and **17** formed whereas the site-selectivity of the products were not satisfactory (The alkylation proceeded at C5- and C6- positions). When acetyl group is used to protect C6-OH, the site-selectivity of C6-H was reduced, probably due to the steric hindrance. Mono-alkylated sorbose derivatives **18** and **19** were produced in 40% and 54% yields, respectively, by the reaction of L-sorbofuranose derivative **3-1g** or its methylated saccharide **3-1h** with **3-2a**.

Scheme 3-14. Scope of Protected Saccharides for TBADT-catalyzed C(sp³)-H Alkylation.



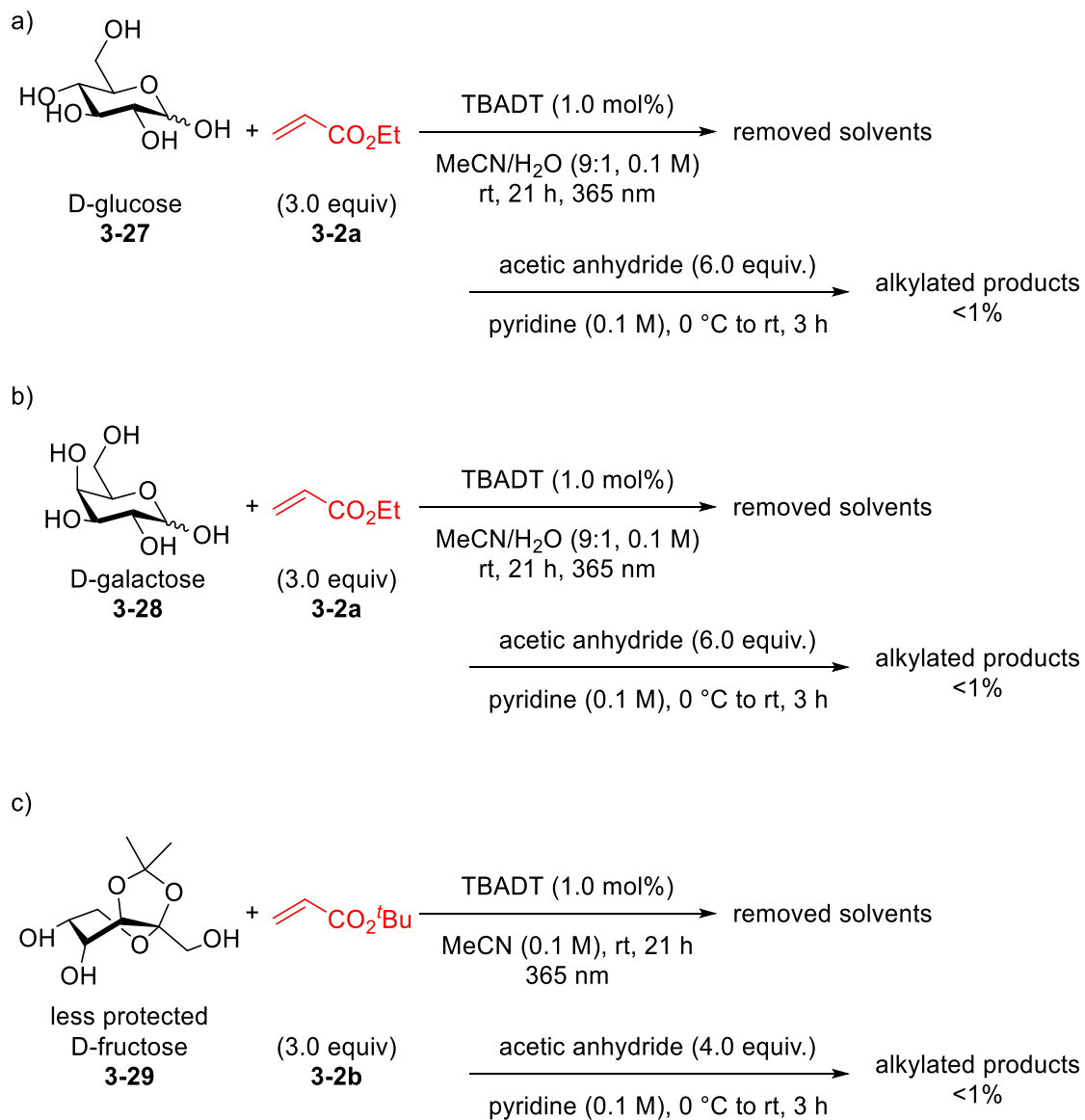
^a**3-2a** (1.0 equiv); The ratio of isomers is reported in parentheses.

3) Scope of Less or Unprotected Saccharides for TBADT-catalyzed C(sp³)-H Alkylation

By the reactions of unprotected glucose **3-27** or galactose **3-28** with **3-2a**, alkylated products were not formed (Scheme 3-15a, b). Similarly, in the reaction of less protected fructose **3-29** with **3-2b**, alkylated product was not obtained (Scheme 3-15c). In the second step of each reaction, the hydroxy groups of the reaction mixture were protected with acetic anhydride after first step, in order to facilitate the detection of alkylated product. I considered that saccharides contain many OH groups, which form strong

hydrogen bonding with the decatungstate anion of TBADT, and thus the catalytic activity of TBADT is inhibited.

Scheme 3-15. Scope of Less or Unprotected Protected Saccharides for TBADT-catalyzed C(sp³)-H Alkylation.

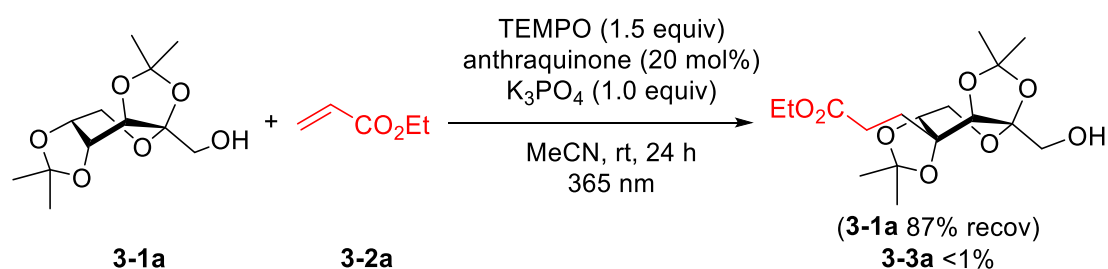


3.2.7 Proposed Reaction Mechanism

1) Radical Trapping Experiments

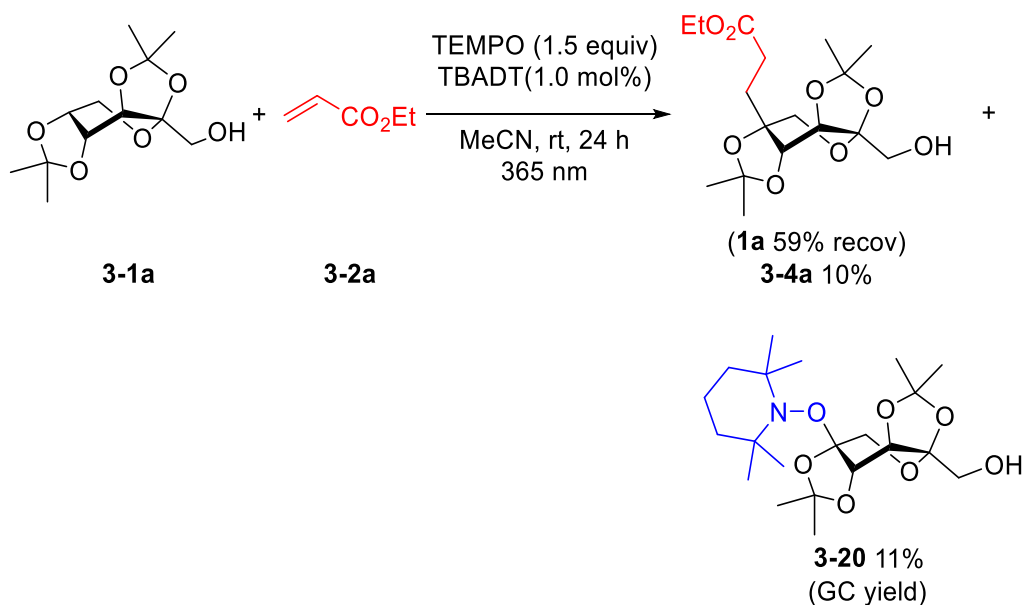
When adding 1.5 equivalents of TEMPO into anthraquinone-catalyzed C(sp³)-H alkylation under the reaction conditions in Table 3-3, entry 6, alkylated products **3-3a** and **3-4a** were not obtained. (Scheme 3-16). This result indicated that the C(sp³)-H alkylation proceeded via a radical pathway.

Scheme 3-16. Radical trapping experiment of anthraquinone-catalyzed C(sp³)-H alkylation using TEMPO.



When 1.5 equivalents of TEMPO were added to the TBADT-catalyzed C(sp³)-H alkylation under the reaction conditions described in Table 3-6, entry 2, a significant decrease in the yield of **3-3a** was observed (Scheme 3-17). Additionally, the formation of TEMPO-adduct **3-20** was observed. This result strongly suggested that C(sp³)-H alkylation proceeds through a radical pathway. The presence of TEMPO-adduct **20** indicated the generation of C5 radical during the reaction.

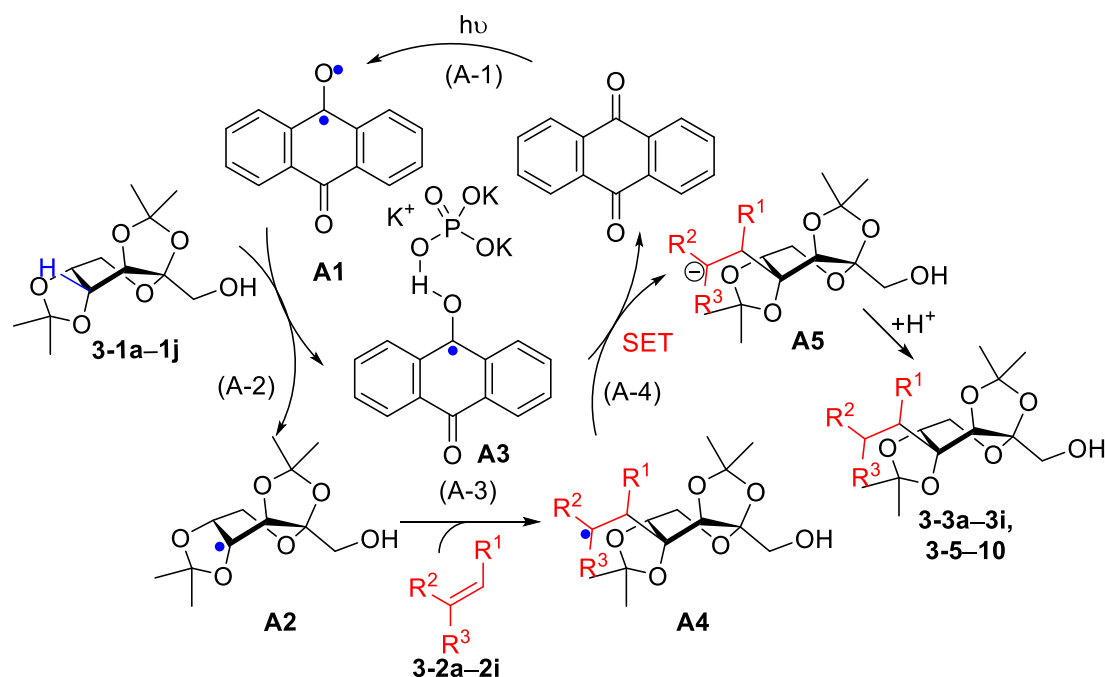
Scheme 3-17. Radical trapping experiment of TBADT-catalyzed C(sp³)-H alkylation using TEMPO.



2) Plausible Reaction Mechanism of Anthraquinone-catalyzed C(sp³)-H Alkylation

Based on the above results and previous reports, the plausible reaction mechanism of anthraquinone-catalyzed site-selective C(sp³)-H alkylation of saccharides is shown in Scheme 3-18a. For anthraquinone-catalyzed C(sp³)-H alkylation: (A-1) the photoexcitation of anthraquinone to generate excited anthraquinone **A1**; (A-2) the hydrogen abstraction from saccharide **3-1a–1j** with **A1** to give radical intermediate **A2** and radical species **A3**; (A-3) the nucleophilic addition of radical intermediate **A2** to electron-deficient alkene **3-2a–2i** to give radical intermediate **A4**; and (A-4) an electron transfer from **A3** to radical intermediate **A4** to form anion intermediate **A5** and regenerate anthraquinone photocatalyst. Finally, the intermediate **A5** was protonated to afford alkylated products **3-3a–3i** and **3-5–3-10**. In step A-4, the hydrogen bonding was formed between K₃PO₄ and OH of **A3**, which facilitated one electron transfer from **A3** to radical intermediate **A4**. The rate-determining step of the HAT process is the generation of a carbon radical species.²² The small-sized anthraquinone serves as a HAT photocatalyst, and site-selectivity was controlled by the C-H BDEs.

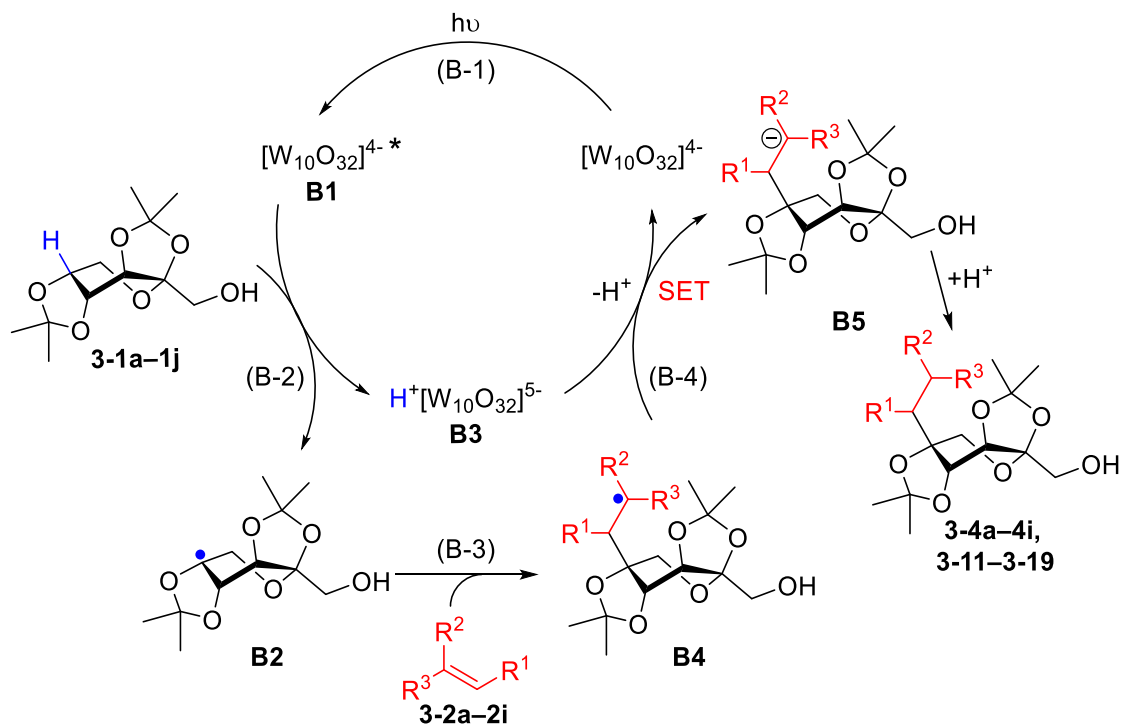
Scheme 3-18a. Plausible reaction mechanism of anthraquinone-catalyzed C(sp³)-H alkylation.



3) Plausible Reaction Mechanism of TBADT-catalyzed C(sp³)-H Alkylation

The plausible reaction mechanism of TBADT-catalyzed C(sp³)-H alkylation is shown in Scheme 3-18b: (B-1) the photoexcitation of the decatungstate [W₁₀O₃₂]⁴⁻ to generate the excited species [W₁₀O₃₂]^{4-*} (**B1**) by oxygen-to-metal charge-transfer (LMCT) upon UV-LED irradiation;²³ (B-2) the abstraction of a hydrogen atom from saccharide **3-1a-1j** by photoexcited **B1** to give radical intermediate **B2** and H⁺[W₁₀O₃₂]⁵⁻ (**B3**); (B-3) the nucleophilic attack of radical intermediate **B2** to electron-deficient alkene **3-2a-2i** to generate radical intermediate **B4**; and (B-4) an electron transfer from **B3** to radical intermediate **B4**, to generate anion intermediate **B5** and regenerate the decatungstate photocatalyst [W₁₀O₃₂]⁴⁻. Finally, the intermediate **B5** was protonated to produce C(sp³)-H alkylated product **3-4a-4i** and **3-11-3-19**. In step B-2, the reaction site is the sterically less-hindered C5 position to avoid the steric repulsion between the bulky decatungstate **B2** and substituent(s) of **3-1a-1j**.

Scheme 3-18b. Plausible reaction mechanism of TBADT-catalyzed C(sp³)-H alkylation.



4) Exploration of the rate-determining step of in TBADT Catalytic System

In kinetic theory, if C–H bond activation is the rate-determining step, the reaction rate depends on the activation energy of the C–H bond, which is the difference between the zero-point energies of the reactants and the transition state. According to the Einstein-Planck and Hooke's laws, the vibrational energies of chemical bonds can be calculated using equation (1).

Transition states are typically unstable, with weak bonds. Consequently, there is a slight difference in the transition state energies between **3-1a** and **3-1a-D** (Scheme 3-19). Additionally, due to the difference in reduced mass (μ), the zero-point energies of **3-1a** and **3-1a-D** also differ. The calculation processes for μ of C–H and C–D bonds are shown in equations (2) and (3) respectively. The calculated reduced masses of C–H and C–D bonds are 1.1 and 2.8, respectively.

When the reduced mass is larger, the zero-point energy of the corresponding substance is smaller. Therefore, the zero-point energy of **3-1a** is higher than that of **3-1a-D**. Consequently, the activation energies of **3-1a** and **3-1a-D** are primarily determined by their zero-point energies. If the rate-determining step is the C–H bond

cleavage, the reaction rate of **3-1a** would be faster than that of **3-1a-D**. This can be supported by kinetic isotope effect (KIE) experiments.

The equation for the vibrational energy of a chemical bond is as follows:

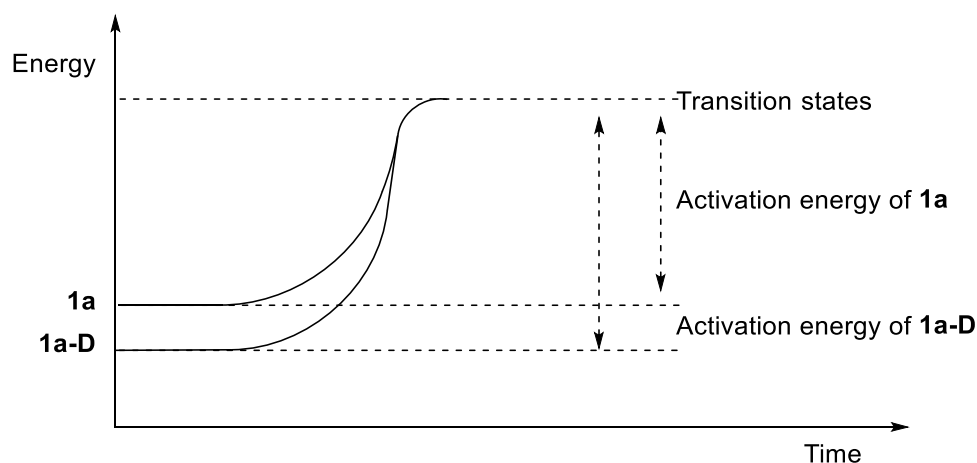
$$E_n = h\nu = h(n + 1/2) \sqrt{\frac{k}{\mu}} \quad (1)$$

h is Planck constant; ν is the vibration frequency; k is the force constant of the bond; $\mu = \frac{m_1 * m_2}{m_1 + m_2}$, reduced mass; n is energy level.

$$\mu_{C-H} = \frac{m_1 * m_2}{m_1 + m_2} = \frac{12.011 * 1.008}{12.011 + 1.008} = 1.1 \quad (2)$$

$$\mu_{C-D} = \frac{m_1 * m_2}{m_1 + m_2} = \frac{12.011 * 2.274}{12.011 + 2.274} = 2.8 \quad (3)$$

Scheme 3-19. Activation energies of **3-1a** and **3-1a-D**.



The kinetic isotope effect (KIE) experiments of **3-1a** and **3-1a-D**

Based on the above analysis results, KIE experiments were conducted for **3-1a** and **3-1a-D** in TBADT-catalyzed C(sp³)-H alkylation as shown in Scheme 3-20. The experimental results are shown in Table 3-7. Based on the experimental results, two straight lines were obtained when the reaction times were plotted on the horizontal axis and the yields on the vertical axis by least-squares method. The slopes of these lines represent the rate equilibrium constants (K) for the respective reactions of **3-1a** and **3-1a-D**. However, since 11% of **3-1a** still existed in **3-1a-D**, the calculation process of K_D for **3-1a-D** was shown in equation (4). The ratio of K_H for **3-1a** to K_D for **3-1a-D** was

calculated to be 5.5. Generally, when the ratio of K_H to K_D is higher than 2, it indicates that the cleavage of the C–H bond is the rate-determining step. Therefore, these results suggested that the cleavage of the C–H bond in **3-1a** is the rate-determining step.

Adjusted initial rate of deuterium species

$$0.1931 = K_H \times 0.11 + K_D \times 0.89 \quad (4)$$

Putting the $K_H = 0.6651$ in equation (4):

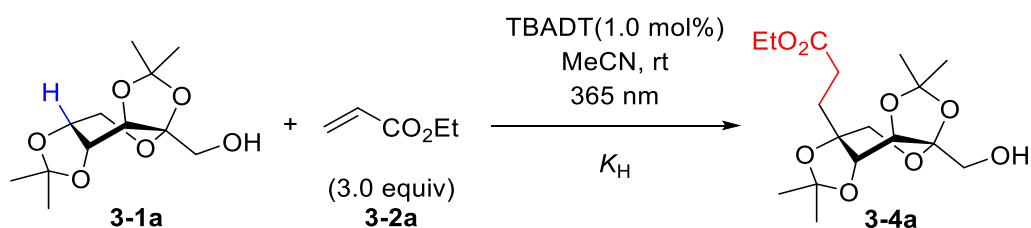
$$K_D = 0.1199$$

Then, the calculation of ratio of K_H to K_D :

$$\frac{K_H}{K_D} = \frac{0.6651}{0.1199} = 5.5$$

Scheme 3-20. Parallel reactions of the kinetic isotope effect (KIE) reaction.

a)



b)

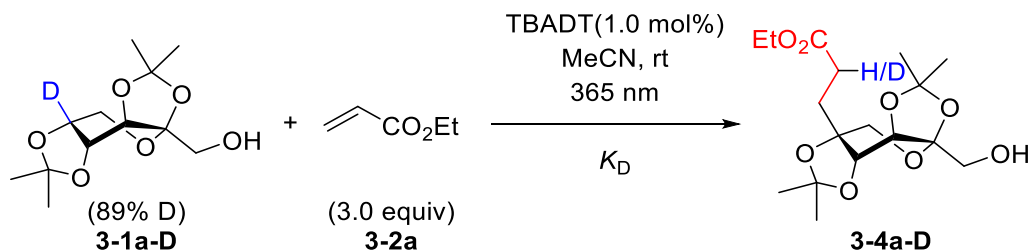


Table 3-7. KIE experiments of TBADT-catalyzed C(sp³)–H alkylation.

time (min)	3-4a yield (%)	3-4a-D yield (%)
10	10.6	1.6
20	18.3	3.5
30	23.7	6.1
40	28.7	7.5
50	36.4	9.4
60	45.3	11.3

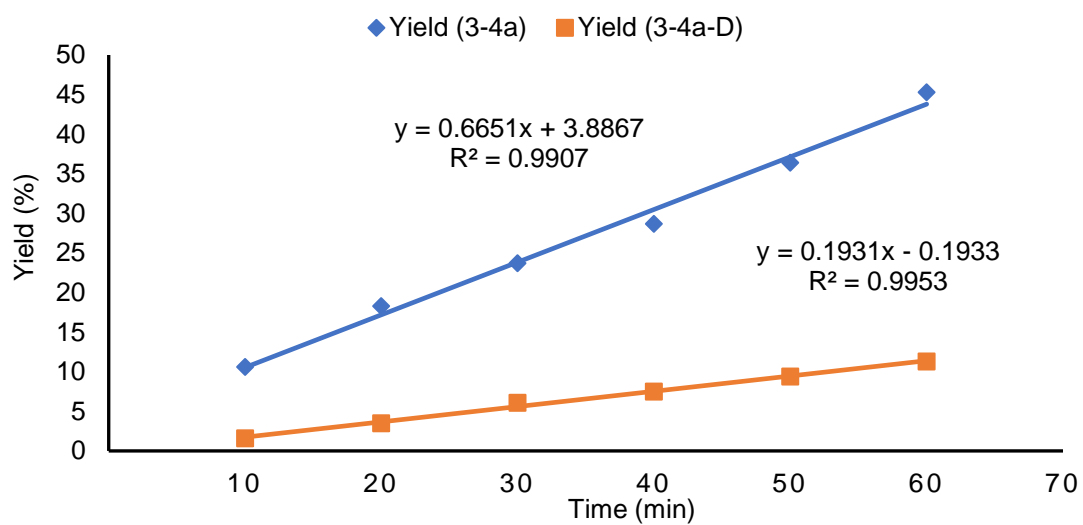


Figure 3-2. Kinetic analysis of the yields of **3-1a** and **3-1a-D** over time

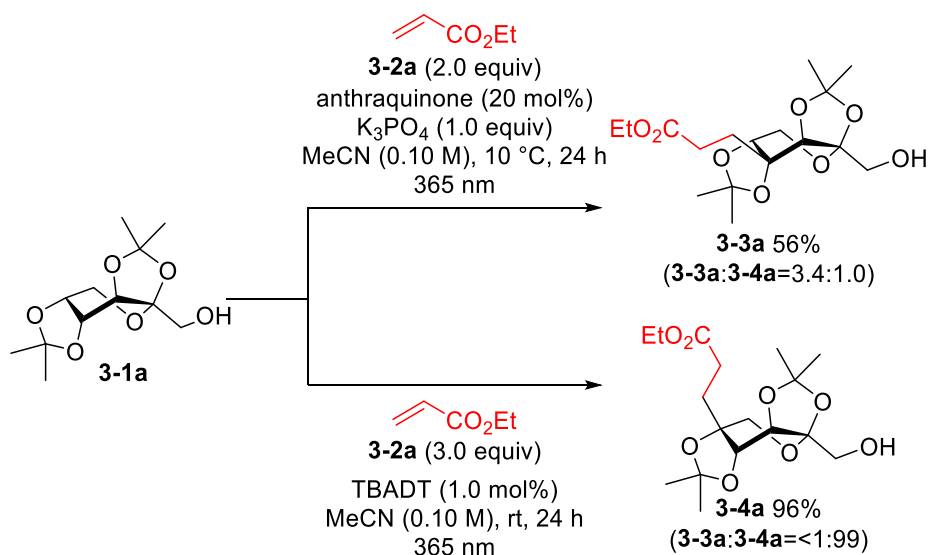
3.2.8 Exploring the Potential Application

1) Switching the Reaction Sites by Catalyst Control

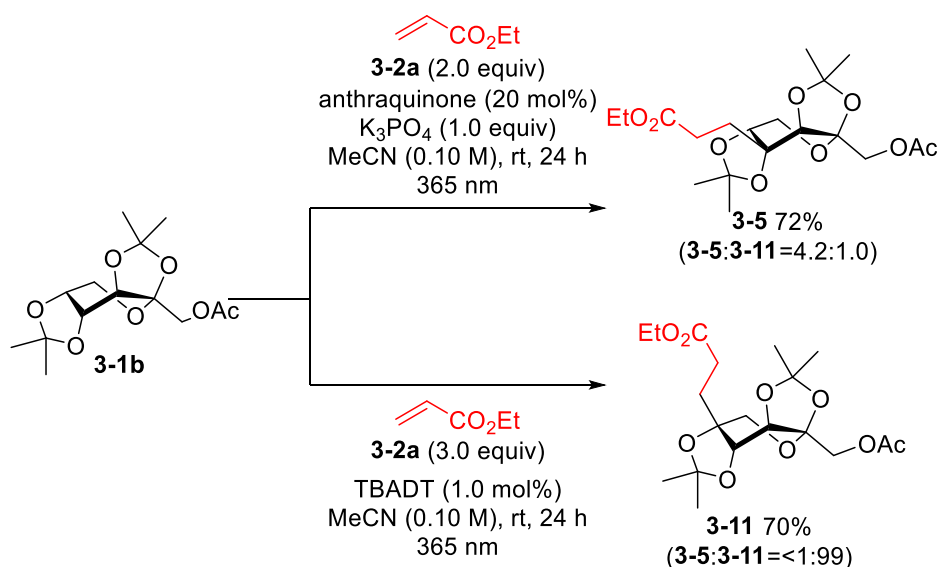
The use of different catalysts, anthraquinone and TBADT, in the alkylation reactions using saccharides **3-1a**, **3-1b**, and **3-1f** as the substrates allowed for a switch in the reaction sites. Under the anthraquinone-catalyzed system, the reaction between **3-1a** and **3-2a** resulted in the formation of both **3-3a** and **3-4a**, with 72% yield and the ratio of **3-3a** to **3-4a** was 3.4 (Scheme 3-21a). In contrast, when using TBADT as the catalyst, the same reaction exclusively yielded **3-4a** with a higher yield of 96%. For the reaction between **3-1b** and **3-2a**, the anthraquinone-catalyzed system produced both **3-5** and **3-11** in 89% yield, with the ratio of **3-5** to **3-11** of 4.2 (Scheme 3-21b). However, in the TBADT-catalyzed system, only compound **3-11** was obtained with 70% yield. Similarly, when **3-1f** reacted with **3-2a**, the anthraquinone-catalyzed system yielded both **3-8** and **others** in 84% yield, with the ratio of **3-8** to **others** of 17 (Scheme 3-21c). On the other hand, the TBADT-catalyzed system exclusively produced **3-15** with 80% yield.

Scheme 3-21. Switching the reaction sites by changing catalysts.

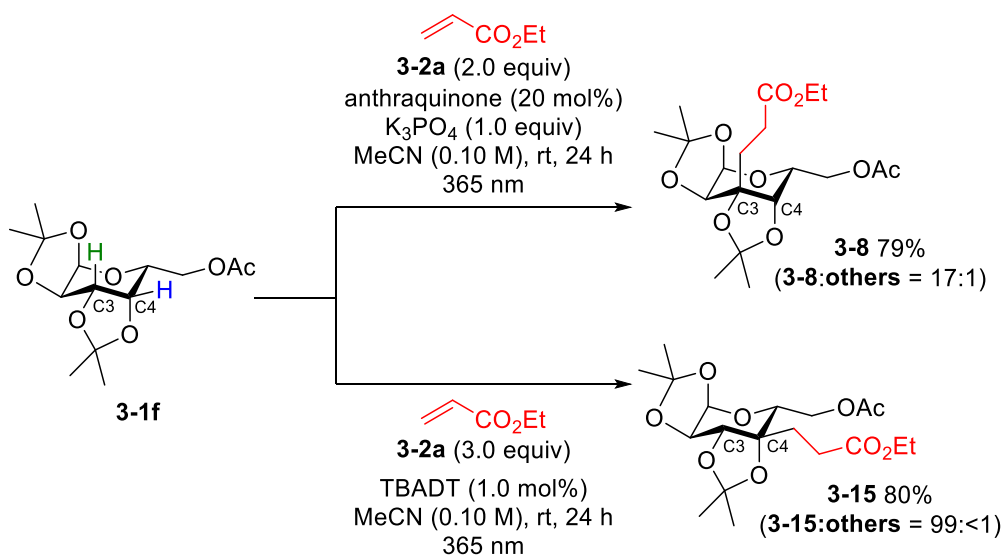
a) **3-1a** was used as substrate



b) **3-1e** was used as substrate



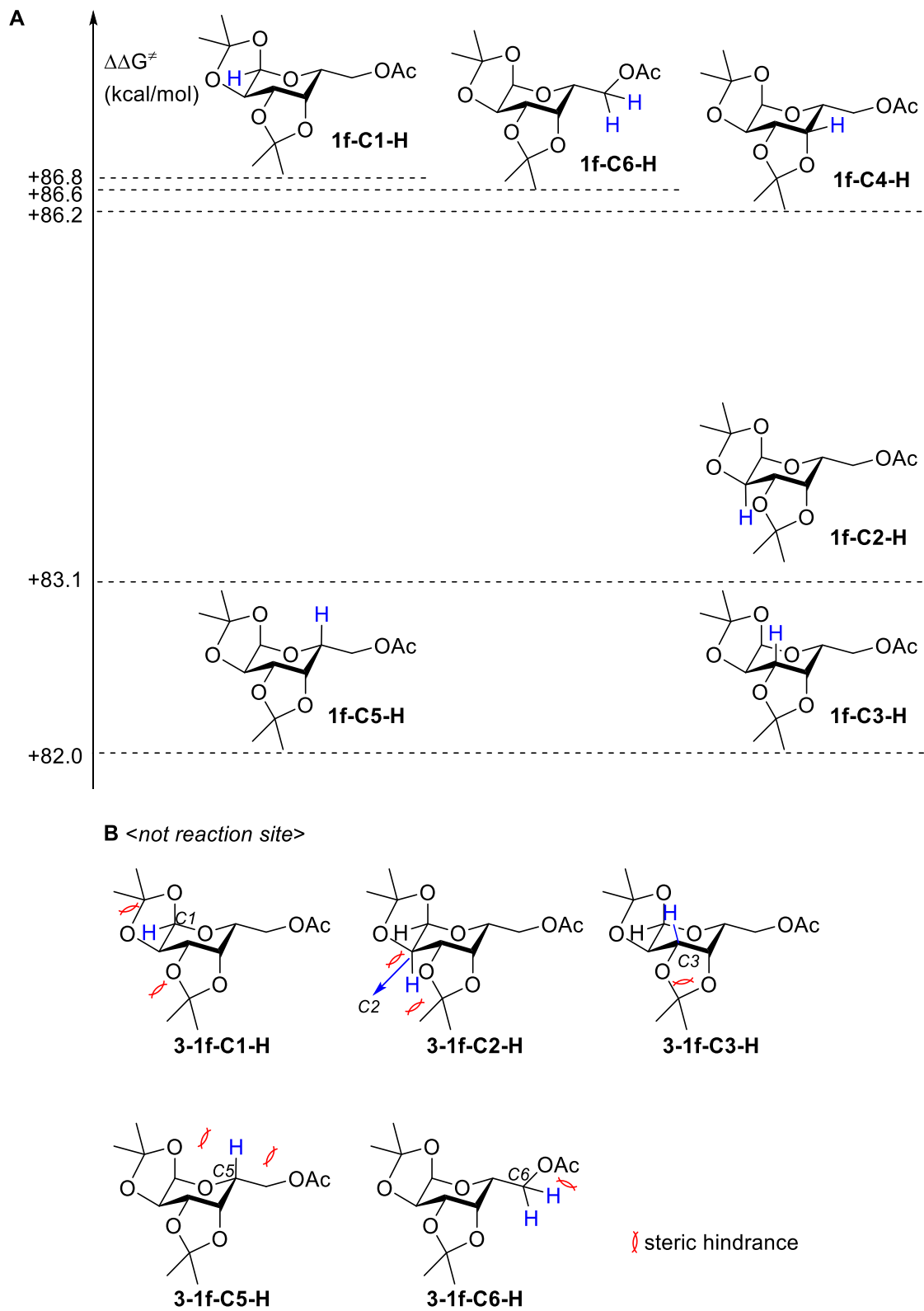
c) **3-1f** was used as substrate



Given the superior selectivity of **3-1f** compared to **3-1a** and **3-1e** in the anthraquinone-catalyzed system, further investigations were conducted. DFT calculations using the UB3LTP/6-31G(d) method in Gaussian 16 were employed to evaluate the bond dissociation energies (BDE) of all C–H bonds of **3-1f** (Scheme 3-21). This analysis aimed to investigate the influence of C–H bond BDE on the reaction selectivity. These results indicated that the C3–H bond exhibited the lowest bond dissociation energy (BDE, 82.0 kcal/mol), which was the reaction position in anthraquinone-catalyzed system. In contrast, TBADT-catalyzed reaction occurred at C4–H position, and the BDE was 86.2 kcal/mol. The energy difference between these

two positions was 4.2 kcal/mol. Due to steric hindrance, anthraquinone predominantly reacted with C3(sp³)-H alkylation of **3-1f**, while TBADT catalyzed C4(sp³)-H alkylation of **3-1f**. The remaining positions (C1-H, C2-H, C3-H, C5-H, C6-H) had significant steric hindrance and thus the reactions were difficult to be promoted (Scheme 3-22b). There was steric hindrance between C1-H bond and the methyl group of isopropylidene moiety on C1 and C2 as well as the methyl group of isopropylidene moiety on C3 and C4. The C2-H is affected by steric hindrance from the methyl group of isopropylidene moiety on C1 and C2 as well as the adjacent oxygen atom on C3. Additionally, steric hindrance was observed between the C3-H and the methyl group of the isopropylidene moiety on C3 and C4. Furthermore, the C5-H was affected by steric hindrance from the methyl group of isopropylidene moiety on C1 and C2 and adjacent oxygen atom on C6. The C6-H encountered steric hindrance from the acetyl group.

Scheme 3-22. C–H bond dissociation energies of **3-1f** and the steric hindrance at non-reaction sites



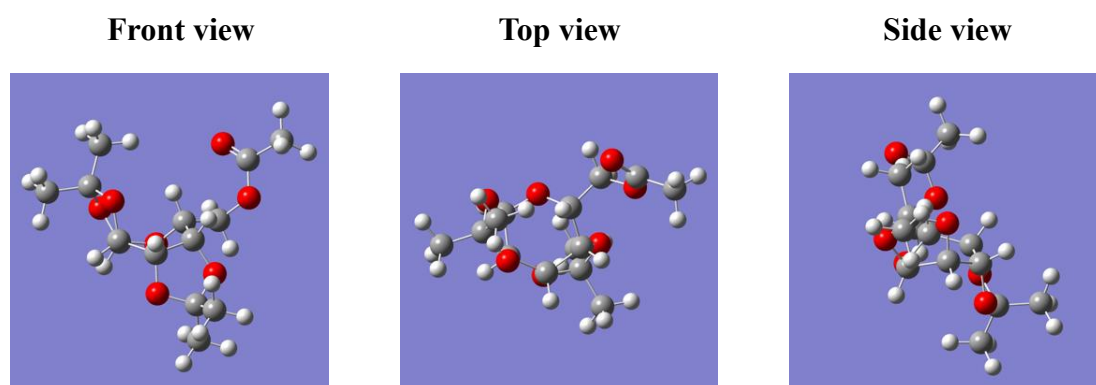


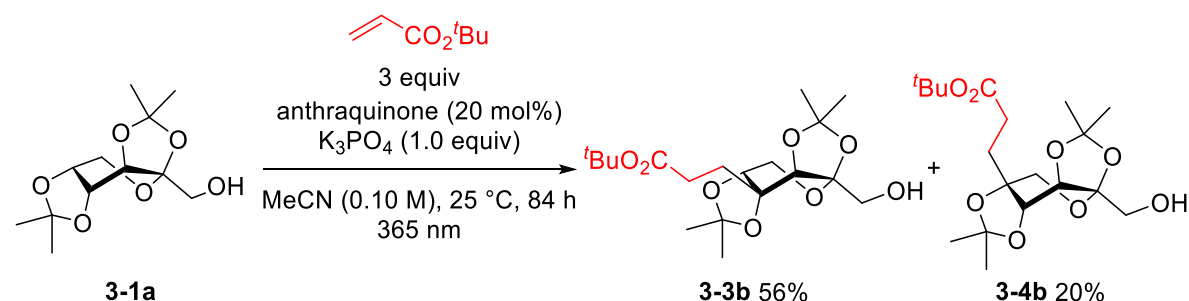
Figure 3-3. Chair conformation of **3-1f**.

2) Exploring Potential Application of Anthraquinone-catalyzed C(sp³)-H Alkylation

Synthesis of **3-3b** on gram scale

Using 1.50 g of **3-1a** and 2.22 g of **3-2b**, in the presence of 1.22 g of K₃PO₄ and anthraquinone catalyst, the reaction was carried out at room temperature for 84 h under UV-LED (365 nm) irradiation (Scheme 3-23). As a result, a mixture of mono-alkylated products, **3-3b** and **3-4b**, was obtained with 76% yield, and the ratio of **3-3b** to **3-4b** was 2.6. The major product **3-3b** was isolated by column chromatography on silica gel to give 1.25 g. The result showed that **3-3b** can be synthesized at the gram level without affecting the yield of the reaction using the commercially available cheap anthraquinone as photocatalyst. This provides a good synthetic method for C4-H alkylation of fructose.

Scheme 3-23. Synthesis of **3-3b** on gram scale.

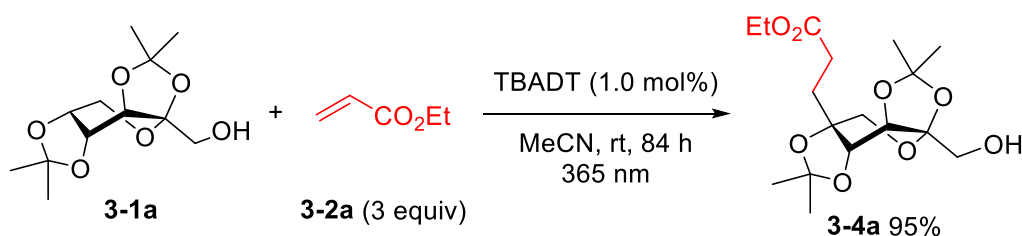


3) Exploring Potential Application TBADT-catalyzed C(sp³)-H Alkylation

Synthesis of 3-4a on gram scale

By utilizing 1.50 g of **3-1a**, 1.97 g of mono-alkylated product **3-4a** was obtained in 95% yield, in the presence of TBADT catalyst. The reaction was conducted at room temperature for 84 h under UV-LED (365 nm) irradiation (Scheme 3-24). The result demonstrated that **3-4a** could be synthesized at the gram level without affecting the yield of the reaction using TBADT as photocatalyst. This provides a good synthetic method for C5-H alkylation of fructose.

Scheme 3-24. Synthesis of **3-4a** on gram scale.



4) C(sp³)-H Alkylation of Glycoconjugates and Drug Molecules

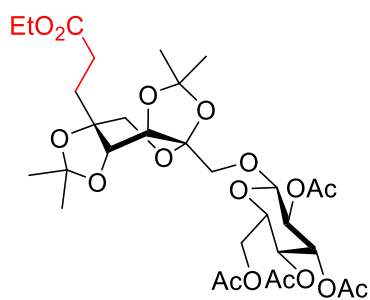
This method was also applied to the site-selective C(sp³)-H alkylation of several glycoconjugates and drug molecules (Scheme 3-25). The disaccharide **3-21**, composed of D-glucose and D-fructose, was successfully alkylated in 75% yield with perfect site-selectivity at the C5-position of the D-fructose moiety. The corresponding dialkylated product **3-22** was obtained in 72% yield from the disaccharide of D-fructose. The protected glycosyl phosphate derivative provided mono-alkylated product **3-23** in 79% yield with perfect site-selectivity. The glycolipid derived from D-fructose and stearic acid produced alkylated product **3-24** in 64% yield. Alkylated topiramate **3-25** was obtained in 92% yield.

The successful application of this method to diverse glycoconjugates and drug derivatives showcases its potential for site-selective C(sp³)-H alkylation in a broad range of bioactive and natural compounds. Glycoconjugates, including disaccharides and glycosyl phosphates, serve as vital intermediates in biochemical metabolic pathways and biosynthesis, respectively.²⁴ The site-selective C(sp³)-H alkylation of these compounds offers a powerful tool for synthesizing complex carbohydrates and

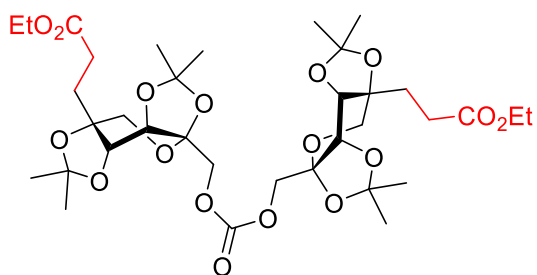
glycoconjugates with precise stereo- and regiochemistry. Glycolipids are significant molecules that play a crucial role in maintaining cell membrane stability and facilitating cell recognition.²⁵ The successful synthesis of alkylated products derived from a glycolipid obtained from D-fructose and stearic acid opens new avenues for creating structurally diverse glycolipids, which have profound implications in various biological processes. Furthermore, the site-selective C(sp³)-H alkylation of the antiseizure drug, topiramate, is of great significance as it provides a potential strategy for modifying its pharmacological properties. Topiramate, used for treating epilepsy and migraines, has demonstrated additional therapeutic effects, such as weight loss and alcohol dependence treatment.²⁶ The high-yield production of alkylated topiramate products presents an opportunity for further optimizing its therapeutic properties.

Additionally, the utilization of decatungstate as a catalyst in this reaction offers a practical advantage, as it is a polyoxometalate that can be easily separated from the organic mixture by filtration. This enhances the convenience and scalability of the method for synthesizing large quantities of alkylated products. Overall, the successful application of this method to a variety of glycoconjugates and drug derivatives highlights its potential for efficiently and selectively synthesizing complex bioactive and natural compounds with diverse functional groups.

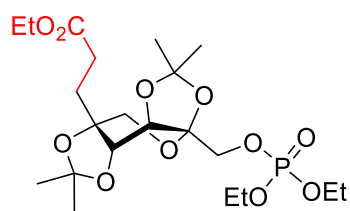
Scheme 3-25. TBADT-catalyzed C(sp³)-H alkylation of glycosyl derivatives.



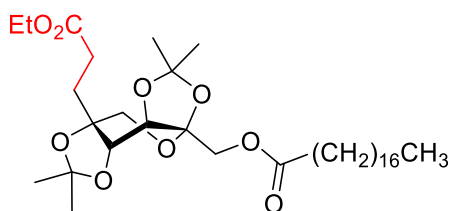
Alkylated disaccharide
(D-Glucose + D-Fructose)
3-21 75%



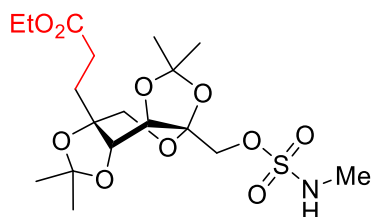
Alkylated disaccharide
(D-Fructose + D-Fructose)
3-22 72%



Alkylated glycosyl phosphate
3-23 79%



Alkylated glycolipid
3-24 64%



Alkylated Tapiramate
(antiseizure drug)
3-25 92%

3.3 Conclusion

In Chapter 3, the site-selective intermolecular C(sp³)-H alkylation of saccharides was realized under anthraquinone and TBADT photocatalysis without using a directing group or a substrate HAT site.

When using **3-1a** as the substrate, anthraquinone demonstrated better performance compared to other photocatalysts. The addition of a base to the anthraquinone-catalyzed reaction resulted in the reduction of side reactions, probably due to the polarity change of C-H bond of substrate. Notably, the presence of K₃PO₄ inhibited the C5-H alkylation of **3-1a**. During solvent screening, the good yield of **3-3a** was obtained in acetonitrile and acetone. According to the Nernst equation, the equilibrium constant for the homolysis reaction of the C4-H bond was 188 times higher than that of the C5-H bond at room temperature, indicating a significantly higher reactivity of the C4-H bond compared to the C5-H bond. However, despite the higher reactivity, the ratio of **3-3a** to **3-4a** was 3.4 at 15 °C. This suggested that there was still steric hindrance between the C4-H of **3-1a** and excited anthraquinone. Therefore, further exploration is needed to identify better catalysts that can improve the yield of **3-3a**.

Consequently, metal photocatalysts were also investigated. Since the ammonium cation of TBADT is larger than the sodium cation of NaDT, TBADT has greater steric hindrance compared to NaDT. As a result, the TBADT-catalyzed alkylation exhibited higher selectivity towards the C5-position than NaDT. Additionally, in the TBADT-catalyzed reaction, the addition of a base likely inhibited the formation of **3-4a**. The screening of solvents revealed that acetonitrile and acetone also provided good yields.

Furthermore, these reactions allow for the incorporation of various functional groups, including ester, carbonyl, cyano, and sulfonyl groups, into diverse saccharide structures. Additionally, by altering the photocatalysts, especially in the case of fructose and galactose derivatives, the reaction sites can be switched. Anthraquinone-catalyzed C(sp³)-H alkylation targeted the weak BDE of C(sp³)-H bond of saccharides, whereas the site-selectivity of TBADT-catalyzed C(sp³)-H alkylation was dominated by steric effects. In TBADT-catalyzed C(sp³)-H alkylation, the mono-alkylated product is obtained in excellent yield, even on a gram scale. This reaction was also applicable for site-selective C(sp³)-H alkylation of glycoconjugates and drug derivatives. We hope

that this strategy will contribute to the development of C(sp³)-H transformations in bioactive and natural compounds, including saccharides.

3.4 Experimental Section

3.4.1 General

^1H (400 MHz) and ^{13}C (100 MHz) NMR spectra were recorded using a JEOL ECZ400 spectrometer. ^1H (600 MHz) and ^{13}C (150 MHz) NMR spectra were recorded using a JEOL JNM-ECA600 spectrometer. Proton chemical shifts are reported relative to the residual solvent peak (CDCl_3 at 7.26 ppm). Carbon chemical shifts are reported relative to CDCl_3 at 77.0 ppm. IR spectra were recorded on a JASCO FT/IR-4200. High-resolution mass spectra were recorded on JEOL JMS-700 (EI, FAB) spectrometer. Gel Permeation Chromatography (GPC) was performed by Japan Analytical Industry LC-5060 with series-connected JAIGEL-1H (f 20 mm x 600 mm) and JAIGEL-2H (f 20 mm x 600 mm). Photo reactions were carried out UV-LED light head AC8361 ($\lambda = 365$ nm, Controller 8332A (CCS)).

Acetonitrile (MeCN, Wako) was dried over with molecular sieve 4A and then was frozen-thaw two times to remove air. 1,2-Dichloroethane (1,2-DCE, Wako) was distilled over CaH_2 before use. H_2O (Takasugi Seiyaku) was deionized. Saccharide derivatives (Figure 3-4) were prepared according to the reported procedures.²⁸ Other reagents including alkenes (Figure 3-5) were purchased from commercial sources and used without further purification.

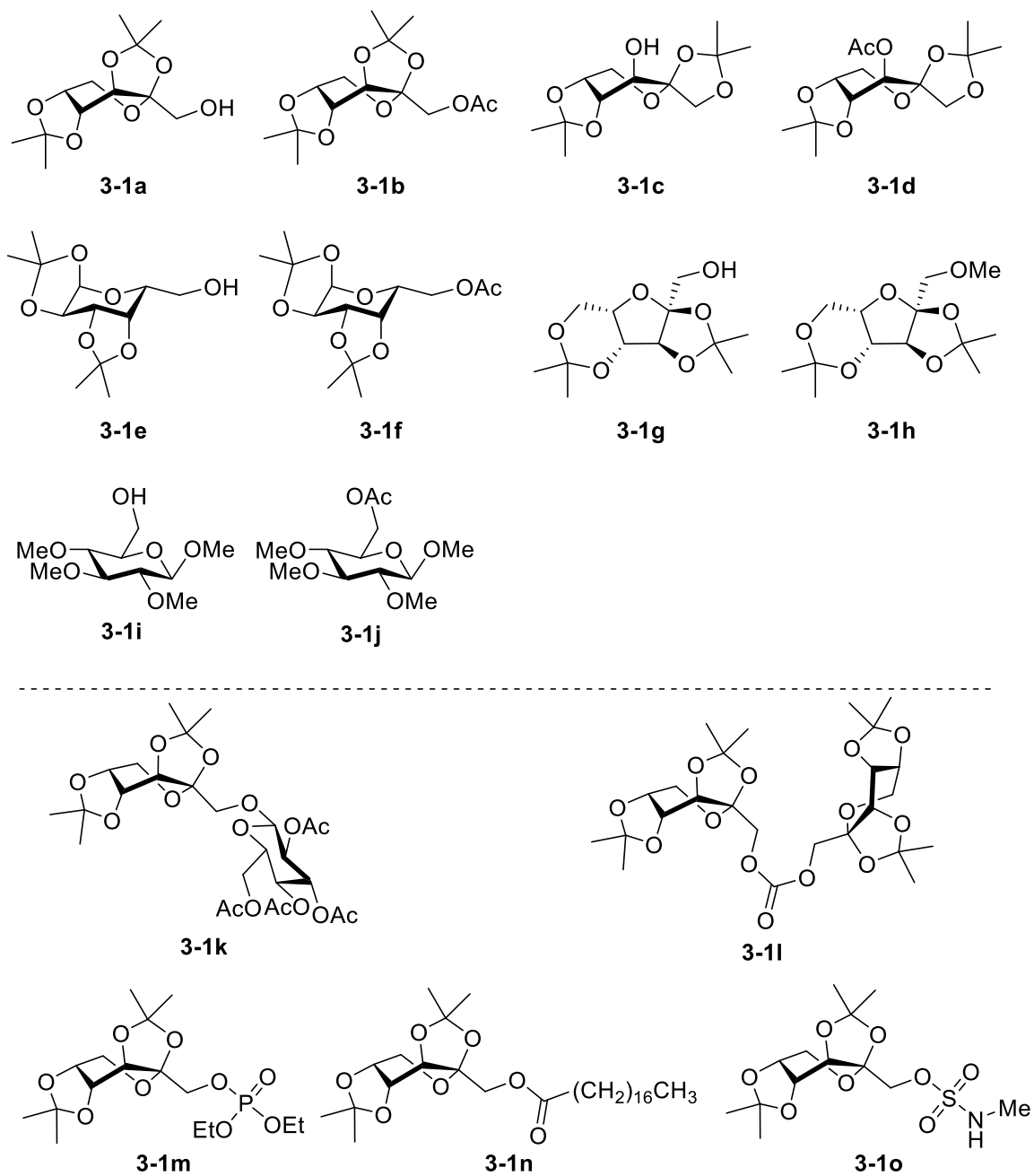


Figure 3-4. Structures of saccharide derivatives.

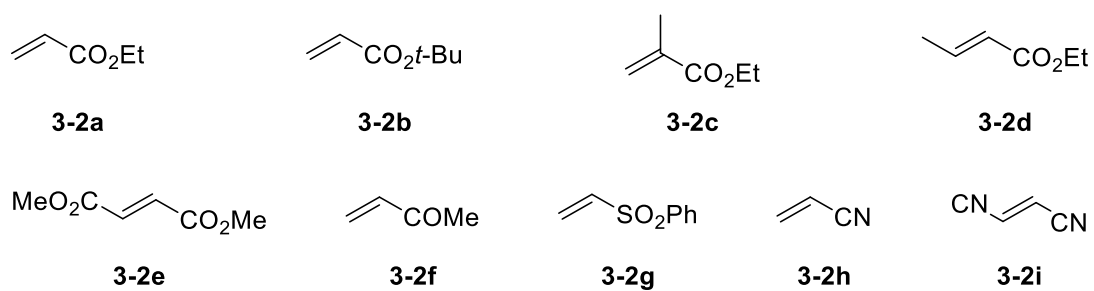


Figure 3-5. Scope of alkenes.

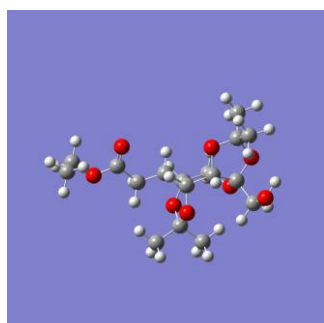
3.4.2 Synthesis and Characterization of Substrates

1) Conformation of alkylated products 3-3a and 3-4a

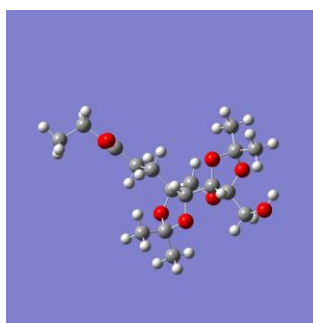
The conformations of alkylated products **3-3a** and **3-4a** were calculated. As shown in the 3D images below, their conformations were twisted boat forms, which are similar to the starting material **3-1a**.

3D images of alkylated products 3-3a and 3-4a (Front view)

3-3a



3-4a



2) C–H bond lengths of 3-1a (DFT calculations)

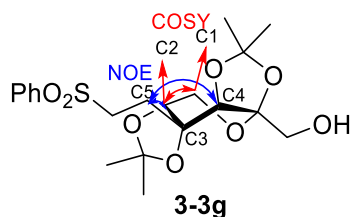
The C–H bond lengths on methylene C1 and C6 were much shorter than those on methine C3, C4 and C5. Because the C–H bond lengths on C3, C4 and C5 were almost the same, it was difficult to discuss the steric hindrance by the bond lengths (Table 3-8).

Table 3-8. C–H bond length of boat form of **3-1a**.

Reaction site	Bond length (Å)	BED (kcal/mol)
3-1a -C1–H	1.107 (1.106 and 1.108)	85.4
3-1a -C3–H	1.115	83.2
3-1a -C4–H	1.116	82.8
3-1a -C5–H	1.113	87.2
3-1a -C6–H	1.107 (1.105 and 1.109)	85.6

3) Confirm the Reaction Site

Confirmation of the structure of **3-3g**



In DEPT-135 spectrum of **3-3g**, nine upward and four downward signals were assigned as CH₃ and CH signals and CH₂ signals, respectively (Figure 3-6). The spectrum indicated that the bond cleavage occurred at the tertiary C(sp³)-H bond of **3-1a**. The result is suitable for **3-3g**. The DEPT-135 spectra of **3-3a-3h** were also measured and the results were consistent with C(sp³)-H alkylated products.

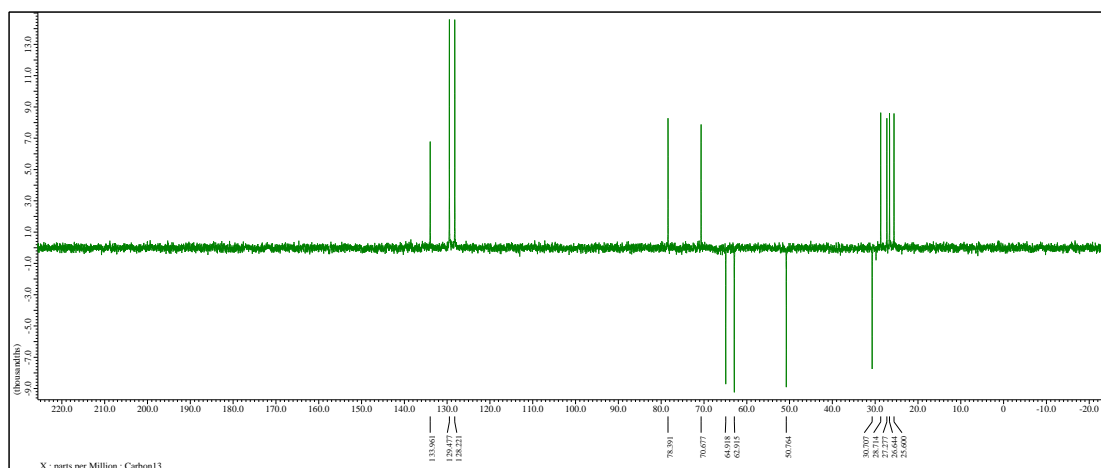


Figure 3-6. DEPT-135 spectrum of **3-3g** (400 MHz, CDCl₃).

In COSY spectrum of **3-3g**, the correlation between hydrogen atoms on C1 and C2 was observed. This result showed that the hydrogen atoms are vicinal (Figure 3-7). This result supports the structure of **3-3g**.

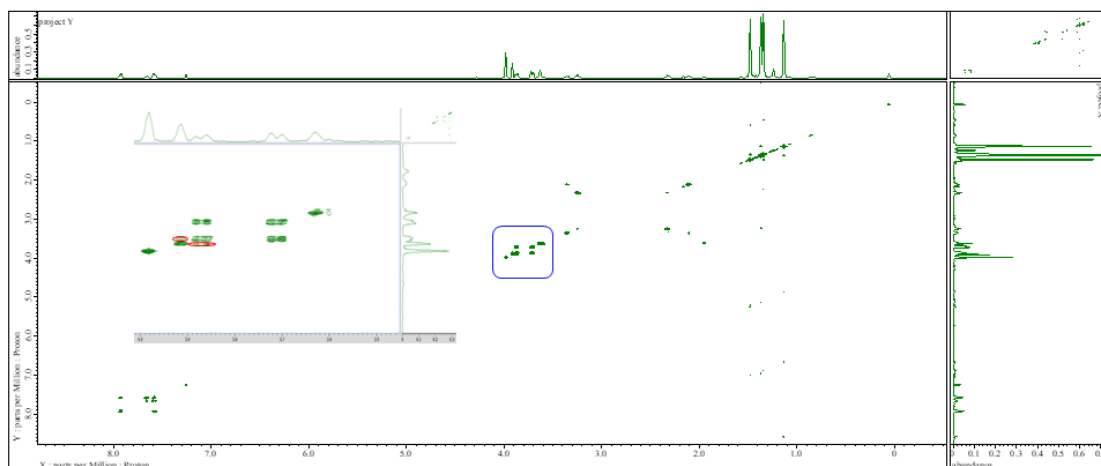


Figure 3-7. COSY spectrum of **3-3g** (600 MHz, CDCl_3).

In NOE spectrum of **3-3g**, the correlation between hydrogen atoms on C2 and C5, and C4 and C5 was observed. This result showed that the hydrogen atoms on C5 are close to hydrogen atoms on C2 and C4, and support the structure of **3-3g** (Figure 3-8).

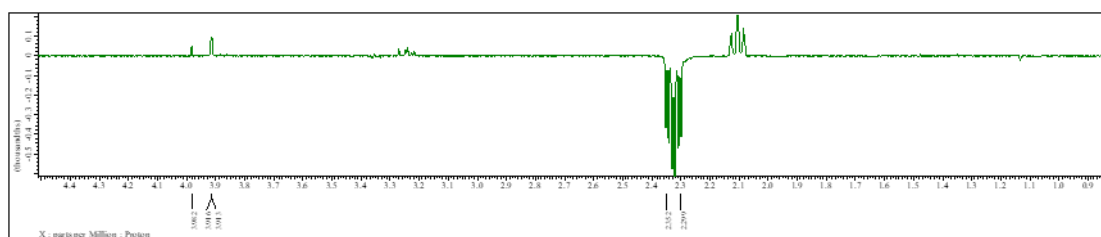
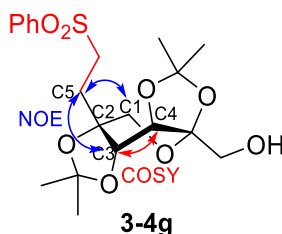


Figure 3-8. NOE spectrum of **3-3g** (600 MHz, CDCl_3).

Confirmation of the structure of **3-4g**



In DEPT-135 spectrum of **3-4g**, nine upward and four downward signals were assigned as CH_3 and CH signals and CH_2 signals, respectively (Figure 3-9). This result

indicated the bond cleavage occurred at the tertiary C(sp³)-H bond of **3-1a**. The result is suitable for **3-4g**. The DEPT-135 spectra of **3-4a-4i** were also measured and the results were consistent with C(sp³)-H alkylated products.

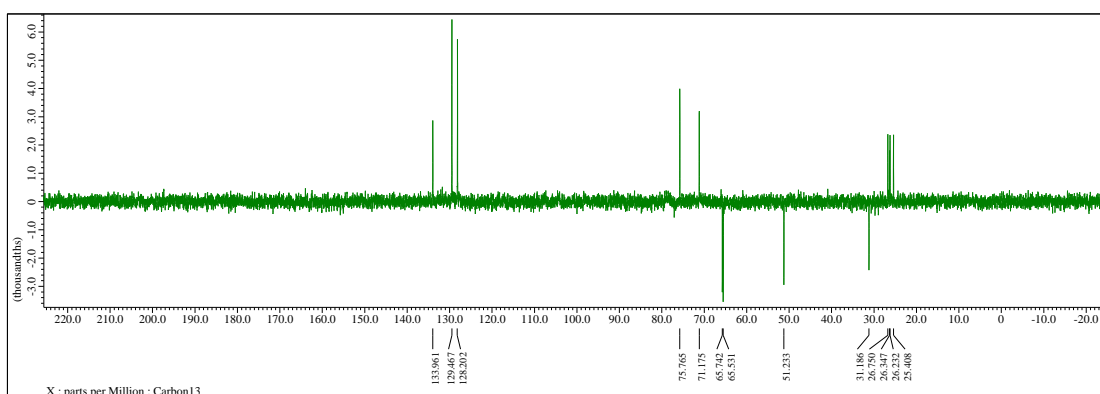


Figure 3-9. DEPT-135 spectrum of **3-4g** (400 MHz, CDCl₃).

In COSY spectrum of **3-4g**, the correlation between hydrogen atoms on C3 and C4 was observed. This result showed that the hydrogen atoms are vicinal, and support the structure of **3-4g** (Figure 3-10).

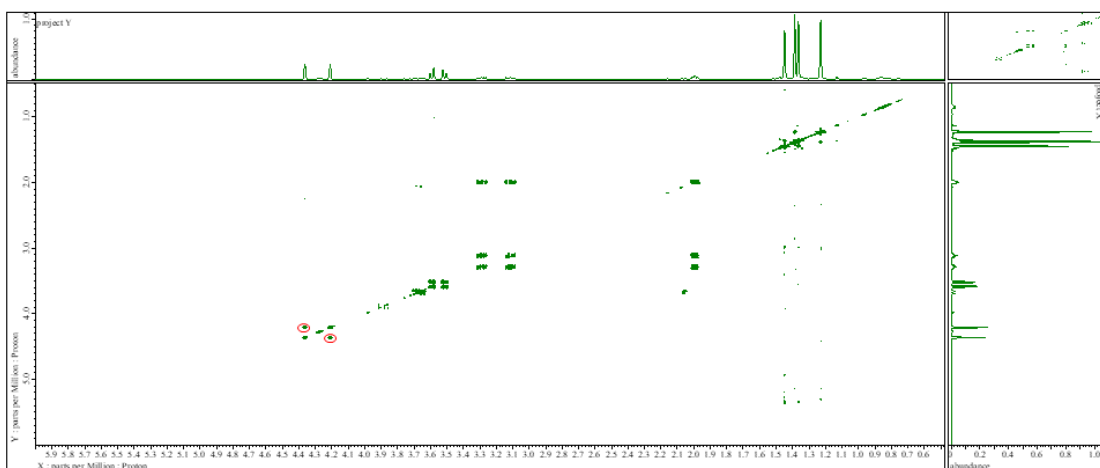


Figure 3-10. COSY spectrum of **3-4g** (600 MHz, CDCl₃).

In NOE spectrum of **3-4g**, the correlation between hydrogen atoms on C1, C3 and C5 was observed. This result showed that the hydrogen atoms on C5 are close to hydrogen atoms on C1 and C3, and support the structure of **3-4g** (Figure 3-11).

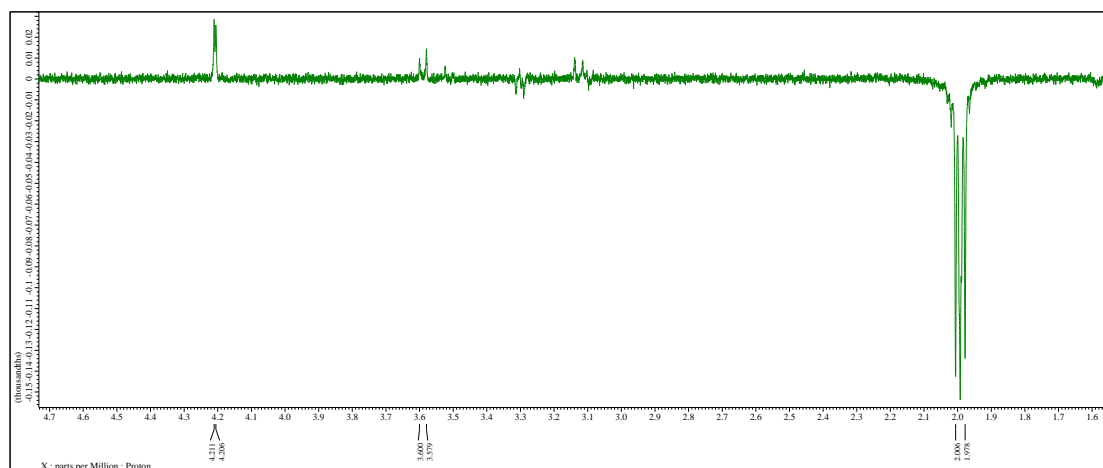
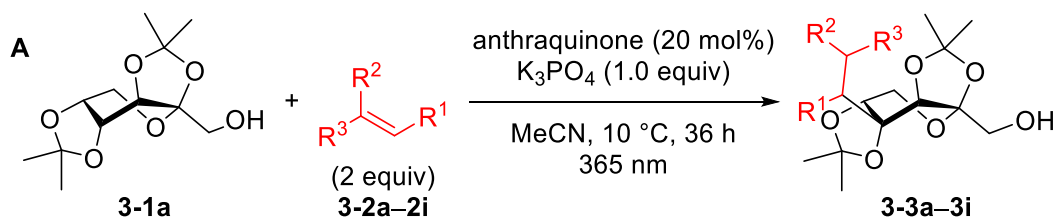


Figure 3-11. NOE spectrum of **3-4g** (600 MHz, CDCl₃).

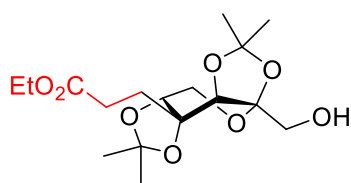
4) Synthesis of Compounds

General procedure A (Scheme 3-26): Saccharide **3-1a** (26.0 mg, 0.100 mmol), anthraquinone (4.2 mg, 20.0 μ mol, 20.0 mol%), K₃PO₄ (21.2 mg, 0.100 mmol, 1.0 equiv) and acetonitrile (1.0 mL) were added to a test tube under N₂ atmosphere. Then alkylene (**3-2**, 0.200 mmol, 2.0 equiv) was added via a syringe into the tube and the tube was sealed with a Teflon-lined screw cap. The reaction was carried out at rt for 24 h under 365 nm UV-LED irradiation. Then, the reaction mixture was evaporated and extracted with dichloromethane (2 \times 2 mL). The organic layer was washed with water and brine, dried over Na₂SO₄, filtrated, and concentrated in vacuo. The reaction mixture was purified by column chromatography on silica gel.

Scheme 3-26. Substrate scope of anthraquinone-catalyzed C(sp³)-H alkylation.



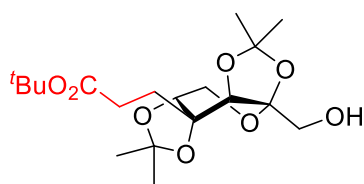
Synthesis of compound 3-3a



Ethyl acrylate (**3-2a**). Mixture of mono-alkylated products: Yellowish oil, 25.9 mg, 72% (**3-3a:3-4a** = 3.3:1.0).

^1H NMR (400 MHz, CDCl_3) δ 1.27 (t, $J = 6.8$ Hz, 3H), 1.39 (s, 3H), 1.44 (s, 3H), 1.45 (s, 3H), 1.53 (s, 3H), 2.16-2.21 (m, 2H), 2.41-2.49 (m, 1H), 2.56-2.64 (m, 1H), 3.69 (d, $J = 2.0$ Hz, 2H), 3.75 (d, $J = 12.8$, 1H), 3.93 (dd, $J = 12.8$, 2 Hz, 1H), 3.96 (d, $J = 2$ Hz, 1H), 4.14 ((dq, $J = 6.8$, 2 Hz, 2H), 4.15 (s, 1H), (OH is missing); ^{13}C NMR (100 MHz, CDCl_3) δ 14.2, 25.4, 26.6, 27.3, 27.9, 29.2, 32.8, 60.5, 63.0, 65.2, 70.9, 78.5, 79.3, 103.5, 108.1, 111.3, 173.4; HRMS (EI^+) calculated for $\text{C}_{17}\text{H}_{28}\text{O}_8$ $[\text{M}+\text{H}]^+$ 360.1784, found 360.1786.

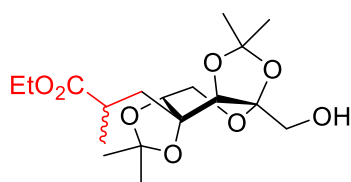
Synthesis of compound 3-3b



Tert-butyl acrylate (**3-2b**), 36 h. Mixture of mono-alkylated products: Yellowish oil, 34.2 mg, 88% (**3-3b:3-4b** = 2.1:1.0.)

^1H NMR (400 MHz, CDCl_3) δ 1.36 (s, 3H), 1.40 (s, 3H), 1.404 (s, 3H), 1.42 (s, 9H), 1.49 (s, 3H), 2.09 (dd, $J = 10.0$, 7.2 Hz, 2H), 2.26-2.36 (m, 1H), 2.44-2.52 (m, 1H), 3.64-3.66 (m, 2H), 3.70 (d, $J = 12.8$ Hz, 1H), 3.89 (dd, $J = 12.8$, 2.0 Hz, 1H), 3.92 (d, $J = 2.0$ Hz, 1H), 4.11 (s, 1H), (OH is missing); ^{13}C NMR (100 MHz, CDCl_3) δ , 25.3, 26.5, 27.3, 28.0 (3C), 29.0, 29.1, 32.7, 63.0, 64.9, 70.8, 78.4, 79.3, 80.3, 103.4, 108.0, 111.1, 172.6; HRMS (EI^+) calculated for $\text{C}_{19}\text{H}_{32}\text{O}_8$ $[\text{M}+\text{H}]^+$ 388.2097, found 388.2098.

Synthesis of compound 3-3c

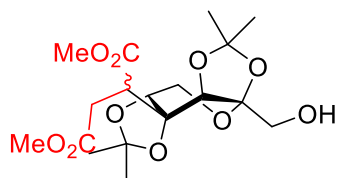


Ethyl crotonate (**3-2c**), rt, 36 h. Mixture of mono-alkylated products: Yellowish oil, 26.5 mg, 71% (**3-3c:3-4c** = 2.1:1.0). The ratio of two diastereomers of **3-3c** was 1.4:1.0.

^1H NMR (400 MHz, CDCl_3) δ 1.19 (d, $J = 6.8$ Hz, 3H), 1.26 (t, $J = 7.2$ Hz, 3H), 1.39 (s, 3H), 1.41 (m, 6H), 1.53 (s, 3H), 1.90 (dd, $J = 14.4$, 4.4 Hz, 1H), 2.10 (m, 1H), 2.55 (dd, $J = 14.4$, 9.2 Hz, 1H), 2.70-2.79 (m, 1H), 3.90 (d, $J = 5.6$ Hz, 2H), 3.73 (d, $J = 12.8$

Hz, 1H), 3.87 (d, $J = 2.0$ Hz, 1H), 3.91 (dd, $J = 12.8, 2.0$ Hz, 1H), 4.01-4.16 (m, 1H), 4.41 (s, 1H); ^{13}C NMR (100 MHz, CDCl_3) δ 14.0, 18.8, 25.3, 26.6, 27.4, 28.8, 34.4, 42.3, 60.4, 62.8, 65.1, 71.0, 78.4, 79.5, 103.3, 107.9, 111.5, 176.6; HRMS (EI^+) calculated for $\text{C}_{18}\text{H}_{30}\text{O}_8$ $[\text{M}+\text{H}]^+$ 374.1941, found 374.1940.

Synthesis of compound 3-3e

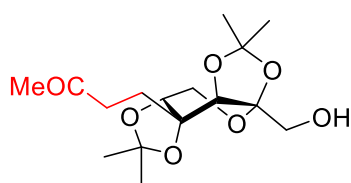


Dimethyl fumarate (**3-2e**), rt, 36 h. Mixture of mono-alkylated products: Yellowish oil, 25.4 mg, 63% (**3-3e**: **3-4e** = 2.0:1.0).

The ratio of two diastereomers of **3-3d** was 1.6:1.0.

^1H NMR (400 MHz, CDCl_3) δ 1.33 (s, 3H), 1.36-1.37 (m, 3H), 1.45-1.46 (m, 3H), 1.52 (s, 3H), 2.76-2.89 (m, 2H), 3.48 (d, $J = 10$ Hz, 0.5H), 3.61 (d, $J = 10$ Hz, 0.5H), 3.68-3.73 (m, 3.5H), 3.76-3.80 (m, 3.5H), 3.90 (dd, $J = 10.5, 1.2$ Hz, 0.5H), 3.96 (d, $J = 10.5$ Hz, 0.5H), 4.20-4.23 (m, 1H), 4.35-4.36 (m, 1H), 4.39 (dd, $J = 7.6, 2.6$ Hz, 0.5H), 4.48 (d, $J = 2.6$ Hz, 0.5H), 4.58-4.60 (m, 1H), (OH is missing); ^{13}C NMR (100 MHz, CDCl_3) δ , 23.9, 24.0, 25.1, 25.2, 25.8, 25.9, 26.54 (2C), 37.3, 37.5, 51.96, 52.03, 52.2, 52.3, 60.9, 61.0, 69.7 (2C), 70.1 (2C), 70.9 (2C), 71.8, 71.9, 75.6, 76.0, 102.0 (2C), 108.5, 108.6, 108.8, 108.9, 170.2, 170.4, 171.2, 171.5; HRMS (EI^+) calculated for $\text{C}_{18}\text{H}_{28}\text{O}_{10}$ $[\text{M}+\text{H}]^+$ 404.1682, found 404.1685.

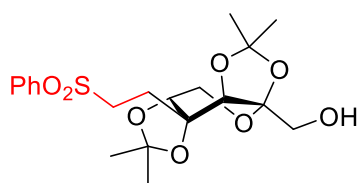
Synthesis of compound 3-3f



Methyl vinyl ketone (**3-2f**), 36 h. Mixture of mono-alkylated products: Yellowish oil, 15.5 mg, 47% (**3-3f**: **3-4f** = 2.2:1.0).

^1H NMR (400 MHz, CDCl_3) δ 1.39 (s, 3H), 1.42 (s, 3H), 1.44 (s, 3H), 1.52 (s, 3H), 2.07-2.14 (m, 2H), 2.20 (s, 3H), 2.55-2.77 (m, 2H), 3.70 (s, 2H), 3.74 (d, $J = 12.8$ Hz, 1H), 3.92 (dd, $J = 12.8, 2.4$ Hz, 1H), 3.97 (d, $J = 2.4$ Hz, 1H), 4.14 (s, 1H), (-OH, missing); ^{13}C NMR (100 MHz, CDCl_3) δ 25.4, 26.6, 27.3, 29.2, 30.1, 31.4, 37.0, 63.0, 65.1, 71.0, 78.6, 79.3, 103.5, 108.1, 111.2, 208.1; HRMS (EI^+) calculated for $\text{C}_{16}\text{H}_{26}\text{O}_7$ $[\text{M}+\text{H}]^+$ 330.1679, found 330.1676.

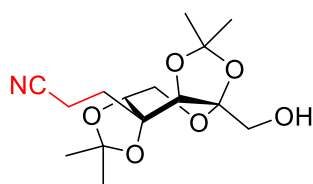
Synthesis of compound 3-3g



Phenyl vinyl sulfone (**3-2g**), 36 h. Mixture of mono-alkylated products: White solid, 32.5 mg, 76% (**3-3g**: **3-4g** = 3.5:1.0).

$^1\text{H NMR}$ (400 MHz, CDCl_3) δ 1.13 (s, 3H), 1.34 (s, 3H), 1.37 (s, 3H), 1.48 (s, 3H), 2.07-2.14 (m, 1H), 2.29-2.37 (m, 1H), 3.21-3.40 (m, 2H), 3.57-3.66 (m, 2H), 3.71 (d, $J = 13.2$ Hz, 1H), 3.87 (dd, $J = 13.2, 2.4$ Hz, 1H), 3.92 (d, $J = 2.4$ Hz, 1H), 3.98 (s, 1H), 7.56-7.69 (m, 3H), 7.92-7.94 (m, 2H), (OH is missing); $^{13}\text{C NMR}$ (100 MHz, CDCl_3) δ , 25.4, 26.5, 27.1, 28.6, 30.6, 50.6, 62.8, 64.8, 70.5, 78.2, 78.6, 103.4, 108.4, 111.6, 128.1 (2C), 129.3 (2C), 133.8, 138.6; HRMS (EI^+) calculated for $\text{C}_{20}\text{H}_{28}\text{O}_8\text{S}$ [$\text{M}+\text{H}$] $^+$ 428.1505, found 428.1504.

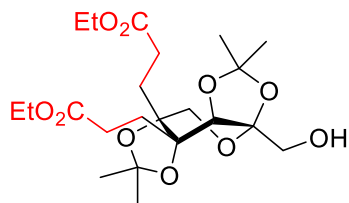
Synthesis of compound 3-3h



Acrylonitrile (**3-2h**), rt, 36 h. Mixture of mono-alkylated products: Yellowish oil, 22.5 mg, 72% (**3-3h**: **3-4h** = 2.6:1.0).

$^1\text{H NMR}$ (400 MHz, CDCl_3) δ 1.42 (s, 3H), 1.46 (s, 6H), 1.54 (s, 3H), 2.07-2.15 (m, 1H), 2.30-2.38 (m, 1H), 2.51-2.64 (m, 2H), 3.67-3.78 (m, 3H), 3.91-3.96 (m, 2H), 4.17 (s, 1H), (-OH, missing); $^{13}\text{C NMR}$ (100 MHz, CDCl_3) δ , 11.1, 25.5, 26.6, 27.2, 29.3, 33.4, 62.8, 64.9, 70.2, 78.3, 78.8, 103.4, 108.5, 111.8, 119.5; HRMS (EI^+) calculated for $\text{C}_{15}\text{H}_{23}\text{NO}_6$ [$\text{M}+\text{H}$] $^+$ 313.1525, found 313.1526.

Synthesis of compound 3-26



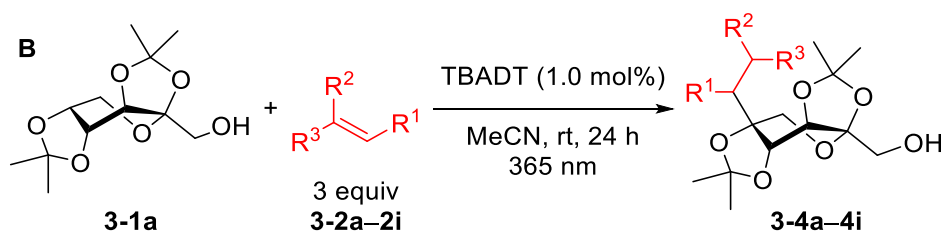
Following Procedure in Table 3-3-1 entry 3 (ethyl acrylate (**3-2a**, 0.300 mmol), 25 °C, 24 h). Dialkylated product **3-26**: Yellowish oil, 18.4 mg, 40%.

$^1\text{H NMR}$ (400 MHz, CDCl_3) δ 1.26 (t, $J = 6.8$ Hz, 3H), 1.27 (t, $J = 6.8$ Hz, 3H), 1.38 (s, 3H), 1.41 (s, 3H), 1.43 (s, 3H), 1.54 (s, 3H), 1.76-1.84 (m, 1H), 2.01-2.24 (m, 3H), 2.32-2.61 (m, 4H), 3.64-3.3.75 (m, 2H), 3.68 (d, $J = 12.8$, 1H), 3.81 (d, $J = 12.8$, 1H), 4.13 ((q, $J = 6.8$ Hz, 2H), 4.15 ((q, $J = 6.8$ Hz, 2H), 4.18 (s, 1H), (OH is missing); $^{13}\text{C NMR}$ (100 MHz, CDCl_3) δ 14.3 (2C), 25.5, 26.4, 27.5, 27.9,

28.2, 28.4, 29.1, 30.1, 30.3, 60.7, 65.8, 67.1, 71.3, 80.6, 82.0, 104.0, 108.7, 109.9, 173.3, 173.5; HRMS (EI⁺) calculated for C₂₂H₃₆O₁₀ [M+H]⁺ 460.2308, found 460.2310.

General procedure B (Scheme 3-27): To a test tube, saccharide **3-1a** (26.0 mg, 0.100 mmol), TBADT (3.3 mg, 1.00 μ mol, 1.0 mol%), and acetonitrile (1.0 mL) were added under N₂ atmosphere. To the mixture, alkylene (**3-2a–2i**, 0.300 mmol, 3.0 equiv) was added via a syringe, and the tube was sealed with a Teflon-lined screw cap. The mixture was stirred at rt for 24 h under 365 nm UV-LED irradiation. Then, the reaction mixture was concentrated under reduced pressure, and the crude mixture was purified by column chromatography on silica gel.

Scheme 3-27. Substrate scope of TBADT-catalyzed C(sp³)-H alkylation.



Synthesis of compound 3-4a

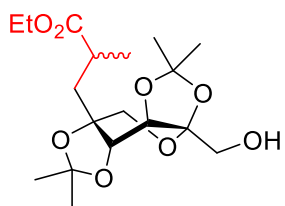
Ethyl acrylate (**3-2a**). **3-4a**: colorless oil, 34.5 mg, 96% yield. ¹H NMR (400 MHz, CDCl₃) δ 1.26 (t, J = 7.2 Hz, 3H), 1.38 (s, 3H), 1.40 (s, 3H), 1.44 (s, 3H), 1.56 (s, 3H), 2.23 (t, J = 8.2 Hz, 2H), 2.35-2.53 (m, 2H), 3.61-3.76 (m, 4H), 3.73 (q, J = 7.2 Hz, 2H), 4.28 (d, J = 3.2 Hz, 1H), 4.40 (d, J = 3.2 Hz, 1H); ¹³C NMR (100 MHz, CDCl₃) δ 14.2, 25.3, 26.2, 26.5, 26.8, 28.6, 33.0, 60.6, 65.7, 66.0, 71.4, 75.4, 79.1, 103.4, 109.1, 109.6, 173.2; HRMS (EI⁺) calculated for C₁₇H₂₈O₈ [M+H]⁺ 360.1784, found 360.1784.

Synthesis of compound 3-4b

tert-Butyl acrylate (**3-2b**). **3-4b**: white solid, 34.1 mg, 88% yield. ¹H NMR (400 MHz, CDCl₃) δ 1.25 (s, 3H), 1.40 (s, 3H), 1.44 (m, 12H), 1.56 (s, 3H), 1.90 (t, J = 8.0 Hz, 2H), 2.26-2.44 (m,

2H), 3.60-3.75 (m, 4H), 4.28 (d, $J = 3.2$ Hz, 1H), 4.40 (d, $J = 3.2$ Hz, 1H), (OH is missing); ^{13}C NMR (100 MHz, CDCl_3) δ , 25.3, 26.2, 26.5, 26.8, 28.0, 29.8, 33.1, 65.7, 66.0, 71.4, 75.4, 79.2, 80.5, 103.4, 109.1, 109.5, 173.4; HRMS (EI^+) calculated for $\text{C}_{19}\text{H}_{32}\text{O}_8$ $[\text{M}+\text{H}]^+$ 388.2097, found 388.2099.

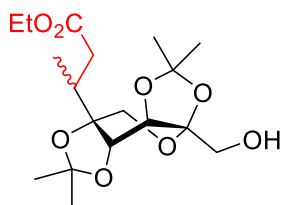
Synthesis of compound 3-4c



Ethyl methacrylate (**3-2c**). **3-4c**: colorless oil, 28.4 mg, 71% yield. The ratio of two diastereomers was 1.1:1.0.

^1H NMR (400 MHz, CDCl_3) δ 1.16-1.27 (m, 6H), 1.34 (s, 1.5H), 1.37 (s, 1.5H), 1.40 (s, 4.5H), 1.44 (s, 1.5H), 1.53-1.63 (m, 1H), 1.55 (s, 1.5H), 1.57 (s, 1.5H), 2.13-2.28 (m, 1H), 2.53-2.73 (m, 1H), 3.59-3.85 (m, 4H), 4.06 (m, 2H), 4.22 (d, $J = 3.2$ Hz, 1H), 4.40 (d, $J = 3.2$ Hz, 1H), (OH is missing); ^{13}C NMR (100 MHz, CDCl_3) δ 14.0, 14.1, 19.4, 19.6, 25.3, 25.4, 26.0, 26.1, 26.2, 26.5, 26.79, 26.83, 35.2 (2C), 42.0, 43.6, 60.4, 60.5, 65.7 (2C), 65.8, 66.0, 71.4, 71.5, 76.1, 76.3, 79.1, 79.5, 103.35, 103.39, 109.0, 109.2, 109.6, 109.7, 176.4, 176.7; HRMS (EI^+) calculated for $\text{C}_{18}\text{H}_{30}\text{O}_8$ $[\text{M}+\text{H}]^+$ 374.1941, found 374.1942.

Synthesis of compound 3-4d



Ethyl crotonate (**3-2d**), TBADT (5 mol%), 36 h. **3-4d**: colorless oil, 22.8 mg, 61% yield. The ratio of two diastereomers was 4.7:1.0. Because the signals of the minor diastereomer overlapped with those of the major diastereomer,

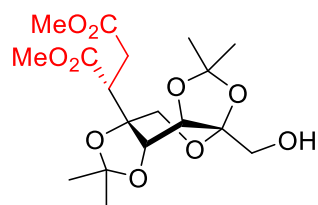
only the signals of the major diastereomer are assigned.

^1H NMR (400 MHz, CDCl_3) δ 1.06 (d, $J = 7.2$ Hz, 3H), 1.26 (t, $J = 7.2$ Hz, 3H), 1.40 (s, 6H), 1.45 (s, 3H), 1.57 (s, 3H), 2.00 (dd, $J = 15.6, 10.8$ Hz, 1H), 2.25-2.36 (m, 1H), 2.67 (dd, $J = 15.6, 3.2$ Hz, 1H), 3.64 (d, $J = 12.8$ Hz, 1H), 3.71 (s, 2H), 3.74 (d, $J = 12.8$ Hz, 1H), 4.14 (dq, $J = 7.2, 2.4$ Hz, 2H), 4.36 (d, $J = 3.2$ Hz, 1H), 4.42 (d, $J = 3.2$ Hz, 1H), (OH is missing); ^{13}C NMR (100 MHz, CDCl_3) δ 14.2, 14.9, 25.4, 26.2, 26.8, 26.9, 37.3, 37.5, 60.5, 63.3, 65.8, 71.2, 74.5, 82.0, 103.5, 109.1, 109.3, 172.8; HRMS (EI^+) calculated for $\text{C}_{18}\text{H}_{30}\text{O}_8$ $[\text{M}+\text{H}]^+$ 374.1941, found 374.1940.

Synthesis of compound 3-4e

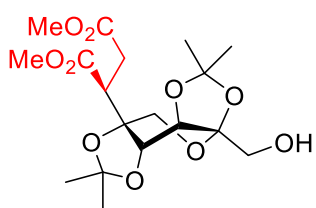
Dimethyl fumarate (**3-2e**). **3-4e**: Colorless oil, 32.4 mg, 80% yield. The ratio of two diastereomers was 2.5:1.0.

Isomer 1 (23.0 mg)



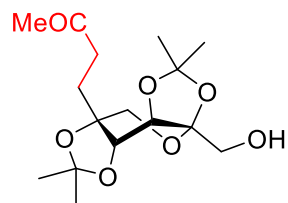
^1H NMR (400 MHz, CDCl_3) δ 1.39 (s, 3H), 1.41 (s, 3H), 1.44 (s, 3H), 1.58 (s, 3H), 2.77 (d, $J = 7.6$, 2H), 3.16 (t, $J = 7.6$ Hz, 1H), 3.67 (s, 3H), 3.73 (s, 3H), 3.67-3.73 (m, 3H), 3.83 (d, $J = 13.2$ Hz, 1H), 4.36 (d, $J = 3.2$ Hz, 1H), 4.52 (d, $J = 3.2$ Hz, 1H), (OH is missing); ^{13}C NMR (100 MHz, CDCl_3) δ 25.4, 26.2, 26.5, 26.8, 32.4, 49.2, 52.0, 52.2, 63.2, 65.5, 71.0, 74.9, 80.0, 103.3, 109.4, 110.2, 172.0, 172.1; HRMS (EI^+) calculated for $\text{C}_{18}\text{H}_{28}\text{O}_{10}$ $[\text{M}+\text{H}]^+$ 404.1682, found 404.1682.

Isomer 2 (9.4 mg)



^1H NMR (400 MHz, CDCl_3) δ 1.36 (s, 3H), 1.41 (s, 3H), 1.44 (s, 3H), 1.50 (s, 3H), 2.81-2.84 (m, 2H), 3.17 (dd, $J = 9.2$, 6.0 Hz, 1H), 3.54 (d, $J = 12.8$ Hz, 1H), 3.65-3.73 (m, 2H), 3.67 (s, 3H), 3.70 (s, 3H), 3.93 (d, $J = 12.8$ Hz, 1H), 4.34 (d, $J = 3.2$ Hz, 1H), 4.80 (d, $J = 3.2$ Hz, 1H), (OH is missing); ^{13}C NMR (100 MHz, CDCl_3) δ 25.5, 26.0, 26.1, 26.6, 31.7, 50.1, 52.0, 52.1, 62.1, 65.5, 71.0, 74.1, 79.0, 103.2, 109.4, 109.6, 171.4, 172.5; HRMS (EI^+) calculated for $\text{C}_{18}\text{H}_{28}\text{O}_{10}$ $[\text{M}+\text{H}]^+$ 404.1682, found 404.1683.

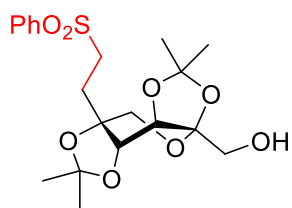
Synthesis of compound 3-4f



Methyl vinyl ketone (**3-2f**). **3-3f**: Colorless oil, 32.1 mg, 97% yield.

^1H NMR (400 MHz, CDCl_3) δ 1.37 (s, 3H), 1.39 (s, 3H), 1.44 (s, 3H), 1.55 (s, 3H), 1.87-1.94 (m, 2H), 2.16 (s, 3H), 2.48-2.69 (m, 2H), 3.58-3.75 (m, 4H), 4.27 (d, $J = 3.2$ Hz, 1H), 4.39 (d, $J = 3.2$ Hz, 1H), (OH is missing); ^{13}C NMR (100 MHz, CDCl_3) δ 25.3, 26.2, 26.5, 26.8, 29.9, 31.8, 37.7, 65.7, 66.0, 71.4, 75.7, 79.1, 103.4, 109.1, 109.4, 207.6; HRMS (EI^+) calculated for $\text{C}_{16}\text{H}_{26}\text{O}_7$ $[\text{M}+\text{H}]^+$ 330.1679, found 330.1679.

Synthesis of compound 3-4g



Phenyl vinyl sulfone (**3-2g**). **3-4g**: White solid, 20.2 mg, 47% yield.

$^1\text{H NMR}$ (400 MHz, CDCl_3) δ 1.24 (s, 3H), 1.37 (s, 3H), 1.39 (s, 3H), 1.46 (s, 3H), 1.98-2.04 (m, 2H), 3.08-3.16 (m, 1H), 3.26-3.34 (m, 1H), 3.50-3.71 (m, 4H), 4.22 (d, $J = 3.2$ Hz, 1H), 4.37 (d, $J = 3.2$ Hz, 1H), 7.56-7.70 (m, 3H), 7.90-7.94 (m, 2H), (OH is missing); $^{13}\text{C NMR}$ (100 MHz, CDCl_3) δ , 25.3, 26.1, 26.2, 26.7, 31.1, 51.1, 65.4, 65.6, 71.1, 75.7, 78.2, 103.3, 109.2, 109.9, 128.1, 129.4, 133.8, 138.6; HRMS (EI^+) calculated for $\text{C}_{20}\text{H}_{28}\text{O}_8\text{S}$ $[\text{M}+\text{H}]^+$ 428.1505, found 428.1505.

Synthesis of compound 3-4h



Acrylonitrile (**3-2h**), TBADT (5 mol%), 36 h. **3-4h**: Colorless oil, 9.4 mg, 30% yield.

$^1\text{H NMR}$ (400 MHz, CDCl_3) δ 1.38 (s, 3H), 1.41 (s, 3H), 1.46 (s, 3H), 1.56 (s, 3H), 1.99 (t, $J = 7.6$ Hz, 2H), 2.39-2.59 (m, 2H), 3.65 (d, $J = 12.4$ Hz, 1H), 3.71 (s, 2H), 3.73 (d, $J = 12.4$ Hz, 1H), 4.28 (d, $J = 3.2$ Hz, 1H), 4.43 (d, $J = 3.2$ Hz, 1H), (OH is missing); $^{13}\text{C NMR}$ (100 MHz, CDCl_3) δ , 25.3, 26.2, 26.6, 26.7, 29.7, 33.8, 65.4, 65.7, 71.5, 75.3, 78.4, 103.4, 109.3, 110.1, 119.4; HRMS (EI^+) calculated for $\text{C}_{15}\text{H}_{23}\text{NO}_6$ $[\text{M}+\text{H}]^+$ 313.1525, found 313.1525.

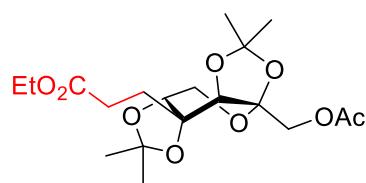
Synthesis of compound 3-4i



Fumaronitrile (**3-2i**). **3-4i**: White solid, 23.9 mg, 71% yield. The ratio of two diastereomers was 1.2:1.0.

$^1\text{H NMR}$ (400 MHz, CDCl_3) δ 1.42 (s, 1.5H), 1.43 (s, 3H), 1.480 (s, 1.5H), 1.483 (s, 1.5H), 1.53 (s, 1.5H), 1.57 (s, 1.5H), 1.62 (s, 1.5H), 2.77-2.98 (m, 2H), 3.15-3.19 (m, 1H), 3.71-3.82 (m, 3.5H), 3.98 (d, $J = 12.4$ Hz, 0.5H), 4.44-4.46 (m, 1H), 4.50 (d, $J = 3.2$ Hz, 0.5H), 4.65 (d, $J = 3.2$ Hz, 0.5H), (OH is missing); $^{13}\text{C NMR}$ (100 MHz, CDCl_3) δ 16.97, 17.05, 25.3, 25.4, 26.2, 26.3, 26.7, 26.8, 26.86, 26.91, 35.9, 37.3, 63.7, 64.8, 64.9 (2C), 70.2, 70.5, 74.6, 75.0, 78.5, 78.6, 103.30, 103.33, 109.9, 110.2, 111.8, 112.2, 115.66, 115.72, 115.8, 116.7; HRMS (EI^+) calculated for $\text{C}_{16}\text{H}_{22}\text{N}_2\text{O}_6$ $[\text{M}+\text{H}]^+$ 338.1478, found 338.1476.

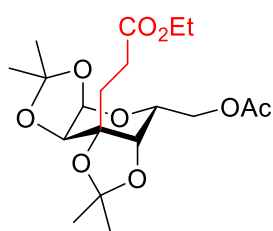
Synthesis of compound 3-5 (General Procedure A)



6-*O*-Acetyl-2,3:4,5-di-*O*-isopropylidene- β -D-fructopyranose (**3-1b**), ethyl acrylate (**3-2a**). Mixture of mono-alkylated products: Yellowish oil, 35.7 mg, 89% (**3-5**: **3-11** = 4.2:1.0).

^1H NMR (400 MHz, CDCl_3) δ 1.27 (t, $J = 6.8$ Hz, 3H), 1.38 (s, 3H), 1.44 (s, 6H), 1.52 (s, 3H), 2.12 (s, 3H), 2.18 (t, $J = 7.6$ Hz, 2H), 2.39-2.49 (m, 1H), 2.56-2.63 (m, 1H), 3.74 (d, $J = 13.2$ Hz, 1H), 3.91 (dd, $J = 13.2, 2.4$ Hz, 1H), 3.96 (d, $J = 2.4$ Hz, 1H), 4.01 (d, $J = 12$ Hz, 1H), 4.10 (s, 1H), 4.15 ((dq, $J = 6.8, 1.2$ Hz, 2H), 4.43 (d, $J = 12$ Hz, 1H); ^{13}C NMR (100 MHz, CDCl_3) δ 14.2, 21.0, 25.1, 26.6, 27.3, 27.9, 29.2, 32.8, 60.6, 62.9, 65.3, 70.9, 78.4, 79.2, 101.1, 108.4, 111.4, 170.2, 173.3; HRMS (EI^+) calculated for $\text{C}_{19}\text{H}_{30}\text{O}_9$ $[\text{M}+\text{H}]^+$ 402.1890, found 402.1888.

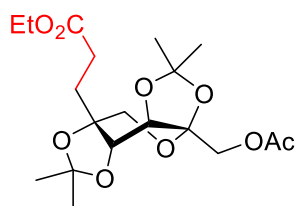
Synthesis of compound 3-8 (General Procedure A)



6-*O*-acetyl-1,2:3,4-di-*O*-isopropylidene- β -D-galactopyranose (**3-1f**), ethyl acrylate (**3-2a**). Mixture of mono-alkylated products: Yellowish oil, 33.7 mg, 84% (**3-8**:**3-15** = 17.0:1.0).

^1H NMR (400 MHz, CDCl_3) δ 1.27 (t, $J = 7.2$ Hz, 3H), 1.31 (s, 3H), 1.42 (s, 3H), 1.43 (s, 3H), 1.49 (s, 3H), 2.08-2.19 (m, 5H), 2.38-2.49 (m, 1H), 2.55-2.63 (m, 1H), 3.95 (d, $J = 2$ Hz, 1H), 4.00-4.03 (m, 1H), 4.11-4.19 (m, 4H), 4.27 (dd, $J = 11.6, 4.8$ Hz, 1H), 4.50 (d, $J = 4.8$ Hz, 1H); ^{13}C NMR (100 MHz, CDCl_3) δ 14.2, 20.9, 24.9, 26.3, 27.5, 28.1, 29.2, 33.1, 60.5, 63.4, 67.0, 71.4, 78.7, 79.6, 96.4, 108.8, 111.8, 170.9, 173.3; HRMS (EI^+) calculated for $\text{C}_{19}\text{H}_{30}\text{O}_9$ $[\text{M}+\text{H}]^+$ 402.1890, found 402.1888.

Synthesis of compound 3-11 (General Procedure B)

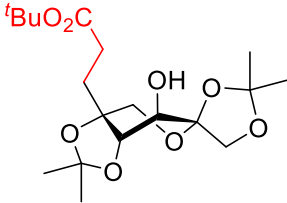


6-*O*-Acetyl-2,3:4,5-di-*O*-isopropylidene- β -D-fructopyranose (**3-1b**), ethyl acrylate (**3-2a**). **3-11**: Yellowish oil, 28.1 mg, 70% yield.

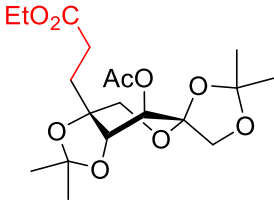
^1H NMR (400 MHz, CDCl_3) δ 1.25 (t, $J = 6.8$ Hz, 3H), 1.36 (s, 3H), 1.40 (s, 3H), 1.43 (s, 3H), 1.54 (s, 3H), 1.94 (t, $J = 8.4$ Hz, 2H), 2.10 (s, 3H),

2.36-2.52 (m, 2H), 3.62 (d, $J = 12.8$ Hz, 1H), 3.70 (d, $J = 12.8$ Hz, 1H), 4.17 (d, $J = 12$ Hz, 1H), 4.13 (q, $J = 6.8$ Hz, 2H), 4.27 (d, $J = 3.2$ Hz, 1H), 4.36 (d, $J = 3.2$ Hz, 1H), 4.42 (d, $J = 12$ Hz, 1H); ^{13}C NMR (100 MHz, CDCl_3) δ 14.2, 20.9, 25.2, 26.3, 26.6, 26.9, 28.6, 33.1, 60.6, 65.4, 65.8, 71.0, 75.5, 79.0, 101.9, 109.3, 109.6, 170.2, 173.1; HRMS (EI^+) calculated for $\text{C}_{19}\text{H}_{30}\text{O}_9$ $[\text{M}+\text{H}]^+$ 402.1890, found 402.1891.

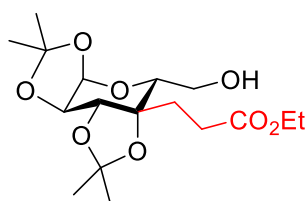
Synthesis of compound 3-12 (General Procedure B)

 2,3:5,6-di-*O*-isopropylidene- β -D-fructopyranose (**3-1c**), *tert*-Butyl acrylate (**3-2b**). **3-12**: Yellowish oil, 27.1 mg, 70% yield. ^1H NMR (400 MHz, CDCl_3) δ 1.38 (s, 3H), 1.42 (s, 3H), 1.43 (s, 9H), 1.44 (s, 3H), 1.51 (s, 3H), 1.91-2.00 (m, 2H), 2.23-2.43 (m, 2H), 3.60 (d, $J = 12$ Hz, 1H), 3.88 (d, $J = 12$ Hz, 1H), 3.96-4.02 (m, 3H), 4.18 (d, $J = 4$ Hz, 1H), (OH is missing); ^{13}C NMR (100 MHz, CDCl_3) δ 25.6, 26.9, 27.0, 27.4, 28.1 (3C), 29.9, 32.9, 67.4, 70.0, 74.6, 78.3, 79.8, 80.4, 103.0, 109.7, 110.3, 172.6; HRMS (EI^+) calculated for $\text{C}_{19}\text{H}_{32}\text{O}_8$ $[\text{M}+\text{H}]^+$ 388.2097, found 388.2096.

Synthesis of compound 3-13 (General Procedure B)

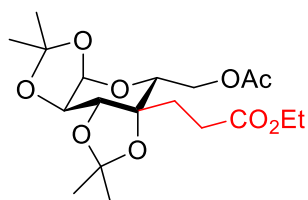
 4-*O*-Acetyl-2,3:5,6-di-*O*-isopropylidene- β -D-fructopyranose (**3-1d**), ethyl acrylate (**3-2a**). **3-13**: White solid, 26.3 mg, 65% yield. ^1H NMR (400 MHz, CDCl_3) δ 1.26 (t, $J = 7.2$ Hz, 3H), 1.35 (s, 3H), 1.39 (s, 3H), 1.46 (s, 3H), 1.47 (s, 3H), 1.87-2.10 (m, 2H), 2.13 (s, 3H), 2.29-2.38 (m, 1H), 2.44-2.54 (m, 1H), 3.73 (d, $J = 12.4$ Hz, 1H), 3.85 (d, $J = 12.4$ Hz, 1H), 3.98 (s, 2H), 4.10-4.16 (m, 3H), 5.33 (d, $J = 4.8$ Hz, 1H); ^{13}C NMR (100 MHz, CDCl_3) δ 14.2, 20.8, 26.00, 26.03, 27.7, 27.8, 28.4, 32.3, 60.6, 66.7, 69.2, 74.0, 78.3, 80.3, 102.4, 110.2, 111.1, 169.7, 173.1; HRMS (EI^+) calculated for $\text{C}_{19}\text{H}_{30}\text{O}_9$ $[\text{M}+\text{H}]^+$ 402.1890, found 402.1892.

Synthesis of compound 3-14 (General Procedure B)



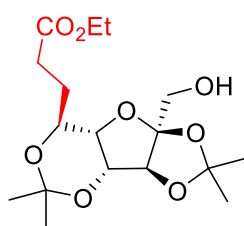
1,2:3,4-di-*O*-isopropylidene- β -D-galactopyranose (**3-1e**), ethyl acrylate (**3-2a**). **3-14**: Yellowish oil, 27.0 mg, 75% yield. ^1H NMR (400 MHz, CDCl_3) δ 1.26 (t, $J = 6.8$ Hz, 3H), 1.33 (s, 3H), 1.37 (s, 3H), 1.43 (s, 3H), 1.54 (s, 3H), 1.88-1.96 (m, 1H), 2.08-2.17 (m, 1H), 2.32-2.40 (m, 1H), 2.45-2.53 (m, 1H), 3.68 (dd, $J = 6.8, 3.6$ Hz, 1H), 3.79-3.85 (m, 2H), 4.14 (q, $J = 6.8, 2\text{H}$), 4.28 (d, $J = 3.2, 1\text{H}$), 4.43 (dd, $J = 5.2, 3.2$ Hz, 1H), 5.58 (d, $J = 5.2$ Hz, 1H), (-OH, missing); ^{13}C NMR (100 MHz, CDCl_3) δ 14.2, 24.9, 25.7, 27.0, 27.1, 28.6, 30.8, 60.6, 61.6, 70.8, 72.0, 74.8, 80.4, 96.3, 109.3, 110.4, 173.1; HRMS (EI^+) calculated for $\text{C}_{17}\text{H}_{28}\text{O}_8$ $[\text{M}+\text{H}]^+$ 360.1784, found 360.1784.

Synthesis of compound 3-15 (General Procedure B)



6-*O*-acetyl-1,2:3,4-di-*O*-isopropylidene- β -D-galactopyranose, (**3-1f**) ethyl acrylate (**3-2a**). **3-15**: Yellowish oil, 32.1 mg, 80% yield. ^1H NMR (400 MHz, CDCl_3) δ 1.25 (t, $J = 7.2$ Hz, 3H), 1.32 (s, 3H), 1.36 (s, 3H), 1.42 (s, 3H), 1.51 (s, 3H), 1.91-2.01 (m, 1H), 2.07-2.16 (m, 1H), 2.08 (s, 3H), 2.34-2.55 (m, 2H), 3.83 (dd, $J = 8.4, 2.4$ Hz, 1H), 4.06 (dd, $J = 12.4, 8.4$ Hz, 1H), 4.13 (dq, $J = 7.2, 1.6$ Hz, 2H), 4.29 (d, $J = 3.2, 1\text{H}$), 4.40 (dd, $J = 5.2, 3.2$ Hz, 1H), 4.45 (dd, $J = 12.4, 2.4$ Hz, 1H), 5.56 (d, $J = 5.2$ Hz, 1H); ^{13}C NMR (100 MHz, CDCl_3) δ 14.2, 20.9, 24.9, 25.7, 27.0, 27.1, 28.6, 31.0, 60.6, 63.7, 70.0, 70.6, 74.9, 80.1, 96.3, 109.3, 110.5, 171.2, 173.0; HRMS (EI^+) calculated for $\text{C}_{19}\text{H}_{30}\text{O}_9$ $[\text{M}+\text{H}]^+$ 402.1890, found 402.1889.

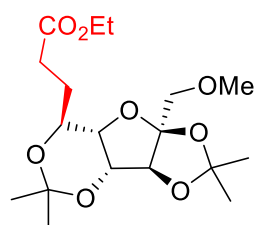
Synthesis of compound 3-18 (General Procedure B)



2,3:4,6-di-*O*-isopropylidene- α -L-sorbofuranose (**3-1g**), ethyl acrylate (**3-2a**). **3-18**: Yellowish oil, 17.3 mg, 48% yield. ^1H NMR (400 MHz, CDCl_3) δ 1.25 (t, $J = 6.8$ Hz, 3H), 1.32 (s, 3H), 1.33 (s, 3H), 1.38 (s, 3H), 1.51 (s, 3H), 1.80-1.90 (m, 1H), 2.01-2.09 (m, 1H), 2.33-2.49 (m, 2H), 3.47-3.52 (m, 1H), 3.67-3.78 (m, 2H), 4.12 (q, $J = 6.8$ Hz, 2H), 2.24-2.27 (m, 1H), 4.25 (s, 1H), 4.52 (s, 1H), (-OH, missing); ^{13}C NMR (100 MHz, CDCl_3) δ 14.2, 23.6, 24.0, 26.8, 27.6, 28.8, 30.3,

60.4, 63.3, 71.4, 74.5, 83.8, 83.9, 100.9, 112.7, 115.8, 173.1; HRMS (EI⁺) calculated for C₁₇H₂₈O₈ [M-CH₃]⁺ 345.1549, found 345.1548.

Synthesis of compound 3-19 (General Procedure B)



1-*O*-methyl-2,3:4,6-di-*O*-isopropylidene- α -L-sorbofuranose (**3-1h**), ethyl acrylate (**3-2a**). **3-19**: Yellowish oil, 19.4 mg, 54% yield.

¹H NMR (400 MHz, CDCl₃) δ 1.24 (t, *J* = 6.8 Hz, 3H), 1.31 (s, 6H), 1.38 (s, 3H), 1.50 (s, 3H), 1.78-1.88 (m, 1H), 2.00-2.09 (m, 1H), 2.32-2.48 (m, 2H), 3.43 (s, 3H), 3.43-3.48 (m, 1H), 3.52 (d, *J* = 10.8 Hz, 1H), 3.62 (d, *J* = 10.8 Hz, 1H), 4.11 (q, *J* = 6.8 Hz, 2H), 2.22-2.25 (m, 1H), 4.23 (s, 1H), 4.51 (s, 1H); ¹³C NMR (100 MHz, CDCl₃) δ 14.2, 23.7, 23.9, 26.6, 27.7, 28.8, 30.4, 59.8, 60.3, 71.3, 72.7, 74.7, 83.6, 83.8, 100.7, 112.7, 115.2, 173.1; HRMS (EI⁺) calculated for C₁₇H₂₇O₈ [M-CH₃]⁺ 359.1706, found 359.1704.

Synthesis of 3-3b on gram scale

2,3:4,5-di-*O*-isopropylidene- β -D-fructopyranose (**3-1a**, 1.50 g, 5.76 mmol), anthraquinone (240 mg, 1.15 mmol, 20 mol%), K₃PO₄ (1.22 g, 5.76 mmol, 1.0 equiv) and acetonitrile (57.6 mL) were added to a 100 mL round-bottomed flask under N₂ atmosphere. Then *tert*-butyl acrylate (**3-2b**, 2.22 g, 17.3 mmol, 3.0 equiv) was added and the mixture was stirred at rt, for 84 h under UV-LED (365 nm) irradiation. The reaction mixture was evaporated to remove solvent, then added dichloromethane 20 mL, washed with water and brine, dried over Na₂SO₄, and concentrated in vacuo. The mixture of mono-alkylated products **3-3b** and **3-4b** was obtained in 76% yield and the ratio of **3-3b**: **3-4b** was 2.6:1.0. The major product **3-3b** was isolated by column chromatography on silica gel to give 1.25 g.

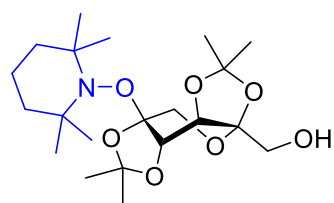
Synthesis of 3-4a on gram scale

2,3:4,5-Di-*O*-isopropylidene- β -D-fructopyranose (**3-1a**, 1.50 g, 5.76 mmol), TBADT (191 mg, 57.6 μ mol, 1.0 mol%), and acetonitrile (57.6 mL) were added to a 100 mL round-bottomed flask under N₂ atmosphere. Then ethyl acrylate (**3-2a**, 1.73 g, 17.3 mmol, 3.0 equiv) was added and the mixture was stirred at rt, for 84 h under UV-

LED (365 nm) irradiation. The reaction mixture was evaporated to remove the solvent and was extracted with dichloromethane (2×10 mL). The organic layer was washed with water and brine, dried over Na_2SO_4 , filtered, and concentrated in vacuo. Monoalkylated product **3-4a** was isolated by column chromatography on silica gel to give 1.97 g (95%) of **3-4a**.

Isolation of compound 3-20

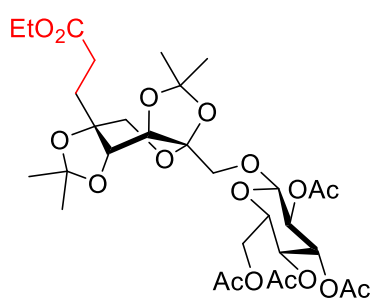
To confirm the structure of TEMPO-adduct **3-20**, **3-20** was synthesized by another route. **3-1a**: (260 mg, 1.00 mmol), **3-2a** (3.00 mmol, 3.0 equiv), TEMPO (1.50 mmol, 1.5 equiv), TBADT (33 mg, 10.0 μmol , 1.0 mol%), and acetonitrile (10 mL) were added into a flask (50 mL) under N_2 atmosphere, and the mixture was stirred at rt for 24 h, under UV-LED (365 nm) irradiation. The mixture was concentrated under reduced pressure, and the crude mixture was purified by column chromatography on silica gel to give **3-20** as a yellowish oil.



^1H NMR (400 MHz, CDCl_3) δ 1.09 (s, 3H), 1.12 (s, 3H), 1.20 (s, 3H), 1.35 (s, 3H), 1.40 (s, 3H), 1.40-1.58 (m, 6H), 1.46 (s, 3H), 1.52 (s, 3H), 1.58 (s, 3H), 3.64-3.71 (m, 2H), 4.04 (d, $J = 12.8$ Hz, 1H), 4.16 (d, $J = 12.8$ Hz, 1H), 4.29 (d, $J = 2.4$ Hz, 1H), 4.50 (d, $J = 2.4$ Hz, 1H), (OH is missing); ^{13}C NMR (100 MHz, CDCl_3) δ 16.8, 20.2, 20.4, 25.1, 26.0, 26.3, 26.4, 34.0, 34.9, 40.3, 41.0, 60.0, 60.3, 61.3, 65.1, 72.3, 78.2, 103.0, 105.5, 108.4, 109.0; HRMS (EI^+) calculated for $\text{C}_{21}\text{H}_{37}\text{O}_7$ $[\text{M}+\text{H}]^+$ 415.2570, found 415.2569.

General procedure: Glycoconjugate **3-21–25** (0.100 mmol), TBADT (3.3 mg, 1.0 μmol , 1.0 mol%), and acetonitrile (1.0 mL) were added to a test tube under N_2 atmosphere. To the mixture, ethyl acrylate (**3-2a**, 0.300 mmol, 3.0 equiv) was added, and the mixture was stirred at rt for 24 h under UV-LED (365 nm) irradiation. The reaction mixture was evaporated and extracted with dichloromethane (2×2 mL). The organic layer was washed with water and brine, dried over Na_2SO_4 , filtered, and concentrated in vacuo. The reaction mixture was purified by column chromatography on silica gel.

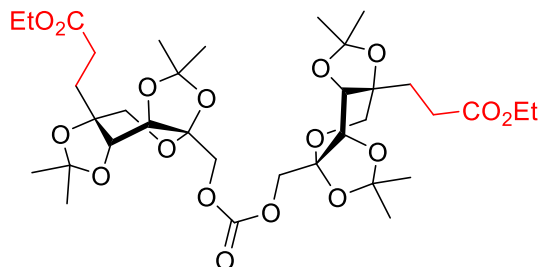
Synthesis of compound 3-21



3-1k, ethyl acrylate (**3-2a**). **3-21**: Yellowish oil, 51.8 mg, 75% yield.

^1H NMR (400 MHz, CDCl_3) δ 1.25 (t, $J = 7.2$ Hz, 3H), 1.33 (s, 3H), 1.36 (s, 3H), 1.40 (s, 3H), 1.52 (s, 3H), 1.91-1.95 (m, 2H), 1.99 (s, 3H), 2.01 (s, 3H), 2.02 (s, 3H), 2.07 (s, 3H), 2.34-2.51 (m, 2H), 3.57 (d, $J = 12.4$ Hz, 1H), 3.68-3.73 (m, 3H), 3.93 (d, $J = 12.4$ Hz, 1H), 4.10-4.15 (m, 3H), 4.21-4.26 (m, 2H), 4.45 (d, $J = 3.2$ Hz, 1H), 4.64 (d, $J = 8.4$ Hz, 1H), 5.03 (t, $J = 8.4$ Hz, 1H), 5.08 (t, $J = 9.6$ Hz, 1H), 5.18 (t, $J = 9.6$ Hz, 1H); ^{13}C NMR (100 MHz, CDCl_3) δ 14.2, 20.6, 20.7, 25.4, 26.3, 26.6 (2C), 26.8 (2C), 28.7, 33.0, 60.6, 62.1, 65.7, 68.5, 69.9, 70.2, 71.3, 71.8, 73.1, 75.6, 79.2, 100.2, 102.3, 109.2, 109.4, 169.2, 169.4, 170.3, 170.6, 173.2; HRMS (EI^+) calculated for $\text{C}_{31}\text{H}_{46}\text{O}_{17}$ $[\text{M}+\text{H}]^+$ 690.2735, found 690.2736.

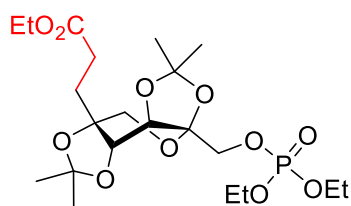
Synthesis of compound 3-22



3-1l, ethyl acrylate (**3-2a**). **3-22**: White solid, 52.6 mg, 72% yield.

^1H NMR (400 MHz, CDCl_3) δ 1.25 (t, $J = 7.2$ Hz, 6H), 1.36 (s, 6H), 1.38 (s, 6H), 1.42 (s, 6H), 1.54 (s, 6H), 1.93 (t, $J = 7.6$ Hz, 4H), 2.34-2.51 (m, 4H), 3.61 (d, $J = 12.4$ Hz, 2H), 3.70 (d, $J = 12.4$ Hz, 2H), 4.11 (d, $J = 11.6$ Hz, 2H), 4.12 (q, $J = 7.2$ Hz, 4H), 4.27 (d, $J = 3.2$ Hz, 2H), 4.38 (d, $J = 3.2$ Hz, 2H), 4.44 (d, $J = 11.6$ Hz, 2H); ^{13}C NMR (100 MHz, CDCl_3) δ 14.2, 25.1, 26.3, 26.6, 26.8, 28.6, 33.0, 60.6, 65.8, 67.9, 70.6, 75.4, 79.0, 101.6, 109.5, 109.6, 154.4, 173.1; HRMS (FAB^+) calculated for $\text{C}_{34}\text{H}_{51}\text{O}_{17}$ $[\text{M}-\text{CH}_3]^+$ 731.3126, found 731.3124.

Synthesis of compound 3-23

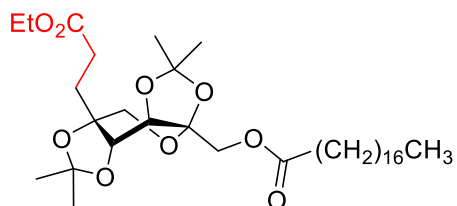


3-1m, ethyl acrylate (**3-2a**). **3-23**: White solid, 39.3 mg, 79% yield.

^1H NMR (400 MHz, CDCl_3) δ 1.24 (t, $J = 6.8$ Hz, 3H), 1.32 (dt, $J = 6.8, 2.8$ Hz, 6H), 1.35 (s, 3H), 1.40 (s, 6H),

1.54 (s, 3H), 1.92 (t, $J = 7.6$ Hz, 2H), 2.33-2.51 (m, 2H), 3.59 (d, $J = 12.4$ Hz, 1H), 3.69 (d, $J = 12.4$ Hz, 1H), 4.01-4.17 (m, 8H), 4.27 (d, $J = 3.2$ Hz, 1H), 4.42 (d, $J = 3.2$ Hz, 1H); ^{13}C NMR (100 MHz, CDCl_3) δ 14.1, 16.0, 16.1, 25.4, 26.3, 26.6, 26.8, 28.0, 28.6, 32.9, 60.6, 63.86, 63.92, 65.8, 67.2, 70.1, 75.4, 79.0, 101.9, 109.5, 173.1; HRMS (FAB^+) calculated for $\text{C}_{21}\text{H}_{37}\text{O}_{11}\text{P}$ $[\text{M}+\text{H}]^+$ 497.2152, found 497.2152.

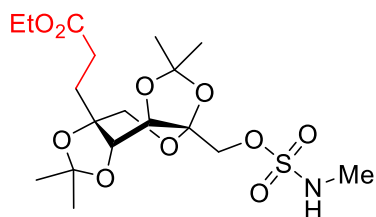
Synthesis of compound 3-24



3-1n, ethyl acrylate (**3-2a**). **3-24**: White solid, 40.1 mg, 64% yield.

^1H NMR (400 MHz, CDCl_3) δ 0.87 (t, $J = 6.4$ Hz, 3H), 1.24-1.27 (m, 33 H), 1.37 (s, 3H), 1.40 (s, 3H), 1.44 (s, 3H), 1.55 (s, 3H), 1.94 (t, $J = 7.6$ Hz, 2H), 2.32-2.53 (m, 2H), 2.34 (t, $J = 7.6$ Hz, 2 H), 3.62 (d, $J = 12.4$ Hz, 1H), 3.70 (d, $J = 12.4$ Hz, 1H), 4.04-4.16 (m, 3H), 4.27 (d, $J = 3.2$ Hz, 1H), 4.37 (d, $J = 3.2$ Hz, 1H), 4.40 (m, 1H); ^{13}C NMR (100 MHz, CDCl_3) δ 14.08, 14.14, 22.6, 24.7, 25.2, 26.2, 26.6, 26.8, 28.6, 29.0, 29.2, 29.3, 29.4, 29.5, 29.58 (3C), 29.62 (4C), 31.8, 33.0, 34.1, 60.5, 65.1, 65.7, 70.8, 75.4, 79.0, 101.9, 109.2, 109.6, 173.0, 173.1; HRMS (EI^+) calculated for $\text{C}_{35}\text{H}_{62}\text{O}_9$ $[\text{M}+\text{H}]^+$ 626.4394, found 626.4393.

Synthesis of compound 3-25

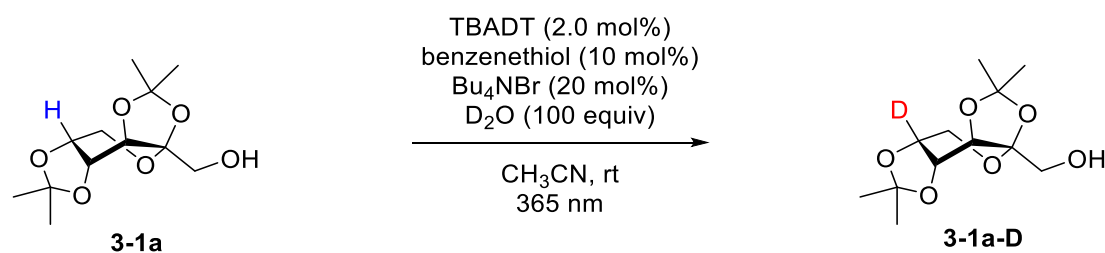


3-1o, ethyl acrylate (**3-2a**). **3-25**: Yellowish oil, 41.7 mg, 92% yield.

^1H NMR (400 MHz, CDCl_3) δ 1.25 (t, $J = 7.2$ Hz, 3H), 1.36 (s, 3H), 1.42 (s, 6H), 1.55 (s, 3H), 1.94 (t, $J = 8.4$ Hz, 2H), 2.34-2.52 (m, 2H), 2.83 (d, $J = 4.8$ Hz, 3H), 3.62 (d, $J = 12.4$ Hz, 1H), 3.70 (d, $J = 12.4$ Hz, 1H), 4.10-4.22 (m, 4H), 4.29 (d, $J = 3.2$ Hz, 1H), 4.38 (d, $J = 3.2$ Hz, 1H), 4.62 (q, $J = 4.8$ Hz, 1H); ^{13}C NMR (100 MHz, CDCl_3) δ 14.2, 25.2, 26.3, 26.5, 26.8, 28.6, 29.8, 32.9, 60.6, 65.8, 70.1, 70.5, 75.3, 78.9, 101.2, 109.6, 109.8, 173.1; HRMS (EI^+) calculated for $\text{C}_{18}\text{H}_{31}\text{NO}_{10}\text{S}$ $[\text{M}+\text{H}]^+$ 453.1669, found 453.1667.

Preparation of deuterated 3-1a-D

The prepared procedure referred to Wu's report.²⁹ To a 50 mL two-neck flask was added **3-1a** (260 mg, 1.00 mmol), TBADT (66.4 mg, 20.0 μmol , 2.0 mol%), tetrabutylammonium bromide (64.5 mg, 0.200 mmol, 20 mol%) under N_2 atmosphere. Dichloromethane (DCM, 10 mL), D_2O (2.0 mL, 100 equiv), benzenethiol (0.100 mmol, 10 mol%) were added dropwise via syringe. The mixture was stirred at rt for 24 h under UV-LED (365 nm) irradiation. The reaction mixture was concentrated under reduced pressure, and was added DCM (10 mL) and H_2O (10 mL). The organic phase was separated and was washed with sat. brine (10 mL), dried over MgSO_4 , filtered, and concentrated under reduced pressure. The crude mixture was purified by column chromatography on silica gel to give **3-1a-D** as a white solid. The product contains 89% deuterium atom on C1 determined by NMR.



¹H NMR (400 MHz, CDCl_3) δ 1.34 (s, 3H), 1.39 (s, 3H), 1.48 (s, 3H), 1.54 (s, 3H), 2.12-2.16 (m, 1H), 3.64-3.73 (m, 2H), 3.77 (d, $J = 12.8$ Hz, 1H), 3.91 (d, $J = 12.8$ Hz, 1H), 4.24 (dd, $J = 6.4, 1.2$ Hz, 0.11H), 4.34 (d, $J = 2.8$ Hz, 1H), 4.60 (d, $J = 2.8$ Hz, 0.78H);
¹³C NMR (100 MHz, CDCl_3) δ 23.9, 25.3, 25.7, 26.4, 61.1, 65.5, 69.9, 70.8, 70.9, 103.0, 108.5, 109.0; HRMS (EI^+) calculated for $\text{C}_{11}\text{H}_{16}\text{DO}_6$ $[\text{M}-\text{CH}_3]^+$ 246.1084, found 246.1086.

The Kinetic Isotope Effect (KIE) Experiments of 3-1a and 3-1a-D

Experimental Procedure A for 3-1a

The method is according to reported work.³⁰ Six parallel reactions were carried out at the same time. To a 10 mL Schlenk tube were added **3-1a** (26.0 mg, 0.100 mmol) and TBADT (3.3 mg, 10 μmol , 1.0 mol%). It was evacuated and back-filled with

nitrogen (three times). Then CH₃CN (1.0 mL) and ethyl acrylate (**3-2a**, 0.300 mmol, 3.0 equiv) were added via syringe. The mixture was stirred at rt for fixed time (10 min, 20 min, 30 min, 40 min, 50 min and 60 min) under UV-LED (365 nm) irradiation. After the reaction, the mixture was concentrated under reduced pressure, and was added 1,1,2,2-tetrachloroethane (0.100 mmol) as an internal standard. The yield of product **3-4a** was determined by ¹H NMR (Scheme 3-13a).

Experimental Procedure B for 3-1a-D

3-1a-D (26.1 mg, 0.10 mmol) was substrate. Six parallel reactions were prepared at the same time. And the procedure is same as procedure A (Scheme 3-13b).

3.5 References

1. (a) Comini, L. R.; Fernandez, I. M.; Vittar, N. R.; Montoya, S. N.; Cabrera, J. L.; Rivarola, V. A. *Phytomedicine* **2011**, *18*, 1093–1095. (b) Comini, L. R.; Montoya, S. N.; Páez, P. L.; Argüello, G. A.; Albesa, I.; Cabrera, J. L. *J. Photochem. Photobiol. B, Biol.* **2011**, *102*, 108–114. (c) Ma, W.; Liu, C.; Li, J.; Hao, M.; Ji, Y.; Zeng, X. *Photochem. Photobiol. Sci.* **2020**, *19*, 485–494. (d) Mugas, M. L.; Calvo, G.; Marioni, J.; Céspedes, M.; Martinez, F.; Sáenz, D.; Venosa, G. D.; Cabrera, J.; Montoya, S. N.; Casas, A. *J. Photochem. Photobiol. B, Biol.* **2021**, *214*, 112089. (e) Ma, W.; Zhang, M.; Cui, Z.; Wang, X.; Niu, X.; Zhu, Y.; Yao, Z.; Ye, F.; Geng, S.; Liu, C. *Microb. Biotechnol.* **2022**, *15*, 499–512.
2. (a) Egerton, G. S.; Morgan, A. G. *J. Soc. Dye. Colour.* **1971**, *87*, 268–277. (b) Bachman, J. E.; Curtiss, L. A.; Assary, R. S. *J. Phys. Chem. A* **2014**, *118*, 8852–8860.
3. (a) Ando, Y.; Suzuki, K. *Chem. Eur. J.* **2018**, *24*, 15955–15964. (b) Cervantes-González, J.; Vosburg, D. A.; Mora-Rodriguez, S. E.; Vázquez, M. A.; Zepeda, L. G.; Villegas Gomez, C.; Lagunas-Rivera, S. *ChemCatChem* **2020**, *12*, 3811–3827. (c) Lee, W.; Jung, S.; Kim, M.; Hong, S. *J. Am. Chem. Soc.* **2021**, *143*, 3003–3012.
4. Norrish, R. G. W.; Bamford, C. H. *Nature* **1937**, *140*, 195–196.
5. (a) Cameron, D. W.; Giles, R. G. F. *Chem. Commun.* **1965**, 573–574. (b) Cameron, D. W.; Giles, R. G. F. *J. Chem. Soc. C* **1968**, 1461–1464.
6. Ando, Y.; Matsumoto, T.; Suzuki, K. *Synlett* **2017**, *28*, 1040–1045.
7. Kamijo, S.; Takao, G.; Kamijo, K.; Tsuno, T.; Ishiguro, K.; Murafuji, T. *Org. Lett.* **2016**, *18*, 4912–4915.
8. (a) Du, D.-Y.; Qin, J.-S.; Li, S.-L.; Su, Z.-M.; Lan, Y.-Q. *Chem. Soc. Rev.* **2014**, *43*, 4615–4632. (b) Wang, S.-S.; Yang, G.-Y. *Chem. Rev.* **2015**, *115*, 4893–4961. (c) Yang, G.-P.; Zhang, N.; Ma, N.-N.; Yu, B.; Hu, C.-W. *Adv. Synth. Catal.* **2017**, *359*, 926–932. (d) Chen, L.; Chen, W.-L.; Wang, X.-L.; Li, Y.-G.; Su, Z.-M.; Wang, E.-B. *Chem. Soc. Rev.* **2019**, *48*, 260–284. (e) Huang, B.; Yang, D.-H.; Han, B.-H. *J. Mater. Chem. A* **2020**, *8*, 4593–4628.
9. For the reports on the mechanism of decatungstate photocatalysis and the application to C–H transformations, see: (a) Renneke, R. F.; Pasquali, M.; Hill, C. L. *J. Am. Chem. Soc.* **1990**, *112*, 6585–6594. (b) Renneke, R. F.; Kadkhodayan, M.; Pasquali, M.; Hill, C. L. *J. Am. Chem. Soc.* **1991**, *113*, 8357–8367. (c) Hill, C. L. *Synlett* **1995**, 127–132.

- (d) Texier, I.; Delaire, J. A.; Giannotti, C. *Phys. Chem. Chem. Phys.* **2000**, *2*, 1205–1212. (e) Ravelli, D.; Protti, S.; Fagnoni, M. *Acc. Chem. Res.* **2016**, *49*, 2232–2242. (f) Waele, V. D.; Poizat, O.; Fagnoni, M.; Bagno, A.; Ravelli, D. *ACS Catal.* **2016**, *6*, 7174–7182. (g) Perry, I. B.; Brewer, T. F.; Sarver, P. J.; Schultz, D. M.; DiRocco, D. A.; MacMillan, D. W. C. *Nature* **2018**, *560*, 70–75. (h) Sarver, P. J.; Bacauanu, V.; Schultz, D. M.; DiRocco, D. A.; Lam, Y. H.; Sherer, E. C.; MacMillan, D. W. C. *Nat. Chem.* **2020**, *12*, 459–467. (i) Jiang, H.; Yu, X.; Daniliuc, C. G.; Studer, A. *Angew. Chem. Int. Ed.* **2021**, *60*, 14399–14404.
10. Duncan, D. C.; Netzel, T. L.; Hill, C. L. *Inorg. Chem.* **1995**, *34*, 4640–4646.
11. Waele, V. D.; Poizat, O.; Fagnoni, M.; Bagno, A.; Ravelli, D. *ACS Catal.* **2016**, *6*, 7174–7182.
12. Raviola, C.; Ravelli, D. *Synlett* **2019**, *3*, 803–808.
13. Shih, Y. L.; Huang, S. H.; Wu, Y. K.; Ryu, I. *Bull. Chem. Soc. Jpn.* **2022**, *95*, 1501–1505.
14. Matsuo, T.; Mayer, J. M. *Inorg. Chem.* **2005**, *44*, 2150–2158.
15. (a) Binkley, J. S.; Pople, J. A.; Hehre, W. J. *J. Am. Chem. Soc.* **1980**, *102*, 939–947. (b) Lee, C.; Yang, W.; Parr, R. G. *Phys. Rev. B* **1988**, *37*, 785–789. (c) Antony, J.; Grimme, S. *Phys. Chem. Chem. Phys.* **2006**, *8*, 5287–5293.
16. Frisch, J. J. et al., *Gaussian 16*, Rev. B.01; Gaussian, Inc.: Wallingford, CT, **2016**.
17. Li, C.; Danovich, D.; Shaik, S. *Chem. Sci.* **2012**, *3*, 1903–1918.
18. Jeffrey, J. L.; Terrett, J. A.; MacMillan, D. W. *Science* **2015**, *349*, 1532–1536.
19. (a) Naguib, Y. M. A.; Steel, C.; Cohen, S. G.; Young, M. A. *J. Phys. Chem.* **1987**, *91*, 3033–3036. (b) Dondi, D.; Fagnoni, M.; Albin, A. *Chem. Eur. J.* **2006**, *12*, 4153–4163. (c) Tanielian, C.; Cougnon, F.; Seghrouchni, R. *J. Mol. Catal. A: Chem.* **2007**, *262*, 164–169. (d) Lai, W.; Li, C.; Chen, H.; Shaik, S. *Angew. Chem., Int. Ed.* **2012**, *51*, 5556–5578.
20. Duncan, D. C.; Netzel, T. L.; Hill, C. L. *Inorg. Chem.* **1995**, *34*, 4640–4646.
21. Li, C.; Danovich, D.; Shaik, S. *Chem. Sci.* **2012**, *3*, 1903–1918.
22. Shu, W.; Zhang, H.; Huang, Y. *Org. Lett.* **2019**, *21*, 6107–6111.
23. Duncan, D. C.; Netzel, T. L.; Hill, C. L. *Inorg. Chem.* **1995**, *34*, 4640–4646.

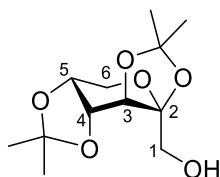
24. (a) Heidlas, J. E.; Williams, K. W.; Whitesides, G. M. *Acc. Chem. Res.* **1992**, *25*, 307–314. (b) Plante, O. J.; Palmacci, E. R.; Andrade, R. B.; Seeberger, P. H. *J. Am. Chem. Soc.* **2001**, *123*, 9545–9554.
25. Hyenne, V.; Labouesse, M. *Nat. Cell Biol.* **2011**, *13*, 1185–1187.
26. Maryanoff, B. E.; Nortey, S. O.; Gardocki, J. F.; Shank, R. P.; Dodgson, S. P. *J. Med. Chem.* **1987**, *30*, 880–887.
27. Ishigaki, Y.; Shimajiri, T.; Takeda, T.; Katoono, R.; Suzuki, T. *Chem.* **2018**, *4*, 795–806.
28. (a) Duncan, D. C.; Netzel, T. L.; Hill, C. L. *Inorg. Chem.* **1995**, *34*, 4640–4646. (b) Lowry, M. S.; Goldsmith, J. I.; Slinker, J. D.; Rohl, R.; Pascal, R. A.; Malliaras, G. G.; Bernhard, S. *Chem. Mater.* **2005**, *17*, 5712–5719. (c) Serra, F.; Coutrot, P.; Esteve-Quellejeu, M.; Herson, P.; Olszewski, T. K.; Grison, C. *Eur. J. Org. Chem.* **2011**, *10*, 1841–1847.
29. Kuang, Y.; Cao, H.; Tang, H.; Chew, J.; Chen, W.; Shi, X.; Wu, J. *Chem. Sci.* **2020**, *11*, 8912–8918.
30. (a) Simmons, E. M.; Hartwig, J. F. *Angew. Chem. Int. Ed.* **2012**, *51*, 3066–3072. (b) Shu, W.; Zhang, H.; Huang, Y. *Org. Lett.* **2019**, *21*, 6107–6111.

3.6 Supporting Information

3.6.1 DFT Calculation Data of 3-1a

Bond dissociation enthalpies of chair conformation of 3-1a

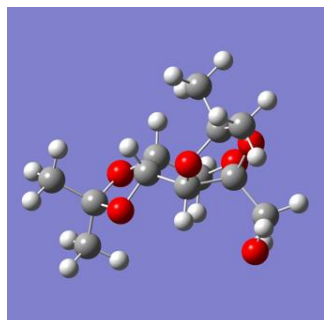
DFT calculations were carried out using the Gaussian 16 suite of programs at the UB3LTP/6-31G(d) level of theory.^{15,16} Vibrational frequency calculations were carried out for each stationary point to ensure they were energy minimum (no imaginary frequencies). Frequency calculations were carried out at 1 atm and 298.15 K.



3-1a

3D images of chair conformation of 3-1a

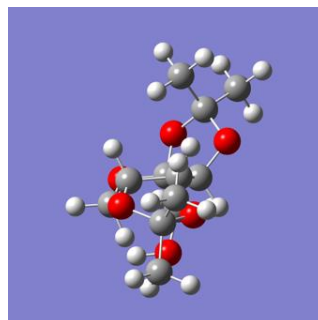
Front view



Top view



Side view



Bond dissociation enthalpy calculations

Geometry optimizations and frequency calculations were carried out for chair conformation of **3-1a**.

Calculated energies and geometries

Chair conformation of 3-1a

Energy

Electronic Energy (EE)	-920.64918
Zero-point Energy Correction	0.322515
Thermal Correction to Energy	0.340058
Thermal Correction to Enthalpy	0.341002
Thermal Correction to Free Energy	0.277977
EE + Zero-point Energy	-920.32667
EE + Thermal Energy Correction	-920.30912
EE + Thermal Enthalpy Correction	-920.30818
EE + Thermal Free Energy Correction	-920.37121
Imaginary Freq	0

Energies in Hartree, calculated in MeCN.

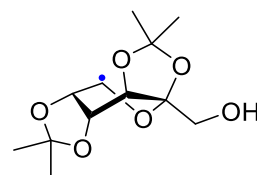
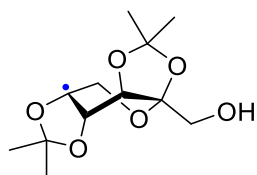
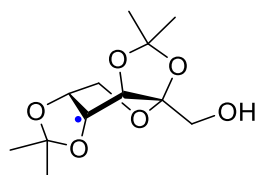
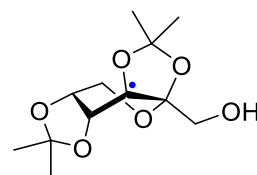
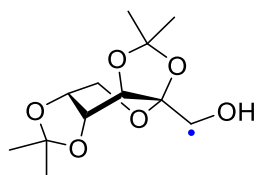
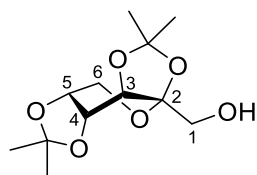
Geometry:

Atom	X	Y	Z
C	-0.74371900	-0.68091100	-0.15938300
C	0.55614800	-0.07798300	-0.74488200
C	1.37826800	0.88623500	0.17125900
C	-0.70556900	1.32565300	1.33230900
C	-1.22362900	-0.09813100	1.17936400
H	0.27198700	0.43472200	-1.66768000
H	-0.61810400	-1.76941500	-0.10494900
H	-1.02304800	1.76276200	2.28243400
H	-1.08920200	1.94514200	0.51139700
H	-0.90385000	-0.70174500	2.03643700
O	-1.82724000	-0.34814700	-1.02919900
O	-2.64371600	-0.11518200	1.09124200
O	2.51423600	0.13493100	0.54679200
O	1.50190300	-1.08413900	-1.08501000
C	1.89965200	2.12810200	-0.56633700
H	2.70709300	2.55792400	0.04230300
H	2.31948200	1.82664800	-1.53105500
O	0.87780600	3.07341600	-0.83850600
H	0.62678500	3.45631300	0.01663400
O	0.72283800	1.32049200	1.35768800
C	-3.02676300	-0.42176500	-0.26517200
C	2.48927300	-1.16333600	-0.05644600
C	-3.62311100	-1.83065600	-0.30470500
H	-4.49866400	-1.88720100	0.34950800
H	-3.92590100	-2.08810500	-1.32467500
H	-2.89265100	-2.56906400	0.03983900
C	-3.98797700	0.64214600	-0.77679600
H	-4.26262900	0.43756000	-1.81618500

H	-4.89718600	0.65150400	-0.16827000
H	-3.51461200	1.62602500	-0.72385600
C	3.83516100	-1.43189100	-0.71577200
H	4.63034800	-1.44103000	0.03556500
H	3.81926600	-2.40077500	-1.22434800
H	4.04686100	-0.65028200	-1.44989100
C	2.13370700	-2.21425100	0.99905000
H	2.06380600	-3.20634600	0.54184500
H	2.90436100	-2.23682300	1.77580200
H	1.18059600	-1.97805600	1.48015400

Bond dissociation enthalpies of boat conformation of 3-1a

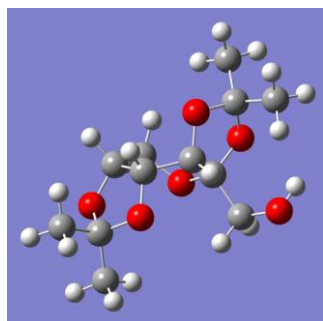
Species of calculation



3D images of boat conformation of 3-1a

3-1a

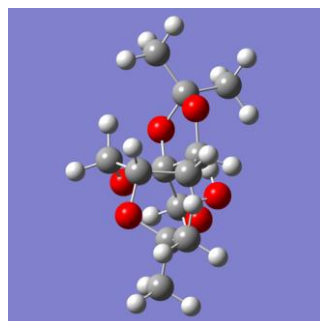
Front view



Top view

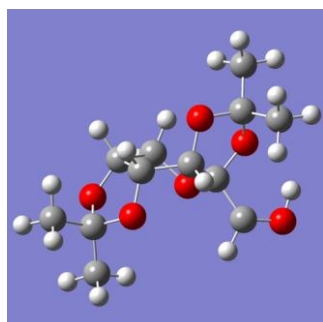


Side view



[3-1a-C1-H]•

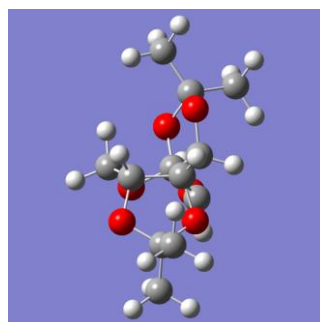
Front view



Top view

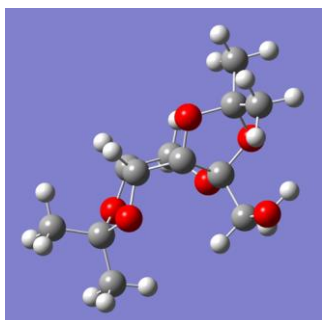


Side view

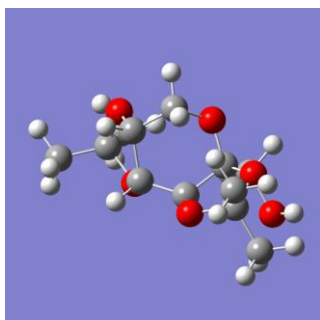


[3-1a-C3-H]•

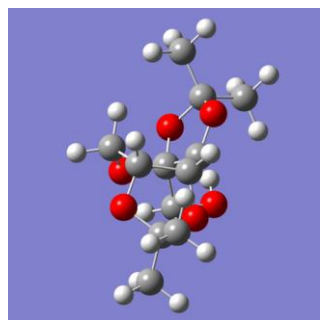
Front view



Top view



Side view

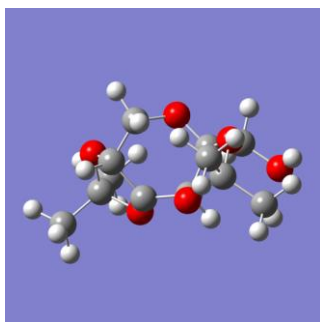


[3-1a-C4-H]•

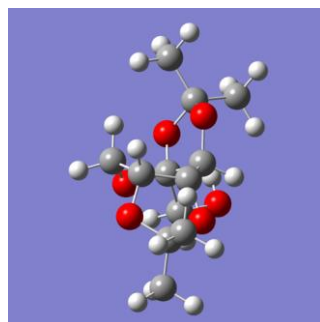
Front view



Top view

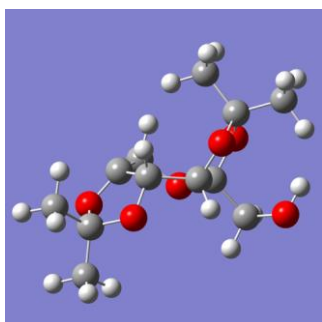


Side view



[3-1a-C5-H]•

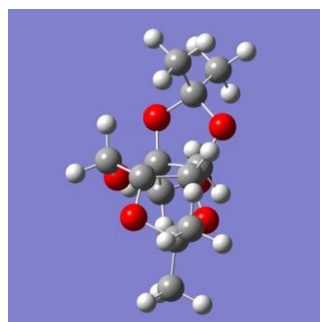
Front view

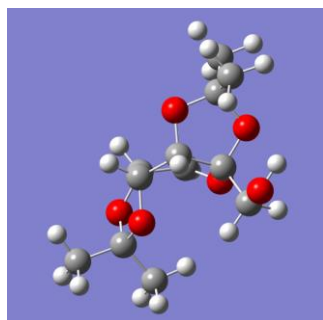
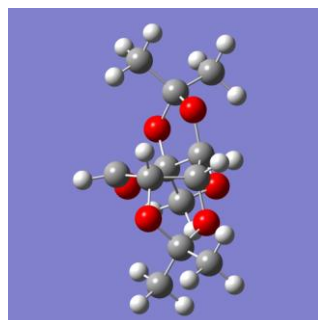


Top view



Side view



[3-1a-C6-H]•**Front view****Top view****Side view****Calculated energies and geometries****3-1a****Energy**

Electronic Energy (EE)	-920.66217
Zero-point Energy Correction	0.322925
Thermal Correction to Energy	0.340254
Thermal Correction to Enthalpy	0.341198
Thermal Correction to Free Energy	0.279203
EE + Zero-point Energy	-920.33925
EE + Thermal Energy Correction	-920.32192
EE + Thermal Enthalpy Correction	-920.32097
EE + Thermal Free Energy Correction	-920.38297
Imaginary Freq	0

Energies in Hartree, calculated in MeCN.

Geometry

Atom	X	Y	Z
C	-0.88737000	-0.62156700	-0.82763200
C	-1.31068800	-1.35919100	0.47108200
C	-0.33578300	-1.11531000	1.61521900
C	0.88834600	0.65670800	0.55868200
C	0.51346100	-0.01905300	-0.78062700
H	-0.83140000	-1.29717200	2.57226800
H	-1.41224100	-2.43786200	0.30126900
H	0.62405400	0.70251400	-1.59980900
H	-0.94826000	-1.29083500	-1.69487800
H	0.52085300	-1.79403100	1.53367900
O	0.09667000	0.24790900	1.64761400
O	2.25500800	0.27621300	0.74079900
O	1.45618500	-1.08370600	-0.90469600
O	-1.82287000	0.44809700	-0.94435300

O	-2.58319100	-0.79222400	0.80046500
C	2.66868600	-0.65145500	-0.28761200
C	3.35009400	-1.85049000	0.35247700
H	2.68859000	-2.32243300	1.08452100
H	3.61308400	-2.58636900	-0.41422300
H	4.26867000	-1.53456200	0.85686500
C	3.57047100	0.06442100	-1.29346400
H	4.46433800	0.44863400	-0.79042500
H	3.88666700	-0.63225800	-2.07685100
H	3.04613900	0.90335500	-1.75992400
C	0.80087400	2.18779200	0.56096600
H	-0.19815500	2.48950200	0.23693200
H	0.95044800	2.53213400	1.59442700
O	1.72785000	2.78277800	-0.33083900
H	2.60624100	2.47335400	-0.04771600
C	-3.01991100	0.04666800	-0.27209900
C	-3.68343500	1.28315600	0.31138300
H	-3.96482400	1.97710100	-0.48703200
H	-4.58770100	1.00262800	0.86074700
H	-2.99210900	1.78300800	0.99604000
C	-3.93412600	-0.73278500	-1.22022500
H	-4.82566200	-1.07666400	-0.68535300
H	-4.25112400	-0.09687400	-2.05376600
H	-3.41853600	-1.60907200	-1.62758400

[3-1a-C1-H]•

Energy

Electronic Energy (EE)	-920.00047
Zero-point Energy Correction	0.309087
Thermal Correction to Energy	0.326505
Thermal Correction to Enthalpy	0.327449
Thermal Correction to Free Energy	0.264062
EE + Zero-point Energy	-919.69138
EE + Thermal Energy Correction	-919.67396
EE + Thermal Enthalpy Correction	-919.67302
EE + Thermal Free Energy Correction	-919.7364
Imaginary Freq	0

Energies in Hartree, calculated in MeCN.

Geometry

Atom	X	Y	Z
C	-0.94170500	-0.87105100	-0.59803400
C	-1.32635700	-1.07899600	0.89055200
C	-0.32430000	-0.43185500	1.83657200
C	0.91768700	0.77318300	0.18617300
C	0.46375500	-0.32297100	-0.82676300
H	-0.79400900	-0.24045200	2.80477900

H	-1.42658700	-2.14400900	1.13170500
H	0.52311300	0.07258800	-1.84782000
H	-1.04447800	-1.80570400	-1.16372100
H	0.53775600	-1.09147400	1.99166200
O	0.09921700	0.84383200	1.33953300
O	2.23387400	0.34695500	0.57080800
O	1.39886700	-1.38292600	-0.63521500
O	-1.86400800	0.11081500	-1.06303300
O	-2.59427100	-0.42735500	1.02156700
C	2.63024300	-0.79504400	-0.22156800
C	3.36739900	-1.77951200	0.66870300
H	2.73892700	-2.06747500	1.51641700
H	3.62841600	-2.67630100	0.09797900
H	4.29069900	-1.32862800	1.04510000
C	3.46050900	-0.33808900	-1.42091800
H	4.37588700	0.15525200	-1.07786900
H	3.73949400	-1.20105800	-2.03437800
H	2.89998200	0.36791100	-2.04194700
C	1.02199800	2.14926800	-0.40134300
H	0.12737800	2.69026900	-0.69240900
O	2.04083700	2.94665700	0.02661600
H	2.72780000	2.34125000	0.37465500
C	-3.04529900	0.00566900	-0.26527800
C	-3.65820700	1.39015600	-0.13100100
H	-3.96409600	1.76881200	-1.11154000
H	-4.54032100	1.35191200	0.51597800
H	-2.92469100	2.07408200	0.30581500
C	-4.00859300	-1.02283400	-0.86187500
H	-4.88807100	-1.13297200	-0.21873400
H	-4.34094700	-0.70386900	-1.85560400
H	-3.52515500	-2.00149800	-0.95359400

[3-1a-C3-H]•

Energy

Electronic Energy (EE)	-920.00449
Zero-point Energy Correction	0.309565
Thermal Correction to Energy	0.327025
Thermal Correction to Enthalpy	0.327969
Thermal Correction to Free Energy	0.264849
EE + Zero-point Energy	-919.69492
EE + Thermal Energy Correction	-919.67746
EE + Thermal Enthalpy Correction	-919.67652
EE + Thermal Free Energy Correction	-919.73964
Imaginary Freq	0

Energies in Hartree, calculated in MeCN.

Geometry

Atom	X	Y	Z
C	-0.88000300	-0.67724000	-0.79609400
C	-1.37719300	-1.32561300	0.54528900
C	-0.37035600	-1.12443500	1.67291000
C	0.90071500	0.61038200	0.58653400
C	0.49937300	-0.12112200	-0.66728300
H	-0.85029500	-1.29028600	2.64083100
H	-1.56430800	-2.39920000	0.41381400
H	-0.91064200	-1.40732500	-1.61347700
H	0.44994700	-1.84677200	1.57041400
O	0.13181800	0.21616900	1.71120700
O	2.28186100	0.25282900	0.73852500
O	1.50468300	-0.97218900	-1.03612400
O	-1.80675200	0.39120300	-1.01887100
O	-2.58780600	-0.63571100	0.84747500
C	2.71546800	-0.59965100	-0.32907500
C	3.34752900	-1.85934900	0.23918200
H	2.64869100	-2.36949200	0.90837400
H	3.62943900	-2.54019800	-0.56998800
H	4.24921600	-1.59731300	0.80180900
C	3.63128000	0.15834000	-1.28285700
H	4.52420600	0.50021900	-0.74921700
H	3.94542700	-0.49371300	-2.10405000
H	3.10698000	1.02426400	-1.69613000
C	0.78265800	2.14298000	0.56915800
H	-0.22624900	2.41334800	0.24994800
H	0.93212200	2.50201600	1.59785400
O	1.68566700	2.75342200	-0.33500400
H	2.57827000	2.52030700	-0.02624200
C	-3.01354600	0.07090400	-0.32079900
C	-3.68195900	1.36504000	0.11053300
H	-3.95044500	1.96371300	-0.76550800
H	-4.59469400	1.14852300	0.67467900
H	-3.00072600	1.94041700	0.74422300
C	-3.91986000	-0.81079100	-1.18381000
H	-4.82089100	-1.08609000	-0.62562600
H	-4.22095900	-0.27407800	-2.08975900
H	-3.40547700	-1.73080300	-1.48174700

[3-1a-C4-H]•

Energy

Electronic Energy (EE)	-920.00572
Zero-point Energy Correction	0.309467
Thermal Correction to Energy	0.326868
Thermal Correction to Enthalpy	0.327812

Thermal Correction to Free Energy	0.265038
EE + Zero-point Energy	-919.69625
EE + Thermal Energy Correction	-919.67885
EE + Thermal Enthalpy Correction	-919.67791
EE + Thermal Free Energy Correction	-919.74068
Imaginary Freq	0

Energies in Hartree, calculated in MeCN.

Geometry

Atom	X	Y	Z
C	-0.90312600	-0.51189800	-0.68657600
C	-1.35043500	-1.24263400	0.55491200
C	-0.34940500	-1.02327100	1.69116700
C	0.95874700	0.66780700	0.57550800
C	0.48726300	0.01393700	-0.76493100
H	-0.84224500	-1.15498300	2.65770600
H	-1.49424500	-2.32310500	0.40432500
H	0.58947100	0.73912700	-1.58135400
H	0.46278900	-1.75467600	1.61157600
O	0.16350600	0.31106600	1.68419600
O	2.29685700	0.20503100	0.72031900
O	1.38859400	-1.08991900	-0.92445200
O	-1.89383200	0.35069500	-1.07361000
O	-2.60790100	-0.61887200	0.86418700
C	2.63430100	-0.72497100	-0.33700500
C	3.27324500	-1.96482700	0.26829800
H	2.60439800	-2.41893300	1.00513200
H	3.48604700	-2.69812800	-0.51618900
H	4.21548400	-1.70107700	0.75893300
C	3.54286300	-0.03663000	-1.35561100
H	4.46612800	0.29965600	-0.87152700
H	3.80647500	-0.73635900	-2.15557000
H	3.04532600	0.83082800	-1.79848800
C	0.95027400	2.20107000	0.57326200
H	-0.04218600	2.55553200	0.28110800
H	1.14875200	2.54189100	1.59949800
O	1.87552600	2.74637400	-0.35081300
H	2.74907600	2.40625000	-0.08898600
C	-3.09176300	0.01922600	-0.31030100
C	-3.78397700	1.31294000	0.07570800
H	-4.09749900	1.85951800	-0.81893500
H	-4.67191000	1.09353900	0.67712000
H	-3.10400100	1.93800300	0.66180700
C	-3.96179500	-0.91973100	-1.14179600
H	-4.85287000	-1.20218500	-0.57193900
H	-4.27954300	-0.42774500	-2.06675200
H	-3.40860500	-1.82826300	-1.40189700

[3-1a-C5-H]•**Energy**

Electronic Energy (EE)	-919.99736
Zero-point Energy Correction	0.309181
Thermal Correction to Energy	0.326744
Thermal Correction to Enthalpy	0.327688
Thermal Correction to Free Energy	0.263714
EE + Zero-point Energy	-919.68817
EE + Thermal Energy Correction	-919.67061
EE + Thermal Enthalpy Correction	-919.66967
EE + Thermal Free Energy Correction	-919.73364
Imaginary Freq	0

Energies in Hartree, calculated in MeCN.

Geometry

Atom	X	Y	Z
C	-0.89370600	-0.64466900	-0.48933700
C	-1.36092800	-0.66126800	0.94717200
C	-0.42604200	-0.23407400	2.01902400
C	1.08246300	0.84336500	0.46469900
C	0.44136800	0.10855900	-0.75781000
H	-0.96539900	0.03969100	2.92828200
H	0.23944500	0.82692300	-1.55742800
H	-0.77248400	-1.65479900	-0.90640500
H	0.30439400	-1.01092600	2.26573200
O	0.27645900	0.96549200	1.60482500
O	2.26218500	0.07998700	0.73474300
O	1.45182800	-0.77429400	-1.22388800
O	-1.95780300	0.04203000	-1.16868600
O	-2.62482500	-0.12819300	0.99866800
C	2.42756500	-0.99692800	-0.20218000
C	2.19967900	-2.34290600	0.48530500
H	1.17766100	-2.42482900	0.86569800
H	2.36655300	-3.15733400	-0.22731400
H	2.89754700	-2.46493700	1.32049700
C	3.81069300	-0.90923100	-0.83502700
H	4.58721400	-0.99234000	-0.06797900
H	3.94683000	-1.72190400	-1.55583800
H	3.92349600	0.04212000	-1.36238500
C	1.49231800	2.29441400	0.16171000
H	0.60361200	2.86326900	-0.12571900
H	1.89530100	2.72747400	1.08817500
O	2.41351900	2.39370500	-0.90879500
H	3.22812900	1.95367000	-0.61049000
C	-3.12670100	-0.03532900	-0.36169200
C	-3.90763800	1.25895600	-0.49581000

H	-4.25138300	1.38114400	-1.52781300
H	-4.78218900	1.24566600	0.16183600
H	-3.27005600	2.10725500	-0.22986800
C	-3.94641500	-1.28312100	-0.68085100
H	-4.80888100	-1.35372400	-0.01017100
H	-4.30895200	-1.23729500	-1.71287600
H	-3.33767200	-2.18554700	-0.56208300

[3-1a-C6-H]•

Energy

Electronic Energy (EE)	-919.99948
Zero-point Energy Correction	0.30846
Thermal Correction to Energy	0.326119
Thermal Correction to Enthalpy	0.327063
Thermal Correction to Free Energy	0.263284
EE + Zero-point Energy	-919.69102
EE + Thermal Energy Correction	-919.67336
EE + Thermal Enthalpy Correction	-919.67242
EE + Thermal Free Energy Correction	-919.7362
Imaginary Freq	0

Energies in Hartree, calculated in MeCN.

Geometry

Atom	X	Y	Z
C	-0.84815000	-0.60796600	-0.90758000
C	-1.21132300	-1.44452400	0.32608800
C	-0.45484100	-1.01805800	1.54023500
C	0.88279700	0.68842800	0.49516600
C	0.54794300	-0.00523700	-0.83829800
H	-0.74160800	-1.38808400	2.52057900
H	-1.08580800	-2.51798600	0.16131100
H	0.69413400	0.70850500	-1.65849500
H	-0.94563300	-1.20106600	-1.82590000
O	0.08980800	0.24020200	1.60322200
O	2.23821100	0.35646900	0.70731000
O	1.48668100	-1.07595300	-0.91011000
O	-1.79596000	0.45659200	-0.88366000
O	-2.64047900	-1.22035300	0.44196700
C	2.66584000	-0.68409700	-0.20738600
C	3.17896100	-1.87747100	0.58241200
H	2.39709100	-2.23979600	1.25666500
H	3.46467500	-2.68546400	-0.09897200
H	4.05734900	-1.59298800	1.17022900
C	3.70136800	-0.09753100	-1.16192400
H	4.57236200	0.26077500	-0.60312100

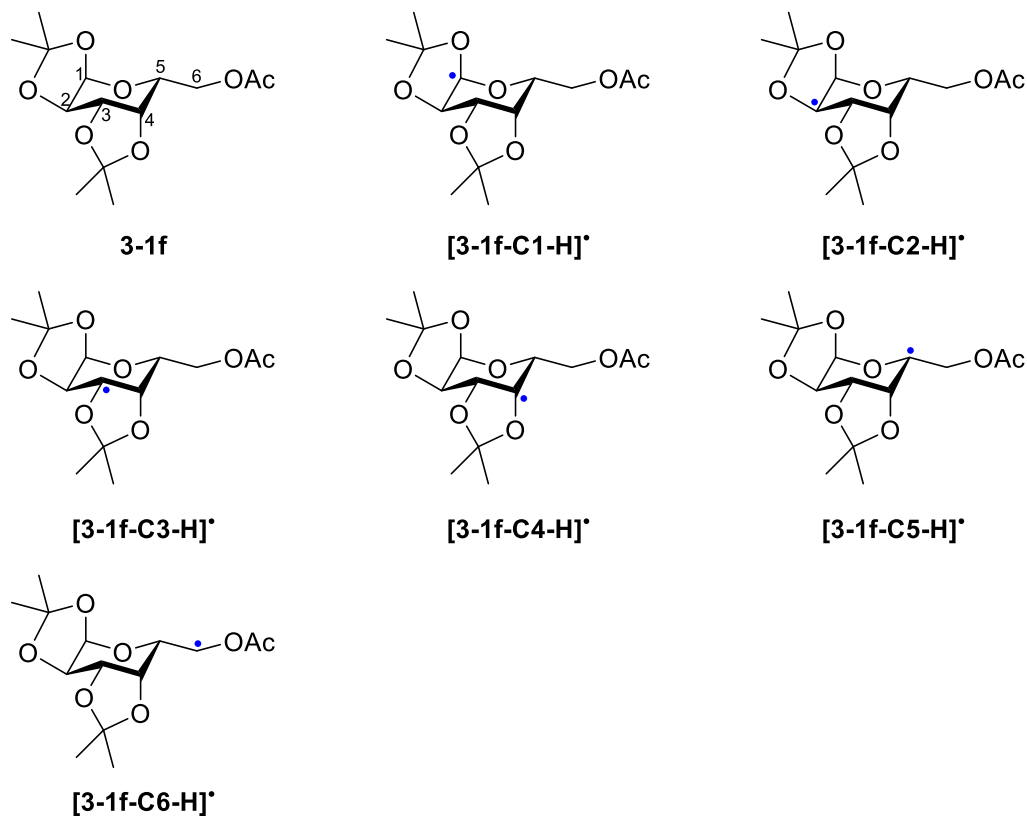
H	4.03438200	-0.86178400	-1.87165400
H	3.27497500	0.74111900	-1.72146000
C	0.74734000	2.21411300	0.50123900
H	-0.26509700	2.48633300	0.19504500
H	0.90842700	2.56538600	1.53053400
O	1.64240400	2.82366600	-0.41214400
H	2.53536200	2.54586300	-0.14127800
C	-2.98764500	0.00502500	-0.21643100
C	-3.39502900	1.06673100	0.79888400
H	-3.61036700	2.01525900	0.29518300
H	-4.29451200	0.74866000	1.33626200
H	-2.58678400	1.22295300	1.51908500
C	-4.08006100	-0.29577400	-1.23907700
H	-4.96633700	-0.70126500	-0.73952400
H	-4.36802100	0.61799100	-1.76968800
H	-3.72311600	-1.03121500	-1.96745300

3.6.2 DFT Calculation Data of 3-1f

Bond dissociation enthalpies of chair conformation of 3-1f

Summary

Species of calculation



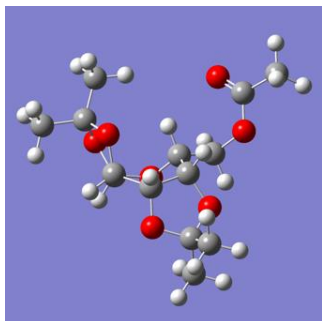
Bond dissociation enthalpy calculations

Geometry optimizations and frequency calculations were carried out for **3-1f** and for the radical species resulting from H-atom abstraction from each site **[3-1f-C1-H][•]**, **[3-1f-C2-H][•]**, **[3-1f-C3-H][•]**, **[3-1f-C4-H][•]**, **[3-1f-C5-H][•]**, and **[3-1f-C6-H][•]**. The calculated energies of these species are listed and the calculated BDEs are summarized.

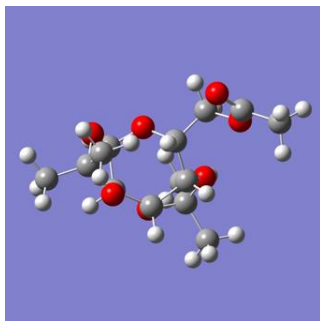
3D images of chair conformation of 3-1f

3-1f

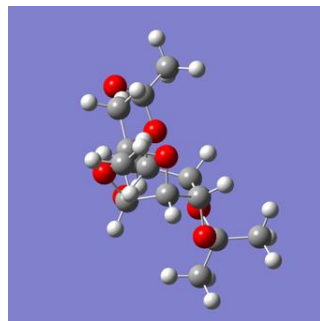
Front view



Top view



Side view

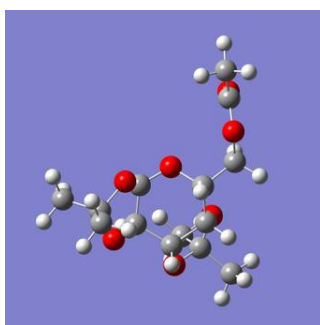


[1f-C1-H]^{*}

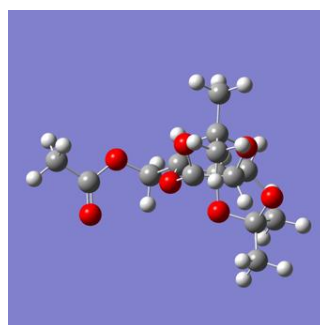
Front view



Top view

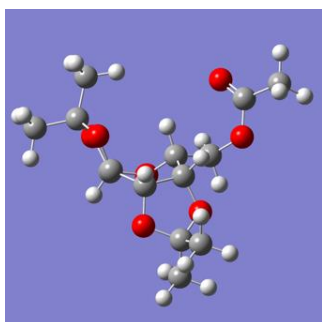


Side view



[1f-C2-H]^{*}

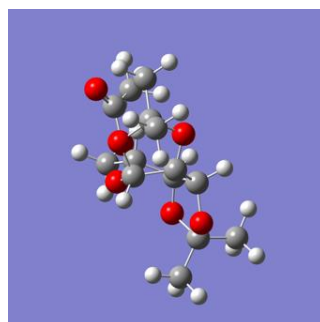
Front view



Top view

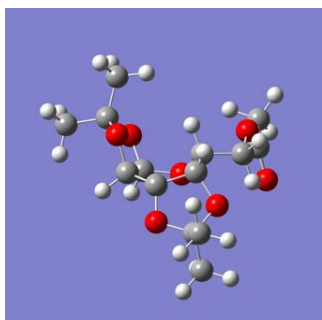


Side view



[1f-C3-H]

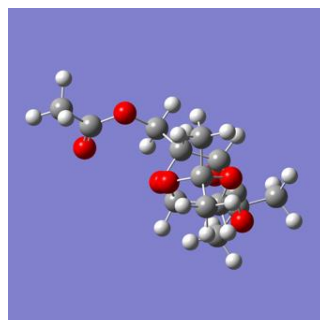
Front view



Top view

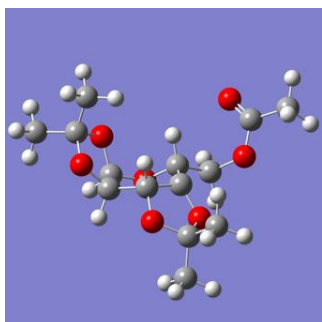


Side view

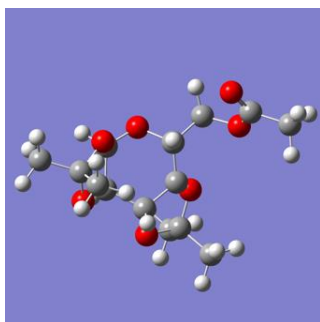


[1f-C4-H]

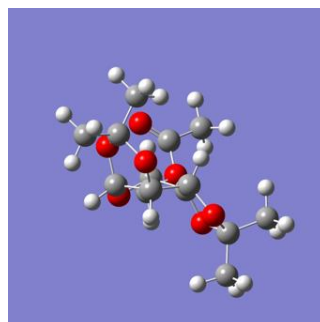
Front view



Top view

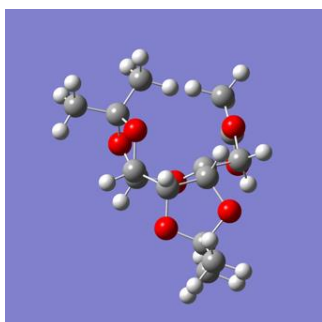


Side view

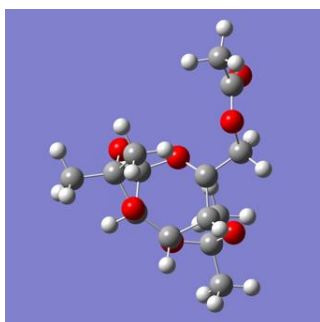


[1f-C5-H]

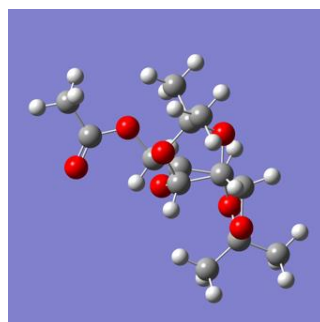
Front view



Top view

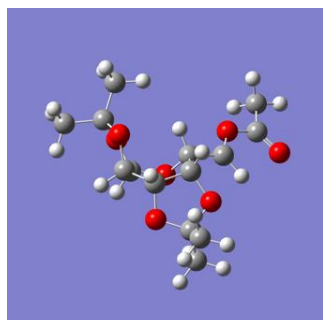


Side view

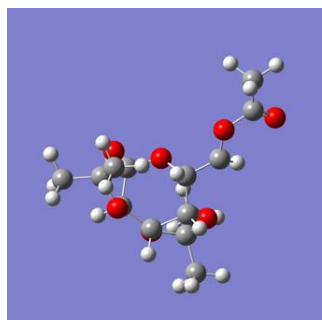


[1f-C6-H]•

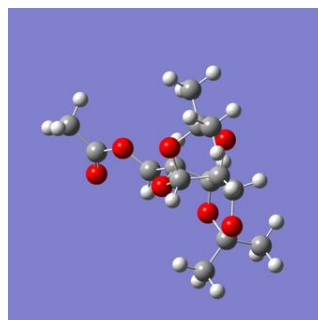
Front view



Top view



Side view



Bond Dissociation Enthalpy Calculations

Geometry optimizations and frequency calculations were carried out for **1f** and for the radical species resulting from H-atom abstraction from each site [1f-C1-H]•, [1f-C2-H]•, [1f-C3-H]•, [1f-C4-H]•, [1f-C5-H]•, and [1f-C6-H]•. The calculated energies of these species are listed and the calculated BDEs are summarized.

Calculated energies and geometries

3-1f

Energy

Electronic Energy (EE)	-1073.3291
Zero-point Energy Correction	0.361375
Thermal Correction to Energy	0.382245
Thermal Correction to Enthalpy	0.383189
Thermal Correction to Free Energy	0.310475
EE + Zero-point Energy	-1072.9677
EE + Thermal Energy Correction	-1072.9468
EE + Thermal Enthalpy Correction	-1072.9459
EE + Thermal Free Energy Correction	-1073.0186
Imaginary Freq	0

Energies in Hartree, calculated in MeCN.

Geometry

Atom	X	Y	Z
C	0.11075000	-1.54836800	-0.86556900
C	1.50758600	-1.31825000	-0.29726300
C	1.52929800	-0.72511300	1.12967800
C	-0.37270400	0.56336300	0.48926700
C	-0.92127200	-0.43215600	-0.53868000

H	1.74969500	-1.46744900	1.89983200
H	2.05966600	-2.26641400	-0.31664300
H	0.19208000	-1.69553600	-1.94975900
H	0.31779800	1.24348700	-0.02163800
H	-1.22100700	0.10575300	-1.44489300
O	0.31232100	-0.14167900	1.53096500
O	2.57253800	0.23665800	1.08305500
O	2.16544400	-0.32730600	-1.08518000
O	-0.41792900	-2.70979900	-0.23121000
O	-2.04077300	-1.13483600	0.00353400
C	-1.44567400	1.38656300	1.19611900
H	-2.16962600	0.73068200	1.67981300
H	-0.98020400	2.04166600	1.93470500
O	-2.20468400	2.16926800	0.25080600
C	-1.70942800	3.38457400	-0.08662500
O	-0.67047800	3.83400000	0.35457000
C	-2.62091600	4.08084200	-1.06224300
H	-2.71910000	3.48267000	-1.97483300
H	-3.62162700	4.18989000	-0.63040300
H	-2.21552900	5.06328200	-1.30873900
C	-1.83206800	-2.54589900	-0.12362400
C	3.13783600	0.29313000	-0.24154400
C	4.45737000	-0.47965100	-0.26529200
H	4.89534500	-0.45165000	-1.26864100
H	5.16713000	-0.03119500	0.43749400
H	4.30402100	-1.52510000	0.02182300
C	3.30008600	1.74377400	-0.66457600
H	4.01598900	2.24772100	-0.00771300
H	3.67783800	1.79629400	-1.69074100
H	2.34147000	2.26808700	-0.61151700
C	-2.29765500	-3.22730000	1.15269200
H	-3.37270000	-3.07592900	1.29213700
H	-2.10277200	-4.30336600	1.10327700
H	-1.76268100	-2.80419100	2.00791000
C	-2.53480900	-3.06894000	-1.37781300
H	-2.36211400	-4.14451900	-1.49126000
H	-3.61351600	-2.89436600	-1.30651000
H	-2.16205700	-2.55967700	-2.27317000

[3-1f-C1-H]•

Energy

Electronic Energy (EE)	-1072.6642
Zero-point Energy Correction	0.347147
Thermal Correction to Energy	0.368286
Thermal Correction to Enthalpy	0.36923
Thermal Correction to Free Energy	0.294424
EE + Zero-point Energy	-1072.3171

EE + Thermal Energy Correction	-1072.296
EE + Thermal Enthalpy Correction	-1072.295
EE + Thermal Free Energy Correction	-1072.3698
Imaginary Freq	0

Energies in Hartree, calculated in MeCN.

Geometry

Atom	X	Y	Z
C	1.69543600	-0.59461500	-0.66966900
C	1.71777500	0.57363800	0.35985600
C	0.35478500	1.15809100	0.68433700
C	-0.87058700	-0.27866800	-0.73675900
C	0.31052700	-1.22159200	-0.92083800
H	2.22903400	0.21265100	1.26138100
H	2.13326500	-0.21283200	-1.59678600
H	-0.85215300	0.46030300	-1.54784800
H	0.27192100	-1.63162900	-1.94010700
O	-0.77291700	0.42463700	0.53217300
O	0.29837000	2.43162700	0.15508500
O	2.42702000	1.68716300	-0.19650500
O	2.46718700	-1.70363800	-0.21642200
O	0.26362000	-2.26843900	0.04645500
C	-2.19966800	-1.01099900	-0.74178000
H	-2.27823000	-1.63407500	-1.63739000
H	-2.30731000	-1.62907500	0.14919000
O	-3.27031500	-0.04739000	-0.80174600
C	-4.12937900	0.02311400	0.24393200
O	-4.10192900	-0.72241000	1.20162100
C	-5.11469400	1.14394300	0.03939000
H	-4.58436500	2.10241500	0.01087500
H	-5.63170700	1.02418600	-0.91851500
H	-5.84016900	1.15082800	0.85427900
C	1.59072300	-2.77877800	0.18794800
C	1.66195600	2.88255900	0.00441700
C	2.10791000	3.60346200	1.27355200
H	3.15433600	3.91119500	1.17968800
H	1.49468100	4.49472100	1.44252400
H	2.01138000	2.94253300	2.14126200
C	1.75082000	3.73810900	-1.24575500
H	1.14408700	4.64197000	-1.13353200
H	2.78987900	4.03643200	-1.41736300
H	1.39611300	3.17169500	-2.11198200
C	1.82047800	-3.11295500	1.65480700
H	1.14385800	-3.91307100	1.97293500
H	2.85075400	-3.44963500	1.80784500
H	1.63836800	-2.22927700	2.27400500
C	1.82121900	-3.96914800	-0.74058000

H	2.86354500	-4.29938700	-0.67921800
H	4.97436900	-1.64200500	-0.83877700
H	4.64716800	0.03399200	-1.33573700

[3-1f-C2-H][•]

Energy

Electronic Energy (EE)	-1072.6716
Zero-point Energy Correction	0.347813
Thermal Correction to Energy	0.368841
Thermal Correction to Enthalpy	0.369785
Thermal Correction to Free Energy	0.295937
EE + Zero-point Energy	-1072.3238
EE + Thermal Energy Correction	-1072.3028
EE + Thermal Enthalpy Correction	-1072.3018
EE + Thermal Free Energy Correction	-1072.3757
Imaginary Freq	0

Energies in Hartree, calculated in MeCN.

Geometry

Atom	X	Y	Z
C	-0.52788600	1.38197100	-0.88339800
C	-1.72646200	0.71474600	-0.29824200
C	-1.66475600	0.16630900	1.10341900
C	0.55712700	-0.47704800	0.50750300
C	0.81523800	0.67404300	-0.47307000
H	-2.10325500	0.80558200	1.87667700
H	-0.62091200	1.42902300	-1.97467700
H	0.12044700	-1.31421500	-0.05168200
H	1.33515800	0.28884200	-1.35828800
O	-0.34163800	-0.05929800	1.54527200
O	-2.39915900	-1.05561100	1.01291400
O	-2.37266100	-0.18459000	-1.10043400
O	-0.40509200	2.69009600	-0.31352200
O	1.58168200	1.69503600	0.15542300
C	1.80605000	-0.96445900	1.23748900
H	2.26836300	-0.14139600	1.78324500
H	1.54204700	-1.76857200	1.92682100
O	2.80860000	-1.42114100	0.30636200
C	2.72793000	-2.70855800	-0.11032200
O	1.85897600	-3.47783500	0.24827700
C	3.85452900	-3.03532600	-1.05431800
H	3.82656900	-2.36379700	-1.91930100
H	4.81746000	-2.88731200	-0.55325800
H	3.76791800	-4.07047300	-1.38785400
C	0.98311900	2.96532400	-0.12571700

C	-3.08582100	-1.11423200	-0.23737400
C	-4.52809200	-0.64213200	-0.08326700
H	-5.03947300	-0.65277400	-1.05112000
H	-5.06399800	-1.30546800	0.60303800
H	-4.55409900	0.37605400	0.31876200
C	-2.95899100	-2.50664300	-0.82627700
H	-3.45326700	-3.23090100	-0.17123700
H	-3.43654100	-2.54672600	-1.81012800
H	-1.90488800	-2.78135300	-0.92739200
C	1.13564100	3.85324000	1.09773100
H	2.19490700	4.04030700	1.30024300
H	0.63906400	4.81482100	0.93375800
H	0.68690700	3.36100700	1.96558700
C	1.59377900	3.57229700	-1.39068600
H	1.11546300	4.53017000	-1.62120300
H	2.66616000	3.74290000	-1.24874500
H	1.46188500	2.90382700	-2.24842600

[3-1f-C3-H][•]

Energy

Electronic Energy (EE)	-1072.6733
Zero-point Energy Correction	0.347625
Thermal Correction to Energy	0.368663
Thermal Correction to Enthalpy	0.369608
Thermal Correction to Free Energy	0.295771
EE + Zero-point Energy	-1072.3257
EE + Thermal Energy Correction	-1072.3046
EE + Thermal Enthalpy Correction	-1072.3037
EE + Thermal Free Energy Correction	-1072.3775
Imaginary Freq	0

Energies in Hartree, calculated in MeCN.

Geometry

Atom	X	Y	Z
C	-1.81599300	0.59570000	0.24109300
C	-1.03128400	1.66870700	-0.42931400
C	0.27449500	1.11943700	-1.09800000
C	0.39087400	-0.50751700	0.64960600
C	-1.11083400	-0.50561500	0.99334400
H	0.20621500	1.09952000	-2.18866900
H	-1.64590900	2.18402900	-1.17704000
H	0.87628800	0.25909300	1.26600300
H	-1.22677200	-0.43655700	2.08524400
O	0.58174200	-0.20601700	-0.73696700
O	1.28801500	2.01614500	-0.68366200

O	-0.53286100	2.57958000	0.55955400
O	-2.82767500	0.04637700	-0.49878500
O	-1.75016200	-1.69617500	0.50945800
C	1.03945500	-1.85189300	0.92699400
H	0.82186600	-2.16800200	1.95110500
H	0.68882600	-2.60688000	0.22453600
O	2.47283200	-1.71883300	0.82672600
C	3.11008300	-2.38215500	-0.16671600
O	2.56753400	-3.15105800	-0.93417400
C	4.57624200	-2.03482700	-0.17513100
H	4.70243700	-0.97420500	-0.42085200
H	5.01252700	-2.19796800	0.81578900
H	5.09606000	-2.64494400	-0.91545400
C	-2.99469400	-1.33857800	-0.08326800
C	0.70744900	3.09317000	0.07773100
C	0.48769900	4.30468000	-0.82994700
H	0.03339200	5.12450100	-0.26357200
H	1.44419400	4.64958700	-1.23629100
H	-0.17042800	4.05217900	-1.66802700
C	1.60213400	3.40104900	1.26639600
H	2.58204600	3.74526000	0.92111400
H	1.15528700	4.18980200	1.87997900
H	1.73530900	2.50553000	1.88072000
C	-3.21212200	-2.18323700	-1.32492000
H	-3.29568300	-3.23854100	-1.04658600
H	-4.13362700	-1.88419900	-1.83377900
H	-2.36587500	-2.06055700	-2.00725400
C	-4.13372000	-1.41827200	0.92838800
H	-5.07303100	-1.08927200	0.47237800
H	-4.25415300	-2.45073700	1.27181900
H	-3.92306600	-0.78167300	1.79409600

[3-1f-C4-H][•]

Energy

Electronic Energy (EE)	-1072.6661
Zero-point Energy Correction	0.34752
Thermal Correction to Energy	0.3686
Thermal Correction to Enthalpy	0.369544
Thermal Correction to Free Energy	0.295285
EE + Zero-point Energy	-1072.3186
EE + Thermal Energy Correction	-1072.2975
EE + Thermal Enthalpy Correction	-1072.2966
EE + Thermal Free Energy Correction	-1072.3708
Imaginary Freq	0

Energies in Hartree, calculated in MeCN.

Geometry

Atom	X	Y	Z
C	-0.73501500	-1.16963000	0.58759600
C	-1.93386100	-0.71438000	-0.30146300
C	-1.64664000	0.50261800	-1.21756800
C	0.66421800	0.64779100	-0.59566600
C	0.59965700	-0.65686500	0.11298800
H	-2.25068300	0.44859200	-2.13115800
H	-2.24123000	-1.57952800	-0.89681500
H	-0.96025300	-0.87397200	1.62138700
H	0.43549500	1.45678800	0.10517800
O	-0.34056900	0.67752600	-1.65825700
O	-2.05983900	1.60330700	-0.40775200
O	-3.03802400	-0.27533000	0.47749000
O	-0.59290000	-2.59419700	0.50218300
O	1.30984100	-1.71053700	-0.40018300
C	1.98328400	0.93935800	-1.30680500
H	2.24538900	0.12403800	-1.98200800
H	1.89537800	1.87181200	-1.86708600
O	3.07069200	1.02659300	-0.36660300
C	3.27263300	2.22421300	0.23512000
O	2.58596800	3.20444600	0.02723100
C	4.45215100	2.16024200	1.16845500
H	4.29721900	1.37640100	1.91758600
H	5.35849400	1.90598400	0.60783100
H	4.58379500	3.12379100	1.66289200
C	0.75983900	-2.92128200	0.17785900
C	-3.14175000	1.16783300	0.41438500
C	-4.48261600	1.52363500	-0.22326900
H	-5.30466700	1.12085000	0.37777600
H	-4.59766100	2.61088200	-0.28624800
H	-4.55075800	1.10221900	-1.23148200
C	-2.96894100	1.76157900	1.80515400
H	-3.02501000	2.85438100	1.76184200
H	-3.76089300	1.40010200	2.46890000
H	-1.99850300	1.47383900	2.22122500
C	0.77342800	-4.00575900	-0.88414100
H	1.80162400	-4.23985000	-1.17699500
H	0.30904600	-4.91546500	-0.49092600
H	0.21505500	-3.67349600	-1.76438500
C	1.54556700	-3.28060600	1.43510500
H	1.10767600	-4.16638600	1.90637300
H	2.58989200	-3.49646000	1.18686900
H	1.51752600	-2.45147300	2.14987300

[3-1f-C5-H][•]**Energy**

Electronic Energy (EE)	-1072.6721
Zero-point Energy Correction	0.347334
Thermal Correction to Energy	0.368508
Thermal Correction to Enthalpy	0.369452
Thermal Correction to Free Energy	0.294669
EE + Zero-point Energy	-1072.3248
EE + Thermal Energy Correction	-1072.3036
EE + Thermal Enthalpy Correction	-1072.3027
EE + Thermal Free Energy Correction	-1072.3775
Imaginary Freq	0

Energies in Hartree, calculated in MeCN.

Geometry

Atom	X	Y	Z
C	1.81668200	0.99994900	-0.49585800
C	0.77738800	1.84261100	0.22621000
C	-0.10571600	1.05722800	1.20301500
C	0.00594800	-0.75174300	-0.38949000
C	1.24042700	-0.29044700	-1.09387300
H	0.24012000	1.08215900	2.23612900
H	1.26444700	2.66840200	0.76112900
H	2.31154300	1.60029900	-1.26987000
H	1.05006700	-0.20867800	-2.16700400
O	-0.22671200	-0.34294500	0.89994700
O	-1.34900800	1.69607400	1.11789300
O	-0.15835200	2.32629800	-0.73457000
O	2.75365100	0.53943200	0.47392100
O	2.34917500	-1.21852500	-0.95088400
C	-0.66094400	-2.02960600	-0.74324700
H	-0.34094700	-2.36450800	-1.73264700
H	-0.46581300	-2.82148900	-0.01262800
O	-2.10780800	-1.84294400	-0.82250100
C	-2.87673800	-2.44277000	0.11490600
O	-2.45124700	-3.18020500	0.98204900
C	-4.32481700	-2.06486600	-0.06512500
H	-4.94996300	-2.68111000	0.58317300
H	-4.46126900	-1.00923600	0.19738300
H	-4.62914100	-2.18845000	-1.10905600
C	3.22689100	-0.76215300	0.08851200
C	-1.40525100	2.53223000	-0.06566300
C	-1.55002000	3.98361400	0.38084800
H	-1.59722300	4.64354300	-0.49162100
H	-2.46815700	4.11081100	0.96375400
H	-0.69915000	4.28012300	1.00281700

C	-2.52897000	2.06602500	-0.97770500
H	-3.49529300	2.19223900	-0.47886900
H	-2.53652800	2.65775200	-1.89898100
H	-2.39252800	1.01066600	-1.23051300
C	3.14349300	-1.67519400	1.30658000
H	3.46980800	-2.68670000	1.04343100
H	3.78844700	-1.30112900	2.10897900
H	2.11326400	-1.71535800	1.67216200
C	4.63560500	-0.66083800	-0.48961400
H	5.33535700	-0.30289900	0.27297800
H	4.97434000	-1.64207600	-0.83879300
H	4.64716100	0.03392400	-1.33575700

[3-1f-C6-H]'

Energy

Electronic Energy (EE)	-1072.6644
Zero-point Energy Correction	0.346419
Thermal Correction to Energy	0.36767
Thermal Correction to Enthalpy	0.368614
Thermal Correction to Free Energy	0.294244
EE + Zero-point Energy	-1072.318
EE + Thermal Energy Correction	-1072.2968
EE + Thermal Enthalpy Correction	-1072.2958
EE + Thermal Free Energy Correction	-1072.3702
Imaginary Freq	0

Energies in Hartree, calculated in MeCN.

Geometry

Atom	X	Y	Z
C	-1.73567600	0.92318100	-0.57173400
C	-2.12189100	-0.36965000	0.13661000
C	-1.08977900	-0.84719200	1.18411800
C	0.62154000	-0.04740300	-0.29296200
C	-0.24102900	1.02591200	-0.97311200
H	-1.40590100	-0.65346900	2.21192200
H	-3.10360700	-0.23774700	0.60902200
H	-2.37970500	1.05545400	-1.45039300
H	0.49645800	-0.99205900	-0.83559700
H	-0.11391900	0.94810200	-2.05857200
O	0.17302500	-0.23751000	1.07799200
O	-1.00993600	-2.25058900	0.96671900
O	-2.15290900	-1.42635700	-0.82101000
O	-1.91749900	1.98586100	0.35944300
O	0.14874700	2.33000600	-0.53846000
C	2.05457100	0.31705000	-0.28393700

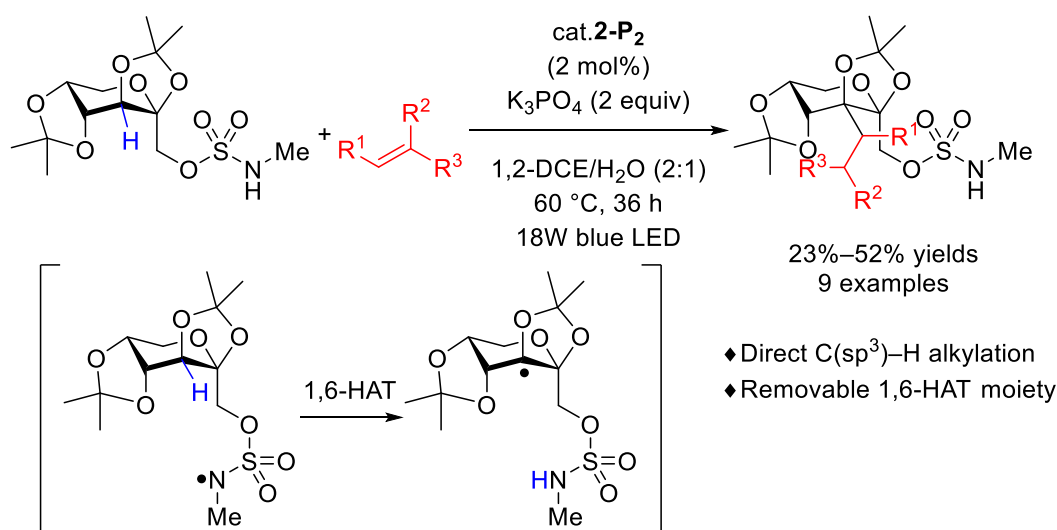
H	2.43711200	1.30622200	-0.07855700
O	2.92499500	-0.73699100	-0.17406400
C	4.26515900	-0.47664700	-0.01068400
O	4.71175400	0.64767600	0.04015900
C	5.03906000	-1.75869500	0.09210400
H	4.70207600	-2.33077800	0.96399600
H	4.86571400	-2.37724000	-0.79520500
H	6.10304100	-1.53734300	0.18713200
C	-0.96920300	3.00721200	0.05483600
C	-1.88684800	-2.63666600	-0.10797300
C	-3.17463800	-3.22857300	0.46768100
H	-3.85422700	-3.51685600	-0.34121400
H	-2.94461900	-4.11818500	1.06315700
H	-3.68465600	-2.50612500	1.11328600
C	-1.16281400	-3.60016300	-1.03358100
H	-0.90726600	-4.51767200	-0.49434800
H	-1.80542400	-3.86451300	-1.87951000
H	-0.24396500	-3.14509200	-1.41480800
C	-0.52286100	3.64981600	1.35841800
H	0.24473500	4.40574400	1.16474300
H	-1.36990700	4.13505200	1.85402700
H	-0.11119600	2.88203200	2.01985100
C	-1.55243800	4.00731800	-0.94401600
H	-2.41481700	4.52275800	-0.50789200
H	-0.79925600	4.75494400	-1.21397800
H	-1.87501100	3.49700600	-1.85790200

Chapter 4. Conclusion

In Chapter 1, I introduced the potential applications of saccharide derivatives in various fields and provided a brief discussion on different approaches for modifying saccharides. Specifically, I focused on two main methods for achieving alkylation of saccharides, which involved the functionalization of hydroxy groups of saccharides and direct C(sp³)-H alkylation of saccharides, respectively.

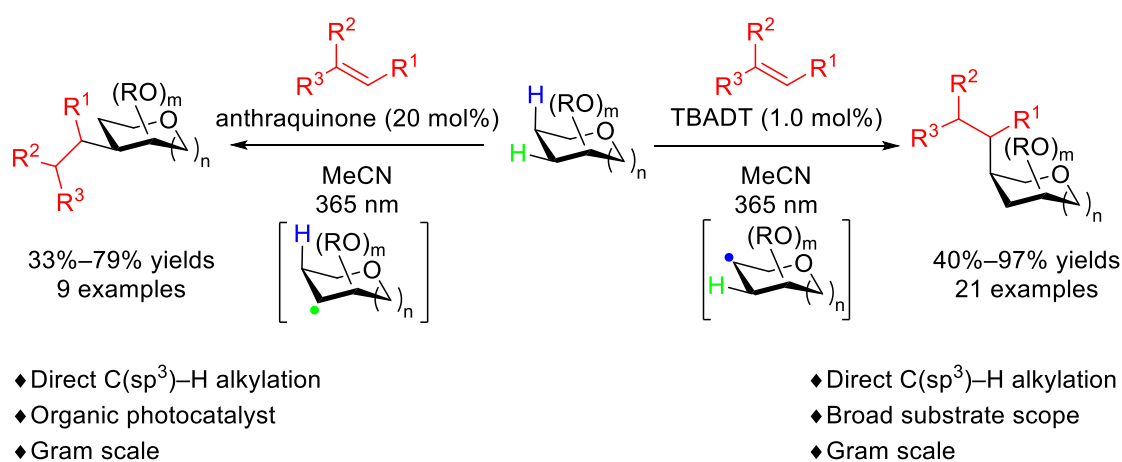
In Chapter 2, the C3(sp³)-H alkylation was achieved using 2,3:4,5-bis-*O*-(1-ethylethylidene)- β -D-fructopyranose methyl sulfamate as a model substrate. As a result, nine alkylated-D-fructopyranose derivatives were obtained in moderate yields (23% to 52%). Additionally, this work demonstrated that the alkylation at the target positions, which are not easily accessible through the transformations of hydroxy groups, can be achieved by introducing a 1,6-HAT moiety of saccharides. Several functional groups, such as ester, aryl, carbonyl, cyano, and sulfonyl groups, could be introduced using the reaction. Furthermore, the 1,6-HAT moiety, which presented in the alkylated D-fructopyranose derivatives, could be removed, and the introduced siloxy group also could be transformed to a hydroxy group. The alkylation of D-fructopyranose derivatives with alkenes bearing the functional groups will promote the synthesis of complex carbohydrates.

Scheme 4-1. Iridium-photocatalyzed C3(sp³)-H alkylation of 2,3:4,5-bis-*O*-(1-ethylethylidene)- β -D-fructopyranose methyl sulfamate via 1,6-HAT.



In Chapter 3, the site-selective C(sp³)-H alkylation of saccharides successfully was achieved without using a directing group or a HAT site. These reactions were accomplished using anthraquinone or TBADT photocatalyst. Under anthraquinone photocatalysis, nine alkylated saccharides were obtained in moderate to good yields (33% to 79%). In addition, under TBADT photocatalysis, twenty-one alkylated saccharides were obtained in moderate to excellent yields (40% to 97%). Various functional groups could be introduced into different saccharide frameworks using the two reaction systems. Anthraquinone-catalyzed C(sp³)-H alkylation targeted the weak bond dissociation energy (BDE) of C(sp³)-H bond of saccharides. On the other hand, the site-selectivity of TBADT-catalyzed C(sp³)-H alkylation was mainly governed by steric effects. By changing the photocatalysts, the reaction sites could be switched due to the different factors influencing the site-selectivity. Moreover, in both anthraquinone- and TBADT-catalyzed C(sp³)-H alkylation, the mono-alkylated products were obtained on a gram scale. Hopefully, these reactions will contribute to the development of glycochemistry.

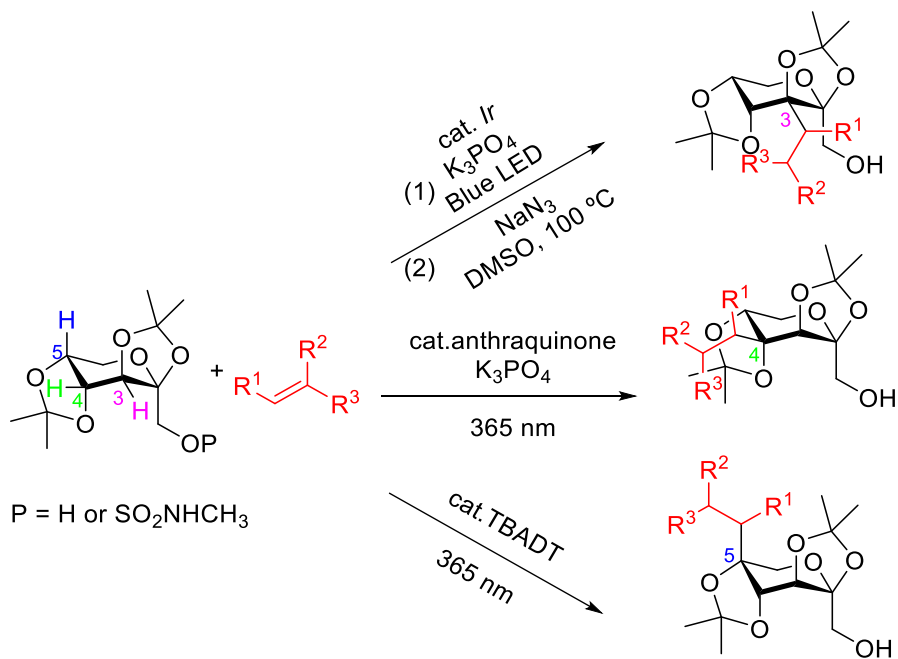
Scheme 4-2. Anthraquinone- and TBADT-catalyzed site-selective alkylation of saccharides via HAT.



In this thesis, the site-selective alkylation of D-fructopyranose at C3–H, C4–H, and C5–H positions was successfully achieved, as illustrated in Scheme 4-3. Through the site-selective introduction of diverse functional groups, the transformations of D-fructopyranose provide valuable insights into the field of glycochemistry.

Furthermore, site-selective C(sp³)–H alkylation of various saccharides, including D-fructose, D-galactose, L-sorbose, and other saccharide derivatives, was successfully accomplished under TBADT photocatalysis. This strategy holds the potential to foster advancements in C(sp³)–H transformations in bioactive and natural compounds.

Scheme 4-3. Site-selective alkylation of 2,3:4,5-bis-*O*-(1-ethylethylidene)- β -D-fructopyranose in this thesis.



Publication List

Chapter 2: Li, Y.; Miyamoto, S.; Torigoe, T.; Kuninobu, Y.

Regioselective C(sp³)-H alkylation of a fructopyranose derivative by 1,6-HAT.

Org. Biomol. Chem. **2021**, *19*, 3124–3127.

Chapter 3: Li, Y.; Kuninobu, Y.

Site-selective Direct Intermolecular C(sp³)-H Alkylation of Saccharides and Switching of Reaction Sites by Changing Photocatalysts

Adv. Synth. Catal. **2023**, in press. DOI 10.1002/adsc.202300329

Acknowledgements

I would like to express my deepest gratitude to my thesis advisor, Professor Yoichiro Kuninobu, for his invaluable guidance, support, and encouragement throughout my research journey. His expertise, patience, and dedication have been instrumental in shaping this thesis and developing my academic skills. I am grateful for his mentorship and the opportunity to learn from him.

I would also like to extend my sincere appreciation to Assistant Professor Takeru Torigoe for his guidance and help on my first project. His teachings and advice have broadened my knowledge and skills and have enabled me to grow both personally and professionally. And thanks to Mr. Shoto Miyamoto for investigating of the reaction conditions on my first project. Thanks to the faculty members of the Institute for Materials Chemistry and Engineering Ms. Ideta Keiko, Mr. Hiroshi Toshima and Kanako Imamura, for their valuable measurement work during my academic journey.

I would also like to thank Assistant Professor Kohei Sekine, and lab mates Mr. Zeng Jialin, Mr. Jiang Zhiyan, Mr. Chen Qi and others for their help during my research work and life. I am grateful for their companionship, which has made my academic journey enjoyable and memorable.

I am especially thankful to Professor Mitsuru Shindo and Professor Go Hirai for their kind and patient guidance on this thesis.

I would like to thank my family, for their unwavering support, and encouragement. Their moral support helps me achieve my academic goals.

Finally, I would like to thank the Japan Science and Technology Agency (JST) that have provided financial support for my research work. Their generous support has made this research possible, and I am grateful for their assistance.

In conclusion, I acknowledge the contributions of all those who have helped me in my academic journey. Without their support, guidance, and encouragement, this thesis would not have been possible.